CHARACTERIZATION OF PUTATIVE REGULATORS OF THE SMALL GTPASE, RAC, IN *DROSOPHILA*

by

Caillin Langmann
B.Sc., Simon Fraser University 1999

THESIS
SUBMITTED IN PARTIAL FULFILLMENT OF
THE REQUIREMENTS FOR THE DEGREE OF
DOCTOR OF PHILOSOPHY

In the Department
of
Molecular Biology and Biochemistry

SIMON FRASER UNIVERSITY

June 2004

APPROVAL

Name: **Caillin Langmann**

Degree: Doctor of Philosophy (Science)

Title of Thesis: Characterization of Putative Regulators of the Small GTPase, Rac, in *Drosophila*.

Examining Committee:

Chair: _____

Dr. Lynne Quarmby, Ph.D. Associate Professor
Department of Biology, SFU

_____

Dr. N. Harden, Ph.D. Associate Professor
Senior Supervisor
Department of Molecular Biology and Biochemistry, SFU

_____

Dr. B. Brandhorst, Ph.D. Professor
Supervisor
Department of Molecular Biology and Biochemistry, SFU

_____

Dr. E. Verheyen, Ph.D. Assistant Professor
Supervisor
Department of Molecular Biology and Biochemistry, SFU

_____

Dr. C. Beh, Ph.D. Assistant Professor
Internal Examiner
Department of Molecular Biology and Biochemistry, SFU

_____

Dr. Vanessa Auld, Ph.D. Associate Professor
External Examiner
Department of Zoology, University of British Columbia

Date Approved: _____

SIMON FRASER UNIVERSITY

Partial Copyright Licence

ABSTRACT

The Rho subfamily GTPases (Rho, Rac, Cdc42) are small GTP-binding proteins that act as switches, controlling many cellular functions. These GTPases fluctuate between a GTP-bound 'on' state and a GDP-bound 'off' state, this being catalyzed by guanine nucleotide exchange factors (GEFs) and GTPase-activating proteins (GAPs). Rac, a possible oncogene, has diverse roles including regulation of cell adhesion, the release of arachidonic acid, formation of F-actin based membrane ruffles/lamellipodia, assembly of multi-molecular focal complexes, apoptosis, and regulation of the JNK MAP kinase pathway.

Model systems such as *Drosophila* have furthered the understanding of the functional roles of Rac in neuronal development, epithelial morphogenesis, and apoptosis. The use of model systems allows the study of molecular processes at levels not possible in cell culture. These include genetic approaches and the study of gene function at the level of tissue morphogenesis. Three putative interactors of Rac, originally identified in mammals, were studied in *Drosophila*. Sra-1, a cytoskeletal effector, was found to interact with Rac and had roles in neuronal development and F-actin regulation. POSH, a modulator of JNK signaling in mammals, was found to indirectly modulate Rac in *Drosophila* but was not required for JNK signaling during embryonic development. *Drosophila* POSH also had a role in apoptosis during development. RhoGAP68F, a GAP protein, was found to preferentially negatively regulate activated Rho rather than Rac in *Drosophila* and was therefore not investigated further.

DEDICATION

To Mom, Dad and Deanna.

ACKNOWLEDGEMENTS

Thanks for help from Dr. Esther Verheyen, Dr. Bruce Brandhorst, Ryan Conder, Justina Sanny, Barton Xu, Bari Zahedi, Kai-Ping Sem, Darrell Bessette, Marina 'Hoss' Kanjer, Jobi 'wan Kinobi' McKenzie, Krista 'Krispy' Ryz, Daniel 'Han Solo' Han, Claire Hou, Richard 'Oh, Heck!' Heck, Micheal 'The Sleeper' Sha, Miles 'Dr. Lean' Chu, Ricky 'Martin' Choi. Also thank you to the Esther Verheyen Laboratory and the Susan Parkhurst Laboratory.

Finally thank you to Dr. Nick Harden for being an extremely supportive supervisor.

TABLE OF CONTENTS

LIST OF FIGURES

LIST OF TABLES

LIST OF ABBREVIATIONS AND ACRONYMS

AEL – after egg laying

CNS – central nervous system

CRIB – Cdc42 Rac1 interacting binding domain

DSra-1 – *Drosophila* Specifically Rac1 Associated protein

DPOSH – Plenty of SH3s

Rac1V12 – Constitutively active Rac1

Rac1N17 – Dominant negative functioning Rac1

GTP – guanine triphosphate

GDP – guanine diphosphate

PCR – polymerase chain reaction

INTRODUCTION

1.1 The Rho subfamily of small GTPases

The Rho subfamily of small GTPases, so called due to their ability to cleave GTP to GDP, are members of the large family of Ras GTP-binding proteins of 20-30kD in size. The Rho GTPases, which include Rho, Rac, and Cdc42 first characterized in the early 1990s, act as molecular switches controlling many actin-dependent processes by signalling to downstream effector proteins (Hall, 1998). These GTPases cycle between a GTP-bound 'on' state and a GDP-bound 'off' state (Van Aelst and D'Souza-Schorey, 1997).

1.2 Regulation of the Rho GTPases

The Rho GTPases are required to be anchored to the cell membrane by farnesylation of a C-terminal CAAX box in order that they can be locally activated through upstream mechanisms by receptor tyrosine and serine/threonine kinases (Hancock et al., 1992) (Van Aelst and D'Souza-Schorey, 1997). While the exact mechanisms are relatively unknown, several receptor tyrosine kinases have been implicated in the activation of the Rho GTPases in mammalian cultured cells, such as the insulin receptor (INR), the epidermal growth factor receptor (EGFR), platelet derived growth factor β-receptor (PDGF β-R) and the activation of Rac by cadherins through the epidermal growth factor receptor (EGFR) (Kotani et al., 1994) (Hawkins et al., 1995) (Nobes et al., 1995) (Betson et al., 2002).

It is likely guanine nucleotide exchange factors (GEFs) are responsible for the upstream activation of the Rho GTPases. GEFs function by causing a conformational change in the inactive GTPase allowing for the release of GDP from its catalytic domain. Many GEFs have little in common except for a DH domain, a conserved domain first recognized in Dbl, a Cdc42 GEF and oncogene (Schmidt and Hall, 2002).

The methods of transduction of the signal between an active receptor and a GEF are not clear and are probably quite complicated, however the study of the Vav family of GEFs has provided one mechanism. Vav has been shown to be activated by several receptors including EGFR, PDGFR, and the B- and T-cell receptors (Bustelo, 1996). When stimulated, the T-cell receptor (TCR) is auto-phosphorylated allowing the Src tyrosine kinase, Fyn, to bind to the TCR SH2 binding domain, and subsequently activate the Fyn kinase. Once activated, Fyn phosphorylates Vav stimulating in turn, the GEF catalytic domain that mediates the conformational change in Rac allowing the exchange of GDP with GTP (Schmidt and Hall, 2002).

Another Rac GEF, DOCK180 (*Drosophila* Myoblast City (MBC)), has also been shown to act upstream of Rac (Nolan et al., 1998). DOCK180 contains a DOCK homology region-2 (DHR-2), rather than a DH domain, which is responsible for GEF function (Cote and Vuori, 2002).

In addition, Rho GTPases are negatively regulated by GTPase activating proteins (GAPs) which increase the GTPase intrinsic rate of hydrolysis of GTP to GDP thereby rapidly shutting down the activated molecule (Van Aelst and D'Souza-Schorey, 1997). While at first glance the role of a GAP as a negative regulator seems straightforward, GAPs may also function as effectors themselves. n-Chimaerin, a GAP demonstrated to

inhibit Rac1 induced cytoskeletal rearrangements, was shown to co-operate with Rac1 in the formation of lamellipodia and filopodia when a mutant form lacking the GAP domain was microinjected into fibroblasts (Kozma et al., 1996).

Just as there are proteins to enhance the GTPase function, there also exist proteins known as guanine dissociation inhibitors (GDIs) that inhibit the exhange of GDP and the hydrolysis of bound GTP (Van Aelst and D'Souza-Schorey, 1997). As mentioned, Rho GTPases appear to be required to be anchored to the membrane and GTP-bound in order to be in an active state. As such, GDIs primarily function as inhibitors by controlling the translocation of the GTPases from the cytosol to the membrane by forming a complex preventing the farnesylated CAAX box from associating with the membrane (Takahashi et al., 1997).

1.3 Rac acts to regulate the cytoskeleton and cell migration

This thesis principally focused on putative regulators of signaling by the Rho GTPase, Rac. Rac has been shown to have a multitude of roles including the release of arachidonic acid, vesicle formation, membrane ruffling and lamellipodia formation, assembly of multimolecular focal complexes, regulation of the c-Jun N-termal kinase pathway (JNK), and cell cycle progression (Coso et al., 1995; Malecz et al., 2000; Nobes and Hall, 1995; Peppelenbosch et al., 1995; Ridley et al., 1992). Most of these processes involve the cytoskeleton of the cell, and Rac has been shown to be a key mediator.

Lamellipodia are small protrusive filamentous actin (F-actin) rich structures generated at the leading edges of migrating cells when exposed to growth factors. A dominant negative version of Rac, Rac1N17, was created by mutating a Thr to Asn at

amino acid 17, based upon an analogous mutation in the related GTPase, Ras. The microinjection of RacN17 into Swiss 3T3 cells exposed to growth factors inhibited the formation of lamellipodia (Ridley et al., 1992). Constitutively active Rac, RacV12, also constructed based upon a Ras mutant by mutating a Gly to a Val at amino acid 12, was microinjected into cells and shown to induce lamellipodia in the absence of growth factors, indicating that Rac is involved in the regulation of the cytoskeleton (Ridley et al., 1992).

Real time localization studies have also revealed an associated role of Rac with lamellipodia. The fluorescent activation indicator for Rho proteins (FLAIR) technique has shown that a gradient of activated Rac protein is seen in migrating fibroblasts with the highest concentrations in the leading edge (Kraynov et al., 2000).

The exact mechanisms behind how Rac interacts with the cytoskeleton have not been completely solved and it is likely that several mechanisms are responsible, however a model has been proposed by recent research into the WAVE/Scar protein. Activated Rac was shown to cause the inactive WAVE/Scar complex to dissociate and allow the subsequent WAVE/Scar activation of Arp2/3 (Eden et al., 2002). In turn WAVE/Scar leads to the Arp2/3 driven actin polymerization (Volkmann et al., 2001). Arp2/3 is a complex of seven proteins that binds to the slow growing 'pointed' end of existing F-actin and acts to initiate the nucleation of F-actin branches by providing a template upon which actin monomers can bind and quickly grow in the fast 'barbed' direction (Volkmann et al., 2001).

Arp2/3 and WAVE/Scar are not the only mechanisms for the regulation of actin as studies in animal systems, such as *Drosophila*, have revealed that certain F-actin

structures are uneffected by mutations in these genes (Kiehart and Franke, 2002). Another Rac binding effector, p21-Activated Kinase (PAK), has also been shown to cause the formation of lamellipodia and cytoskeletal rearrangements through phosphorylation of a number of actin regulating proteins (Bokoch, 2003; Sells et al., 1997; Vadlamudi et al., 2002).

1.4 Rac and cell adhesions

The regulation of cell adhesions has been shown to be closely linked with Rac (Evers et al., 2000). Adherens junctions are critical in development and morphogenesis and exist as cell-cell homophilic interactions between the extracellular regions of E-cadherins. The cytoplasmic region of E-cadherin forms a complex with α–catenin, β–catenin and F-actin and F-actin is thought to stabilize the cadherin receptors at cell-cell contact sites (Braga et al., 1997). Expression of RacN17 in the wing disc epithelium of *Drosophila*, inhibited actin assembly at the adherens junctions and microinjection of RacN17 into human keratinoctyes disrupted the adherens junctions suggesting that Rac's ability to regulate F-actin stabilizes these cell-cell adhesions (Braga et al., 1997; Eaton et al., 1995). Not only does Rac stabilize the junctions but it is also likely recruited to and activated by initial cell-cell contact at these junctions themselves, leading to their stabilization (Kovacs et al., 2002; Nakagawa et al., 2001; Noren et al., 2001).

Integrins are dual pass transmembrane proteins that provide a link between the extracellular matix and the cytoskeleton through the basal surface of the cell (Brown et al., 2000). The integrin complex consists of α- and β-integrins plus a variety of intracellular proteins, such as talin, filamin, vinculin, and α-actinin, that serve as a link

with F-actin. While Rac cannot affect the affinity of integrin mediated adhesion to the extracellular matrix, it does seem to be able to recruit integrins to new membrane protrusions (Kiosses et al., 2001). The recruitment of integrins produces clusters which probably serve to strengthen the adhesions.

1.5 Rac, the JNK pathway, and transcriptional activation

One of the known functions of Rac is the activation of the c-Jun N-terminal Kinase (JNK) signaling pathway. JNK is a member of the mitogen-activated protein (MAP) kinase family and was originally identified in human cells as two proteins that phosphorylate the transcription factor c-Jun (Hibi et al., 1993). MAPKs have been shown to have roles in many cell functions such as migration, proliferation, differentiation, and apoptosis (Davis, 2000). There are five groups of MAPKs identified in mammals, extracellular regulated kinase 1 and 2 (ERK1/2), JNK, p38, ERK3/4, and ERK5. Each is activated by dual phosphorylation of a specific tripeptide motif, Thr-X-Tyr, by a MAPK kinase (MAPKK) which is itself phosphorylated by a MAPKK kinase (MAPKKK) (Davis, 2000).

Constitutively active Rac, RacV12, as well as oncogenic Rac GEFs were shown to specifically activate the JNK pathway in COS-7 cells, while dominant negative Rac, RacN17, blocks the JNK pathway in COS-7 cells induced with cytokines and growth factors (Coso et al., 1995).

The exact link between Rac and the JNK pathway is not completely clear. It has been shown that a large variety of mammalian kinases can act as JNKKKs or JNKKKKs, including MLK, LZK, TAK, ASK, MEKK, TPL, PAK and GCK, and sorting out the

precise mechanisms particular to each cell type and specific signal is likely to be complex (Bokoch, 2003; Davis, 2000). For example, evidence has been described for an interaction between Rac, MLK3 and the members of the germinal center kinases (GCK) – IV family of Ste20 proteins in mammalian cells that could activate JNKK (Dan et al., 2001; Leung and Lassam, 2001). It is also important to note that the MLKs have a Cdc42 Rac interactive binding (CRIB) domain that can facilitate the direct binding of the MLK to Rac (Burbelo et al., 1995; Leung and Lassam, 2001).

The end result of the JNK pathway is the activation of a transcription factor complex known as activating protein-1 (AP-1) (Davis, 2000). AP-1 is not a single transcription factor but rather a family of transcription factors such as Jun, Fos, ATF and Maf, that dimerize using a basic region-leucine zipper (bZIP) to form an active complex (Shaulian and Karin, 2002). The AP-1 transcription factors have been demonstrated to control a variety of cellular functions including proliferation, death, survival, differentiation, and motility, and studies done on gene expression after AP-1 activation have revealed a large number of transcribed genes (Ozanne et al., 2000).

1.6 Drosophila as a model system for studying epithelial migration

Epithelial morphogenetic events in the late *Drosophila* embryo are of interest in the study of *Drosophila* Rac. During stage 12 (7-9 hours after egg laying (AEL)), the germ band, retracts caudally revealing the egg yolk covered by a layer of simple squamous tissue called the amnioserosa (Campos-Ortega and Hartenstein, 1985) (Fig. 1.1). During stage 13 to 15 (9-13 hours AEL) the process known as dorsal closure

Figure 1.1 Stages of *Drosophila* Embryogenesis.

Figure depicts the stages of *Drosophila* embryogenesis. Number on top right of each figure indicates the stage. Amnioserosa is indicated by 'as', and germ band is indicated by 'gb'.

Stage 5, cellularization, occurs 2 – 2:30 hours AEL, and is the first stage of nuclear cellularization. Stage 8, germ band extension, occurs 3 – 3:40 hours AEL, mesoderm and endoderm have formed in the previous stages while the germ band extends over the amnioserosa. Stage 9, germ band elongation, occurs 3:40 – 4:20 hours AEL. Stage 11, germ band retraction begins, 5:20 – 7:20 hours AEL. Stage 12, germ band retraction, occurs 7:20 – 9:20 hours AEL. Ventral nerve cord forms axons. Stage 13, dorsal closure begins, 9:20 – 10:20 hours AEL. Stage 14, head involution occurs and dorsal closure continues 10:20 – 11:20 hours AEL. Stage 15, dorsal closure completes during this stage, 11:20 – 13 hours AEL. Stage 17, 16 hours have elapsed, the embryo has completed embryogenesis, cuticle has been secreted and hatching into a larval Stage 1 will soon occur. (Hartenstein, 1993).

Figure reproduced with permission from Hartenstein (1993).

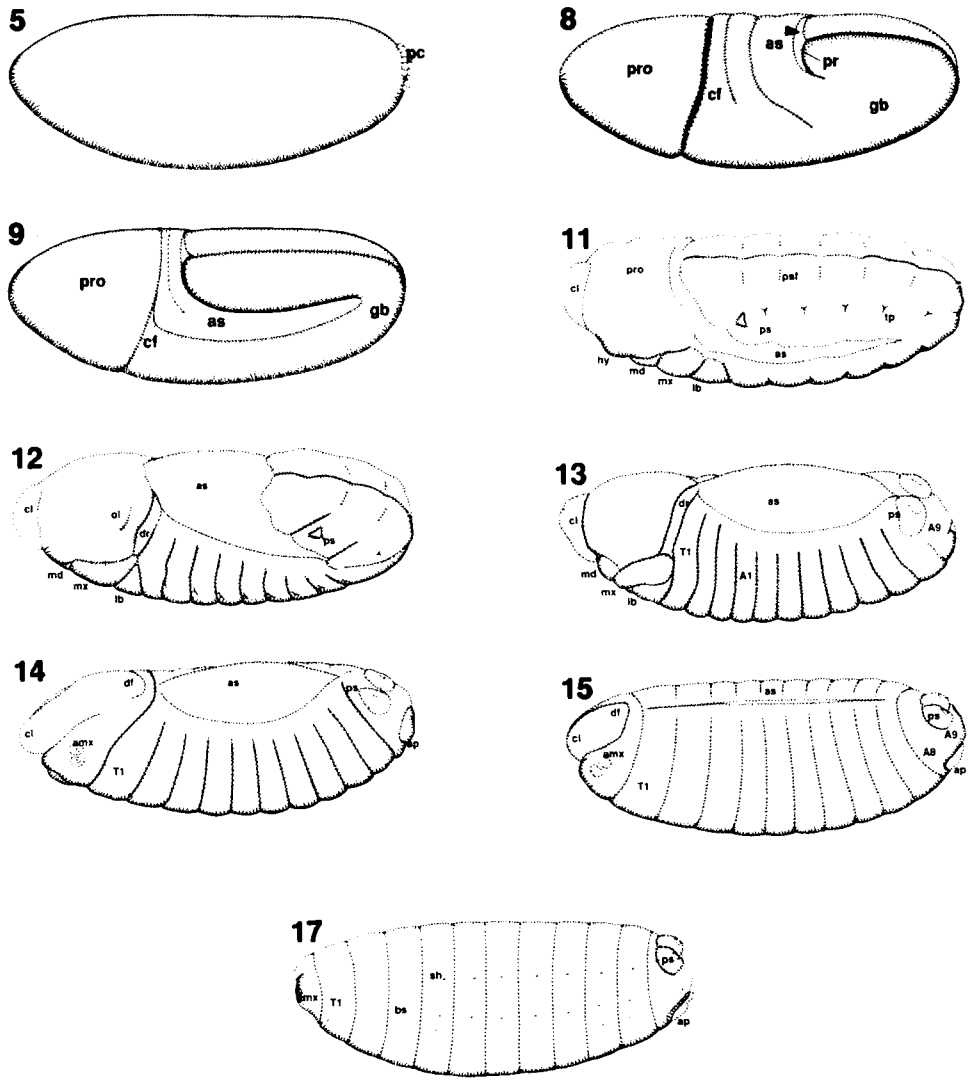

Figure reproduced with permission from Hartenstein (1993). (Hartenstein, 1993)

occurs. Dorsal closure is a morphogenetic process where the lateral epidermis of both sides of the embryo migrates dorsally to cover the amnioserosa and completely seals the embryo (Campos-Ortega and Hartenstein, 1985).

The process of dorsal closure appears to be largely mechanical. Nonmuscle myosin-II (referred to as myosin) and F-actin accumulate at the leading edge (LE) cells of the lateral epidermis and it has been suggested these proteins act as a 'purse-string' to draw the hole closed (Fig. 1.2) (Young et al., 1993). On a cellular level one would expect the forces generated by the 'purse-string' to constrict the leading edge cells in an anterior-posterior direction (A-P), leading to an elongation in the dorsal-ventral (D-V) direction (Fig. 1.3). This is supported by the finding that leading edge cell elongation is impaired in *zipper* (myosin) mutant embryos and in embryos expressing *DRac1N17* (Harden et al., 1996; Young et al., 1993). *zipper* mutant embryos are lacking in non-muscle myosin II heavy chain, whereas DRac2N17-expressing embryos are deficient in leading edge F-actin. Interestingly, anti-phosphotyrosine staining of embryos reveals a series of triangular nodes at the LE that are associated with adherens junctions (Harden et al., 1996). These are lost in embryos expressing RacN17, as would be expected considering the cell culture evidence for the role of Rac in stabilizing these structures.

Laser ablation studies of cells on the lateral epidermis and the LE have demonstrated that while cell constriction is a major force behind dorsal closure, there are other forces contributing to epidermal migration (Kiehart et al., 2000). Live embryo imaging has revealed the existence of lamellipodia and filopodia at the LE that appear to act to correctly align opposite LE cells (Jacinto et al., 2000).

Figure 1.2 Dorsal closure is a model for epithelial movement in the *Drosophila* embryo.

(A – D) Panels show dorsal views of progressively older embryos stained with anti-phosphotyrosine antibodies to show closure of the epidermis over the large flat cells of the amnioserosa.

Figure reproduced with permission from Harden (2002).

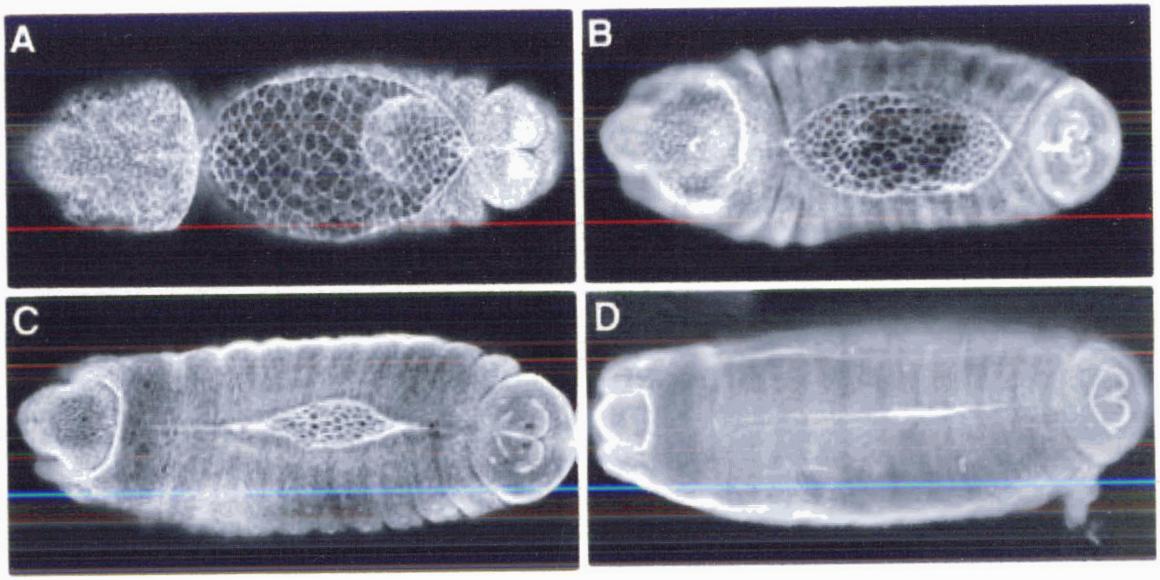

Figure reproduced with permission from Harden (2002).

Figure 1.3 Views of the leading edge (LE) during DC.

(A) The boundary between the amnioserosa *(top of figure)* and the epidermis in phalloidin-stained embryo showing accumulation of F-actin along the LE, and extension of F-actin-rich filopodia from the amnioserosa and LE cells *(arrows).* (B) Accumulation of myosin along the LE. (C) Accumulation of phosphotyrosine along the LE in triangular nodes *(arrows).* (D) View of the dorsal midline after the migrating epidermal flanks have met up at the end of DC. Note that cells flanking segment borders (marked with *bars)* are wider than their neighbors. (E) Phosphotyrosine-stained *kay* mutant embryo lacking DFos, showing loss of LE phosphotyrosine nodes and failure of cell elongation in the epidermis. (F) Embryo expressing dominant negative Dcdc42 showing bunched epidermis characterized by ectopic adhesions between LE cells *(arrows).*

Figure reproduced with permission from Harden (2002).

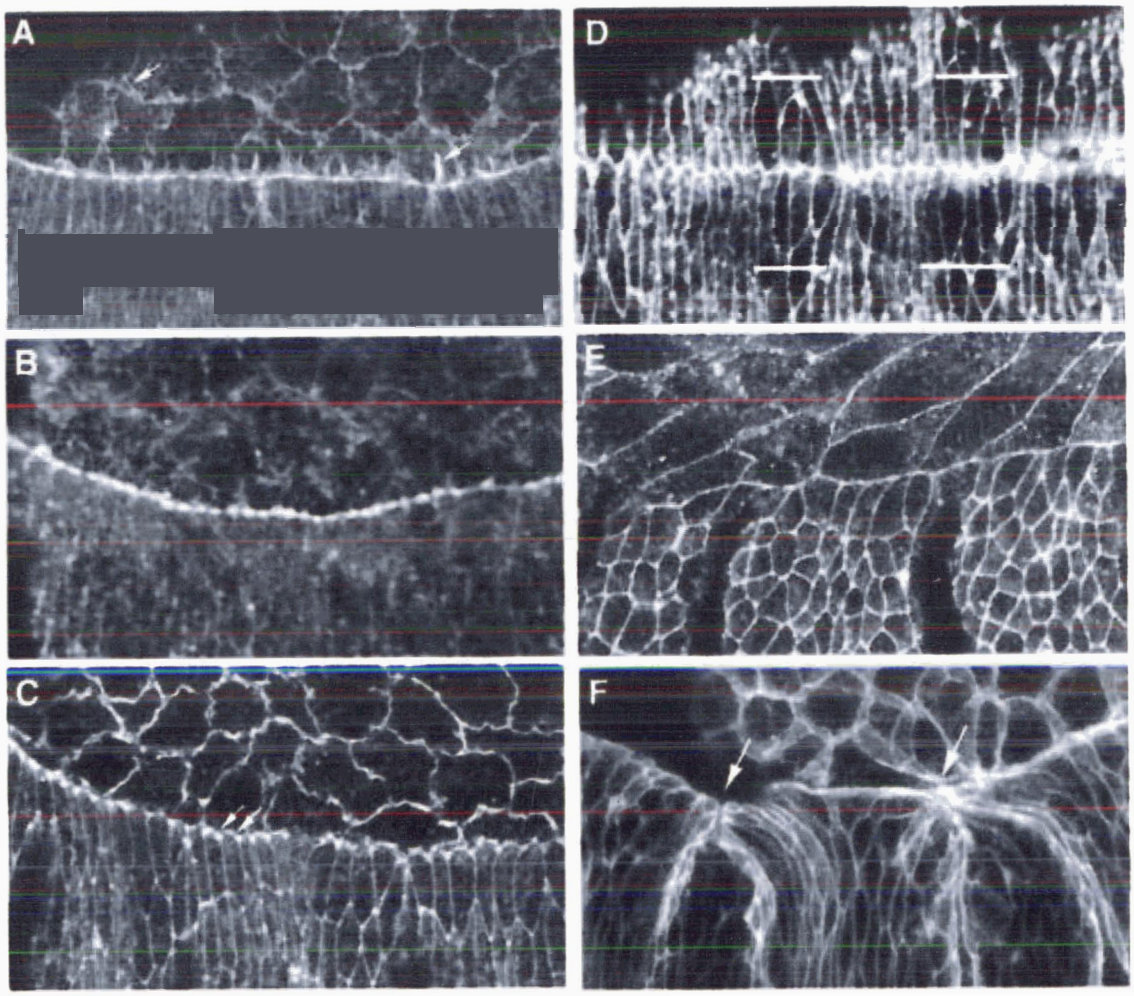

Figure reproduced with permission from Harden (2002).

Now that a model has been described for epithelial sheet movement and morphogenesis, it can be used to examine cell signaling pathways driving cell shape change and motility. The JNK cascade has been found to be a central component of the signaling driving dorsal closure (Fig. 1.4). The first gene cloned encoding a JNK component affecting dorsal closure was *hemipterous* (*hep*), a MAPKK most similar to JNKK (Glise et al., 1995). Following this, *Drosophila* JNK (DJNK) was shown to be encoded by *basket* (*bsk*), *Drosophila* Jun (DJun) encoded by *l(2)IA109*, and *Drosophila* JNKKK (DJNKKK) encoded by a MLK gene, *slipper* (*slpr*) (Hou et al., 1997; Kockel et al., 1997; Nusslein-Volhard et al., 1984; Riesgo-Escovar and Hafen, 1997b; Riesgo-Escovar et al., 1996; Sluss et al., 1996; Stronach and Perrimon, 2002). Mutations in the *Drosophila* JNK components produce non-constricted LE cells, disruption of F-actin and myosin at the LE, and the failure of dorsal closure to complete.

As mentioned, the end result of the JNK cascade is the assembly of AP-1, and in the case of dorsal closure, it is the dimerization of DJun and *Drosophila* Fos (DFos), encoded by *kayak* (*kay*) (Jurgens et al., 1984; Riesgo-Escovar and Hafen, 1997a; Zeitlinger et al., 1997). *kay* mutants exhibit the same dorsal closure defects as seen for mutants in the other JNK components.

Two genes have been studied whose expression in the leading edge cells during dosal closure is dependent on the DJun/DFos transcription factor: *decapentaplegic* (*dpp*) and *puckered* (*puc*) which respectively encode the *Drosophila* homologs of transforming growth factor-β (TGF-β) and a VH-1 family MAPK phosphatase for DJNK (Glise et al., 1995; Jackson and Hoffmann, 1994; Ring and Martinez Arias, 1993; St Johnston and Gelbart, 1987) (Martin-Blanco et al., 1998; Ring and Martinez Arias, 1993).

Figure 1.4 Schematic diagram summarizing signaling occurring during DC.

Note that some of the interactions depicted remain speculative and not all known DC participants are shown. The diagram is centered on the JNK cascade *(highlighted in red)* in a LE cell migrating towards the top right hand corner of the figure. The LE accumulation of F-actin and myosin and extensions of filopodia and lamellipodia are shown in *red.* The triangular adherens junctions at the dorsal end of the LE cell are shown in *green.* Dpp/ TGF-P signaling events *(highlighted in blue)* in LE cells and a more ventrally located epidermal cell are also summarized. See text for details.

Figure reproduced with permission from Harden (2002).

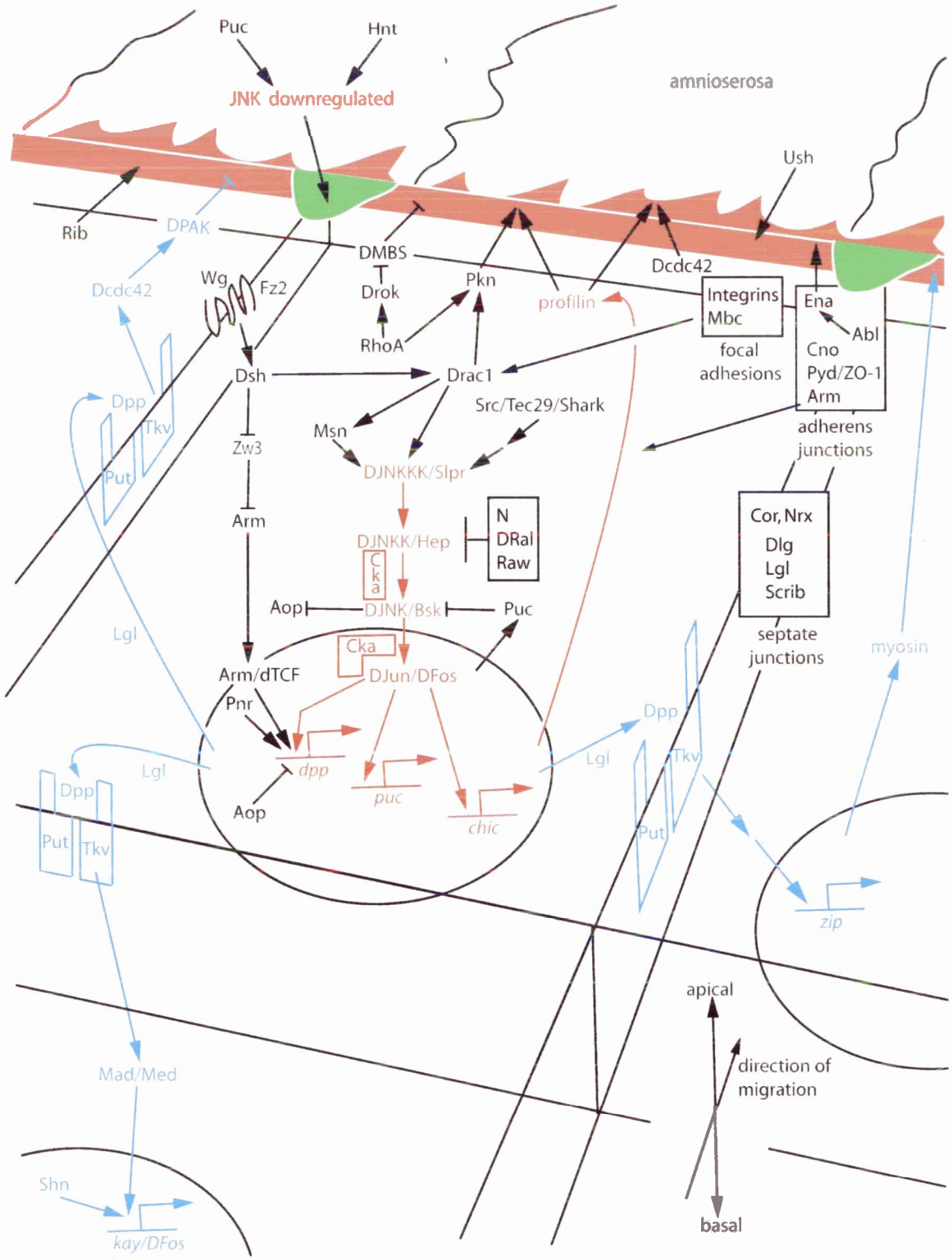
Puc
Hnt
JNK downregulated
amnioserosa
Ush
Rib
DPAK
DMBS
Dcdc42
Wg
Fz2
Drok
Pkn
profilin
Integrins
Mbc
focal
adhesions
Ena
Abl
Cno
Pyd/ZO-1
Arm
adherens
junctions
RhoA
Dsh
Drac1
Src/Tec29/Shark
Msn
Zw3
DJNKKK/Slpr
Dpp
Tkv
Put
Arm
DJNKK/Hep
N
DRal
Raw
Cka
Aop
DJNK/Bsk
Puc
Cor, Nrx
Dlg
Lgl
Scrib
septate
junctions
myosin
Lgl
Arm/dTCF
Pnr
DJun/DFos
dpp
puc
chic
Aop
zip
Mad/Med
Shn
kay/DFos
apical
direction of
migration
basal

Unfortunately *dpp* is required early in the formation of the dorsal epidermis, and an examination of its role during dorsal closure can only be examined by the expression of transgenes (Morisato and Anderson, 1995).

Mutations exist for the type-I and type-II TGF-β receptors, *thick veins* (*tkv*) and *punt* (*put*), both of which cause dorsal closure defects (Affolter et al., 1994; Brummel et al., 1994; Childs et al., 1993; Letsou et al., 1995; Nellen et al., 1994; Penton et al., 1994; Ruberte et al., 1995). Moreover, the over-expression of Dpp or an expression of an activated version of Tkv can rescue dorsal closure defects caused by mutations of the JNK pathway (Ip and Davis, 1998). Therefore, as one of the results of the JNK cascade is the expression of the *dpp,* TGF-β signaling via both receptors is required for successful dorsal closure (Ruberte et al., 1995).

Clearly, TGF-β signaling is required during dorsal closure, but the exact mechanisms of action have not yet been resolved. Several possible explanations have been described: the production of myosin is lost in LE cells deficient in *tkv* mutants, cells ventral to the LE cells fail to elongate in *tkv* and *put* mutants, and there is misdirected migration of the leading edge in the *tkv* and *put* mutants (Harden, 2002).

The relationship between *Drosophila* Rac1 (DRac1) and dorsal closure was first demonstrated by showing that the expression of dominant negative DRac1, DRac1N17, during embryogenesis causes dorsal closure defects similar to those seen in the JNK mutations (Harden et al., 1995; Harden et al., 2002). Expression of constitutively active DJun during dorsal closure can partially rescue DRacN17-induced defects and expression of constitutively active *Drosophila* RacV12 (DRacV12) can cause ectopic expression of *dpp* and *puc* in a *hep* dependent manner (Hou et al., 1997) (Glise et al., 1995). These

results suggested, in agreement with the mammalian data, that DRac1 can activate the JNK cascade.

Embryos mutant for all three *Drosophila Rac* genes, *DRac1*, *DRac2*, and *Mig-2-like* (*Mtl*), have reduced F-actin, myosin, lammellipodia, and filopodia at the LE and exhibit dorsal closure defects (Hakeda-Suzuki et al., 2002). *DRac1* appears to make the greatest contribution to dorsal closure, as double mutations in *DRac1,DRac2* or *DRac1,Mtl* show dorsal closure defects while *DRac2,Mtl* double mutants are viable. The effects of *Drosophila Rac* mutations on the JNK cascade, such as *dpp* transcript levels, have not been examined at this time.

How might Rac activate the JNK cascade in dorsal closure? DRac could act through Slpr and/or Misshapen (Msn), a *Drosophila* Ste20 GCK, by possibly forming a terniary complex to activate the JNK cascade (Stronach and Perrimon, 2002; Su et al., 1998). Slpr can facilitate this by directly binding Rac with its CRIB domain, and as already mentioned, GCKs have been shown to bind MLKs, however there remains little doubt that Slpr is acting as the major JNKKK responsible for dorsal closure (Stronach and Perrimon, 2002).

A possible mechanism of upstream activation of Rac during dorsal closure is through Myoblast City (Mbc), the *Drosophila* DOCK180 GEF homolog (Nolan et al., 1998). Mbc over-expression was shown to increase the levels of phosphorylated DJun and can be inhibited by expression of DRac1N17, suggesting that it could activate the JNK cascade through Rac similar to evidence from cell culture (Kiyokawa et al., 1998; Nolan et al., 1998).

The signaling pathways discovered in dorsal closure closely parallels with that seen in cultured cells. Dorsal closure should be a good model system for the examination of cytoskeletal regulation and cell migration that can lead beyond the level of the study of single cells. The study of development and morphogenesis allows the investigation and construction of tissue specific models of epithelial migration.

1.7 Drosophila as a model for neural development

In *Drosophila* the development of the nervous system involves the organization of polarized neurons with long branches extending through the tissue to precise connections at muscles or neurons (pathfinding). The neuronal branches (neurites) must be carefully and correctly guided through a maze of tissues, pulled in the correct direction by a growth cone, an actin rich tip with strong resemblance to the lammellipodial and filopodial extentions of migrating fibroblasts (Settleman, 2001).

A role for DRac in neural development was shown by expression of DRac1N17 in *Drosophila* neurons during embryogenesis which caused a loss of axons but not dendrites (Luo et al., 1994). Interestingly a similar effect was seen with the expression of DRacV12 and evidence from various systems has led to a model where Rac may function as a positive regulator of axon pathfinding but functioning to both extend and contract the growth cone depending on particular extracellular signals (Luo, 2000). For instance, if lamellipodia are required for both the growth and retraction of the growth cone then interference in Rac signaling by constitutively active and dominant negative mutants could cause inhibition of axon growth.

Recently through examination of the *Drosophila* loss-of-function mutants of the Rac genes, DRac1, DRac2, and Mtl, a role for Rac was confirmed in axon growth, guidance, and branching during embryogenesis (Ng et al., 2002).

Definite roles also exist for Rac in the migration of the neuron associated glial cells which migrate along the neural pathway substrate (Sepp et al., 2000). Expression of DRac1V12 in glial cells results in a balled up cell phenotype, reminiscent of the effects on neurons (Sepp and Auld, 2003). It has also been shown that this glial cell migration is required for the correct migration of peripheral neural cells (Sepp et al., 2001).

How Rac might signal to co-ordinate the growth cone is unclear, but direct signaling through *Drosophila* PAK (DPAK) has been shown to act by organizing F-actin and myosin at the leading edge of cells undergoing shape change and migration (Harden et al., 1996; Manser et al., 1995; Manser et al., 1997). Mutations of DPAK also result in photoreceptor axon guidance defects in the developing adult eye (Hing et al., 1999; Newsome et al., 2000).

1.8 Drosophila as a model for the study of apoptosis

Programmed cell death, or apoptosis, has been shown to be important in the development of multicellular tissues (organogenesis) and a genetic description was originally described in *C. elegans* for which Brenner, Sulston and Horvitz received the 2002 Nobel Prize (Danial and Korsmeyer, 2004).

Since the initial studies in the early 1970s, the number of genes involved in apoptosis has grown dramatically, as has the complexity behind the control of cell death.

The various mechanisms controlling apoptosis in *Drosophila* are complicated and incomplete, and therefore, only the genes relevant to this thesis will be discussed here.

Apoptosis, or programmed cell death, plays an essential role during *Drosophila* embryogenesis and has been well studied from the analysis of mutations in apoptotic genes. A deficiency, *H99*, on the *Drosophila* third chromosome removes three genes, *grim*, *reaper*, *hid*, all shown to encode inhibitors of the *Drosophila* Inhibitor of Apoptosis-1 (DIAP1) protein (Wang et al., 1999; White et al., 1994; Yoo et al., 2002). *H99* homozygous embryos fail to undergo apoptosis and exhibit several phenotypes such as extra cells in the central nervous system, delayed germ band retraction, and head involution defects (Pazdera et al., 1998; Wang et al., 1999; White et al., 1994).

Grim, Reaper, and Hid are though to bind to DIAP1 and in effect, competitively interfere with DIAP1's ability to bind the *Drosophila* Dronc, an initiator caspase similar to mammalian caspase-2 (Danial and Korsmeyer, 2004). Dronc in turn activates the effector caspases that are responsible for activating the cellular apoptotic machinery.

Drosophila caspase-1, or drICE, functions in a similar manner to the mammalian protein, the primary effector caspase responsible for DNA degradation by Caspase Activated DNAse (CAD) and for α-spectrin disruption (Fraser et al., 1997; Nath et al., 1996a; Nath et al., 1996b; Widlak, 2000). During apoptosis, DNA is degraded in two stages. During stage 1, cleavage of DNA into large molecular weight fragments occurs, followed by stage 2 cleavage of DNA into smaller fragments (Widlak, 2000). While there is some evidence that the large molecular weight DNA fragmentation factor (LDFF) under the control of caspase-3 cleaves during stage 1, stage 2 cleavage by CAD under the control of caspase-1 has been well documented (Lu et al., 2004; Widlak, 2000). A

Drosophila homolog of *CAD*, *Rep4*, has been cloned, but no mutants exist at this time (Inohara and Nunez, 1999).

In *Drosophila* S2 cells, drICE was shown to be required for apoptosis, and DIAP1 was demonstrated to inhibit the activation of drICE (Fraser et al., 1997; Kaiser et al., 1998). Silencing of Dronc inhibits the processing of drICE in apoptotic stimulated S2 cells (Muro et al., 2002).

Evidence of studies done on Drosophila imaginal discs points to the activation of transcription of *grim*, *reaper*, and *hid*, through DJNK (Varfolomeev and Ashkenazi, 2004). Upstream of this signaling pathway is the *Drosophila* Tumour Necrosis Factor, Eiger, and its receptor, Wengen which have been shown to activate DJNK through *Drosophila* TRAF1 (Kanda et al., 2002; Kauppila et al., 2003; Moreno et al., 2002).

1.9 The use of Drosophila to study three putative Rac effector proteins

The interest of this thesis was to examine the roles of three putative Rac binding proteins in *Drosophila*. The role of *Drosophila* Rac in morphogenesis had been well studied in *Drosophila* prior to the start of the project and characterized models had been developed, in particular Rac's function in dorsal closure as described earlier in the thesis. The three proteins, Plenty of SH3s (POSH), Specifically Rac1-associated Protein (Sra-1), and p50 Rho GTPase Activating Protein (p50RhoGAP) were originally identified as Rho GTPase binding proteins in mammalian systems, and were considered good candidate Rac effectors that could be studied in an ideal model organism.

Each of the proteins was chosen for study because they likely represented diverse aspects of Rac signaling, and were readily amenable to mutational analysis due to the

presence of P element insertions flanking the genes encoding the *Drosophila* homologs. Sra-1 was investigated as a potential link between Rac and the cytoskeleton, POSH as a link between Rac and the Jun N-terminal Kinase (JNK) signaling pathway, and RhoGAP68F, the *Drosophila* homolog of p50RhoGAP, as a potential Rac regulator and effector protein.

The use of a model organism, such as *Drosophila*, allows the study of genes beyond the limits of investigation in single cells, which are constrained by their particular genetic background and lack of natural environment. Indeed, model organisms have the advantage of allowing the scientist to pry into the limitless study of the function of a gene at the level of the organism itself. This is, after all, the end goal of biomedical research, to apply the knowledge of each level, from cell to tissue to organism, to the understanding of our own.

> "Nature herself must be our advisor; the path she chalks must be our walk. For as long as we confer with our own eyes, and make our ascent from lesser things to higher, we shall be at length received into her closet-secrets."
>
> William Harvey, Doctor of Physic, 1653

1.10 Specifically Rac1-associated Protein (Sra-1)

Specifically Rac1-associated Protein (Sra-1) was originally pulled out of a affinity purification column in a screen of bovine proteins that could bind GTP-bound Rac1 (Kobayashi et al., 1998). Portions of the amino acid sequence of bovine Sra-1 were obtained from a 120 kDa band on a Western blot and a human cDNA homolog,

KIAA0068, was obtained. Human Sra-1 was shown to preferentially bind GTP-bound Rac1 vs GDP-bound Rac1 in an *in vitro* binding assay and was also shown to co-localize with RacV12 and cortical F-actin in the RacV12-induced lamellipodia of KB cells. Interestingly, Sra-1 did not have a CRIB domain or any other recognizable domains. Sra-1 was found to be in the membrane fraction of KB cell lysate and was able to co-sediment with F-actin.

Sra-1 constitutes a potential route for cytoskeletal regulation by Rac, and it was chosen for study in *Drosophila*, where Rac regulation of the cytoskeleton in development had been demonstrated. A single *Drosophila* homolog of human *Sra-1* (*DSra-1*) was found and sequenced, revealing a closely matching amino acid identity of 65%. *DSra-1* transcript was elevated in the embryonic nervous system while anti-human Sra-1 antibodies stained the leading edge during dorsal closure. DSra-1 was found to bind GTP-bound DRac1, over-expression of *DSra-1* caused dorsal closure defects, and over-expression of *DSra-1* could partially rescue DRacN17-induced lethality. Mutants created in *DSra-1* by P element mutagenesis were lethal, but maternal and zygotic *DSra-1* loss-of-function embryos did not have dorsal closure defects. Rather, lethality was due to pathfinding defects in the nervous system. Interestingly, a role for DSra-1 in F-actin organization was identified in the follicle cells covering the *Drosophila* oocyte.

It is possible that DSra-1 acts as a regulator of Rac-mediated F-actin regulation in the nervous system and ovary.

1.11 Plenty of SH3s (POSH)

Plenty of SH3s (POSH), was originally pulled out of a yeast two-hybrid screen of a mouse cDNA library for RacV12 binding partners (Tapon et al., 1998). POSH was shown to bind GTP-bound Rac1 even though it did not have the standard CRIB domain. Named POSH due to its organization of an N-terminal Zinc RING finger domain followed by four SH3 domains, POSH was of particular interest because it could activate the JNK pathway in Cos-1 cells and moreover induce apoptosis in NIH-3T3 cells. Unlike Rac1, POSH could not induce actin polymerization, lamellipodia, or cell motility. POSH was also able to stimulate the nuclear translocation of the transcription factor Necrosis Factor-κB (NF-κB) in Cos-1 cells. TNF-α activates NF-κB through the IKK complex (*Drosophila* Nemo is IKK gamma homolog, part of IKK complex (Choi and Benzer, 1994; Mihaly et al., 2001; Mirkovic et al., 2002)), and it in turn can inhibit apoptosis in some cell types by possibly targeting the IAPs (Lin, 2003).

POSH presented itself as a possible link between Rac and the JNK cascade. Given that JNK signaling and Rac have been genetically positioned in dorsal closure, *Drosophila* was considered to be a good sytem to dissect POSH function. A single *Drosophila* homolog of POSH, DPOSH, was found and embryos showed elevated *DPOSH* transcript at the leading edge during dorsal closure. A *DPOSH* loss-of-function mutation was created by P element mutagenesis, however, the mutation was homozygous viable and did not have dorsal closure defects. Furthermore, DPOSH was not able to bind activated DRac1, nor could it activate the JNK pathway during embryogenesis. Interestingly, *DPOSH* mutant embryos did not stain with Acridine Orange, a dye used as a positive stain for apoptosis in cells but still showed activation of *Drosophila* caspase-1,

drICE (Abrams et al., 1993). A series of experiments indicated that DPOSH interacts genetically with Drosophila Rac, and at least in some cases, functions as a Rac effector. Finally DPOSH was found to bind 14-3-3ζ in a yeast two-hybrid screen of a *Drosophila* embryonic cDNA library, and was shown to increase the level of *tailless*, a product of 14-3-3ζ signaling.

The results indicate a possible role for DPOSH in Rac signaling as well as a role in apoptosis in the *Drosophila* embryo.DPOSH appears to have no role in JNK signaling in the *Drosophila* embryo, but work from our collaborators indicates that it can activate the JNK cascade later in development (Seong et al., 2001).

1.12 Rho GTPase Activating Protein 68F (RhoGAP68F)

The *Drosophila* Rho GTPase Activating Protein, RhoGAP68F, is homologous to p50RhoGAP, a GAP for Cdc42 (Lancaster et al., 1994). p50RhoGAP was purified from human spleen tissue and a portion of its amino acid was sequenced. From this a cDNA clone was obtained from a human library. p50RhoGAP was found to have GAP activity for Rac and Rho but had preferential activity for Cdc42. Cdc42 also contained a SH3 domain suggesting that it could bind other proteins.

While GAPs are commonly associated with their ability to regulate GTPase activity, there is evidence that GAPs can act as effectors of signalling downstream of GTPases. For example, n-chimaerin, a Rac1 GAP, was shown to be able to induce the formation of actin based structures lamellipodia and filopodia (Kozma et al., 1996).

RhoGAP68F, reported in a survey of *Drosophila* GAPs by Billuart et al. 2001, was selected for study in *Drosophila* as it had an EP element, *EP(3)3152*, inserted

upstream of the gene (Billuart et al., 2001). At the origin of the study, this was the Rho family GAP with an EP element so conveniently located, and as described later, P element mutagenesis is an efficient tool for targeted mutagenesis of a gene. Rac and Cdc42 are very closely related, therefore, it was hoped that RhoGAP68F could function as a RacGAP in *Drosophila* (Burridge and Wennerberg, 2004).

RhoGAP68F was found to preferentially bind *Drosophila* GTP-bound Rho in an *in vitro* binding assay.

GAP assays indicated that RhoGAP68F preferentially hydrolyzed GTP-bound Rho vs. Rac or Cdc42. Since RhoGAP68F was not a Rac GAP, no further study was performed.

MATERIALS AND METHODS

2.1 Fly Stocks

Canton S and w^{1118} were used as "wild-type" strains. *hs-GAL4*^{M4}/ *hs-GAL4*^{M4} was provided by J. Roote. *EP(3)3267/EP(3)3267*, *EP(3)0789/EP(3)0789*, *EP(2)1206/ EP(2)1206*, *EP(3)3118 EP(3)3118* were obtained from Szeged Stock Center. GAL4 lines were obtained from the Bloomington Stock Center. They are *ptc-GAL4*$^{5559.1}$/*ptc-GAL4*$^{5559.1}$, *hs-GAL4*^{2077}/*CyO*, *69B-GAL4/69B-GAL4*, *GMR-GAL4/CyO*, *As-GAL4/As-GAL4*, *en-GAL4/en-GAL4*, and *nanos-GAL4/CyO*. *GMR-reaper/TM6B,Tb*, *Df(3R)ea/TM3,Ser*, *puc*^{E69}/*TM3,Sb*, *FRT82B,ovo*^{D}/*TM3,Sb*, *FRT82B,ubi-nls-GFP/FRT82B,ubi-nls-GFP*, *kay*^{1}/*TM3Sb,Ser* (*kayak*), *bsk*^{1}/*CyO* (*basket*), *H99/TM3,Sb*, *cbl*^{KG03080}/*TM3,Sb,Ser*, *Tbp-1*^{04210b}/*TM3,Sb* (*tat-binding protein-1*), *Btk*^{29A}/*CyO*, *UAS-p35/UAS-p35*, *w;Δ2-3CyO/Bc*, and *w;Δ2-3Sb/TM3,Ser* were also obtained from Bloomington. *hep*^{1}/*FM6* (*hemipterous*) was from S. Noselli. *splr*^{921}/*FM6* (*slipper*) was from B. Stronach. *UAS-p53/UAS-p53* was from C. Kopczynski. *14-3-3ζ*^{P1188} from N. Perrimon. *hsFLP;kD/TM3*, *FRT82B,CYFIP*$^{85.1}$, *CYFIP*$^{85.1}$/*TM3B,Sb* from A. Giangrande. *SacI*^{2107}/*TM6,TSb*, *UAS-cdc42V12/UAS-cdc42V12*, *UAS-DRacN17/UAS-DRacN17*, *hs-DRacN17/hs-DRacN17* from N. Harden. *Rac1*^{J11},*Rac2Δ,MtlΔ/TM6,Tb* from B. Dickson. *UAS-DRacV12/UAS-DRacV12* from K. Simons.

2.2 cDNA clones

LD47929, *LD19991*, and *LD45365* were produced by the Berkeley *Drosophila* Genome Project and can be currently obtained from Open Biosystems

(http://www.openbiosystems.com/drosophila_gene_collection_2.php). *ribosomal protein 49* (*rp49*) used as a loading control was provided by D. Sinclair (O'Connell and Rosbash, 1984). *tailless* (*tll*) cDNA was from N. Perrimon (Pignoni et al., 1990) and *decapentaplegic* (*dpp*) cDNA was from S. Parkhurst (Hoffmann and Goodman, 1987).

2.3 Standard molecular techniques

Routine techniques such as restriction digestion, cloning, agarose gels, and Polymerase Chain Reaction (PCR) were performed as described in Sambrook et al. (Sambrook et al., 1989).

PCR reactions where high fidelity was required, such as the cloning of genes, were carried out using Vent polymerase obtained from New England Biolabs and used according to manufacturer's instructions. Screening and analytical PCR was carried out using Taq polymerase from Qiagen used according to manufacturer's instructions.

Cloning was performed using XL1-Blue bacterial competent cells for transformations, obtained from Stratagene and used according to manufacturer's instructions. Transformations of pGEX5X-3 clones for GST-fusion proteins required JM109 and subsequent BL21 bacterial competent cells obtained from Stratagene and used according to manufacturer's instructions. JM109 was used as it is *recA*- and therefore prevents recombination commonly experienced with pGEX5X-3, while being an efficient competent cell. BL21 is used for enhanced expression of GST-fusion proteins, prevention of degradation and formation of inclusion bodies.

2.4 Sequencing

Sequencing – All sequencing was carried out at the University of British Columbia Nucleic Acid and Protein Sequencing center on Applied Biosystems PRISM 373/377 Sequencer.

Sequencing DSra-1 cDNA – The full length *DSra-1* cDNA was strategically cut with restriction enzymes *PstI* and *BamHI* into multiple fragments and cloned into pBluescript KS+. These fragments were sequenced with T7 and T3 primers as described. A full length double pass sequence was obtained. The sequence was verified as correct after the Berkeley Drosophila Genome Project release.

2.5 Site directed mutagenesis

Mutagenesis was performed on the plasmid containing *DPOSH*, *pBluescriptKS-DPOSH,* using the QuikChange site-directed mutagenesis kit, according to the manufacturer's instructions (Stratagene). Both forward and reverse PCR primers were designed to harbour several nucleotide changes, with the rest of the sequence corresponding to the template. A high fidelity PfuTurbo DNA polymerase and a reduced number of cycles were used to minimize errors during PCR amplification.

The *DpnI* endonuclease, which is specific for methylated and hemimethylated DNA, was then used to digest the parental DNA template and to select for mutation-containing synthesized DNA. Almost all DNA from *E.coli* strains is *dam* methylated and therefore susceptible to *DpnI* digestion. The mutation-containing DNA is then transformed into *E.coli* XL1-Blue.

The change in sequence was verified by sequencing using the T7 primer, 5' GTAATACGACTCACTATAGGGCG 3'. The modified cDNA was then excised from *pBluescript* and directionally cloned into *pUAST* using *EcoRI* and *Xhol* for germ line transformation into embryos.

2.6 Generation of transgenic Drosophila lines

Components:

Heptane

Household bleach

Injection buffer: 5mM KCl, 0.1mM sodium phosphate pH 6.8. Filter sterilize using 0.2 micron filter.

The *pUAST* construct has two P-element ends necessary for insertion into chromosomes and contains a marker, the *white* (*w*) gene, which enables visualization of the presence of an insert in w^- flies (Brand and Perrimon, 1993). The gene of interest is placed under the control of a pre-engineered UAS promoter. This, along with another plasmid encoding a transposase, is injected into the pre-blastoderm of an embryo, and should invoke a random insertion into a chromosome resulting in progeny containing transgenic DNA (Ashburner, 1989).

The procedure described by Spradling was used to obtain germ-line transformants (Spradling, 1986). Preblastoderm *yw* embryos obtained from a one hour collection at room temperature were dechorionated in 50% bleach, washed in water and arranged in rows of ~ 40 embryos on a black nitrocellulose disc, with all of the posterior ends facing

the same direction. The embryos were then transferred to a coverslip (made sticky using gum extracted from Sellotape™ in heptane), with their posterior ends facing the edge of the coverslip. Embryos were desiccated in an air tight box filled with desiccant.

After immersion in halocarbon oil (Voltalef), embryos were injected in their posterior ends with 400ug/mL of pUAST + transgene construct mixed with 200ug/mL of pUChsΔ2-3 as helper in injection buffer (Brand and Perrimon, 1993; Rio et al., 1986). Plasmid DNA to be used for injection was prepared using the Qiagen MidiPrep kit and quantified by absorbance spectroscopy at 260nm. The microinjection system used was as described in O'Connor and Chia (O'Connor and Chia, 1993). Injected embryos were allowed to develop at room temperature and surviving adults were individually mated to *yw* flies. Male progeny with eye colour were mated to *yw;Gla/Cyo* and *yw;Tm3Ser/Tm6Tb* to capture and balance insertions on the second or third chromosome.

Integrity of the inserts was verified by Northern analysis after heat shock-induced expression of the transgene as described in section 2.9.

2.7 Generation of Drosophila mutants from excision directed mutagenesis

The EP element is a nonautonomous P element, meaning that it does not contain an active transposase necessary for its mobilization and consequent transposition about the genome (Rorth, 1996a). Introduction of a source of transposase allows for the re-mobilization of a nonautonomous P element in the germ line. The re-mobilization of a P element often results in an imprecise excision event, resulting in random deletions about its insertion point and consequently a mosaic reflecting this in the germ line (Sved et al., 1991). The progeny of the mosaic will bear the resulting genotype.

The EP element line was mated *en masse* to transposase-containing flies of the genotype *w;Δ2-3CyO/Bc* if the EP element was on the 2nd chromosome or *w;Δ2-3Sb/TM3Ser* if the EP element was on the 3rd chromosome. The female virgin F1 progeny of the genotype *EP(2)1206/Δ2-3CyO* or *EP(3)3267/Δ2-3Sb* were selected, and each was mated individually with *w;Gla/CyO* or *w;TM3Sb/TM6Tb* males respectively. Approximately 400 such crosses were performed, and one male white eyed progeny from each cross, which potentially harboured an excision allele of the original EP element, was mated to virgin females of *w;Gla/CyO* or *w;TM3Sb/TMTb*, depending on the chromosomal origin of the EP element, to establish stocks. Homozygous viability was assessed by the loss of the balancer chromosome marker in the stock.

2.8 Generation of Drosophila mosaics

The generation of genetic mosaics or 'clones' has been shown to be an important tool for the analysis of the maternal effect of recessive zygotic mutations as well as the examination of the tissue specific roles of a gene. Genetic mosaics were created based upon the methodology of Chou and Perrimon (1996) for germ line clones and Golic and Lindquist (1989) for somatic clones (Theodosiou and Xu, 1998). This method takes advantage of the site specific recombination activity of the FLP recombinase which can direct recombination between homologous chromosomes at FRT sequences during mitosis.

Alleles of the gene of interest are recombined onto chromosomes containing FRT sequences near the centromere. FLP-mediated recombination allows the creation of clones of cells homozygous for the allele in a heterozygous individual.

FLP is placed under the control of a heat shock promoter, hsp70, and is therefore induced, usually at 37°C, under management by the investigator. In this way specific tissues can be targeted by heat shock inductions at the desired developmental stage.

The generation of germ line clones allows the creation of progeny devoid of the maternal contribution of a gene by creating germ cells homozygous mutant for that gene. A dominant female sterile mutation, ovo^{D}, is used to ensure that only germ cells homozygous for the gene of interest can produce eggs.

The development of the germ line was targeted during larval stage three, when larvae were at their largest and were found crawling along the sides of the vessel. At this time heat shocks were conducted for 2 hours at 37°C in order to drive genetic recombination in cells undergoing mitosis and hence producing a mosaic of genetically different cells.

To generate germ line clones of *DSra-1/CYFIP*$^{85.1}$, *hsFLP;kD/TM3Sb* females were crossed to *FRT82B,ovo*^{D}*/TM3Sb* males. The males from the F1 progeny, *hsFLP;FRT82B,ovo*^{D}*/TM3Sb* males were mated to *FRT82B,CYFIP*$^{85.1}$*/TM3Sb* females. The stage three larvae from this cross were heat shocked for 2 hours and allowed to develop to adults. *hsFLP;FRT82B,ovo*^{D}*/FRT82B,CYFIP*$^{85.1}$ females were mated to *CYFIP*$^{85.1}$*/TM3* males.

After recombination there will be germ line cells which are *CYFIP*$^{85.1}$*/ovo*^{D}, *CYFIP*$^{85.1}$*/CYFIP*$^{85.1}$, or ovo^{D}/ovo^{D}. Because of the ovo^{D} dominant mutation the only embryos produced from the final cross will be from *CYFIP*$^{85.1}$*/CYFIP*$^{85.1}$ germ line cells, and half the embryos will be devoid of both maternal and zygotic *DSra-1/CYFIP*.

To generate follicle cell clones of *DSra-1/CYFIP, hsFLP;kD/TM3Sb* females were crossed to *FRT82B,ub-nls-GFP* males. The ubi-nls-GFP transgene is a reporter that allows visualization of cells that are not homozygous mutant clones. The *hsFLP; FRT82B,ub-nls-GFP/TM3Sb* males from the F1 progeny were mated to *FRT82B,CYFIP*$^{85.1}$*/TM3Sb* females. The females from the F2 progeny of the genotype *hsFLP;FRT82B,ubi-nls-GFP/FRT82B,CYFIP*$^{85.1}$ were heat shocked for 2 hours at 37°C in order to drive genetic recombination in follicle cells undergoing mitosis (Margolis and Spradling, 1995). This was done for two days successively and then the female flies were dissected to retrieve the oocytes. The oocytes were then stained with anti-GFP and phalloidin as described in section 2.16.

2.9 Northern blot analysis

Total RNA from embryos or adult flies were prepared using the TRIzol reagent (Life Technologies) according to manufacturer's instructions. 50mg of tissue or 50 adult flies was homogenized in 1 mL of TRIzol.

Poly A+ mRNA was isolated from total RNA using the Qiagen Oligotex mRNA Mini Kit following manufacturer's instructions.

cDNA clones to be used as probes were purified using Qiagen Mini-Prep columns and labelled by random priming using the Amersham Pharmacia Biotech oligolabelling kit (27925001) according to manufacturer's instructions. 50μCi of [α-^{32}P]dCTP was used as a label. Unincoporated redionucleotides were separated from the labelled DNA using MicroSprin S-200 HR columns from Amersham Pharmacia Biotech (27512001).

Formaldehyde-agarose gels were prepared according to Sambrook et al. (1989). Northern analysis was done using the protocol of Virca et al. with staining of the gels with Acridine Orange omitted (Virca et al., 1990). RNA in the gel was transferred to the Hybond N membranes using capillary action and hybridized as described by Virca et al. Control probe was created from *rp49*.

2.10 Fixation of Drosophila embryos

Components:

20% paraformaldehyde: 10g of paraformaldehyde was added to 50mL Falcon tube. 35mL water and 0.5mL of 1M NaOH was added and the tube was heated at 65°C until paraformaldehyde was dissolved. 10mL of 5x phosphate buffered saline (PBS) was added.

PBS: as per Sambrook et al. (1989).

Heptane

Methanol

0.01% Triton-X

Household Bleach

Embryos were stained as described in Ashburner (1989). Embryos were allowed to develop as indicated and dechorionated using 50% household bleach : 50% 0.01% Triton-X for 3 minutes and rinsed with 0.01% Triton-X. Removal of the protective chorion is required to allow the diffusion of molecular probes into the embryo.

Embryos were fixed in a solution containing 4mL 20% paraformaldehyde, 1mL 10X phosphate buffered saline (PBS), and 5mL heptane. Vigorous shaking was performed for 25 minutes and the bottom aqueous layer was removed. 5mL methanol was added and the tube was shaken vigorously for 1 minute and the embryos were allowed to settle. Embryos were removed and washed with methanol five times.

2.11 Cuticle preparations

Components:

Hoyer's medium: 30g of gum arabic was added to 50mL of water. Once dissolved, 200g of chloral hydrate was added sparingly while stirring. 20g of glycerol was introduced, mix and centrifuged at 5000rpm to 10000rpm for 20 minutes to separate and remove the sediment. Medium must be stored in the dark.

Household Bleach

0.01% Triton-X

Cuticle preparations were performed as described by Ashburner (1989). Embryos were allowed to develop a full 24 hours AEL in order to allow the secretion of the cuticle. Embryos were dechorionated using 50% household bleach : 50% 0.01% Triton-X for 3 minutes and rinsed with 0.01% Triton-X.

Hoyer's medium was placed upon glass slides and dechorionated embryos were added to the medium. A glass coverslip was added to cover the medium and the slides were incubated at 65°C until the embryos had cleared leaving the cuticle.

2.12 RNA in situ hybridization of whole-mount embryos

Components:

4% paraformaldehyde

Methanol

PBSTw: PBS with 0.1% Tween-20

Bovine Serum Albumin (BSA)

Hybridization buffer: 50% deionized formamide, 4X SSC (as per Sambrook et al. (1989), 1X Denharts (as per Sambrook et al. (1989)), 0.1% Tween-20, 5% dextran sulphate, 250µg/mL salmon sperm DNA, 50µg/mL heparin. Store at -20°C.

Wash buffer: 50% formamide, 2X SSC (as per Sambrook et al. (1989)), 0.1% Tween-20.

Ashburner Wash Buffer: 100mM NaCl, 50mM $MgCl_2$, 100mM Tris, pH 9.5, 0.1% Tween-20. As described by Ashburner (1989).

NBT: 4-nitro blue tetrazolium chloride at 100µg/µL (Roche, 92451026)

BCIP: 5-bromo-4-chloro-3-indolyl-phosphate at 50µg/µL (Roche, 1383221)

RNA *in situs* were performed as described in Lehmann and Tautz (1994). Digoxigenin-labelled (DIG) RNA probes were generated by *in vitro* transcription of the antisense strand of the cDNA clones using the DIG RNA labelling kit from Roche Molecular Biochemicals according to manufacturer's instructions.

Fixed embryos stored in methanol were rehydrated 3:1 methanol : 4% paraformaldehyde for two minutes, then 1:3 methanol : 4% paraformaldehyde for five minutes. The embryos were then fixed in 4% paraformaldehyde for ten minutes, followed by rinsing the embryos three times in PBSTw. 0.5mL of hybridization buffer (boiled for ten minutes and put on ice) was added to the embryos and prehybridized for one hour at 52°C. 7μL of probe was added and incubation allowed to proceed at 52°C for 12-16 hours without agitation. The embryos were then washed in wash buffer at 52°C for at least four times, with the last wash allowed to proceed overnight. Room temperature rinses were done 3X with PBSTw followed by washing for 30 minutes in PBSTw. PBSTw was removed and 0.5μL of anti-digoxigenin-alkaline phosphatase (Roche Molecular Biochemicals), and 1mL PBSTw + 5% BSA was added. Samples were incubated for 90 minutes at room temperature. After the antibody solution was discarded, embryos were washed 4 X 20 minutes in PBSTw followed by 3 X 5 minutes in Ashburner wash buffer. The last wash was not removed and 3.4μL of NBT and 3.5μL of BCIP were added. Colour development was allowed to proceed under dissection microscope and halted when desired resolution was obtained. Reaction was stopped by washes in PBSTw. Embryos were rotated in 70% glycerol for two hours and samples were stored at 4°C. Embryos were observed using differential interference contrast (DIC) microscopy on a Zeiss Axioplan microscope.

2.13 Immunostaining of Drosophila embryos

Components:

PBT: PBS + 0.1% Triton-X

BSA

PBB: PBT + 1% BSA

Nickel solution: 2.5% Nickel ammonium sulphate, 0.1% sodium acetate buffer pH 6.

DAB reaction mix: 50μL of 5mg/mL DAB, 10μL of 0.2 g/mL glucose, 2μL of 0.2g/mL NH_4Cl, 1mL of Nickel solution, and 3μL of 2mg/mL glucose oxidase (Sigman, G2133, 250000U).

Immunostaining was performed as described by Harden et. al (1996). Fixed embryos were rehydrated in 1mL PBT for 3 X 20 minutes on a spiral mixer. Embryos were then blocked in PBB for one hour. The blocking solution was then removed and the appropriate concentration of primary antibodies diluted in PBB was introduced to the embryos and incubated at 4°C overnight. Concentrations of antibodies were as follows: mouse monoclonal anti-phosphotyrosine 1:1000, affinity purified rabbit polyclonal anti-human Sra-1 1:50, rabbit polyclonal anti-drICE 1:2000, mouse monoclonal anti-FLAG 1:1000 (Sigma), rabbit polyclonal anti-lacZ 1:1000, rabbit polyclonal anti-DPOSH 1:1000. Solution was then removed, followed by washing 3 X 20 minutes in PBT. The last PBT wash was then removed.

For horse radish peroxidase-mediated (HRP) visualization of antibody staining using DAB, HRP conjugated goat anti-rabbit or goat anti-mouse secondary antibodies were added in a 1/200 dilution (Jackson Immunoresearch). Incubation was done for two hours at room temperature. Embryos were washed 3 X 20 minutes in PBT. Colour development was

with DAB reaction mix and staining was stopped with PBT. PBT was then substituted with 70% glycerol and embryos equilibrated for two hours. Samples were stored at 4°C. Embryos were observed using differential interference contrast (DIC) microscopy.

For fluorescent detection of antibody staining, FITC-conjugated anti-mouse secondary antibodies were added in a 1/200 dilution (Vector Laboratories) in the dark with safelight illumination when needed. Incubation was done for two hours at room temperature. Embryos were washed 3 X 20 minutes in PBT. Additional washes were 2 X 10 minutes in PBS. Following the removal of the last PBS wash, Vectashield mountant (Vector Labs) was added and embryos equilibrated for one hour at room temperature or overnight at 4°C. Samples were stored at 4°C in the dark. Embryos were observed using confocal microscopy.

2.14 Staining of embryos with Acridine Orange

Components:

Sodium phosphate buffer: 0.1M as per Sambrook et al. (1989).

Acridine orange: 5µg/mL in 0.1M sodium phosphate buffer pH 7.4.

Household bleach

0.01% Triton-X

Heptane

PBS

700 Halocarbon oil

Acridine Orange (AO) staining was performed as described by Abrams et al. (1993). Embryos 6-12 hours after egg laying (AEL) were dechorionated for 5 minutes as previously described, rinsed well with distilled water and then placed in equal volumes of heptane and 5μg/ml of AO in 0.1M sodium phosphate buffer pH 7.4. After 4.5 to 5 minutes of shaking, embryos were washed with PBS and then placed on a slide under series 700 Halocarbon oil. AO staining was viewed with a Zeiss fluorescence microscope.

2.15 Fixing and staining of Drosophila optic lobes

Components:

PBT: PBS + 0.1% Triton-X

BSA

PBB: PBT + 1% BSA

4% paraformaldehyde

Optic lobe fixation and staining was performed as described by Natzle et al. (1994). Larval optic lobes were dissected in cold PBT and fix with 4% paraformaldehyde for 15 minutes at 4°C and rinsed 3 X PBT for 5 minutes on a nutator. Then samples were blocked with PBB for 1 hour at room temperature on a nutator. Primary antibody (1:200 mAb24B10) was added and allowed to incubate at 4°C overnight. Samples were washed 3 X 20 minutes with PBT, then incubated with secondary antibody (1:200 anti-mouse-FITC from Vector Labs) at room temperature for 2 hours. Samples were washed 3 X 20

minutes with PBT and Vector Shield (Vector Labs) added. Discs were viewed with confocal microscopy.

2.16 Fixation and staining of Drosophila oocytes

Components:

EBR buffer: 130mM NaCl, 4.7mM KCl, 1.9mM $CaCl_2$, 10mM HEPES pH 6.9 as per Sambrook et al. (1989).

Buffer B: 100mM potassium phosphate pH 6.8 as per Sambrook et al. (1989), 450mM KCl, 150mM NaCl, 20mM MgCl2•6H20.

Devitellinizing buffer: 1 vol buffer B, 1 vol formaldehyde 36%, 4 vol water.

Formaldehyde 36%

BSA

PBS

PBO: 1 X PBS, 0.3% Triton-X, 0.5% BSA.

Heptane

Ovary fixation and staining was performed as described by Verheyen et al. (1994) (Verheyen and Cooley, 1994a). Ovaries were dissected in cold EBR and transferred to an eppendorf containing cold EBR on ice. EBR was removed and add 100μL devitellinizing buffer and 600uL heptane was added. The sample was vigorously agitated to be sure that the buffer was saturated with heptane and then was rotated for 10 minutes at room temperature. The solution was removed with a pipet and rinsed with PBS three times.

The ovaries were washed 3 X in PBS for 10 minutes each. The the ovaries were prehybridized for 10 minutes in PBO and then the antibody was added, in this case a 1:1000 anti-GFP (abcam rabbit polyclonal anti-GFP). Sample was incubated overnight at 4°C on nutator and then washed 3 X in PBO and a secondary antibody added, in this case 1:200 anti-rabbit-biotinylated (Vector Labs). Ovaries were incubated for 2 hours at room temperature on a Nutator, then washed 3 X PBS for 10 minutes, and 1:2000 Texas Red streptavidin was added. Sample was allowed to incubate for 1.5 hours at room temperature in the dark. After one hour, 50μL 1:1000 phalloidin-FITC conjugate (Sigma) was added. Ovaries were then washed 3 X 10 minutes in PBS and Vector Shield was added. Ovaries were viewed with a confocal microscope.

2.17 Western Analysis

Components:

Protein sample buffer: 0.01% mercaptoethanol, 2% SDS, 0.01% bromophenol blue, 6% glycerol, 25mM Tris pH 6.8.

Running buffer: 2.5mM Tris pH 8.3, 19.2mM glycine, 0.01%SDS.

Transfer buffer: 2.5mM Tris pH 8.3, 19.2mM glycine, 0.01%SDS, 20% methanol.

Protein samples were separated on 10% or 12% polyacrylamide gels using the BioRad Mini-Protean II Electrophoresis Cell and transferred to nitrocellulose membrane

using the BioRad Trans-Blot Semi Dry following manufacturer's instructions. Gels were prepared as in Sambrook et al (1989). Protein samples were loaded with sample buffer and electrophoresis carried out in running buffer. The Trans-Blot was run at 15V for 20 minutes using the transfer buffer to transfer the proteins from the gel to the nitrocellulose membrane.

Western blotting was performed as per manufacturer's instructions using reagents from the Western Blotting Chemiluminescence Kit obtained from Roche. Concentrations of primary antibodies as follows: rabbit polyclonal anti-human Sra-1 1:1000 (affinity purified 1:50), mouse monoclonal anti-FLAG 1:1000 (Sigma), rabbit polyclonal anti-DPOSH 1:1000. Secondary antibody was a 1:2000 dilution of an anti-rabbit or anti-mouse coupled horse radish peroxidase (HRP) antibody obtained from Vector Labs. Visualization was performed using the luminol reagent from the kit.

2.18 In vitro binding assays

Components:

LB: 5g bactotryptone, 5g NaCl, 2.5g bacto-yeast extract in 500mL of water. Autoclaved.

LB agar: LB + 7.5g agar. Autoclaved. Cooled to 55°C and ampicillin added to 50μg/mL. Poured on plates.

LB + ampicillin: LB. Autoclaved. Cooled to 55°C and ampicillin added to 50μg/mL.

GST buffer: 50mM Tris pH 7.5 (as per Sambrook et al. (1989)), 150mM NaCl, 0.5mM $MgCl_2$, 0.1% Triton-X.

Lysis buffer: GST buffer, 5mM DTT, Complete Protease Inhibitor no EDTA from Roche Pharmaceuticals per 50mL buffer.

Exchange buffer: 50mM HEPES pH 7.1 (as per Sambrook et al. (1989)), 5mM EDTA, 0.1mM EGTA, 50mM NaCl, 0.1mM DTT.

Wash buffer: GST buffer.

Protein sample buffer: 0.01% mercaptoethanol, 2% SDS, 0.01% bromophenol blue, 6% glycerol, 25mM Tris pH 6.8.

IPTG

PBS

GST-pull down assays were performed as described by Lu and Settleman, (1999). A single bacterial colony of BL21 harbouring the appropriate pGEX-fusion construct was inoculated into 50mL of LB + ampicillin and cultured at 37°C overnight (O/N). 20mL of the O/N culture were added to 200mL of LB + ampillicin and grown at 37°C until the $O.D._{600}$ reached 0.600. The culture was induced with 0.5mM IPTG at 25°C for five hours, and then spun at 9000rpm for 20 minutes in a 250mL or 500mL centrifuge bottle. Pellet was washed with 20mL of cold PBS and spun down at 4000rpm for 10 minutes in a table-top centrifuge. The supernatant was removed and the cell pellet was stored at -70°C. On the next day, pellet was thawed, resuspended in 15mL of lysis buffer by drawing up and down with a 10mL pipette and kept on ice for 10 minutes. The suspension was sonicated until the viscous solution appeared fluid. The debris was spun down and supernatant

passed through a 0.45uM filter. The filtrate was supplemented with 1mL of 80% glycerol, mixed and aliquots of 2mL each were flash frozen and stored at -70°C.

30μg of GST beads were pre-equilibrated with GST buffer. 20μL of beads were then added to 2mL of thawed GST-GTPase extract and mixed by nutator at 4°C for one hour in a 2mL microfuge tube. The tube was then spun at maximum speed for 10 seconds and the supernatant was discarded. Beads were washed 2X with 400μL of GST buffer, inverting a few times, pelleting down and removing the supernatant.

In vitro transcription and translation of ^{35}S labelled DPOSH, DSra-1 and RhoGAP68F was performed using the pXJFLAG-DPOSH, pXJFLAG-DSra-1, and pXJFLAG-RhoGAP68F plasmids respectively, in combination with the TNT Quick Coupled Transcription/Translation kit available from Promega. Manufacturer's instructions were followed.

The GTPases were bound to GTP or GDP as follows. To the 20μL of beads bound to GST-GTPase, 400μL of exchange buffer was added. Tube was then inverted for a few times, beads pelleted down and supernatant removed. A fresh 80μL of exchange buffer together with GTPγS or GDP to a final concentration 0.5mM were then added to the beads. Tubes were then incubated at 30°C for 30 minutes. 2μL of 1M $MgCl_2$ was then added to each tube to stabilize the coupling of the GST-GTPase with either GTPγS or GDP. Beads were pelleted down and supernatant removed.

400μL of wash buffer with protease inhibitors was added to the beads along with desired amounts of *in vitro* transcribed translated reaction. Reaction was mixed on a Nutator at 4°C for 1 hour. 1mL washes with wash buffer were done 4 times.

1X protein sample buffer was added to beads and boiled for 5 minutes. Beads were pelleted down and the supernatant loaded on a 10% polyacrylamide gel. After the gel was run, it was stained with Coomassie and destained. The gel was then dried and subjected to autoradiography.

2.19 GTPase-Activating Protein (GAP) assay

Components:

GST buffer: 50mM Tris pH 7.5 (as per Sambrook et al. (1989)), 150mM NaCl, 0.5mM $MgCl_2$, 0.1% Triton-X.

GST elution buffer: 10mM reduced glutathione, 50mM Tris pH 8.0, 5mM $MgCl_2$. Freeze at -20°C.

Loading buffer: 20mM Tris, pH 8, 1.5uM GTP, 10mM β-mercaptoethanol, 5mM $MgCl_a$, 20mM EDTA, 10% glycerol, 0.5μg/ml BSA

$MgCl_2$: 1M

Reaction buffer: 20mM Tris pH 7.5, 5mM $MgCl_a$, 0.5μg/ml BSA

Wash buffer: 20mM Tris pH 8, 5mM $MgCl_2$, 100mM NaCl

The GST-fusion proteins GST-Rac, GST-Rho, GST-Cdc42, and GST-RhoGAP68F were expressed as described in section 2.18 except that the reactions were scaled up 4 times to produce a large amount of protein. Protein was purified by running the bacterial lysate through 1mL GST columns from Pharmacia Biotech and eluted by 3 volumes of GST elution buffer as described in the manufacturer's instructions. Proteins

were washed in GST buffer (minus 0.1% Triton-X) and concentrated to 1mg/mL volumes by spinning in Centricon 10 kDa filter columns from Millipore as per manufacturer's instructions. Protein concentration was assessed by Bradford assay using Bradford reagent from BioRad as per manufacturer's instructions.

GAP assays were performed as described (Hattori et al., 1992). GST-Rac, GST-Rho, GST-Cdc42, 5uM each, were loaded with [γ-^{32}P]GTP in loading buffer at 30°C for 15 minutes, followed by the addition of 1M $MgCl_2$ to 20 mM. Purified GST-RhoGAP68F was added to 250nM of each small G protein in reaction buffer at 30°C for 10 minutes. The reaction was terminated by the addition of ice-cold wash buffer. Samples were adsorbed to nitrocellulose filters (Schleicher & Schuell). The filters were washed three times with wash buffer, and added to scintillation vials. Scintillation counts were performed and quantified.

2.20 Antibody generation

GST-DPOSH protein was prepared and concentrated as mentioned in the previous section 2.19.

Serum was obtained from two rabbits before the initial injection of the epitope. 100μL containing 400μg of GST-DPOSH protein was mixed with an equal amount of TiterMax Gold adjuvant and vortexed and passed through a blunt 18 gauge needle until viscous. This was then injected subcutaneously into 2 sites on two different rabbits. Boosts were given at two week intervals using the same preparation. After 6 boosts, rabbits were exsanquinated from the ear. The blood was allowed to clot at 37°C for four hours in order to separate and harvest the serum. The serum was stored in aliquots at -

70°C. The rabbits were identified by number 16 and 24. Number 16 appeared to give stronger bands on a Western blot (results not shown) and was used in the figures in this thesis. Both affinity purified 16 and 24 both failed to produce a single band on a Western blot and neither showed a different banding pattern on *DPOSH*^{74} Westerns (results not shown).

2.21 Affinity purification of anti-DPOSH antibodies

Affinity purification of DPOSH antibodies was performed using the method described in Sambrook et al. (Sambrook et al., 1989)1989).

2.22 Yeast two hybrid system

Components:

XGal: dissolve XGal into DMF to prepare a solution of 20mg/mL XGal. Store in dark at -20°C.

10X BU salts: 70g $Na_2HPO_4 \cdot 7H_20$, 30g NaH_2PO_4 1L Water, pH 7.0. Autoclave.

Leu+ dropout powder: 2.5g adenine, 1.2g arginine (HCl), 6.0g aspartic acid, 6.0g glutamic acid (monosodium salt), 3.6g leucine, 1.2g methionine, 3.0g phenylalanine, 22.5g serine, 12.0g threonine, 1.8g tyrosine, 9.0g valine. Amino acid powder was ground with a pestle and mortar until fine and stored in a light protective vessel.

Total dropout powder: as leu+ powder but without the leucine.

CM media: 0.85g yeast nitrogen base, 0.4g leu+ dropout powder, 2.5g $(NH_4)_2SO_4$, 475mL H_20. Adjusted to pH 5.9 with NaOH. 10g agar (if making plates). Autoclaved and allow to cool. 25mL 40% glucose.

Gal/Raff/CM leu+ media: 0.85g yeast nitrogen base, 0.4g leu+ dropout powder, 2.5g $(NH_4)_2SO_4$, 450mL H_20. Adjusted to pH 5.9 with NaOH. Autoclaved and allow to cool. 25mL 40% galactose, 25mL 20% raffinose.

Gal/Raff/CM leu- media: 0.85g yeast nitrogen base, 0.5g leu- dropout powder, 2.5g $(NH_4)_2SO_4$, 450mL H_20. Adjusted to pH 5.9 with NaOH. Autoclaved and allowed to cool. 25mL 40% galactose, 25mL 20% raffinose.

Glu/XGal leu+ plates: 0.85g yeast nitrogen base, 0.4g leu+ dropout powder, 2.5g $(NH_4)_2SO_4$, 425mL H_20. Adjusted to pH 7.0 with NaOH. 10g agar. Autoclaved and allowed to cool. 25mL 40% glucose, 50mL 10X BU salts, 1mL XGal.

Gal/Raf/XGal leu+ plates: 0.85g yeast nitrogen base, 0.4g leu+ dropout powder, 2.5g $(NH_4)_2SO_4$, 400mL H_20. Adjusted to pH 7.0 with NaOH. 10g agar. Autoclaved and allowed to cool. 25mL 40% galactose, 25mL 20% raffinose, 50mL 10X BU salts, 1mL XGal.

Glu leu- plates: 0.85g yeast nitrogen base, 0.5g leu- dropout powder, 2.5g $(NH_4)_2SO_4$, 475mL H_20. Adjusted to pH 7.0 with NaOH. 10g agar. Autoclaved and allowed to cool. 25mL 40% glucose.

Gal/Raf leu- plates: 0.85g yeast nitrogen base, 0.5g leu- dropout powder, 2.5g $(NH_4)_2SO_4$, 450mL H_20. Adjusted to pH 7.0 with NaOH. 10g agar. Autoclaved and allowed to cool. 25mL 40% galactose, 25mL 20% raffinose.

Trp 1% Stock solution: tryptophan dissolved in water to 1% solution. Spread on plates (100uL) and add to liquid media (400μL per 100mL) to replace nutrient.

His 1% Stock solution: histidine dissolved in water to 1% solution. Spread on plates (50μL) and add to liquid media (200μL per 100mL) to replace nutrient.

Ura 0.5% Stock solution: uracil dissolved in water to 0.5% solution. Spread on plates (100μL) and add to liquid media (400μL per 100mL) to replace nutrient.

10X TE: 0.1M Tris pH 7.5, 0.01 M EDTA. Autoclaved.

10X LiAc: 1M lithium acetate. Autoclaved.

50% PEG: 50% polyethylene glycol (PEG) in water, autoclaved.

Sterile Water: Autoclaved distilled water.

15% Glycerol solution: 15% glycerol, 1X TE. Autoclaved.

DMSO: dimethyl sulfoxide.

The EGY48 strain of yeast used in the two-hybrid protocol as described by Golemis et al. (1999) is deficient in the genes *HIS3*, *TRP1*, and *URA3* required respectively in the anabolism of histidine, tryptophan, and uracil (Golemis et al., 1999). Moreover the strain has its production of leucine controlled at the *LEU2* gene under a *LexA* operator. The protein of interest, or "bait" protein is expressed in the yeast cytosol by cloning the cDNA into the pEG202 vector, placing expression of the bait protein as a LexA fusion protein under control of the strongly constitutively active *ADH* promoter. The pEG202 vector also contains a viable copy of the *HIS3* gene allowing the yeast to survive on media deficient in histidine and in this way allow selection of yeast colonies containing the plasmid.

A second plasmid, pJG4-5 is transformed into EGY48. This plasmid contains a fusion cassette with a SV40 nuclear localization sequence and a B42 acid blob domain responsible for activation of transcription, plus a series of sites available for the cloning

of cDNA libraries or known genes that are to be tested for interaction with the bait protein. This is placed under the control of a *GAL1* promoter and is consequently driven by adding galactose to the yeast media. The plasmid also contains a viable copy of the *TRP1* gene allowing for selection of yeast colonies grown on tryptophan deficient media.

A final reporter plasmid, pSH18-34, is transformed into EGY48. The plasmid contains 8 *LexA* operators directing transcription of the *lacZ* gene. β-galactosidase, the product of the *lacZ* gene, produces a blue coloured product in the presence of media containing the substrate X-Gal. The plasmid also contains a viable copy of the *URA3* gene allowing for selection of yeast colonies grown on uracil deficient media.

An interaction trap occurs when the bait protein fused to the LexA DNA binding protein interacts with the protein fused to the B42 acid domain completing a functional transcriptional activator. The *lacZ* and *LEU2* reporter give a positive signal when colonies are able to catalyse the X-Gal substrate yielding blue colonies, and are able to grow on leucine deficient plates.

It is important to test that the bait protein fused to the *LexA* DNA binding domain is not itself able to activate the reporter as it could be possible that the bait protein contains an acidic moiety or functional domain that could act as an activator of transcription. A simple test of EGY48 transformed with pEG202 containing the bait (pBait) and pSH18-34 reporter plasmid grown on leucine deficient media should produce no colonies nor should the colonies turn blue in the presence of X-Gal and galactose. In the same respect it is also important to test that the fusion protein produced from cloning into pSH18-34

does also not self activate transcription of the reporters and this was tested in a similar manner.

Transformation protocol - 150mL of CM media deficient in relevant dependent amino acid(s) to allow maintenance of any previously transformed plasmid(s) was inoculated with EGY48 (possibly containing previously transformed plasmids) and was incubated at 30°C for 16 - 18 hours, shaken at 250rpm until $O.D._{600} = 1.5$. The overnight culture was transferred into 300mL (small scale) or 1L (library) CM media containing relevant dependent amino acid(s) to allow maintenance of any previously transformed plasmid(s) up to an $O.D._{600}$ 0.200 - 0.300. This was incubated at 30°C for 3 hours with shaking at 230rpm until $O.D._{600}$ 0.500 +/- 0.100 and then placed into 50mL Falcon tubes and centrifuged at 1000xg for five minutes at room temperature. The supernatant was discarded and cell pellets were resuspended by vortex in 50mL (small scale) or 500mL (library) sterile 1X TE. Note this did not mean 50mL/500mL into each Falcon but rather a final volume of 50mL/500mL. Resuspended cells were added to an appropriately sized centrifuge tube and centrifuged at 1000xg for 5 minutes at room temperature. The supernatant was then discarded. Cells were resuspended in 1.5mL (small scale) or 8.0mL (library) fresh sterile 1x TE/LiAc (1x TE, 1x LiAc in sterile water). 10mL (small scale) or 100mL (library) PEG/LiAc solution (ie: 8mL 50% PEG, 1mL 10x TE, 1mL 10x LiAc, votexed well) was prepared. The following was added to 15mL falcon tube: 1μL library or 1μL of ~1μg/uL plasmid to be transformed, 0.1mg salmon sperm DNA, and 100μL of yeast competent cells. This was mixed by gentle vortex. 30 of these tubes were used when transforming the library. In order to achieve a library transformation of 2 to 3 x 10^6 primary transformants, and assuming a transformation efficiency of 10^5/μg of library, this

will required 20μg to 30μg of library (Golemis et al., 1989). 600μL of PEG/LiAc solution was then added and the competent cells were well vortexed. The transformation was incubated at 30°C 200rpm for 30 minutes. 70μL of DMSO was then added and mixed well by GENTLE inversion. The cells were then heat shocked for 15 minutes in a 42'C water bath with gentle swirling every five minutes. This was then chilled on ice for two minutes and then centrifuged at room temperature for 5 minutes at 1000xg. The cells were then resuspended in 1.0mL of sterile TE. 100μl were plated per small plate or entire contents of the falcon tube were plated for large 20mm library plates using sterile technique on appropriately amino acid deficient CM agar plates and incubated at 30°C to select for plasmid-containing yeast, until colonies are visible.

Testing for self activation of bait protein – The *pEG202-DSra-1/DPOSH* plasmids were transformed into EGY48 along with the pSH18-34 reporter plasmid. As a positive control, pSH17-4 and pSH18-34 was used. pSH17-4 has a *LexA* domain fused to a *GAL4* domain, thus can form a complete transcription factor. Transformants were grown on Glu/XGal CM trp+ and subsequently on Gal/Raf/XGal trp+ plates for 2 - 3 days at 30°C. Evidence of a blue colour indicates self activation.

Repression assay – The repression assay can detect if the bait fusion protein is being translocated to the nucleus and acting as an efficient DNA binding protein. pJK101 is a reporter plasmid containing *GAL1* activating sequences (UAS) upstream of two *LexA* binding domains and a *lacZ* reporter gene. LexA-bait fusion proteins are able to bind *LexA* operator sites on the pJK101 lacZ reporter plasmid and interfere with transcription of the β-galactosidase caused by the binding of GAL4 to *GAL1*. This indicates that the bait fusion protein is being translocated to the nucleus.

The *pEG202-DSra-1/DPOSH* plasmids were transformed into EGY48 along with the pJK101 reporter plasmid. pJK101 was transformed into yeast and used as a negative control. Assays were performed by streaking colonies on Gal/Raf XGal plates and allowing them to grow for 2 – 3 days at 30°C. Blue colour was not seen for either *pEG202-DPOSH* or *pEG202-DSra-1* transformation indicating that successful nuclear translocation of the fusion bait proteins was achieved.

Harvest of yeast library – The number of colonies were counted in order to calculate the library transformation efficiency (TE). Sterile technique was used when using sterile glass slides to scrape colonies off of a plate and into a 50mL falcon tube. The scraping up of agar was avoided as it could give false positives. Colonies were suspended in 25mL sterile 1X TE and centrifuged at 1000xg for five minutes at room temperature. The supernatant and agar which did not spin down well but remained floating in TE was discarded. Colonies were resuspended in 25mL sterile 1X TE, and centrifuged to remove supernatant. The resuspension was repeated. A volume of sterile Glycerol solution equal to that of the cell pellet was added to the transformed library and resuspended by vortex. Three serial dilutions of 1:100, 1:1000 and 1:10000 were prepared from the transformed library using sterile TE. 100µL of each dilution was plated on CM media plates. The remaining transformed library was stored at –80°C. The plates were allowed to grow for three days at 30°C. Colonies on the dilution plates were counted to determine replating efficiency (RPE). This was calculated per 100µL.

Example:

Plated 100uL of 1:10000 plate has 270 colonies.

270 colonies/100μL x 10000x dilution factor equals 2,700,000 colonies/100uL.

Determined number of colonies to screen to cover primary transformation 300X.

Example:

Transformation efficiency (TE) was 900,000 colonies.

Library plating efficiency (RPE) was 2,700,000 colonies/100uL.

(TE / RPE) x 30000 = Total μL of primary transformation to screen.

(900,000colonies/2,700,000 colonies/100uL) x 30000 = 10000μL.

Screening library – The original complexity of the library was 4.2 x 10^6, and therefore with a primary transformation of 9 x 10^5, this library was covered 0.21 times. 10mL of transformed library was screened to cover the primary transformation 300x. No more than 2,000,000 colonies should be plated per 10mm plate when screening a transformed library and one can scale up as appropriate to larger plates. If the yeast is allowed to grow too confluent then positive colonies will co-operatively feed non-positives giving spurious background growth.

10X transformed library volume was added to Gal/Raff/CM leu+ liquid media and incubated for 3.5 hours at 30°C 200rpm. This activated the expression of the binding domain. This was then centrifuged at 1000xg for five minutes and the supernatant was discarded. The library pellet was added to Gal/Raff/CM leu- liquid media so that each 20mm Gal/Raff/CM leu- plate received a final volume of 300μL. The transformed library was plated with uniform streaking to ensure that the colonies were spread uniformly over the entire plate and did not pool in one area. This was done to prevent confluent growth. If a plate was too dry then sterile TE was added and streaking was continued until the

yeast was uniformly streaked. Plates were incubated at 30°C and checked every day for the next three days for visible colonies. Visible colonies that grew on the first day, second day and third days were separately noted as colonies growing on the first day indicate a strong binding interaction. The positive colonies were replated on CM media plates.

Confirmation of positives - Positive colonies are replated on Gal/Raff/leu-, Glu/leu-, Glu/Xgal and Gal/Raff/Xgal plates and incubated for three to four days at 30°C. Colonies that turned blue on Xgal and grew on leu- plates were positives. Glucose shuts down the production of the activation domain fusion protein, and therefore positive colonies should not grow on Glu/leu- plates or turn blue on Glu/Xgal. This tests for any self activation by the binding domain fusion protein, in this case DPOSH.

2.23 TUNEL staining

Components:

Proteinase K: 2.2mg/mL

PBS: as per Sambrook et al. (1989).

PBSTw: PBS with 0.1% Tween-20

Apoptag Reagents: Serologicals Corp., Norcross, GA

Procedure was performed as described (McCall et al., 2004).

RESULTS PART 1

Drosophila Specific Rac1 Associated Protein-1 (*DSra-1*)

3.1 Cloning and sequencing Drosophila Sra-1

As described in the Introduction, human Sra-1 had been shown to be able to bind activated Rac1 as well co-precipitate and regulate F-actin in mammalian cells. *Drosophila* was used as a model organism to elucidate the functional role of Sra-1 at the level of tissue morphogenesis.

The human *Sra-1* sequence was used to perform a tBLASTn search against all known *Drosophila* ESTs and located several *Drosophila Sra-1* transcript candidates including LD47929 and LD19991. These were cut with *Pst*I and *Bam*HI, re-cloned into pBluescript SK(-) and sequenced using T3, T7 primers with Applied Biosystems (ABI) 373 and 377 sequencers. From this a full-length sequence of the *Drosophila* homologue of *Sra-1*, which we name *DSra-1*, was generated (Fig. 3.1). Strict sequence identity between both ESTs led us to believe that there is only one possible *DSra-1* coding region and transcript. A full length transcript of *DSra-1* was assembled from the 5′ end of LD47929 and the 3′ portion of LD19991 using the restriction enzyme, *Bsr*G1, and cloned into pBluescript SK(-) using *Not*I and *Sma*I (Fig. 3.1). The full-length cDNA sequence was submitted to NCBI and its accession number was designated as AY029211.

During the course of this work the *Drosophila* genome was sequenced (Myers et al., 2000). BLAST searches against the *Drosophila* genome using both the *Sra-1* and *DSra-1* sequence returned only one probable candidate gene, *CG4931*, which

Figure 3.1 Nucleotide sequence and conceptual translation of *DSra-1* cDNA.

*Bsr*G1 recognition site shaded, arrowhead indicates cut site. A full length transcript of *DSra-1* was assembled from the 5′ end of LD47929 and the 3′ portion of LD19991 using *Bsr*G1, and cloned into pBluescript SK(-) using *Not*I and *Sma*I.

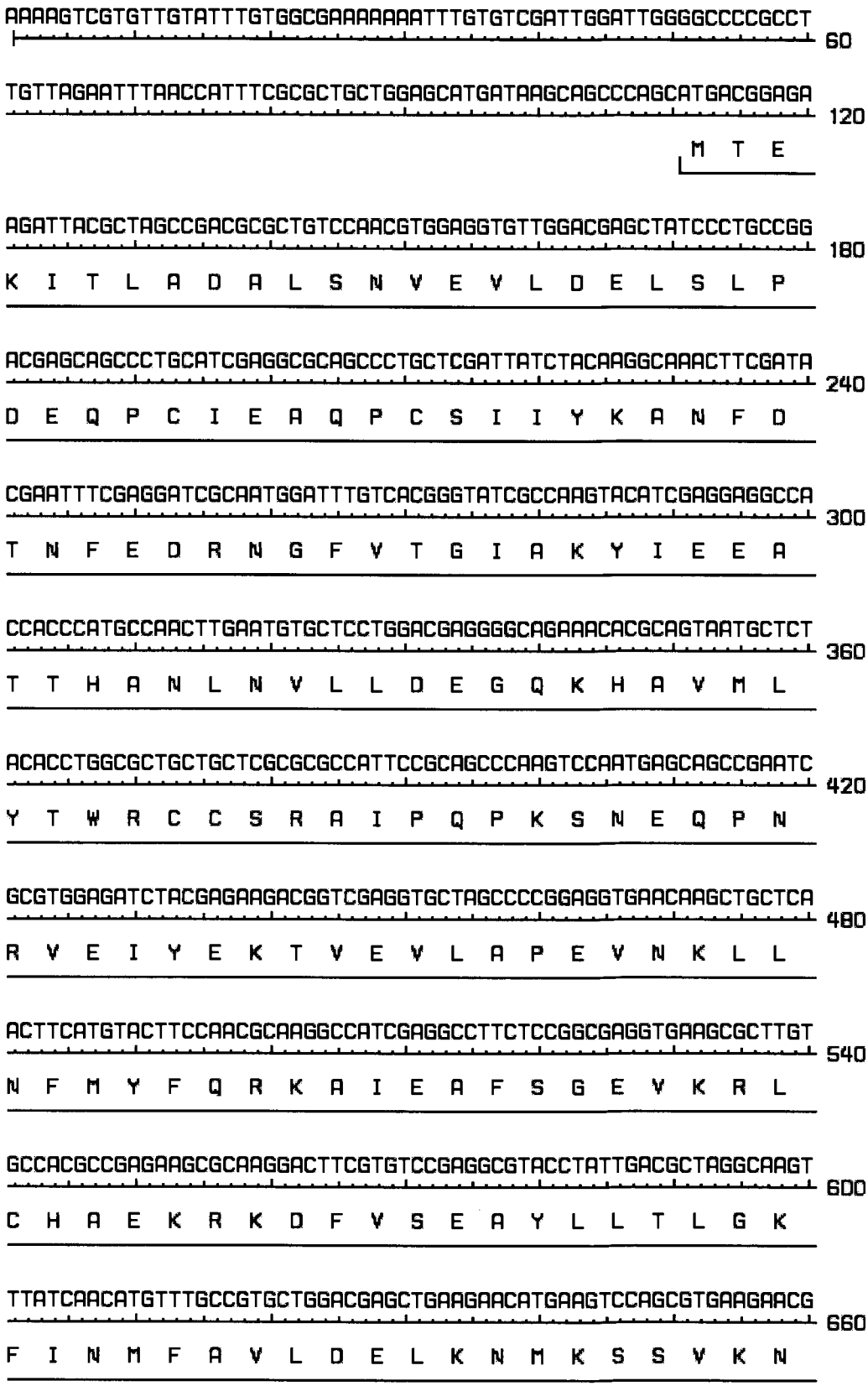
AAAAGTCGTGTTGTATTTGTGGCGAAAAAAATTTGTGTCGATTGGATTGGGGCCCCGCCT
60
TGTTAGAATTTAACCATTTCGCGCTGCTGGAGCATGATAAGCAGCCCAGCATGACGGAGA
120
M T E
AGATTACGCTAGCCGACGCGCTGTCCAACGTGGAGGTGTTGGACGAGCTATCCCTGCCGG
180
K I T L A D A L S N V E V L D E L S L P
ACGAGCAGCCCTGCATCGAGGCGCAGCCCTGCTCGATTATCTACAAGGCAAACTTCGATA
240
D E Q P C I E A Q P C S I I Y K A N F D
CGAATTTCGAGGATCGCAATGGATTTGTCACGGGTATCGCCAAGTACATCGAGGAGGCCA
300
T N F E D R N G F V T G I A K Y I E E A
CCACCCATGCCAACTTGAATGTGCTCCTGGACGAGGGGCAGAAACACGCAGTAATGCTCT
360
T T H A N L N V L L D E G Q K H A V M L
ACACCTGGCGCTGCTGCTCGCGCGCCATTCCGCAGCCCAAGTCCAATGAGCAGCCGAATC
420
Y T W R C C S R A I P Q P K S N E Q P N
GCGTGGAGATCTACGAGAAGACGGTCGAGGTGCTAGCCCCGGAGGTGAACAAGCTGCTCA
480
R V E I Y E K T V E V L A P E V N K L L
ACTTCATGTACTTCCAACGCAAGGCCATCGAGGCCTTCTCCGGCGAGGTGAAGCGCTTGT
540
N F M Y F Q R K A I E A F S G E V K R L
GCCACGCCGAGAAGCGCAAGGACTTCGTGTCCGAGGCGTACCTATTGACGCTAGGCAAGT
600
C H A E K R K D F V S E A Y L L T L G K
TTATCAACATGTTTGCCGTGCTGGACGAGCTGAAGAACATGAAGTCCAGCGTGAAGAACG
660
F I N M F A V L D E L K N M K S S V K N

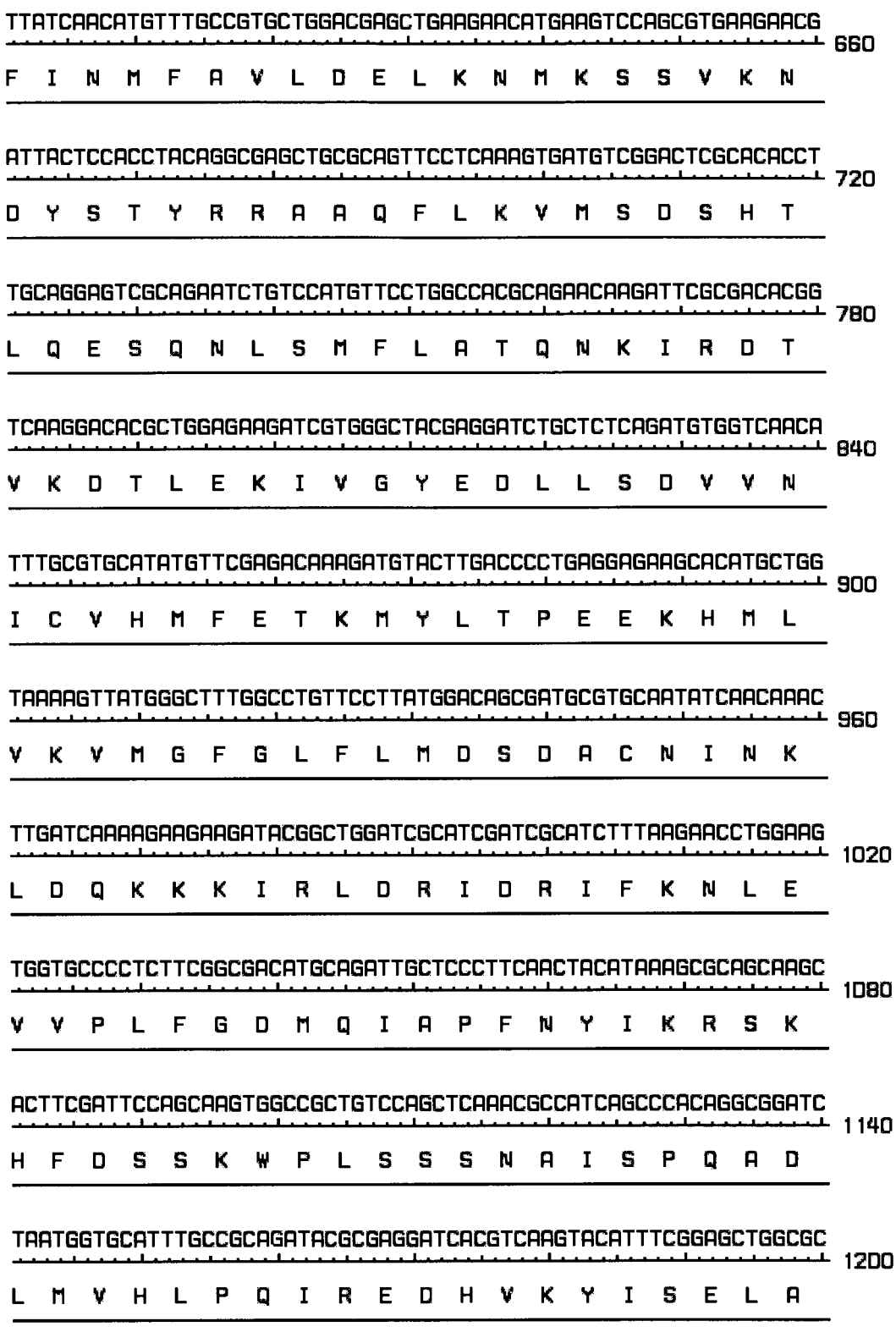
TTATCAACATGTTTGCCGTGCTGGACGAGCTGAAGAACATGAAGTCCAGCGTGAAGAACG
660
F I N M F A V L D E L K N M K S S V K N
ATTACTCCACCTACAGGCGAGCTGCGCAGTTCCTCAAAGTGATGTCGGACTCGCACACCT
720
D Y S T Y R R A A Q F L K V M S D S H T
TGCAGGAGTCGCAGAATCTGTCCATGTTCCTGGCCACGCAGAACAAGATTCGCGACACGG
780
L Q E S Q N L S M F L A T Q N K I R D T
TCAAGGACACGCTGGAGAAGATCGTGGGCTACGAGGATCTGCTCTCAGATGTGGTCAACA
840
V K D T L E K I V G Y E D L L S D V V N
TTTGCGTGCATATGTTCGAGACAAAGATGTACTTGACCCCTGAGGAGAAGCACATGCTGG
900
I C V H M F E T K M Y L T P E E K H M L
TAAAAGTTATGGGCTTTGGCCTGTTCCTTATGGACAGCGATGCGTGCAATATCAACAAAC
960
V K V M G F G L F L M D S D A C N I N K
TTGATCAAAAGAAGAAGATACGGCTGGATCGCATCGATCGCATCTTTAAGAACCTGGAAG
1020
L D Q K K K I R L D R I D R I F K N L E
TGGTGCCCCTCTTCGGCGACATGCAGATTGCTCCCTTCAACTACATAAAGCGCAGCAAGC
1080
V V P L F G D M Q I A P F N Y I K R S K
ACTTCGATTCCAGCAAGTGGCCGCTGTCCAGCTCAAACGCCATCAGCCCACAGGCGGATC
1140
H F D S S K W P L S S S N A I S P Q A D
TAATGGTGCATTTGCCGCAGATACGCGAGGATCACGTCAAGTACATTTCGGAGCTGGCGC
1200
L M V H L P Q I R E D H V K Y I S E L A

GATACACAAACGAGGTGACCACCACCGTCAAGGAGAATCCCTCTGATGCCGAGAACCGGA 1260

R Y T N E V T T T V K E N P S D A E N R

TTACGGCCGACCTGGCTCTGCGCGGCCTTCAATTGCTGTCCGAGTGGACCAGTGTGGTCA 1320

I T A D L A L R G L Q L L S E W T S V V

CCGAGTTGTACTCCTGGAAGCTCCTGCATCCGACTGATCATCACCAGAACAAGGAGTGCC 1380

T E L Y S W K L L H P T D H H Q N K E C

CCGTGGAGGCTGAGGAGTACGAGCGGGCCACCCGCTACAATTACACCTCGGAAGAGAAGT 1440

P V E A E E Y E R A T R Y N Y T S E E K

TCGCGCTGATCGAGGTCATCGCCATGATAAAGGGACTGCAGGTGCTAATGGCGCGCATTG 1500

F A L I E V I A M I K G L Q V L M A R I

AAACCGTATTGTGCGAGGCTATCCGGCGTAACATCTATTCCGAGCTGCAGGACTTCGTGC 1560

E T V L C E A I R R N I Y S E L Q D F V

AGCTTTCGCTTCGTGAACCGCTGCGAAAGGCCGTAAAAAATAAGAAGGATCTTATCCGGA 1620

Q L S L R E P L R K A V K N K K D L I R

GCATCATCATGTCGGTGCGAGAGACATCGGCGGACTGGCAAAAGGGCTATGAGCCCACCG 1680

S I I M S V R E T S A D W Q K G Y E P T

ACGATCCAGTGGCCAAGGGCAAGAAGGATCCCGACGGCGGCTTCCGCATCCAGGTGCCTC 1740

D D P V A K G K K D P D G G F R I Q V P

GCCTCAATGTGGGACCTTCCTCCACTCAGCTATACATGGTGCGCACCATGCTGGAGTCTC 1800

R L N V G P S S T Q L Y M V R T M L E S

TGATTGCCGACAAAAGCGGCGGCAAGCGCACTTTGCGCAAGGACATCGACGGAAACTGTT 1860

L I A D K S G G K R T L R K D I D G N C

TGCTGCAGATCGACACGTTCCACAAGACATCGTTCTACTGGAGCTACTTGCTCAACTTCA 1920

L L Q I D T F H K T S F Y W S Y L L N F

GCGACACGCTTCAGAAGTGCTGCGATCTCTCGCAGCTGTGGTATCGCGAGTTCTACTTGG 1980

S D T L Q K C C D L S Q L W Y R E F Y L

AGATGACCATGGGTCGTAAGGTTAACAAGTGCTTGGTGCGGCATCAGCACAACGAGGAGT 2040

E M T M G R K V N K C L V R H Q H N E E

GCAAGGATCTGATCACCATGGAGAAGCGCATTCAGTTTCCGATTGAAATGTCCATGCCCT 2100

C K D L I T M E K R I Q F P I E M S M P

GGATCCTAACCGATCACATTCTGCAAACGAAGGAGCCCTCAATGATGGAATTTGTCTTGT 2160

W I L T D H I L Q T K E P S M M E F V L

▼

ATCCCCTGGACTTGTACAACGACTCGGCGTACTACGCACTCACTGTCTTCCGAAAGCAGT 2220

Y P L D L Y N D S A Y Y A L T V F R K Q

TCCTGTACGACGAAGTGGAGGCCGAAGTCAATCTGTGCTTCGATCAGTTTGTCTACAAGC 2280

F L Y D E V E A E V N L C F D Q F V Y K

TGAGCGAGCAGATCTTTGCCCATTACAAGCAATTGGCGGGCAGCATCTTCTTGGACAAGC 2340

L S E Q I F A H Y K Q L A G S I F L D K

GATTCCGTTTGGAGTGCGAGGTACTCGGTTTCAACTTCCAGTCGTATCCCCGCAATAATC 2400

R F R L E C E V L G F N F Q S Y P R N N

GTTATGAGACCTTGTTAAAACAACGACATGTCCAACTTTTGGGCCGTTCTATTGACTTGA 2460

R Y E T L L K Q R H V Q L L G R S I D L

ACAAACTGATCACACAACGCATAAACGCCAACATGCACAAGAGCATTGAGTTGGCCATCA 2520

N K L I T Q R I N A N M H K S I E L A I

GTCGTTTCGAGGGCAACGATATAACCGGCATTGTGGAACTCGAAGGCCTGCTAGAGGCGA 2580

S R F E G N D I T G I V E L E G L L E A

ATCGAATTTGCCACAAGTTGCTAAGCAAGTACTTGGCCCTGGATAACTTTGACGGCATGG 2640

N R I C H K L L S K Y L A L D N F D G M

TAAAGGAGGCTAACCACAATGTACTGGCGCCTTACGGCAGAATAACACTGCACGTCTTTG 2700

V K E A N H N V L A P Y G R I T L H V F

TGGAATTGAACTACGACTTTCTGGTCAATTACTGCTATAATGCAGCCACGAATCGTTTCA 2760

V E L N Y D F L V N Y C Y N A A T N R F

TTCGAACCAAAGTGAATCTTTCGTCGTCACAGGCTATTCAGCGTGAGAAGCCGCCACAAA 2820

I R T K V N L S S S Q A I Q R E K P P Q

TGTCCCATTACTATCTGTGGGGTTCCAAGCAGCTGAATGCTGCCTATTCCACACAGTATG 2880

M S H Y Y L W G S K Q L N A A Y S T Q Y

GCCAGTACACTGGCTTTGTAGGTTCACCGCATTTCCATGCCATGTGCCGCCTGCTGGGCT 2940

G Q Y T G F V G S P H F H A M C R L L G

ATCAGGGCATAGCAGTCGTCATGGACATTATACTGAAGGACATTGTTAAGCCACTGATCC 3000

Y Q G I A V V M D I I L K D I V K P L I

AGGGCTCGCTGCTGCAGTTCACCAAGACGCTGATGATTGCCATGCCCAAGTCATGCAAAC 3060

Q G S L L Q F T K T L M I A M P K S C K

TACCCCGTTGCGAATATGGTTCGCCTGGAGTGCTCAGCTACTATCAGGCTCATCTTACAG 3120

L P R C E Y G S P G V L S Y Y Q A H L T

ACATCGTGCAATATCCGGACGCGAAGACAGAGCTATTTCAGTCTTTCCGGGAGTTTGGCA 3180

D I V Q Y P D A K T E L F Q S F R E F G

ACAGCATTATCTTTTGCCTGCTGATCGAACAGGCGCTCTCGCAGGAGGAGGTGTGCGATC 3240

N S I I F C L L I E Q A L S Q E E V C D

TACTGCACGCCGCCCTCTTCCAGAACATCTTTCCCAGACCTTTTTGCAAAGAGAATGAAA 3300

L L H A A L F Q N I F P R P F C K E N E

AACCGGAGGCTAAGCAAAAGCGTCTTGAAGCACAGTTTGCCAATCTGCAGATAGTTTCAA 3360

K P E A K Q K R L E A Q F A N L Q I V S

ACGTGGAAAAGATTGGCACTGCAAAGCAAGCAATGATAGCACGAGAGGGAGATTTGCTGA 3420

N V E K I G T A K Q A M I A R E G D L L

CTCGTGAGCGTCTTTGCTGTGGCCTCAGCATTTTTGAAGTTATTCTCAACCGCGTGAAGA 3480

T R E R L C C G L S I F E V I L N R V K

GCTATTTGGACGACCCTGTGTGGTGTGGTCCTCCACCGGCCAACGGGATTATCCACGTGG 3540

S Y L D D P V W C G P P P A N G I I H V

ATGAGTGCTCGGAGTTCCATCGCCTTTGGTCGGCTCTGCAGTTCGTTTATTGCATTCCAG 3600

D E C S E F H R L W S A L Q F V Y C I P

TCAGGGGAACGGAGTACACCATCGAGGAGCTCTTCGGCGAAGGTCTGAACTGGGCTGGCT 3660

V R G T E Y T I E E L F G E G L N W A G

GCGTCATGATCGTACTGCTGGGACAGCAGCGTCGCTTCGAGGCTCTGGACTTTTGCTACC 3720

C V M I V L L G Q Q R R F E A L D F C Y

ACATTCTGCGGGTACAGCGCGTCGATGGCAAGGATGAGGACGTAAAGGGCATTCAATTGA 3780

H I L R V Q R V D G K D E D V K G I Q L

AGCGAATGGTGGATCGGATTCGTCGGTTCCAAGTATTAAACTCACAAATCTTCTCCATTC 3840

K R M V D R I R R F Q V L N S Q I F S I

TCAACAAGTATCTAAAGGGCGGCGATGGCGAGGGCTCAAATGTGGAGCACGTGCGGTGTT 3900

L N K Y L K G G D G E G S N V E H V R C

TTCCACCGCCTCAGCATCCCTCGGTCATATCGTCCTCGTCGCACTACCAGGATCCCCAGA 3960

F P P P Q H P S V I S S S S H Y Q D P Q

AGCTGCGGCAGAGCATAAACAATTGAAGTCGCCCGGAAAGGGATGCATTTAAGCTAATCG 4020

K L R Q S I N N .

CATACAAATAGGTTACACTTAATCGCAGATGAATTAGTCCCCAGGAAAACAGCGACGTAG 4080

AAGCCGAAAAGCCAAGTTTTCTTGGCTATGCTGCCGAAACTTTGACAGTTTTTTTAGTCA 4140

AAGTGGCGGTCTTGGTTCTATTTGAATTCGATTTTATTGAAAATCTCTTTTGGTATGTCG 4200

CATTCAATCTTACAGTACGTTAAATGTTTTATCCAAGCAATTTATATATATATACATGTAG 4260

ATGTAATTTTGATTCACTTGCTACGGCATTCGATTCAGCTACTCGTACATTATCCCAAAT 4320

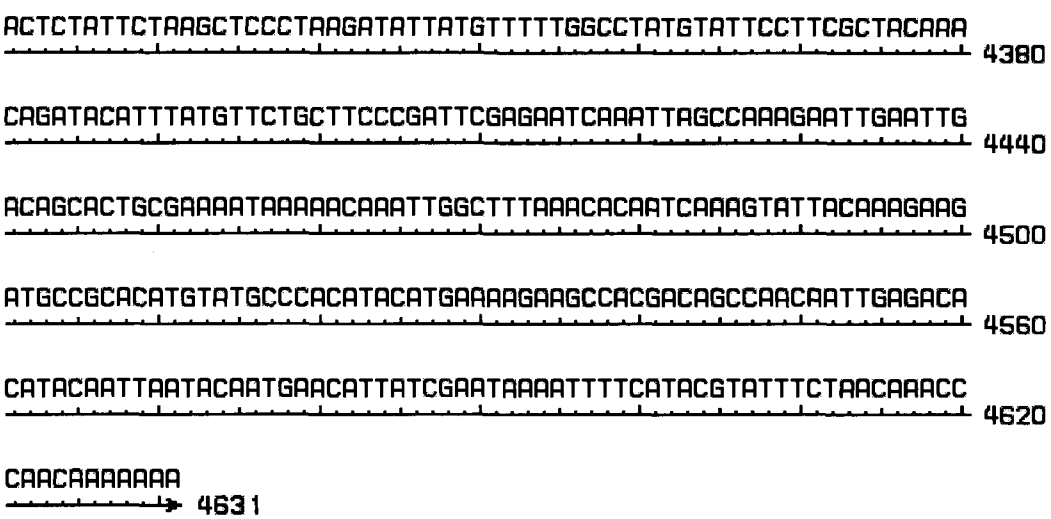
ACTCTATTCTAAGCTCCCTAAGATATTATGTTTTTGGCCTATGTATTCCTTCGCTACAAA
4380
CAGATACATTTATGTTCTGCTTCCCGATTCGAGAATCAAATTAGCCAAAGAATTGAATTG
4440
ACAGCACTGCGAAAATAAAAACAAATTGGCTTTAAACACAATCAAAGTATTACAAAGAAG
4500
ATGCCGCACATGTATGCCCACATACATGAAAAGAAGCCACGACAGCCAACAATTGAGACA
4560
CATACAATTAATACAATGAACATTATCGAATAAAATTTTCATACGTATTTCTAACAAACC
4620
CAACAAAAAAA
4631

localizes to the 88F1 region of the 3R chromosome and has an open reading frame in agreement with our generated *DSra-1* sequence (Fig. 3.2A).

3.2 DSra-1 mRNA

A Northern blot hydrization of total RNA from 0-12 hour old embryos using the *DSra-1* cDNA clone, LD47929, revealed a single hybridizing band of approximately 4.6 kb in size (Fig. 3.2B). This is comparable to the size of the assembled, full-length cDNA and the *Drosophila* Genome Sequencing Project prediction (Myers et al., 2000). A Northern blot analysis of 0-12 hour old embryonic poly A+ mRNA confirmed no evidence for alternative transcripts that may have been occluded by ribosomal RNA shadow bands in the total RNA. The cDNA encodes an open reading frame of 3986 nucleotides and translates to a protein containing 1291 amino acids and a molecular mass of 150 kDa. The translated protein was run against the PubMed translated nucleotide database and bears close similarity to Sra-1 homologs in various species (Fig. 3.3, Table 3.1). InterPro searches indicate that DSra-1 contains no recognizable functional motifs and tBLASTn analysis indicates a 66% identity to human Sra-1. tBLASTn searches for Sra-1 homologs in other organisms were performed and found homologs in *C. elegans* (GenBank accession number AAB92078) and *M. musculus* (GenBank accession number AAC25773.1). Sequence comparison of DSra-1 against these candidates revealed amino acid identities of 48% and 65%, respectively (Table 1).

Two EP-element insertions, *EP(3)0789* and *EP(3)3267*, were available that lie 65 base pairs and 59 base pairs upstream of the predicted start codon of *DSra-1*, respectively (Fig 3.2A). EP-elements contain engineered upstream activating sequences for the yeast GAL4 transcription factor, and can be used to direct GAL4-driven expression of any gene

Figure 3.2 The chromosomal location and organization of *DSra-1*.

(A) Conceptual diagram of chromosomal location of *DSra-1* gene and size of deletions of *DSra-1* alleles. P1 and P2 indicate the sites of primers used for screening P-element remobilised *Drosophila* lines for excision events. Excisions produce aberrant PCR products that are resolved on an agarose gel. P3 indicates an internal primer used to test if the deficiency, *Df(3R)ea*, covered the $DSra\text{-}1^{18b}$ lesion.

(B) Northern blot of 0-12 hour poly A+ *DSra-1* RNA showing a single 4.6kb band.

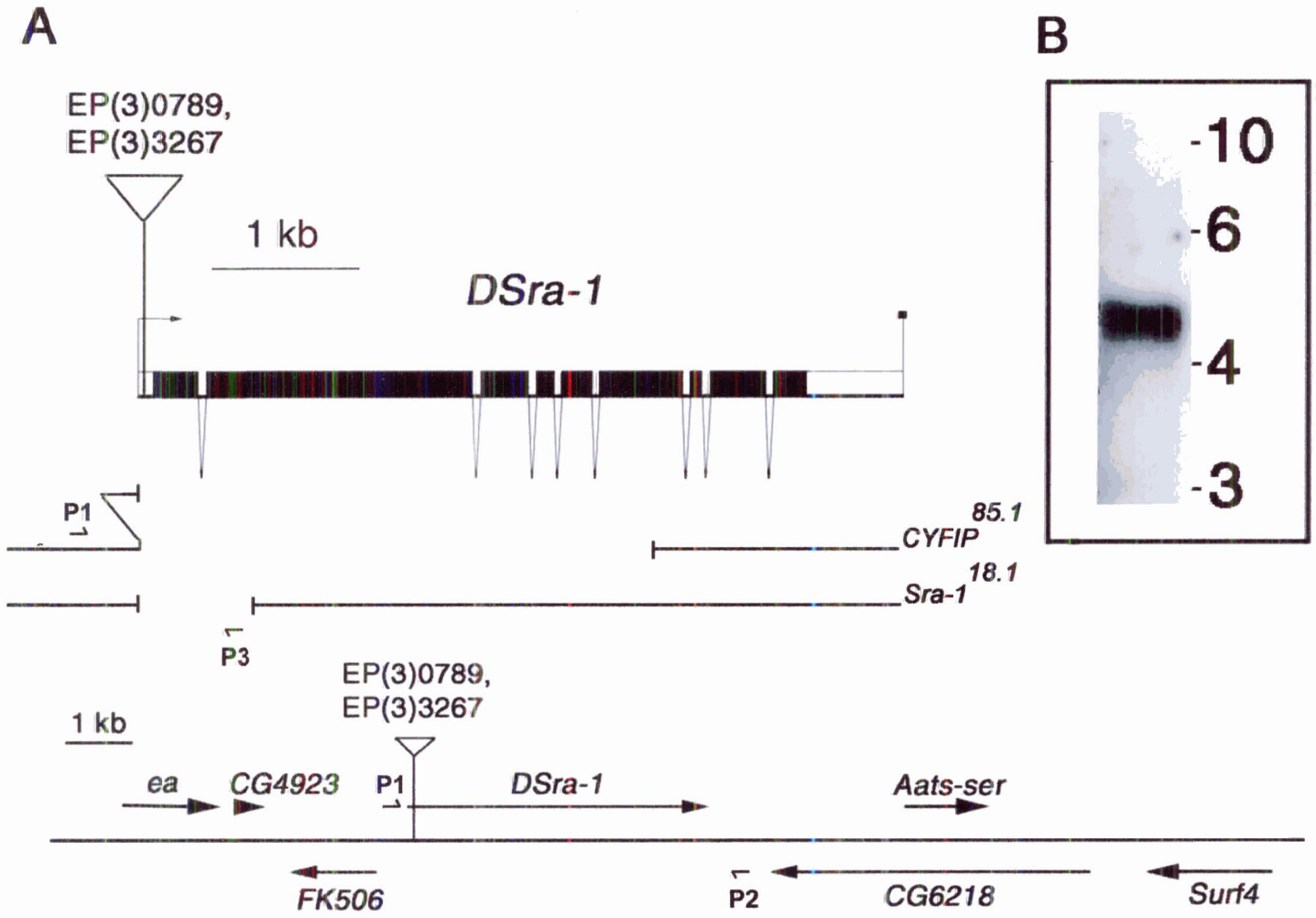

3R, 88E13-88F1

Figure 3.3 Alignment of DSra-1 with homologs from other species.

The Clustal method of the program MEGALIGN of LASERGENE 99 package (DNAStar, Madison WI) was used to produce alignment comparisons of DSra-1 and homologous proteins in other species. Shaded residues match the consensus.

DSra-1 is also known as *Drosophila* CYFIP (Schenck et al., 2003). There are two isoforms of *Sra-1* in humans and *M. musculus*, and these are known as CYFIP1 and PIR121/CYFIP2 and SHYC/CYFIP1 and CYFIP2 respectively (Saller et al., 1999).

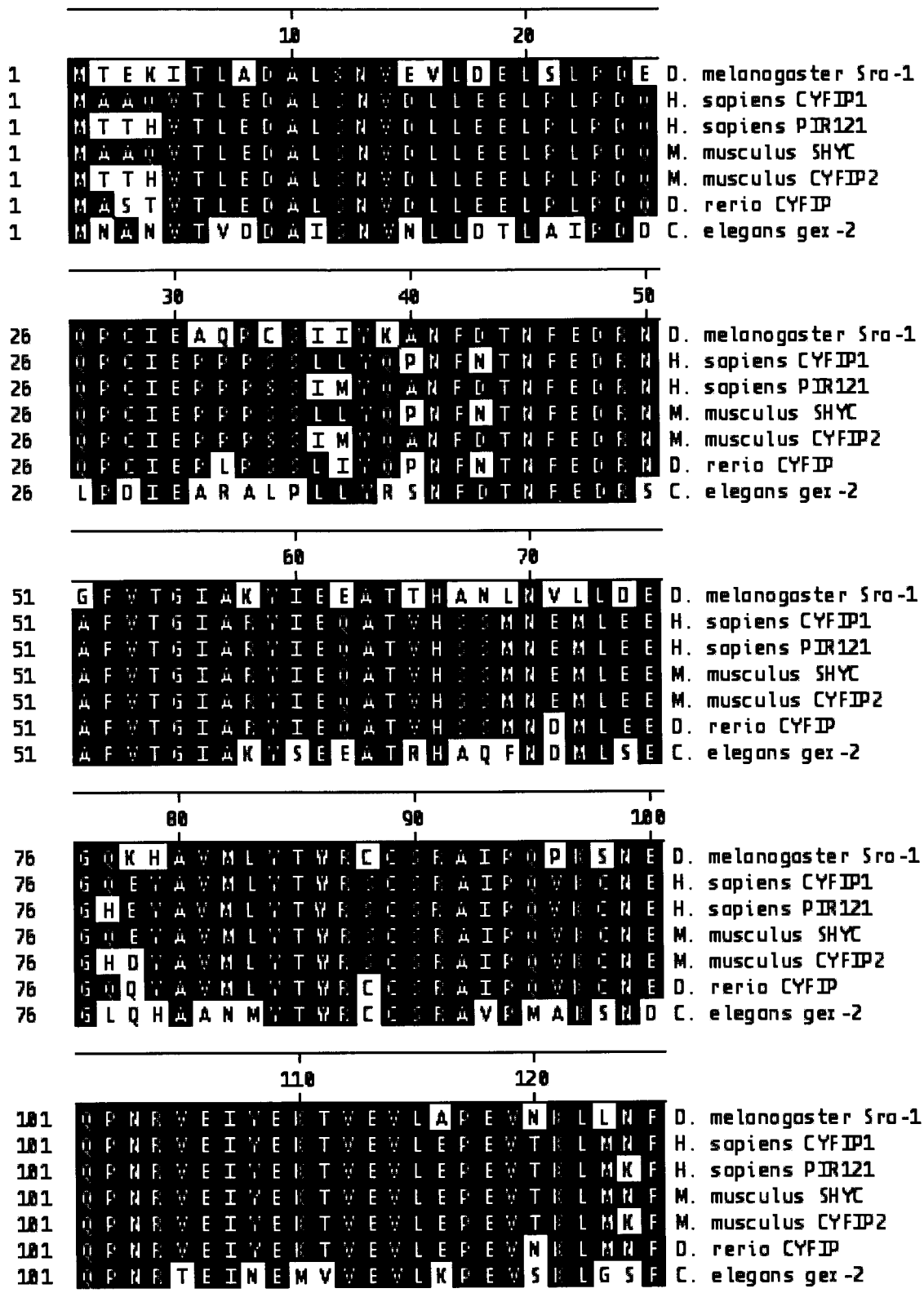
10
20
1 D. melanogaster Sra-1
1 H. sapiens CYFIP1
1 H. sapiens PIR121
1 M. musculus SHYC
1 M. musculus CYFIP2
1 D. rerio CYFIP
1 C. elegans gex-2
30
40
50
26 D. melanogaster Sra-1
26 H. sapiens CYFIP1
26 H. sapiens PIR121
26 M. musculus SHYC
26 M. musculus CYFIP2
26 D. rerio CYFIP
26 C. elegans gex-2
60
70
51 D. melanogaster Sra-1
51 H. sapiens CYFIP1
51 H. sapiens PIR121
51 M. musculus SHYC
51 M. musculus CYFIP2
51 D. rerio CYFIP
51 C. elegans gex-2
80
90
100
76 D. melanogaster Sra-1
76 H. sapiens CYFIP1
76 H. sapiens PIR121
76 M. musculus SHYC
76 M. musculus CYFIP2
76 D. rerio CYFIP
76 C. elegans gex-2
110
120
101 D. melanogaster Sra-1
101 H. sapiens CYFIP1
101 H. sapiens PIR121
101 M. musculus SHYC
101 M. musculus CYFIP2
101 D. rerio CYFIP
101 C. elegans gex-2

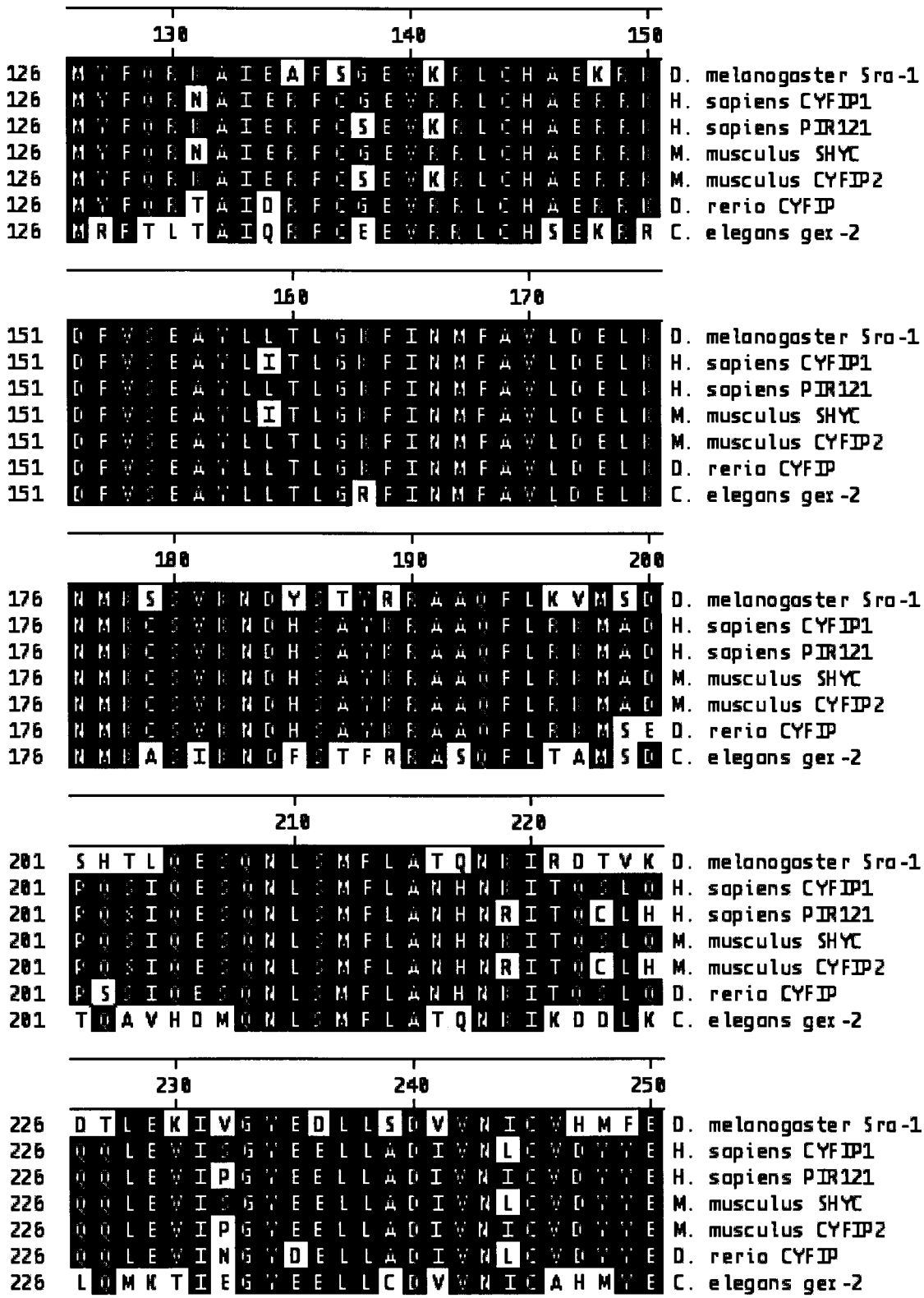
130
140
150
126 D. melanogaster Sra-1
126 H. sapiens CYFIP1
126 H. sapiens PIR121
126 M. musculus SHYC
126 M. musculus CYFIP2
126 D. rerio CYFIP
126 C. elegans gex-2
160
170
151 D. melanogaster Sra-1
151 H. sapiens CYFIP1
151 H. sapiens PIR121
151 M. musculus SHYC
151 M. musculus CYFIP2
151 D. rerio CYFIP
151 C. elegans gex-2
180
190
200
176 D. melanogaster Sra-1
176 H. sapiens CYFIP1
176 H. sapiens PIR121
176 M. musculus SHYC
176 M. musculus CYFIP2
176 D. rerio CYFIP
176 C. elegans gex-2
210
220
201 D. melanogaster Sra-1
201 H. sapiens CYFIP1
201 H. sapiens PIR121
201 M. musculus SHYC
201 M. musculus CYFIP2
201 D. rerio CYFIP
201 C. elegans gex-2
230
240
250
226 D. melanogaster Sra-1
226 H. sapiens CYFIP1
226 H. sapiens PIR121
226 M. musculus SHYC
226 M. musculus CYFIP2
226 D. rerio CYFIP
226 C. elegans gex-2

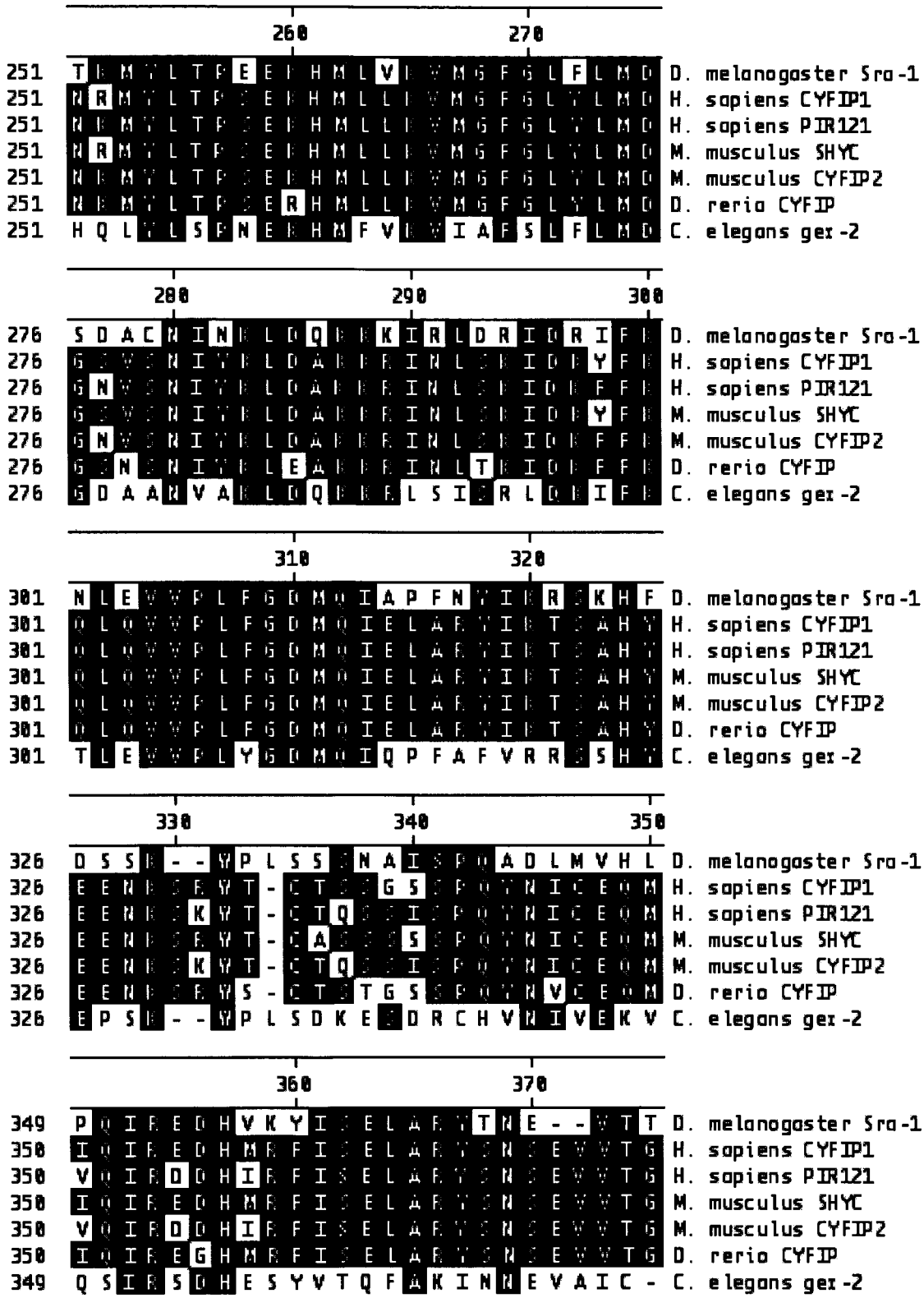
260
270
251 D. melanogaster Sra-1
251 H. sapiens CYFIP1
251 H. sapiens PIR121
251 M. musculus SHYC
251 M. musculus CYFIP2
251 D. rerio CYFIP
251 C. elegans gex-2
280
290
300
276 D. melanogaster Sra-1
276 H. sapiens CYFIP1
276 H. sapiens PIR121
276 M. musculus SHYC
276 M. musculus CYFIP2
276 D. rerio CYFIP
276 C. elegans gex-2
310
320
301 D. melanogaster Sra-1
301 H. sapiens CYFIP1
301 H. sapiens PIR121
301 M. musculus SHYC
301 M. musculus CYFIP2
301 D. rerio CYFIP
301 C. elegans gex-2
330
340
350
326 D. melanogaster Sra-1
326 H. sapiens CYFIP1
326 H. sapiens PIR121
326 M. musculus SHYC
326 M. musculus CYFIP2
326 D. rerio CYFIP
326 C. elegans gex-2
360
370
349 D. melanogaster Sra-1
350 H. sapiens CYFIP1
350 H. sapiens PIR121
350 M. musculus SHYC
350 M. musculus CYFIP2
350 D. rerio CYFIP
349 C. elegans gex-2

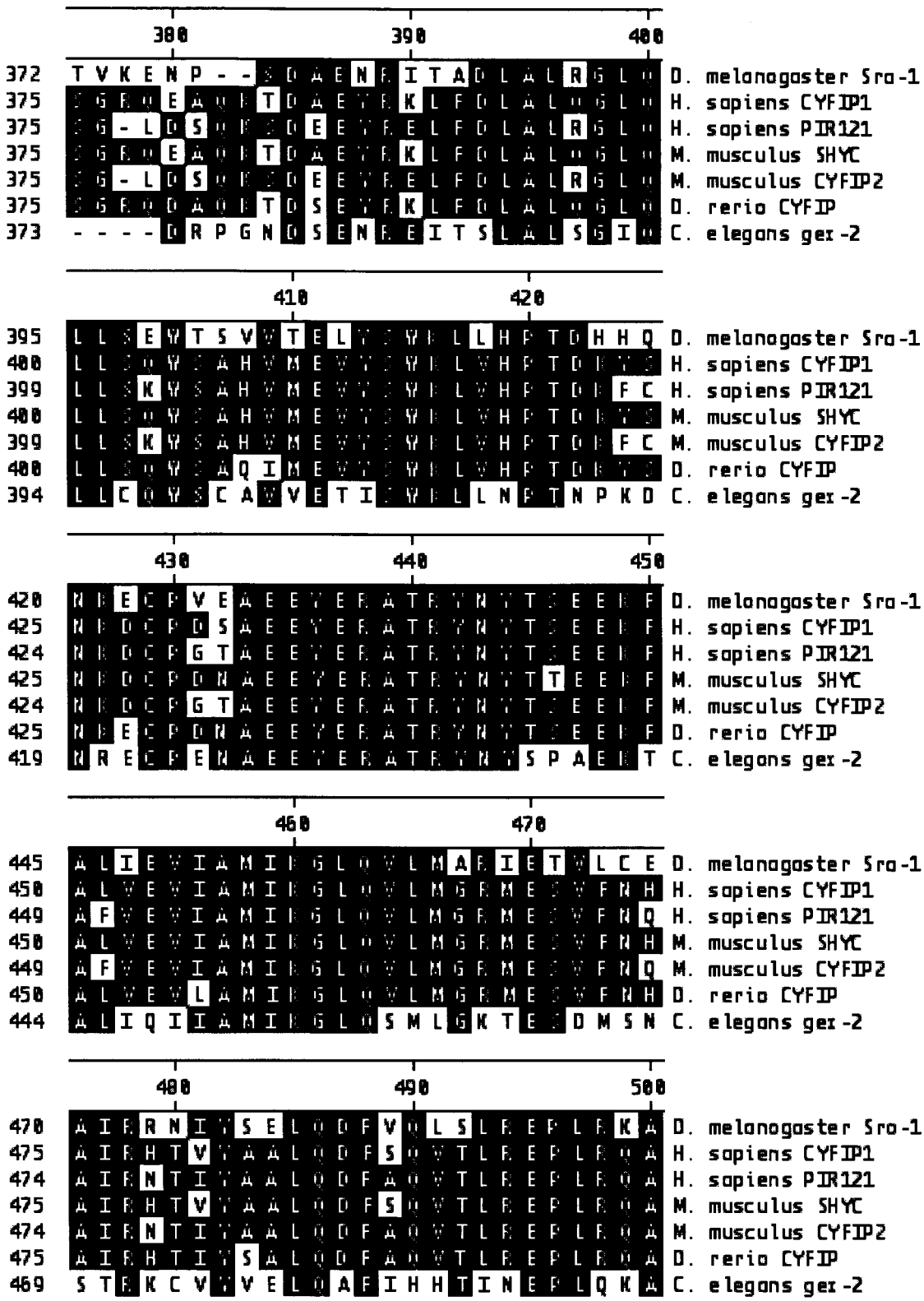
380
390
400
372 TVKENP--SDAENRITADLALRGLQ D. melanogaster Sra-1
375 SGRQEAQRTDAETRKLFDLALQGLQ H. sapiens CYFIP1
375 SG-LDSQRSDEETRELFDLALRGLQ H. sapiens PIR121
375 SGRQEAQRTDAETRKLFDLALQGLQ M. musculus SHYC
375 SG-LDSQRSDEETRELFDLALRGLQ M. musculus CYFIP2
375 SGRQDAQRTDSETRKLFDLALQGLQ D. rerio CYFIP
373 ----DRPGNDSENREITSLALSGIQ C. elegans gex-2
410
420
395 LLSEWTSVWTELWSWRLLHPTDHHQ D. melanogaster Sra-1
400 LLSQWSAHWMEVYSWRLWHPTDRYS H. sapiens CYFIP1
399 LLSKWSAHWMEVYSWRLWHPTDRFC H. sapiens PIR121
400 LLSQWSAHWMEVYSWRLWHPTDRYS M. musculus SHYC
399 LLSKWSAHWMEVYSWRLWHPTDRFC M. musculus CYFIP2
400 LLSQWSAQIMEVYSWRLWHPTDRYS D. rerio CYFIP
394 LLCQWSCAWVETISWRLLNPTNPKD C. elegans gex-2
430
440
450
420 NREQPVEAEEYERATRYNYTSEERF D. melanogaster Sra-1
425 NRDQPDSAEEYERATRYNYTSEERF H. sapiens CYFIP1
424 NRDQPGTAEEYERATRYNYTSEERF H. sapiens PIR121
425 NRDQPDNAEEYERATRYNYTTEERF M. musculus SHYC
424 NRDQPGTAEEYERATRYNYTSEERF M. musculus CYFIP2
425 NREQPDNAEEYERATRYNYTSEERF D. rerio CYFIP
419 NRECPENAEEYERATRYNYSPAERT C. elegans gex-2
460
470
445 ALIEWIAMIRGLQWLMARIETWLCE D. melanogaster Sra-1
450 ALWEWIAMIRGLQWLMGRMESWFNH H. sapiens CYFIP1
449 AFWEWIAMIRGLQWLMGRMESWFNQ H. sapiens PIR121
450 ALWEWIAMIRGLQWLMGRMESWFNH M. musculus SHYC
449 AFWEWIAMIRGLQWLMGRMESWFNQ M. musculus CYFIP2
450 ALWEWLAMIRGLQWLMGRMESWFNH D. rerio CYFIP
444 ALIQIIAMIRGLQSMLGKTESDMSN C. elegans gex-2
480
490
500
470 AIRRNIYSELQDFVQLSLREPLRKA D. melanogaster Sra-1
475 AIRHTVYAALQDFSQWTLREPLRQA H. sapiens CYFIP1
474 AIRNTIYAALQDFAQWTLREPLRQA H. sapiens PIR121
475 AIRHTVYAALQDFSQWTLREPLRQA M. musculus SHYC
474 AIRNTIYAALQDFAQWTLREPLRQA M. musculus CYFIP2
475 AIRHTIYSALQDFAQWTLREPLRQA D. rerio CYFIP
469 STRKCVYVELQAFIHHTINEPLQKA C. elegans gex-2

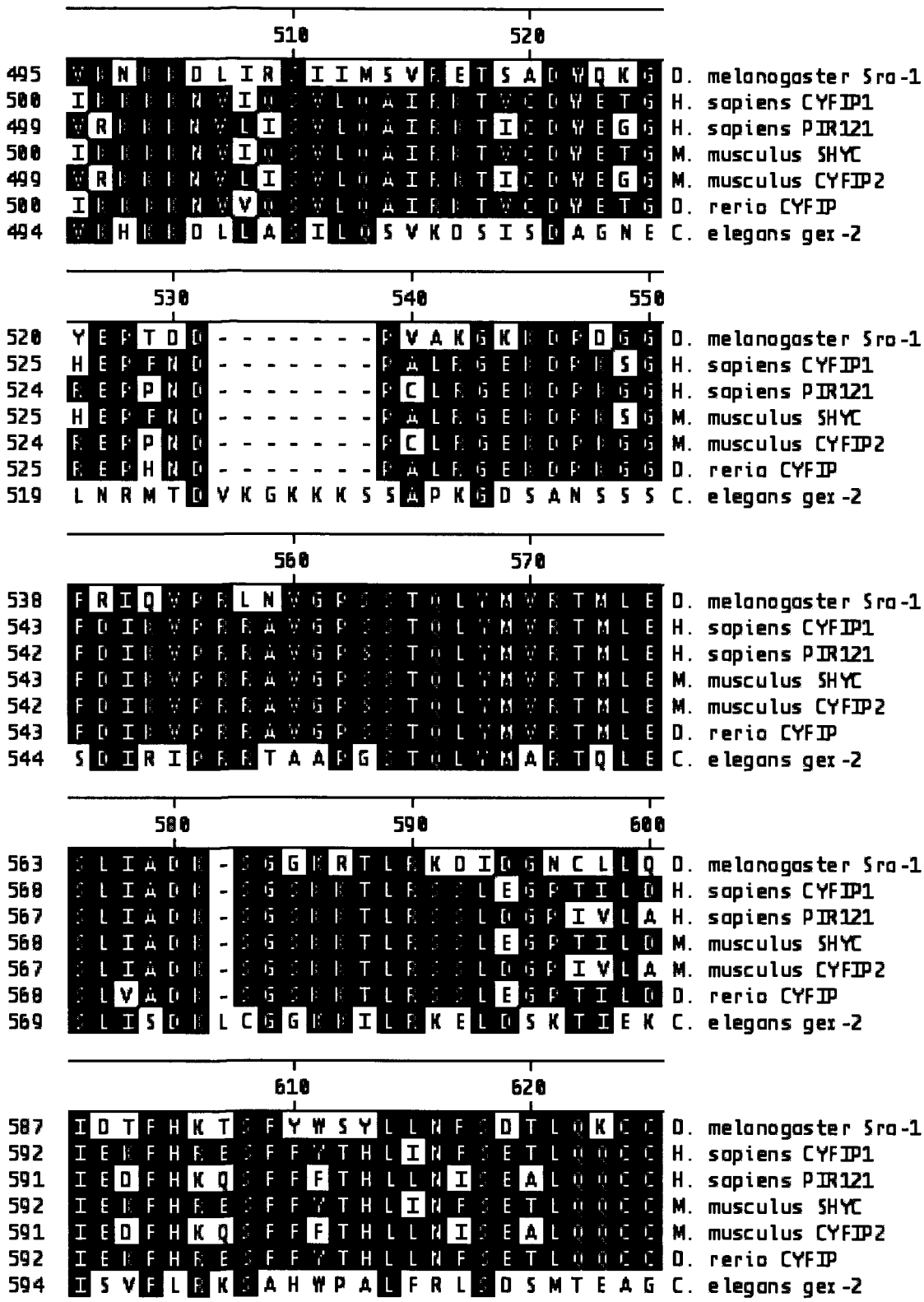
510
520
495 D. melanogaster Sra-1
500 H. sapiens CYFIP1
499 H. sapiens PIR121
500 M. musculus SHYC
499 M. musculus CYFIP2
500 D. rerio CYFIP
494 C. elegans gex-2
530
540
550
520 D. melanogaster Sra-1
525 H. sapiens CYFIP1
524 H. sapiens PIR121
525 M. musculus SHYC
524 M. musculus CYFIP2
525 D. rerio CYFIP
519 C. elegans gex-2
560
570
538 D. melanogaster Sra-1
543 H. sapiens CYFIP1
542 H. sapiens PIR121
543 M. musculus SHYC
542 M. musculus CYFIP2
543 D. rerio CYFIP
544 C. elegans gex-2
580
590
600
563 D. melanogaster Sra-1
560 H. sapiens CYFIP1
567 H. sapiens PIR121
560 M. musculus SHYC
567 M. musculus CYFIP2
560 D. rerio CYFIP
569 C. elegans gex-2
610
620
587 D. melanogaster Sra-1
592 H. sapiens CYFIP1
591 H. sapiens PIR121
592 M. musculus SHYC
591 M. musculus CYFIP2
592 D. rerio CYFIP
594 C. elegans gex-2

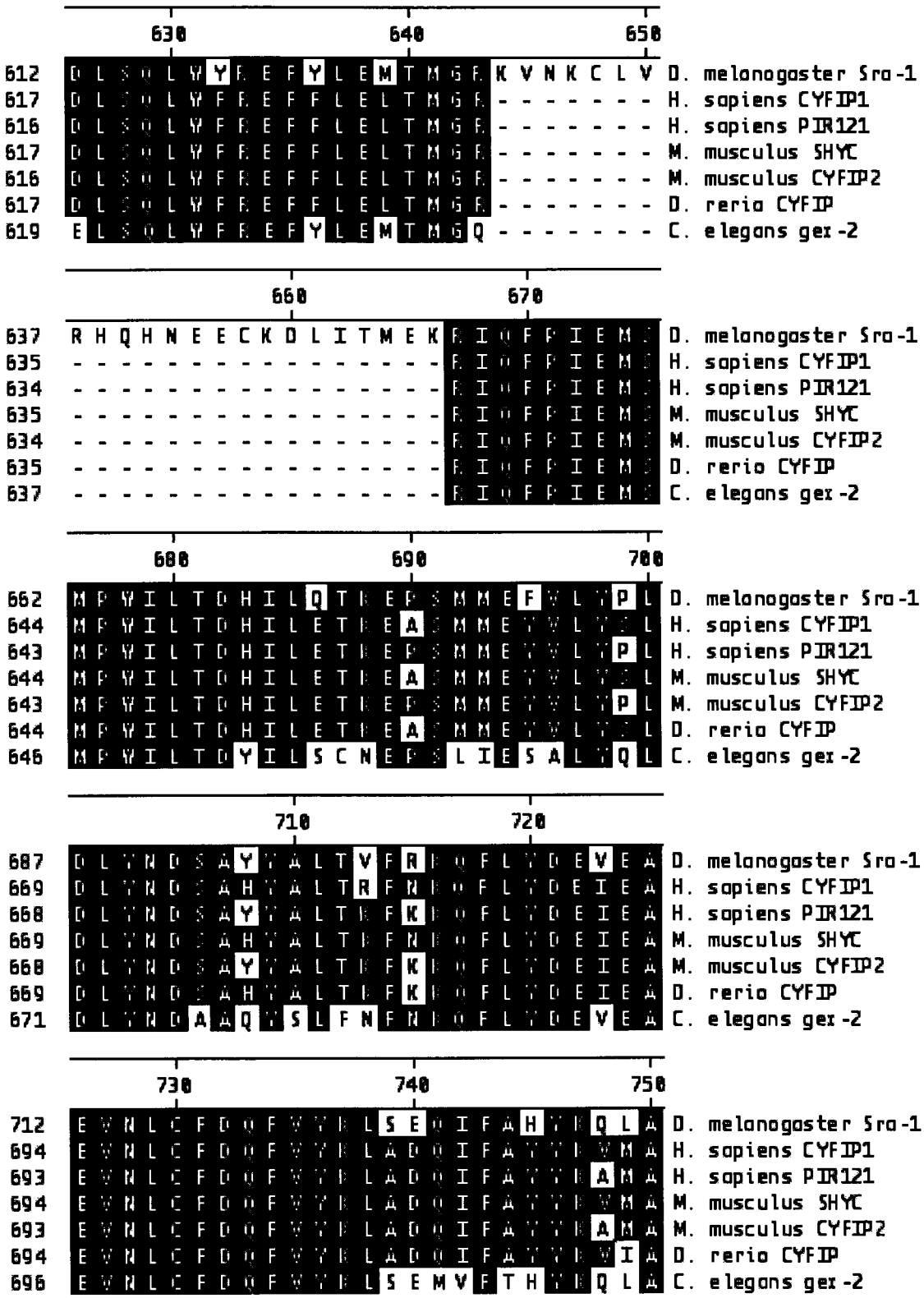
630
640
650
612 D. melanogaster Sra-1
617 H. sapiens CYFIP1
616 H. sapiens PIR121
617 M. musculus SHYC
616 M. musculus CYFIP2
617 D. rerio CYFIP
619 C. elegans gex-2
660
670
637 D. melanogaster Sra-1
635 H. sapiens CYFIP1
634 H. sapiens PIR121
635 M. musculus SHYC
634 M. musculus CYFIP2
635 D. rerio CYFIP
637 C. elegans gex-2
680
690
700
662 D. melanogaster Sra-1
644 H. sapiens CYFIP1
643 H. sapiens PIR121
644 M. musculus SHYC
643 M. musculus CYFIP2
644 D. rerio CYFIP
646 C. elegans gex-2
710
720
687 D. melanogaster Sra-1
669 H. sapiens CYFIP1
668 H. sapiens PIR121
669 M. musculus SHYC
668 M. musculus CYFIP2
669 D. rerio CYFIP
671 C. elegans gex-2
730
740
750
712 D. melanogaster Sra-1
694 H. sapiens CYFIP1
693 H. sapiens PIR121
694 M. musculus SHYC
693 M. musculus CYFIP2
694 D. rerio CYFIP
696 C. elegans gex-2

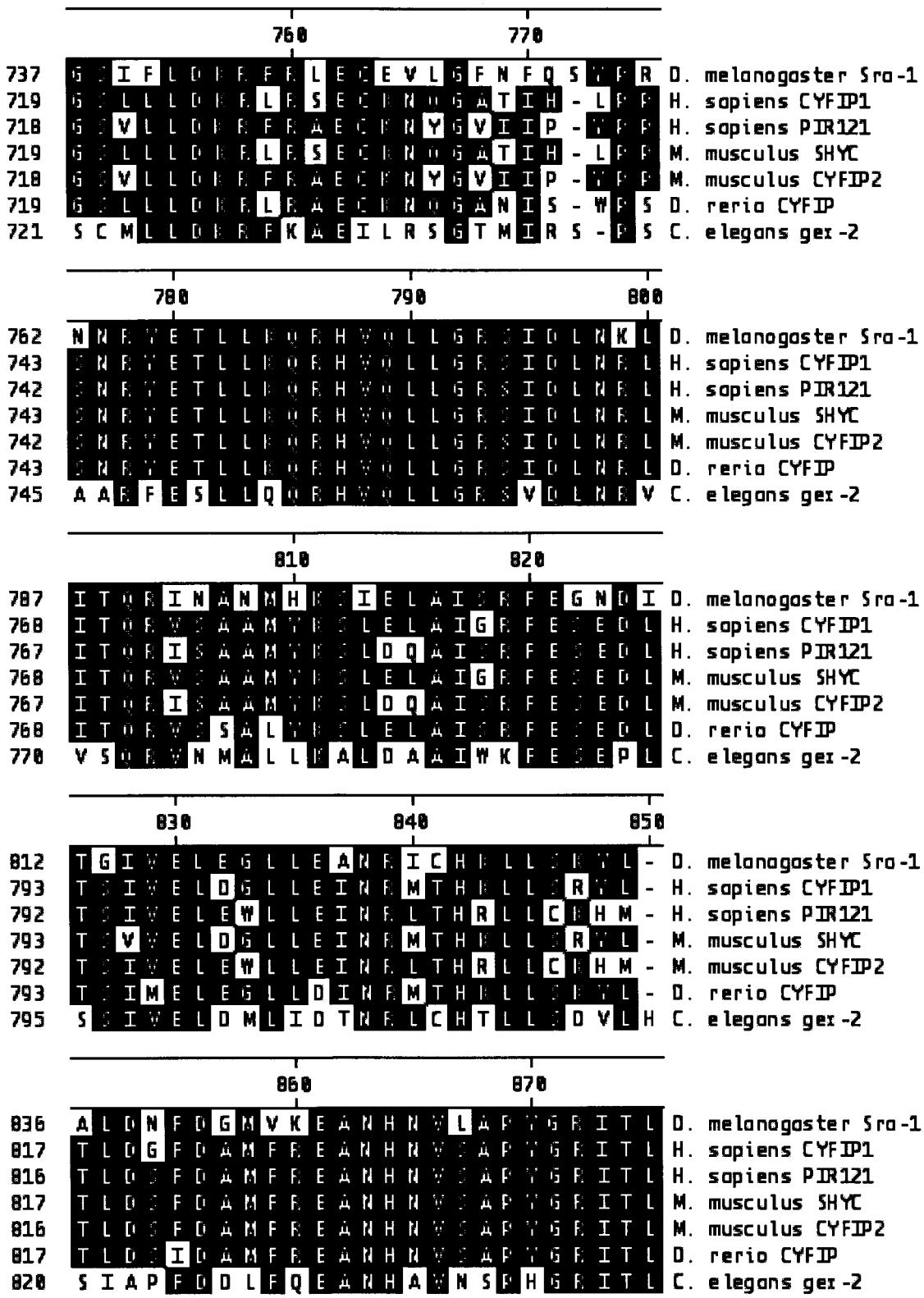
760
770
737 D. melanogaster Sra-1
719 H. sapiens CYFIP1
718 H. sapiens PIR121
719 M. musculus SHYC
718 M. musculus CYFIP2
719 D. rerio CYFIP
721 C. elegans gex-2
780
790
800
762 D. melanogaster Sra-1
743 H. sapiens CYFIP1
742 H. sapiens PIR121
743 M. musculus SHYC
742 M. musculus CYFIP2
743 D. rerio CYFIP
745 C. elegans gex-2
810
820
787 D. melanogaster Sra-1
768 H. sapiens CYFIP1
767 H. sapiens PIR121
768 M. musculus SHYC
767 M. musculus CYFIP2
768 D. rerio CYFIP
770 C. elegans gex-2
830
840
850
812 D. melanogaster Sra-1
793 H. sapiens CYFIP1
792 H. sapiens PIR121
793 M. musculus SHYC
792 M. musculus CYFIP2
793 D. rerio CYFIP
795 C. elegans gex-2
860
870
836 D. melanogaster Sra-1
817 H. sapiens CYFIP1
816 H. sapiens PIR121
817 M. musculus SHYC
816 M. musculus CYFIP2
817 D. rerio CYFIP
820 C. elegans gex-2

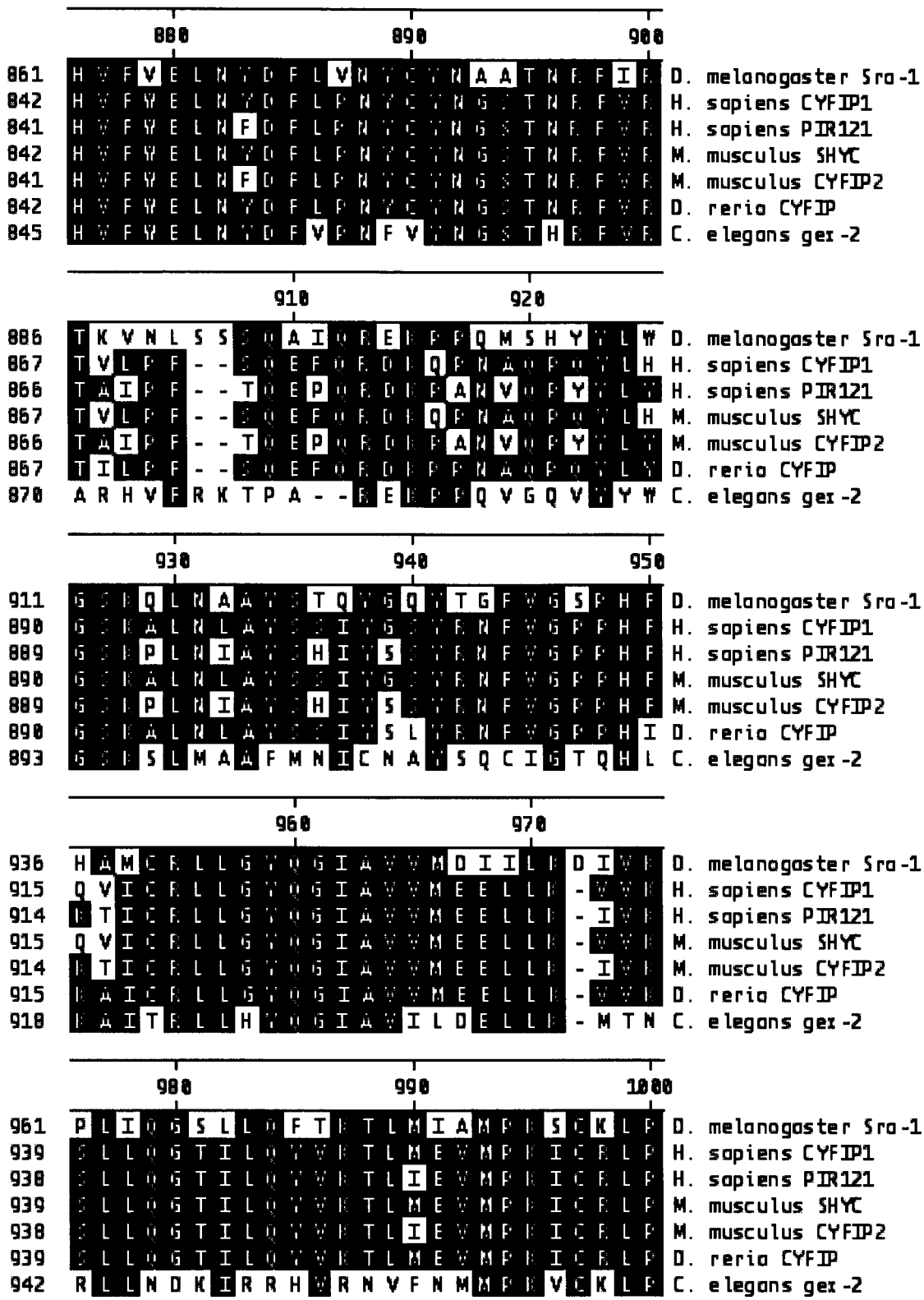
880
890
900
861 D. melanogaster Sra-1
842 H. sapiens CYFIP1
841 H. sapiens PIR121
842 M. musculus SHYC
841 M. musculus CYFIP2
842 D. rerio CYFIP
845 C. elegans gex-2
910
920
886 D. melanogaster Sra-1
867 H. sapiens CYFIP1
866 H. sapiens PIR121
867 M. musculus SHYC
866 M. musculus CYFIP2
867 D. rerio CYFIP
870 C. elegans gex-2
930
940
950
911 D. melanogaster Sra-1
890 H. sapiens CYFIP1
889 H. sapiens PIR121
890 M. musculus SHYC
889 M. musculus CYFIP2
890 D. rerio CYFIP
893 C. elegans gex-2
960
970
936 D. melanogaster Sra-1
915 H. sapiens CYFIP1
914 H. sapiens PIR121
915 M. musculus SHYC
914 M. musculus CYFIP2
915 D. rerio CYFIP
918 C. elegans gex-2
980
990
1000
961 D. melanogaster Sra-1
939 H. sapiens CYFIP1
938 H. sapiens PIR121
939 M. musculus SHYC
938 M. musculus CYFIP2
939 D. rerio CYFIP
942 C. elegans gex-2

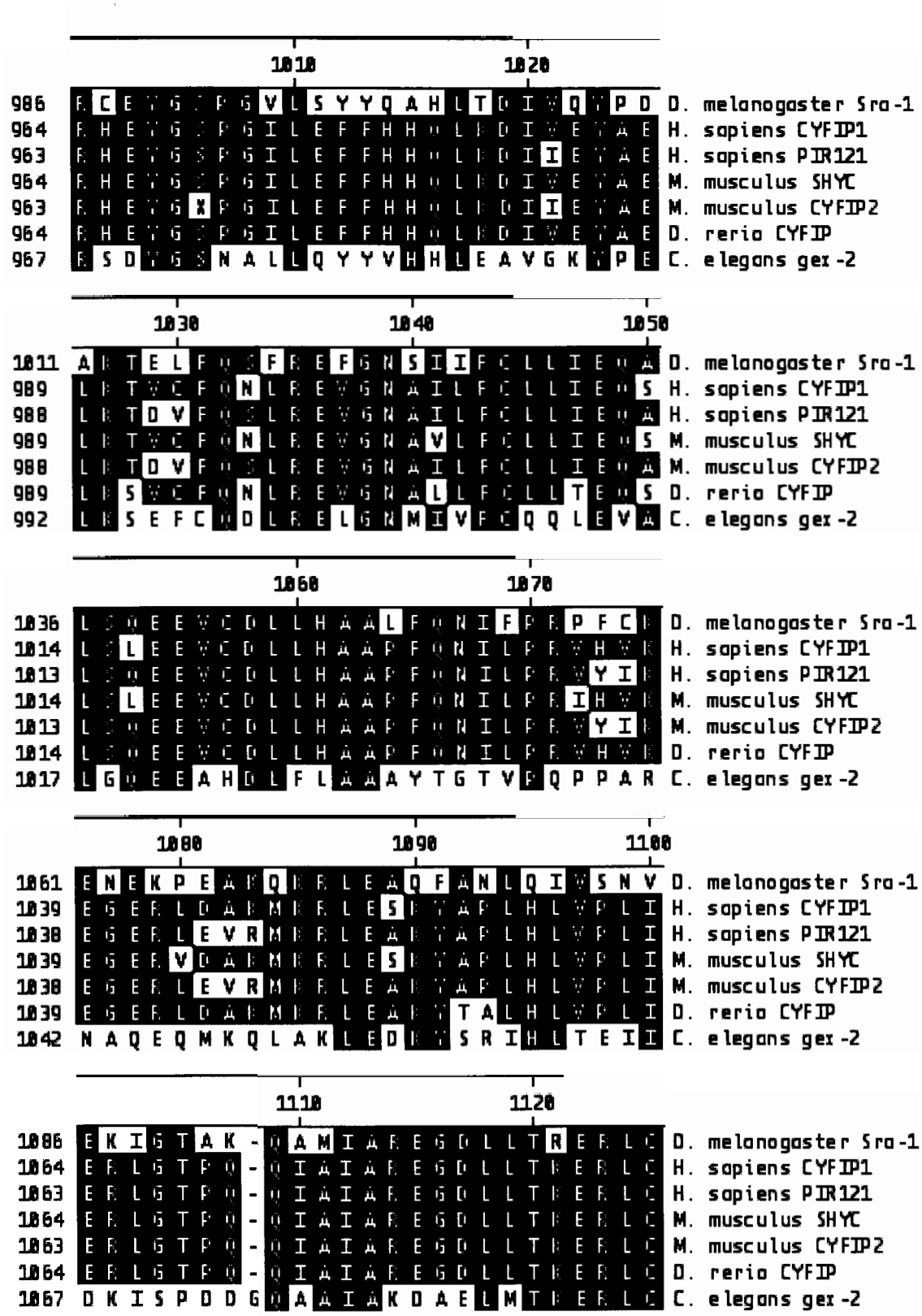
1010
1020
986 D. melanogaster Sra-1
964 H. sapiens CYFIP1
963 H. sapiens PIR121
964 M. musculus SHYC
963 M. musculus CYFIP2
964 D. rerio CYFIP
967 C. elegans gex-2
1030
1040
1050
1011 D. melanogaster Sra-1
989 H. sapiens CYFIP1
988 H. sapiens PIR121
989 M. musculus SHYC
988 M. musculus CYFIP2
989 D. rerio CYFIP
992 C. elegans gex-2
1060
1070
1036 D. melanogaster Sra-1
1014 H. sapiens CYFIP1
1013 H. sapiens PIR121
1014 M. musculus SHYC
1013 M. musculus CYFIP2
1014 D. rerio CYFIP
1017 C. elegans gex-2
1080
1090
1100
1061 D. melanogaster Sra-1
1039 H. sapiens CYFIP1
1038 H. sapiens PIR121
1039 M. musculus SHYC
1038 M. musculus CYFIP2
1039 D. rerio CYFIP
1042 C. elegans gex-2
1110
1120
1086 D. melanogaster Sra-1
1064 H. sapiens CYFIP1
1063 H. sapiens PIR121
1064 M. musculus SHYC
1063 M. musculus CYFIP2
1064 D. rerio CYFIP
1067 C. elegans gex-2

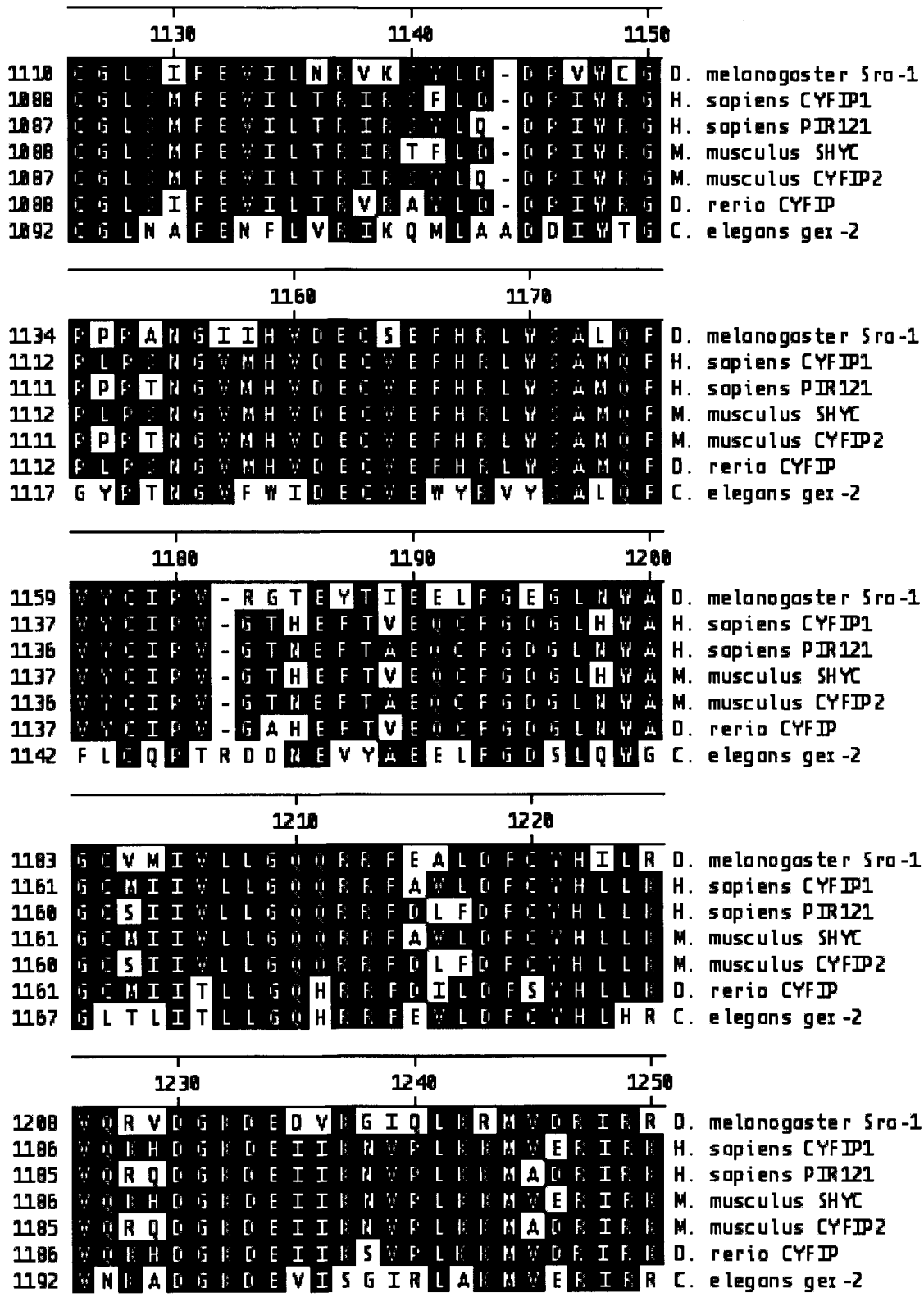
1130
1140
1150
1110 D. melanogaster Sra-1
1088 H. sapiens CYFIP1
1087 H. sapiens PIR121
1088 M. musculus SHYC
1087 M. musculus CYFIP2
1088 D. rerio CYFIP
1092 C. elegans gex-2
1160
1170
1134 D. melanogaster Sra-1
1112 H. sapiens CYFIP1
1111 H. sapiens PIR121
1112 M. musculus SHYC
1111 M. musculus CYFIP2
1112 D. rerio CYFIP
1117 C. elegans gex-2
1180
1190
1200
1159 D. melanogaster Sra-1
1137 H. sapiens CYFIP1
1136 H. sapiens PIR121
1137 M. musculus SHYC
1136 M. musculus CYFIP2
1137 D. rerio CYFIP
1142 C. elegans gex-2
1210
1220
1183 D. melanogaster Sra-1
1161 H. sapiens CYFIP1
1160 H. sapiens PIR121
1161 M. musculus SHYC
1160 M. musculus CYFIP2
1161 D. rerio CYFIP
1167 C. elegans gex-2
1230
1240
1250
1208 D. melanogaster Sra-1
1186 H. sapiens CYFIP1
1185 H. sapiens PIR121
1186 M. musculus SHYC
1185 M. musculus CYFIP2
1186 D. rerio CYFIP
1192 C. elegans gex-2

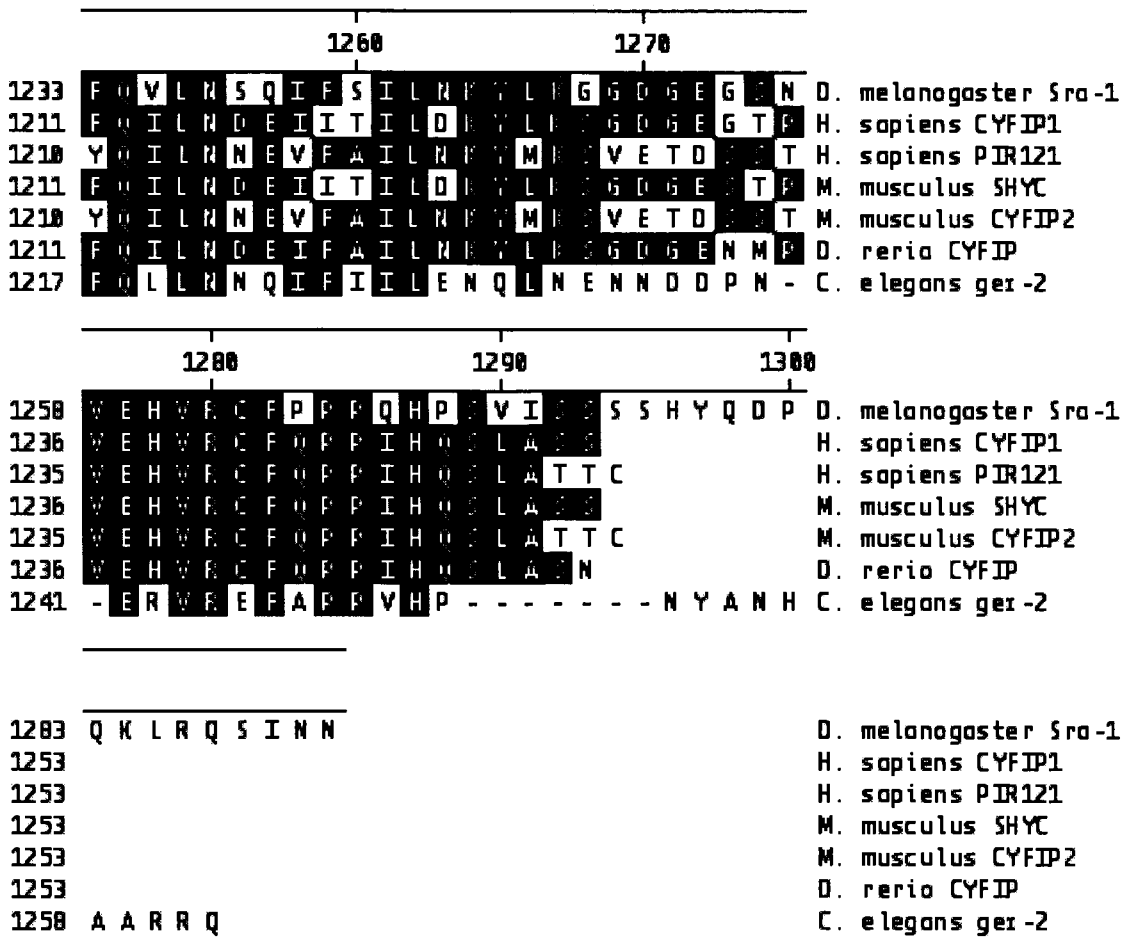
1260
1270
1233 D. melanogaster Sra-1
1211 H. sapiens CYFIP1
1210 H. sapiens PIR121
1211 M. musculus SHYC
1210 M. musculus CYFIP2
1211 D. rerio CYFIP
1217 C. elegans gex-2
1280
1290
1300
1250 D. melanogaster Sra-1
1236 H. sapiens CYFIP1
1235 H. sapiens PIR121
1236 M. musculus SHYC
1235 M. musculus CYFIP2
1236 D. rerio CYFIP
1241 C. elegans gex-2
1283 D. melanogaster Sra-1
1253 H. sapiens CYFIP1
1253 H. sapiens PIR121
1253 M. musculus SHYC
1253 M. musculus CYFIP2
1253 D. rerio CYFIP
1258 C. elegans gex-2

Table 3.1 Similarity and identity comparisons of Sra-1 homologs to DSra-1.

Table depicting similarity and identity comparisons of homologs of DSra-1. Compiled from data returned from tBLASTn search on PubMed database. DSra-1 is also known as *Drosophila* CYFIP (Schenck et al., 2003). There are two isoforms of *Sra-1* in humans and *M. musculus*, and are known as CYFIP1 and PIR121/CYFIP2 and SHYC/CYFIP1 and CYFIP2 respectively (Saller et al., 1999).

	Amino Acid Similarities	Amino Acid Identities
H. sapiens CYFIP1	1032/1284 (80%)	843/1284 (65%)
H. sapiens PIR121 (CYFIP2)	1027/1280 (80%)	845/1280 (66%)
M. musculus SHYC (CYFIP1)	1028/1281 (80%)	833/1281 (65%)
M. musculus CYFIP2	1025/1280 (80%)	844/1280 (65%)
D. rerio CYFIP	1032/1281 (80%)	840/1281 (65%)
C. elegans gex-2	888/1294 (68%)	667/1294 (51%)

that they insert next to in the correct orientation (Rorth, 1996b). *EP(3)0789* and *EP(3)3267* were in the correct orientation to allow GAL4-driven over-expression and misexpression of *DSra-1* .

It is interesting to note that the *S. cerivisiae* gene project had previously revealed that this yeast contains no Sra-1 or Rac candidate. Since we postulate a role for DSra-1 as a Rac-specific effector, a yeast homolog of Sra-1 might not be expected.

3.3 DSra-1 expression pattern

Whole mount RNA *in situ* hybridization experiments were performed on embryos with a DIG labeled anti-sense probe generated from the cDNA LD47929. *DSra-1* was found to be expressed ubiquitously throughout the embryo, but was enriched within the central nervous system (CNS) (Fig. 3.4).

Given the high degree of homology between the human and *Drosophila* forms of Sra-1, the possibility of using antibodies previously generated against the N-terminal 406 amino acids of the human Sra-1 was tested to detect localization of DSra-1 in the developing embryo (Kobayashi et al., 1998). A fragment coding for the N-terminal 406 amino acids of DSra-1 was ligated in frame into pGEX5X-3, transformed into BL-21 cells and expressed. The GST-DSra-1(1-406) was isolated and used in the affinity purification of polyclonal anti-human Sra-1 that had previously been purified against human Sra-1. The antibodies purified against DSra-1(1-406) were used to probe western blots containing *Drosophila* embryo protein extract and GST-DSra-1(1-406) expressed and isolated from BL21 cells. On both blots only single bands were noted (Fig 3.5A).

Figure 3.4 *DSra-1* is expressed in the central nervous system.

Whole mount RNA *in situ* of late stage (17) embryo showing *DSra-1* transcripts in the central nervous system (CNS) (arrows). (A) Lateral view of localization of *DSra-1* transcript in the CNS. (B) Ventral view of localization of *DSra-1* transcript in CNS.

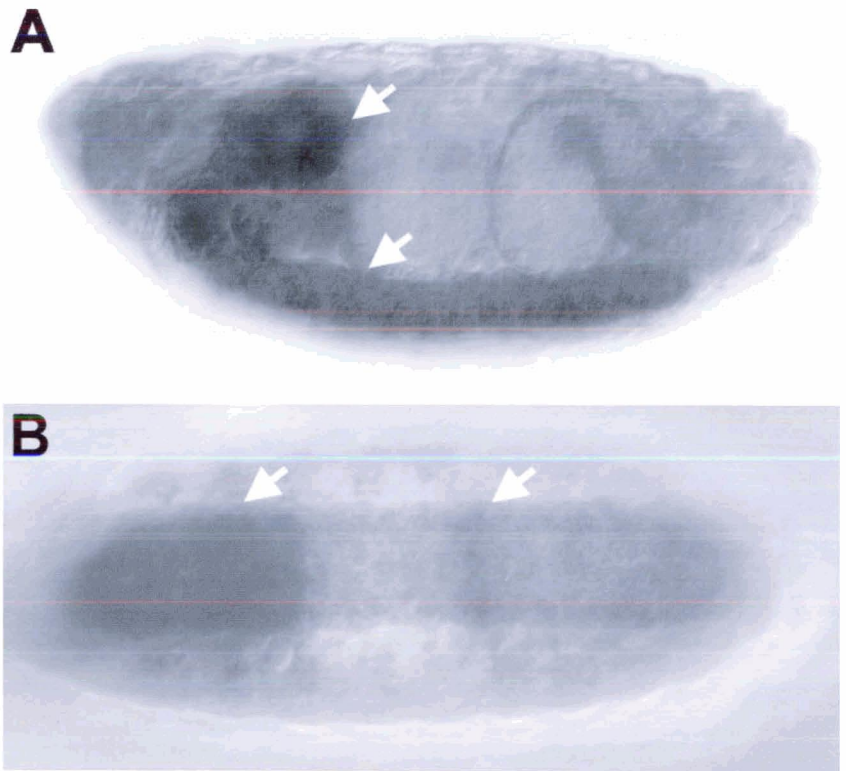
A
B

In order to demonstrate ability of the anti-human Sra-1 antibody to recognize *Drosophila* Sra-1 immunohistochemically, *DSra-1* was over-expressed from a proximal EP insertion line, *EP(3)0789*, in a tissue specific pattern and stained with the antibody. Over-expression of DSra-1 in the amnioserosa of *As-GAL4/EP(3)0789* embryos by the tissue specific driver, *As-GAL4*, and subsequent staining with the antibody revealed strong staining in the amnioserosa as would be expected (Fig. 3.5B). This led us to believe that anti-human Sra-1 antibodies are acceptable for use against DSra-1.

Drosophila embryos aged 0-24 hours after egg laying (AEL) were collected and stained with anti-Sra-1 antibodies. The staining pattern revealed an enrichment of DSra-1 at the leading edge of the epidermis during dorsal closure. Enrichment at the leading edge has also been described for a number of proteins implicated in dorsal closure including DPAK, Puckered, Dpp, non-muscle myosin II and F-actin (Harden et al., 1996; Noselli and Agnes, 1999). Kobayashi et al. (1998), demonstrate an ability of Sra-1 to interact and co-localize with F-actin, thus it was speculated that DSra-1 may be involved in regulation of F-actin at the leading edge during the formation of the actin purse string (Noselli and Agnes, 1999).

Phosphotyrosine levels are also elevated at the leading edge during dorsal closure and are a reliable indicator of the status of the leading edge cytoskeleton, with there being a strong correlation between the distribution of phosphotyrosine and that of F-actin (Harden et al., 1999; Magie et al., 1999) (Fig. 3.5C). Phosphotyrosine is also useful for examining the morphology of the embryo as it localizes to the cellular membrane. The distribution of DSra-1 protein at the leading edge is similar to that of phosphotyrosine, with both remaining elevated at the dorsal midline until shortly after closure (Fig. 3.5D).

Figure 3.5 Human anti-Sra-1 antibodies recognize DSra-1.

(A) Western blot of extracts of untransformed BL21 cells and BL21 cells expressing a 1-406 amino acid portion of DSra-1, as well as whole cell lysate from 0-12hr *Drosophila* embryos, incubated with anti-human Sra-1 antibodies affinity purified against the same 406 amino acid portion of DSra-1. (B) In order to demonstrate affinity of the anti-human Sra-1 antibody to recognize *Drosophila* Sra-1 in tissues, *DSra-1* was expressed from a proximal EP insertion line, *EP(3)0789*, in a tissue specific pattern and stained with the antibody. Over-expression of DSra-1 in the amnioserosa of *As-GAL4/EP(3)0789* embryos by the tissue specific driver, *As-GAL4*, and subsequent staining with the antibody revealed strong staining in the amnioserosa as would be expected (arrow) as compared to (D).

(C) Anti-phosophotyrosine staining of *Drosophila* embryo, with arrows indicating staining at the leading edge of the epidermis. (D) Anti-HumanSra-1 staining of *Drosophila* embryo exhibiting similar staining pattern as indicated by arrows. (E) Anti-human Sra-1 staining of histoblasts as indicated by arrows. (F) Confocal micrograph of embryo stained with anti-human Sra-1 affinity purified antibody depicting staining pattern on leading edge of the epidermis (arrows).

A
BL21
1-406aa DSra-1
0-24hr embryo extract
kDa
177
114
81
64
49
37
B
C
D
E
F

Localization of DSra-1 was also noted in the neuroblasts, and what may be the histoblast nests in the developing embryo (Hartenstein, 1993) (Fig. 3.5E and data not shown).

3.4 DSra-1 binds activated Rac1 in vitro

Mammalian Sra-1 was shown to interact with activated Rac1, that is Rac1 in its GTP bound state (Kobayashi et al., 1998). Sra-1 lacks the Cdc42 Rac interactive binding domain (CRIB) that is commonly present in proteins that bind Rac1, though this domain is not a necessity as there are numerous binders of the Rho subfamily of GTPases that do not have CRIB domains (Noselli and Agnes, 1999) (Bishop and Hall, 2000).

In order to test DSra-1 for its ability to bind GTP-bound Rac1, a GST-pull down assay was performed. DSra-1 coding sequences were cloned into pXJFLAG from which transcription by phage T7 polymerase and translation by rabbit reticulolysate in the presence of ^{35}S-methionine produced ^{35}S-labelled DSra-1. GST-DRac1 and GST-Dcdc42 were expressed in BL21, bound to glutathione sepharose beads, and exchanged with either an unhydrolysable form of GTP (GTP-γS) or GDP to give the active and inactive forms of the p21s, respectively. Under the conditions of a fairly strict wash buffer of Tris pH 7.5 + 0.5% Triton-X, DSra-1 was found to preferentially bind GTP-γS -DRac1 vs. GDP-DRac1, GTP-γS -Dcdc42 and GDP-Dcdc42 (Fig. 3.6).

3.5 DSra-1 does not bind activated Rac1 in yeast two hybrid system

It has been determined by GST-pull down binding assays that a truncated form of human Sra-1 containing the first 406 amino acids is capable of binding GTP-Rac1 (Kobayashi et al., 1998). The yeast two-hybrid system was used in an attempt to

Figure 3.6 DSra-1 preferentially binds GTP-bound DRac1.

In order to test DSra-1 for its ability to bind GTP-bound Rac1, a GST-pull down assay was performed. DSra-1 coding sequences were cloned into *pXJFLAG* from which transcription by phage T7 polymerase and translation by rabbit reticulolysate in the presence of ^{35}S-methionine produced ^{35}S-labelled DSra-1. GST-DRac1 and GST-Dcdc42 were expressed in BL21 cells, bound to glutathione sepharose beads, and exchanged with either an unhydrolysable form of GTP (GTP-γS) or GDP to give the active and inactive forms of the p21s, respectively. Under the conditions of a fairly strict wash buffer of Tris pH 7.5 + 0.5% Triton-X, DSra-1 was found to preferentially bind GTP-γS -DRac1 vs. GDP-DRac1, GTP-γS -Dcdc42 and GDP-Dcdc42.

The lane labelled 10% input contains the protein products of the transcription and translation of *pXJFLAG-DSra-1* and is a control to demonstrate the expression of radiolabelled DSra-1, as well as provide an indicator of its size.

This result is representative of several separate experiments. Coomassie blue staining of the gels indicated equal loading of the small GTPases (data not shown).

10% input
GST-GTPγS
GST-Cdc42-GTPγS
GST-Cdc42-GDP
GST-Rac1-GTPγS
GST-Rac1-GDP
DSra-1

determine the domain necessary for effective binding of DSra-1 to Rac1. The yeast two-hybrid assay has been shown to be very effective for both identifying putative effectors for the Rho family of small GTPases, and mapping interaction domains.

The constitutively active and dominant negative forms of Rac are used in the yeast system to enable the investigator to determine which form of the GTPase the protein of interest favours. In the case of constitutively active RacV12, a glycine at amino acid 12 has been changed to valine, reducing the intrinsic GTPase activity of GTP-bound Rac and preventing GTPase activating proteins from activating Rac's endogenous GTPase activity, effectively maintaining Rac in its active, GTP-bound form (Diekmann et al., 1991). In contrast, by mutating amino acid 17 from threonine to asparagine, RacN17 has a preferential affinity for GDP and is effectively inactive (Ridley et al., 1992). In this manner it is possible to produce the desired form of Rac in a biological system such as yeast.

The interaction trap yeast two-hybrid method (see Materials and Methods section 2.22) was used to test the interaction between DSra-1 and DRac1. A *Drosophila DRac1V12* cDNA was cloned into pJG4-5 via *Eco*RI and *Xho*I. A C-terminal CAAX box in the Rho family of GTPases is responsible for localizing the protein to the cell membrane and the removal of the signal is required to keep the DRac1V12-fusion protein inside the yeast nucleus in order to complete the transcription factor upon a successful interaction (Hancock et al., 1991). To inactivate the CAAX box in DRac1V12, site directed mutagenesis was used to mutate a thymine to an adenosine in order to produce an amino acid mutation of a cysteine to a serine at amino acid position 189. A pJG4-5-DRac1N17 plasmid containing the dominant negative form of DRac1 with an inactive

CAAX box was constructed in a similar manner. When transformed into the EGY48 yeast strain, the pJG4-5-DRac1V12 plasmid causes expression of, under the control of a GAL1 promoter, a fusion protein containing DRac1V12 or DRac1N17, a nuclear localization signal and an acid transcriptional activation domain (Golemis et al., 1999).

Full length *DSra-1* and a truncated *DSra-1* containing only the first 406 amino acids, DSra-1(1-406), were cloned into pEG202, to express these as fusion proteins with a LexA DNA binding domain under the control of the ADH promoter (Golemis et al., 1999).

The lacZ reporter plasmid, pSH18, was used to determine any interaction between Rac1 and DSra-1, and if binding of DRac1V12 is favored over DRac1N17.

DSra-1 was shown not to cause self activation of the lacZ reporter, and it was demonstrated that the fusion protein localizes to the nucleus by a repression assay, where the LexA-Sra-1 fusion protein is able to bind LexA operator sites on a pJK101 lacZ reporter plasmid and interfere with a GAL1 UAS upstream of two LexA domains (Golemis et al., 1999).

Neither form of DRac1 was able to bind DSra-1, therefore this assay was unable to demonstrate binding of DSra-1 to DRac1V12 or DRac1N17.

It is possible that DSra-1 may not bind DRac1 in the context of the yeast environment, and it is also possible that DSra-1 may be deleterious to the yeast, causing degradation of the resulting fusion protein. Truncations of DSra-1 may alleviate this problem, or the *in vitro* binding GST-pull down method may be used to further the analysis of the binding domain instead.

3.6 Over-expression of DSra-1 during embryogenesis causes a failure in dorsal closure

To test whether *DSra-1* expression could be induced from the EP lines by the *GAL4* system, *EP(3)0789* or *EP(3)3267* was crossed with *hs-GAL4*$^{M-4}$ and adult flies of the genotype *EP(3)0789/hs-GAL4*$^{M-4}$ or *hs-GAL4*$^{M-4}$*,EP(3)3267/TM3Sb* were heat shocked and total RNA isolated. The total RNA gathered from these flies was probed for levels of induction using Northern blots with *DSra-1* cDNA as a probe. A cDNA encoding *rp49*, a ribosomal protein, was used as a loading control. Both EP insertions were capable of strongly inducing *DSra-1* transcription, with transcript levels steadily increasing as flies were aged from 0 to 3 h after heat shock (Fig. 3.7). This result demonstrated that *EP(3)0789* and *EP(3)3267* could be used to examine the effects of over-expression of DSra-1 during development and possibly indicate roles for DSra-1 in the process of dorsal closure.

Since the EP-elements induce *DSra-1* expression under the control of a *GAL4* driver, the effects of over expression of *DSra-1* during embryogenesis were determined by collecting and heat shocking embryos 6-12 hours after egg laying (AEL) from a *hs-GAL4*^{2207}*/CyO x EP(3)3267/TM3Sb* cross. Significant numbers of embryos bearing holes in the dorsal surface, germband retraction failures and head defects of their cuticles were seen (Fig. 3.8A, 8B, 8C and 8D). The holes present in the cuticle represent a failure in dorsal closure. Similar phenotypes are seen in the heat shock induced expression of *hs-DRac1N17, UAS-DRac1V12* and in germ line clones of embryos bearing null alleles of the *DRac* family genes, *DRac1*, *DRac2* and *DMtl* (Hakeda-Suzuki et al., 2002; Harden et al., 1995).

Figure 3.7 *EP(3)0789* and *EP(3)3267* can be used to express *DSra-1* with a GAL4 driver.

Northern blots showing upregulation of expression of *DSra-1* induced by *hs-GAL4*^{M4} driver. (A) *EP(3)0789*. (B) *EP(3)3267*. Heat shock (HS) induction was performed at 37°C for 1 hour and embryos allowed to age at 25°C for the indicated time. *rp49* was used as a loading control.

A
Canton S
hs-GAL4M4 / + 1hr HS
hs-GAL4M4 x EP(3)0789
hs-GAL4M4/EP(3)0789 1hr HS
hs-GAL4M4/EP(3)0789 1hr HS aged 1hr
hs-GAL4M4/EP(3)0789 1hr HS aged 2hr
B
Canton S
hs-GAL4M4 / + 1hr HS
hs-GAL4M4 /EP(3)3267 1hr HS
hs-GAL4M4/EP(3)3267 1hr HS aged 1hr
DSra-1
rp49

The use of other drivers such as *69B-GAL4,* expressing GAL4 in the *Drosophila* ectoderm from stage 9 onwards, and *ptc-GAL4,* a GAL4 driver which mimics the segmental expression pattern of *patched,* was investigated with the *EP* lines (Hinz et al., 1994; Staehling-Hampton et al., 1994). Cuticle preparations of *69B-GAL4/EP(3)3267* and *ptc-GAL4/EP(3)3267* embryos revealed a failure to generate cuticle, the morphology of which was further investigated by microscopy of anti-phosphotyrosine stained embryos. A large number of the resulting embryos were in a completely disrupted state, however it was possible to determine a particular phenotype in a number of embryos in which the leading edge had failed to elongate during dorsal closure and a loss of phosphotyrosine nodes at the leading edge was seen, similar to DRacN17-expressing embryos (Fig. 3.8F and 3.8G) (Harden et al., 1995). The phosphotyrosine nodes indicate the sites of adherens junctions therefore the loss of the nodes possibly denotes a disruption of the adherens junctions that participate in dorsal closure (Harden, 2002).

Thus, both cuticle preparations and phosphotyrosine stainings revealed defects in dorsal closure.

3.7 Over-expression of DSra-1 partially rescues the effects of DRac1N17 expression

Since DSra-1 binds activated DRac1 *in vitro*, is localized at the leading edge and the expression of *DSra-1* causes defects in dorsal closure, it was speculated that DSra-1 was a DRac1-effector during dorsal closure. To test the hypothesis, over-expression of *DSra-1* was used to try and rescue *DRac1N17*-induced dorsal closure defects.

Figure 3.8 Defects in embryonic development caused by over-expression of DSra-1.

(A-E) Cuticle preparations of embryos heat shocked 6-12 hours AEL for 1 hour at 37°C and allowed to recover for 36 hours at 21°C. (A) Canton S wild-type cuticle. (B) *hs-GAL4^{M4}/UAS-RacN17* showing dorsal closure failure (arrow). (C) *hs-GAL4^{M4}/EP(3)3267* embryo showing dorsal closure failure similar to that of DRacN17 (arrow). 34.4% of embryos on slide exhibited this phenotype (n = 90) (D) hs-RacV12 embryo showing a failure of the germband to retract during embyogenesis (arrow) (E) *hs-GAL4^{M4}/EP(3)3267* embryo showing failure of germ band retraction similar to DRacV12 phenotypes 14.4% of embryos on slide exhibited this phenotype (n = 90) (arrow).

(F) View of leading edge epidermis of wild-type embryo stained with anti-phosphotyrosine showing elongation of epidermal cells at the leading edge. Note the presence of phosphotyrosine nodes at the leading edge indicating the adherens junctions (arrows). (G) and (H) Anti-phosphotyrosine staining of *ptc-GAL4/EP(3)3267* embryos demonstrating a failure of elongation of the leading edge epithelial cells as compared to a wild type embryo. Note that there is also a loss of the phosphotyrosine nodes at the boundary between the leading edge cells and the amnioserosa (arrows). Loss of the phosphotyrosine nodes is also seen in DRacN17 embryos and possibly indicates a disruption of the adherens junctions that participate in dorsal closure (Harden, 2002).

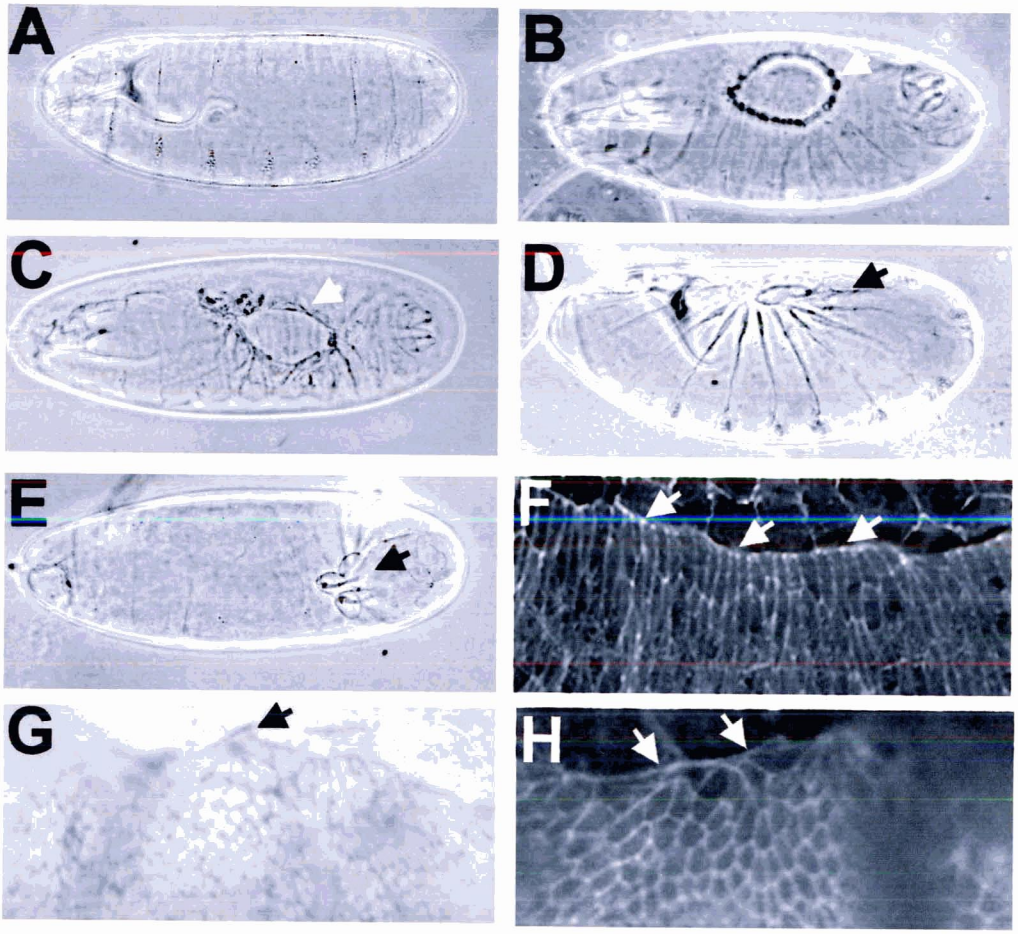
A
B
C
D
E
F
G
H

UAS-DRac1N17,hs-GAL4^{M4} (*N17-104*) flies were mated to *EP(3)0789* and the resultant embryos collected 6-12 hours AEL and heat shocked for 1 hour. As a control, *N17-104* was mated to wild type *Canton S* flies and treated in the same manner. Embryos were then fixed and examined for defects by cuticle preparation.

The inclusion of *EP(3)0789* in the *N17-104* background resulted in an increase of surviving larvae from 27.8% to 35.9% ($p = 0.0006$), however, there did not appear to be any significant rescue of the *DRac1N17*-induced dorsal closure failure phenotype (Table 2).

Further experiments utilizing shorter heat shocks of 30 minutes and 10 minutes were conducted in an attempt to demonstrate rescue of the *DRac1N17*-induced dorsal closure failure. It was thought that since the over-expression of *DSra-1* alone could cause a failure in dorsal closure, it could be possible that a lengthy induction of *DSra-1* could overwhelm any rescue of *DRac1N17*-induced dorsal closure failure by *DSra-1*, with failure caused by *DSra-1* itself. None of the shorter experiments produced significantly differing results.

From this it could be concluded that there is a mild role of DSra-1 acting downstream of Rac1 during embryogenesis but not apparently during dorsal closure.

3.8 Generation of DSra-1 mutants

A null mutant can be used to specifically characterize the functional role of a gene through phenotypic analysis and by interaction studies with other mutants and transgenic lines. The presence of EP-elements upstream of *DSra-1* allowed for targeted deletions of *DSra-1* by re-mobilization of the EP-element (Hawley and Waring, 1988). Two hundred

Table 3.2 Partial rescue of dominant negative RacN17 over-expression by DSra-1.

UAS-Rac1N17, HS-GAL4^{M4} (*N17-104*) flies were mated to *EP(3)0789* and the resultant eggs collected 6-12 hours AEL and heat shocked for 1 hour. As a control *N17-104* was mated to wild type *Canton S* flies and treated in the same manner. Embryos are fixed and examined for defects by cuticle preparation.

The inclusion of *EP(3)0789* in the *N17-104* background resulted in an increase of surviving larvae from 27.8% to 35.9% ($p = 0.0006$), however, there did not appear to be any significant rescue of the *DRac1N17*-induced dorsal closure failure phenotype.

Calculations are based upon embryos that formed a cuticle. No cuticle may represent both unfertilized eggs and embryos that failed to form a cuticle.

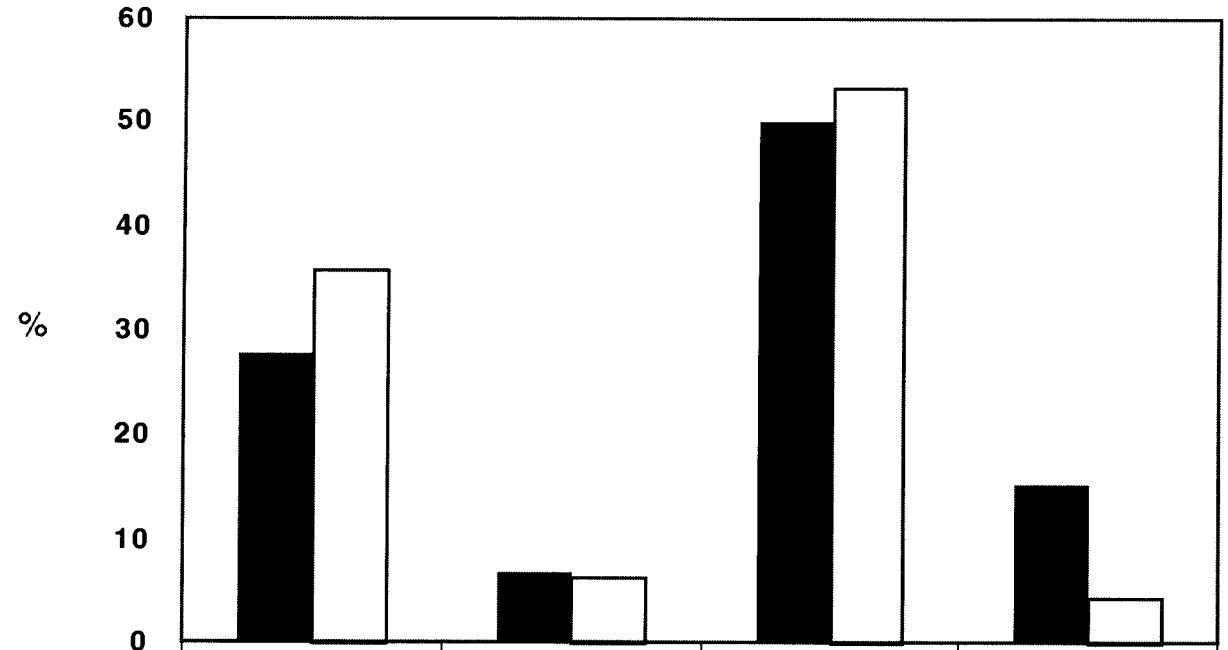

	larvae	WT embryo	dorsal defect	no cuticle	
■Canton S	27.8	6.8	50.2	15.3	n=535
□DSra-1	35.9	6.2	53.5	4.5	n=1066

p=.0006

excision events from the *EP(3)3267* line were produced as described in Materials and Methods.

Since the imprecise excision event results in deletions of random length and direction about the insertion point, many lines needed to be screened in order to obtain a deletion of only *DSra-1*, as it is closely flanked within 500 nucleotides on both sides by neighbouring genes (Fig. 3.2A).

Excision lines were examined by PCR using upstream and downstream primers flanking *DSra-1* in order to determine the precise size of the deletions and check for preservation of the flanking genes. The upstream primer (P1) contained the sequence, CGTCTGCGAGTACTTGCGCTCAGGC, while the downstream primer (P2) contained the sequence, GCGACGAGGACGATATGACCGAGG (Fig. 3.2A). Screening of the 200 lines via PCR revealed a single line of interest, $Sra\text{-}1^{18b}$ (Fig. 3.9A). Line $Sra\text{-}1^{18b}$ has an 709bp excision in the genomic region of *DSra-1*, has a shorter *DSra-1* transcript on a Northern blot, and is not homozygous viable and dies in the early pupal stages (Fig. 3.9B). This deletion is located downstream of the TATA box, covers the start codon, and extends 657 nucleotide bases into the coding region of *DSra-1* (219 amino acids) (Fig. 3.10B). The next two available start codons are out of frame and code for short nonsense products.

3.9 Construction of transgenic DSra-1 flies

In order to ensure that a phenotype is due to a loss of function mutation in *DSra-1*, the phenotypes must be rescued by expression of a *DSra-1* transgene. The creation of

Figure 3.9 PCR and Northern blots reveal *DSra-1*^{18b} to be a deletion of *DSra-1*.

(A) Example of screening method used to search generated P-element excision lines for potential lesions in *DSra-1*. Primers upstream and downstream of *DSra-1* were used to perform PCR within that region on genomic DNA isolated from excision lines. Shorter PCR products reveal the presence of a lesion within the region of *DSra-1*. In this case PCR was performed on genomic DNA of Canton S and *DSra-1*^{18b}*/TM3* flies. A wild type band of 4.6kb and smaller 3.8kb band from the *DSra-1*^{18b} allele is seen in the *DSra-1*^{18b}*/TM3* flies revealing the presence of a lesion. In all cases the TM3 balancer provided an internal wild type control band for rapid screening of potential excisions.

(B) Northern blots of *DSra-1*^{18b}*/TM3* flies reveal a wild-type transcript and a smaller mutant transcript compared to the single wild-type transcript in the Canton S line.

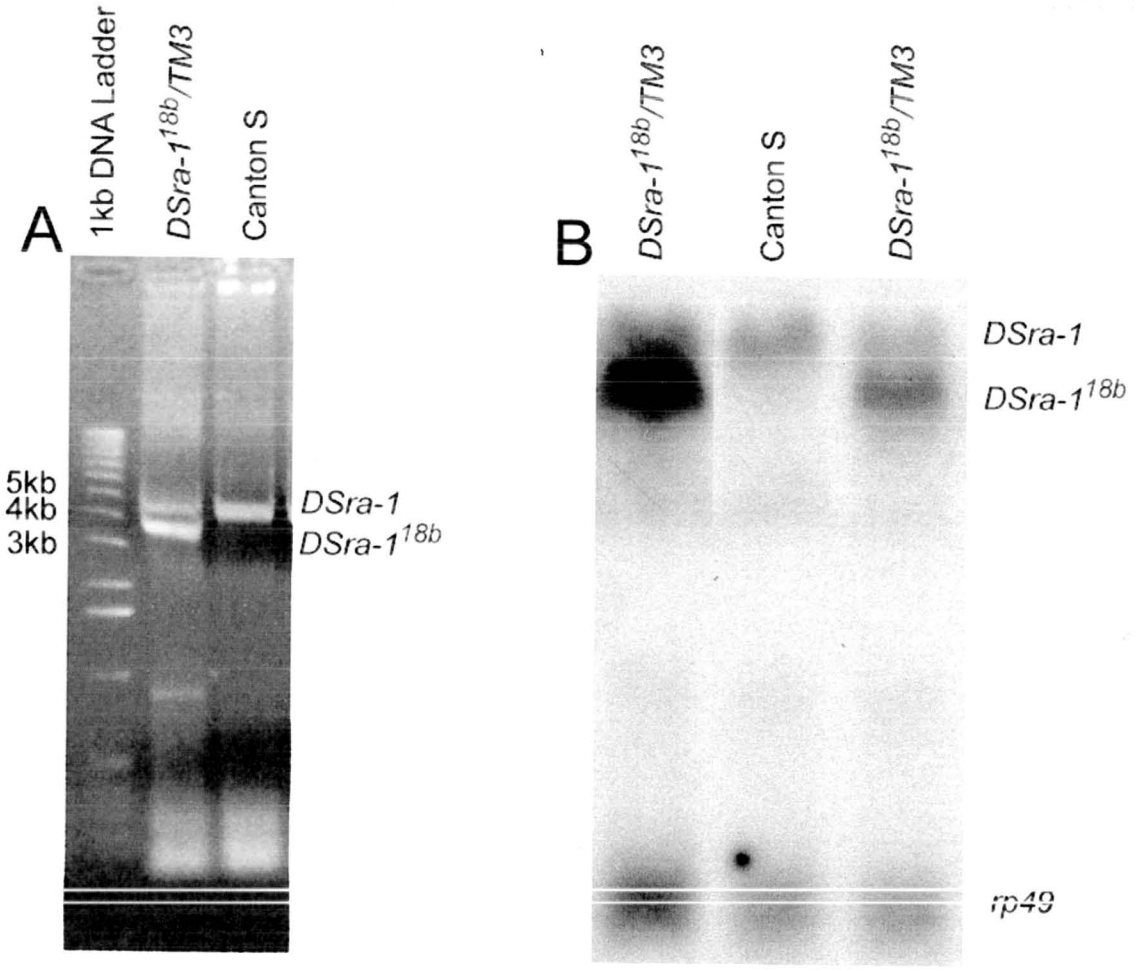
A
1kb DNA Ladder
DSra-1^18b/TM3
Canton S
5kb
4kb
3kb
DSra-1
DSra-1^18b
B
DSra-1^18b/TM3
Canton S
DSra-1^18b/TM3
DSra-1
DSra-1^18b
rp49

Figure 3.10 *DSra-1*^{18b} contains a deletion of 657 nucleotides.

(A) Sequencing results obtained from excising and purifying the smaller 3.8kb band from the gel shown in Fig. 3.9A. (B) Results of sequencing are compared to the wild type cDNA. Alignment performed using the Clustal method of the programme MEGALIGN of LASERGENE 99 package (DNAStar, Madison WI). Numbers indicate the distance from the start of the cDNA. Bent arrow indicated the start codon. Arrows indicate sites of excision. The excision event left a small number of nucleotides that bear no identity to *DSra-1* or the P-element.

A

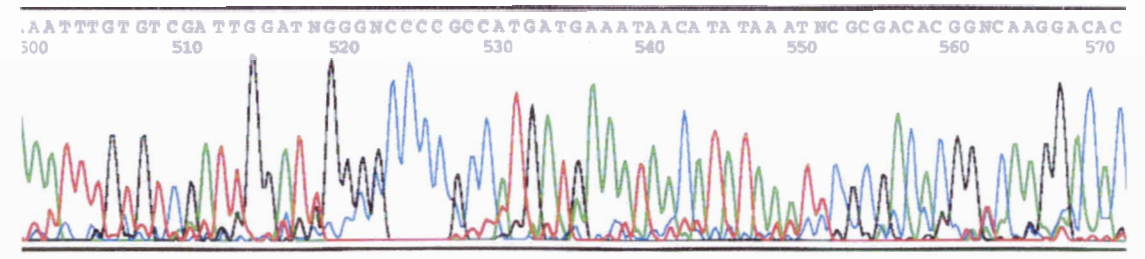
500
510
520
530
540
550
560
570

B

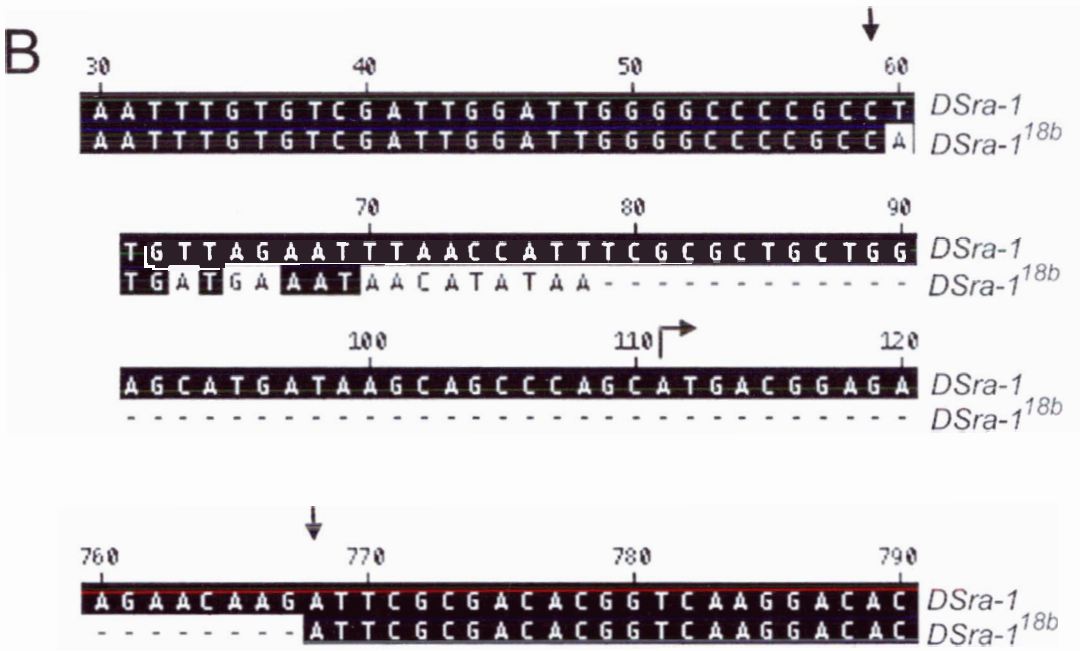
30
40
50
60
DSra-1
DSra-1 18b
70
80
90
DSra-1
DSra-1 18b
100
110
120
DSra-1
DSra-1 18b
760
770
780
790
DSra-1
DSra-1 18b

UAS-DSra-1 transgenes also allows a greater versatility in *DSra-1* over-expression studies.

A *DSra-1* cDNA was cloned into the *Drosophila* nonautonomous P-element vector pUAST, thus placing its expression under the control of a *UAS* promoter as described in Materials and Methods.

Transgenic *Drosophila* lines bearing individual *UAS-DSra-1* insertions in the X, 2nd and 3rd chromosomes were established. The localization of the P-element insertions to each chromosome was determined by crossing the various lines to individual balancers for each chromosome and screening for the maintenance of heterozygosity of the balancer with the insertion in subsequent generations.

Northern blot analysis of these lines crossed with *hs-GAL4*^{M4} and heat shocked for 1 hour at 37°C, were used to test that the *UAS-DSra-1* transgenes were functioning (data not shown).

3.10 Characterization of DSra-1 mutant alleles

To determine if the *DSra-1*^{18b} lethality was due to the mutation within the *DSra-1*^{18b} genomic region, a search for deficiencies in the locus was performed using the Flybase website. Sequences removed by the deficiency *Df(3R)ea* (breakpoints 88E7-13; 89A1) include the genes *easter* (*ea)* and *supernova* (*spno)* (Chasan and Anderson, 1989; Webster et al., 1992) (Fig. 3.2A). As *DSra-1* had been molecularly predicted to be positioned between *ea* and *spno*, it was expected that *Df(3R)ea* should remove the *DSra-1* locus. In an attempt to confirm that *DSra-1* was within the lesion, Northern blot analysis

of *DSra-1* transcript levels in flies heterozygous for *Df(3R)ea* was performed and it appeared that transcript levels were reduced (data not shown).

As was shown from genetic analysis, *DSra-1*^{18b}, itself homozygous lethal, complemented the *Df(3R)ea* deficiency. A Northern Blot was performed at the time on the hemizygote, *Df(3R)ea/DSra-1*^{18b}, and no transcript for full length *DSra-1* was seen. This led us to believe that a second site mutation on the *DSra-1*^{18b} allele was responsible for lethality.

At this time a collaboration was initiated with Annette Schenck and Angela Giangrande of the Department of Molecular Pathology, Institut de Genetique et de Biologie Moleculaire et Cellulaire, Illkirch, France. Their group is primarily interested in the fragile X mental retardation protein (FMRP) and the developing *Drosophila* nervous system and they became interested in DSra-1 as a homolog of human CYFIP1 and CYFIP2, which interact with (Schenck et al., 2001). They had also begun to create excisions at the *DSra-1* locus and had produced a large deletion of *DSra-1*, and had named it *CYFIP*$^{85.1}$. *CYFIP*$^{85.1}$ was homozygous lethal and complemented *Df(3R)ea*, furthermore our collaborators had performed PCR on flies of the genotype *CYFIP*$^{85.1}$*/Df(3R)ea* within the deleted locus and had produced a product indicating that the *Df(3R)ea* deficiency was *not* a deficiency of *DSra-1*. *DSra-1*^{18b} and *CYFIP*$^{85.1}$ failed to complement each other and PCR using an upstream primer, P1 (CGTCTGCGACTACTTGCGCTCAGGC), and a downstream primer, P3 (GCAAGGTGTGCGAGTCCGACATC), within the deleted region of *Sra-1*^{18b}, on flies of the genotype *Df(3R)ea/DSra-1*^{18b} produced a product (Fig. 3.2A). Both *DSra-1*^{18b} and *CYFIP*$^{85.1}$ die in the early pupal stages, and *CYFIP*$^{85.1}$ early pupal lethality can be rescued

by expression of *UAS-DSra-1* with a pan-neuronal driver, *elav-Gal4* (Schenck et al., 2003). These various results indicated that both *DSra-1* alleles are lethal due to mutation of *DSra-1* and not a second site gene.

3.11 DSra-1 has a required role in neurons during development

As part of our collaboration, A. Schenck et al. examined the effects of loss of *DSra-1* on the *Drosophila* developing nervous system. They were able to demonstrate that *DSra-1* alleles produce defects in axon growth, branching, and pathfinding. In addition the organization of the neuromuscular junction was affected.

Our *UAS-DSra-1* transgenes were used in their research. A pan-neuronal driver, *elav-GAL4*, and *UAS-DSra-1* was used to rescue lethality of the $CYFIP^{85.1}$ strain. It was specifically demonstrated that such expression rescued the axon midline crossing defects present in $CYFIP^{85.1}$ embryos. Finally *UAS-DSra-1* was used to demonstrate that DSra-1 antagonizes DRac1 and DFMR1 during neuronal connection of the intersegmental motor nerves to the muscle. (Schenck et al., 2003). A joint publication was produced from our efforts (Schenck et al., 2003).

3.12 DSra-1 is not a member of the JNK cascade

Previous studies suggest that Rac1 is an activator of the JNK cascade during dorsal closure (Harden, 2002). For example, it has been shown that over-expression of *DRacV12* in *Drosophila* embryos can cause ectopic activation of the JNK cascade during dorsal closure (Glise and Noselli, 1997). The experiment utilized the *puc-lacZ* enhancer-trap insertion, puc^{E69}, that allows the transcriptional control of *puckered* (*puc)* gene expression to be visualized by staining for β-galactosidase (Ring and Martinez Arias,

1993). As *puc* transcription is regulated by the JNK cascade, the pattern of β-galactosidase staining in such an experiment reveals areas of JNK cascade activation. Since DSra-1 could bind activated DRac1, a similar method to determine if DSra-1 was a member of the JNK cascade was used.

Flies of the genotypes *en-GAL4/+;puc^{E69}/+* and *EP(3)3267/TM3Sb* were crossed; the resulting embryos collected over 24 hours and stained with anti-β-galactosidase antibodies. Resulting embryos were examined for overstaining of β-galactosidase as evidence of upregulation of *puckered* caused by an over-expression of *DSra-1*. No evidence was found in over 100 embryos (Fig. 3.11A). Thus we conclude that *DSra-1* is not an activator of the JNK cascade.

To investigate further a potential requirement for *DSra-1* in the JNK cascade, we looked at the effects of loss of zygotic and maternal *DSra-1* on the JNK cascade-dependent transcription of *decapentaplegic* (*dpp)* in the leading edge cells. The loss of *dpp* expression in the leading edge cells is seen in mutations of the JNK pathway components such as *hep* (Glise and Noselli, 1997).

Germ line clones were made of the *DSra-1* null allele *CYFIP$^{85.1}$*, utilizing the method of Chou and Perrimon as explained in Material and Methods (Chou and Perrimon, 1996).

CYFIP$^{85.1}$ is a deletion spanning a larger portion of *DSra-1* than *DSra-1^{18b}* (Schenck et al., 2003). Germ line clones were constructed based upon the following crosses: *hsFLP;kD/TM3* x *FRT82B,ovoD/TM3* males, followed by

Figure 3.11. *DSra-1* is not a member of the JNK cascade.

(A) Over-expression of *DSra-1* does not upregulate the transcription of the JNK cascade product, *puckered (puc)*. It has been demonstrated that expression of either constitutively active *DRac1V12* or *Cdc42V12* upregulate the transcription levels of the JNK cascade product, *puc* (Glise and Noselli, 1997). A *puc-lacZ* enhancer-trap insertion, puc^{E69}, that allows the transcriptional control of *puckered (puc)* gene expression to be visualized by staining for β-galactosidase, was used (Ring and Martinez Arias, 1993).

Control *en-GAL4;*puc^{E69}*/UAS-Cdc42V12* embryo, stained with anti-β-galactosidase, demonstrating upregulation of *puc* expression in *engrailed* (*en*) segmental stripes (arrow). No evidence of anti-β-galactosidase staining in *en* stripes was seen in *en-GAL4;*puc^{E69}*/EP(3)3267* embryos driving the expression of *DSra-1* from the *EP(3)3267* P-element. Only a wild type puc pattern at the leading edge was seen (arrow).

(B) *dpp in situ* experiments demonstrating no loss of *dpp* expression in the leading edge of embryos lacking maternal and zygotic *DSra-1*, as compared to wild type Canton S embryos (arrows). The loss of *dpp* expression in the leading edge cells is seen in mutations of the JNK pathway components such as *hep* (Glise and Noselli, 1997).

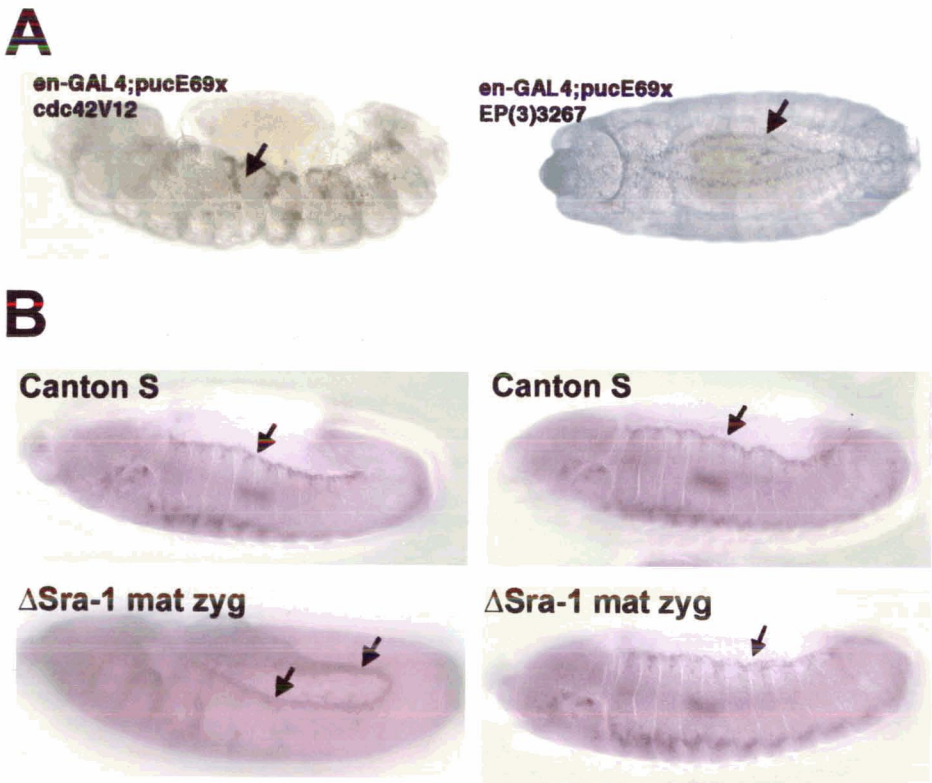
A
en-GAL4;pucE69x
cdc42V12
en-GAL4;pucE69x
EP(3)3267
B
Canton S
Canton S
ΔSra-1 mat zyg
ΔSra-1 mat zyg

hsFLP;FRT82B,ovoD/TM3 males x *FRT82B,CYFIP*$^{85.1}$*/TM3*. The progeny of the last cross were heat shocked during L3 stage of larval development in order to effect recombination in the developing germ line of these organisms. The resultant *FRT82B,ovoD/FRT82B,CYFIP*$^{85.1}$ females were crossed with *CYFIP*$^{85.1}$*/TM3* males, producing embryos deficient in maternal and zygotic *DSra-1*. These embryos were examined by RNA *in situ* for *dpp* expression in order to determine if *DSra-1* had a role in JNK signalling. No loss of *dpp* signal at the leading edge was seen in over 100 embryos, indicating that *DSra-1* has no role in JNK signalling during dorsal closure (Fig. 3.11B).

3.13 DSra-1 is not required for dorsal closure

Embryos deficient in maternal and zygotic *DSra-1* were examined for dorsal closure defects by cuticle preparations; no such defects were found. As further evidence that DSra-1 is not required during dorsal closure, our collaborators could rescue *CYFIP*$^{85.1}$ lethality by using *elav-GAL4*, a pan-neural driver, to express *UAS-DSra-1* (Schenck et al., 2003).

As has been shown, DSra-1 can act as an antagonist of DRac1 signalling (Schenck et al., 2003). Normally over-expression of wild-type *DRac1* during dorsal closure using *hs-DRac1* trangenic flies with *DRac1* under the control of a heat shock promoter, has no effect (Harden et al., 1996). If DSra-1 is acting as a redundant negative regulator of DRac1 during dorsal closure, such defects might be seen if wild-type *DRac1* is over-expressed in a *DSra-1* mutant background. To test for this 6-12 hour AEL *hs-DRac1;CYFIP*$^{85.1}$*/CYFIP*$^{85.1}$ embryos were heat shocked for 1 hour at 37°C, allowed to develop for 24 hours at room temperature and cuticle preparations were performed. *hs-*

DRac1 embryos were used as a control. No evidence of dorsal closure defects was seen in over 100 embryos.

These various results indicate that DSra-1 is not required for dorsal closure to occur.

3.14 DSra-1 regulates basal F-actin in follicle cells

Sra-1 was originally shown to bind F-actin (filamentous actin) *in vitro* and co-localize with cortical F-actin filament at the Rac1V12-induced membrane ruffling area in human KB cells (Kobayashi et al., 1998). The *Drosophila* follicle cells surrounding the developing oocyte develop a basal matrix of F-actin similar to stress fibres in cultured cells, and are thought to enable oocyte elongation by acting as a 'molecular corset' driving constriction of follicle cells perpendicular to the anterior-posterior axis (Gutzeit, 1990b). Proteins, such as Dlar, that have been shown to have a role in regulation of the actin cytoskeleton in other tissues such as the *Drosophila* nervous system, have also been shown to have a role in the regulation of the follicular F-actin (Bateman et al., 2001b). Furthermore, Dlar and Rac have been shown genetically to interact during axon guidance (Kaufmann et al., 1998). While a role of Rac has yet to be demonstrated in regulating follicular F-actin, the general role of Rac in the co-ordination of F-actin and integrins has been well characterized (Harden, 2002).

It was therefore thought that DSra-1 could have a possible role in the regulation of follicular F-actin and follicular clones were designed to investigate that possibility (discussed in Materials and Methods). A ubiquitously expressed green florescent protein (GFP) fused to a nuclear localization signal, *FRT82B,ubi-nls-GFP*, was used along with

FRT82B,CYFIP$^{85.1}$ to generate follicle cell clones deficient in *DSra-1* (see Materials and Methods). In this way *DSra-1* deficient cells could be distinguished from the non-deficient GFP marked cells. As can be seen in clones stained with FITC-phalloidin to mark the F-actin bundles, the *DSra-1* deficient follicle cells were unable to co-ordinate an F-actin basal matrix (Fig. 3.12).

It could be possible that DSra-1 is acting through the SCAR/WAVE complex to enable Arp2/3 to polymerise the F-actin bundles, however this is purely speculative. It does appear that the follicular basal actin could be used as a system to study *in vivo* the roles of DSra-1 in regulating F-actin polymerization (Steffen et al., 2004).

It is interesting to note that the size of the *DSra-1* clone is much smaller than the size of the twin-spot, which consists of a multitude of cells. There are at least two possible explanations for this. The loss of *DSra-1* and subsequent F-actin basal filaments may lead to detachment of extracellular communication and apoptosis (Danial and Korsmeyer, 2004; Margolis and Spradling, 1995). Another explanation is that the loss of F-actin in these cells may cause the impairment of mitosis (Wolf et al., 1999).

3.15 Examination of the effects of p53 upregulation on expression of DSra-1

It has been shown that expression of p53 can cause an induced expression of Sra-1 in mammalian cells (Jin et al., 2000). Transgenic flies with *UAS-p53* insertions were obtained and a heat shock driver, *hs-GAL4*$^{M-4}$, or an *engrailed* driver, *en-GAL4* were used to examine the effects of the induced expression of *p53* on the expression of *DSra-1*. Both Northern blots and whole mount RNA *in situ* failed to demonstrate upregulation of *DSra-1* (Fig. 3.13).

Figure 3.12 Follicle cell clones deficient in *DSra-1* fail to produce a basal F-actin matrix. (A) Follicle cells stained with anti-GFP antibodies. Cells that are brightly stained are those that have undergone recombination and are homozygous for the *82BFRT,ubi-nls-GFP* marker. Cells that are less stained have a *82BFRT,ubi-nls-GFP/FRT82B,CYFIP*$^{85.1}$ genotype, while the two dark cells that did not stain with anti-GFP are those that have undergone recombination to produce homozygous *FRT82B,CYFIP*$^{85.1}$ cells.

(B) *Drosophila* follicle cells in (A) stained with FITC-phalloidin to mark the basal F-actin matrix. A dense matrix of F-actin bundles can been seen in the *82BFRT,ubi-nls-GFP* and *82BFRT,ubi-nls-GFP/FRT82B,CYFIP*$^{85.1}$ cells. These bundles exhibit polarity along an axis perpendicular to the anterior-posterior oocyte axis. The homozygous *FRT82B,CYFIP*$^{85.1}$ cells shown no phalloidin staining.

(C) Merged micrographs of (A) and (B) clearly showing that the unstained cells in (A) are the same cells that fail to stain in (B).

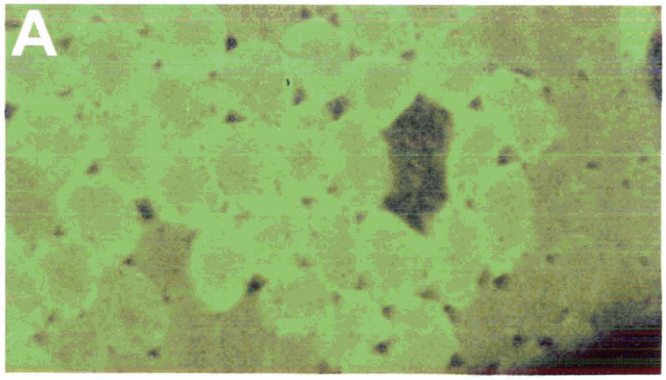
A

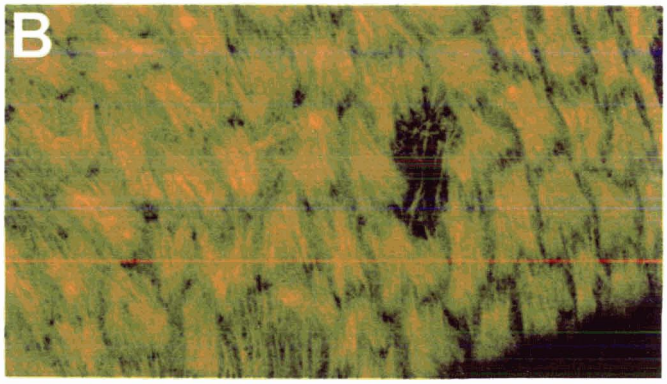
B

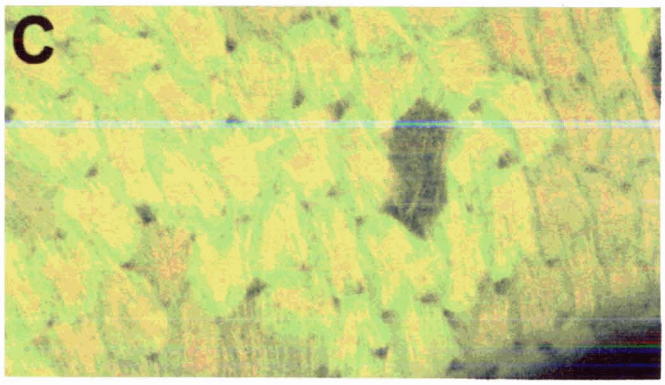
C

Figure 3.13 Over-expression of *p53* does not upregulate *DSra-1*.

Northern blot demonstrating lack of upregulation of *DSra-1* by over-expression of *UAS-p53* in adult flies. *UAS-p53* was driven by the *hs-GAL*^{M4} driver, heat shocked (HS) at 37°C for the indicated time, and aged for 0, 1 or 2 hours after heat shock at room temperature to further induce *p53* expression.

Canton S HS 1hr
hs-GAL4M4 1hr HS
hs-GAL4M4/UAS-p53 1hr HS
hs-GAL4M4/UAS-p53 1hr HS aged 1hr
hs-GAL4M4/UAS-p53 1hr HS aged 2hr
DSra-1
rp49

RESULTS PART 2

Drosophila Plenty of SH3 (*DPOSH*)

4.1 Cloning and sequencing Drosophila POSH

POSH was originally pulled out of yeast two hybrid screen of a *M. musculus* library for new binding proteins of activated Rac (Tapon and Hall, 1997). In mammalian cells it was shown to activate the JNK MAPK pathway and induce apoptosis and was therefore thought to be a good candidate for investigation in *Drosophila*.

The *M. musculus POSH* sequence was used to perform a tBLASTn search against all known *Drosophila* ESTs and located several candidates including LD45365, a full-length clone which was designated *DPOSH*. The clone was ordered and used in the subsequent molecular work. *DPOSH* had already been sequenced by another group and it was therefore unnecessary to repeat that work (Seong, 2000).

During the course of this work the *Drosophila* genome was sequenced (Myers et al., 2000). BLAST searches against the *Drosophila* genome using the *DPOSH* sequence identified only one *DPOSH* like gene, *CG4909*, that according the the gene annotation is located at the 54C9 cytological position on chromosome 2R (Fig. 4.1A).

4.2 DPOSH mRNA

Northern blot hybridization of total RNA from 0-12 hour old embryos using the *DPOSH* cDNA clone, LD45365, as a probe revealed a single hybridizing band of approximately 3.0 kb in size (Fig. 4.1B). This is comparable to the size of the sequenced full-length cDNA and the *Drosophila* Genome Sequencing Project prediction

Figure 4.1 Conceptual diagram of *DPOSH* gene.

(A) Top of the panel shows the organization of the *DPOSH* gene and the position of the *EP(2)1206* P element insertion used to generate *DPOSH* excision alleles as well as drive the expression of *DPOSH*. The extent of the deletion in the $DPOSH^{74}$ allele is shown. Bottom of the panel shows the *DPOSH* genomic region with neighbouring genes and their direction of transcription. P4 and P5 indicate primers used to screen for deletions of *DPOSH* in the generated excision lines.

(B) Northern blot of poly A+ mRNA from 0-12 hour old embryos probed with *DPOSH* LD45365 clones showing a single band of approximately 3kb.

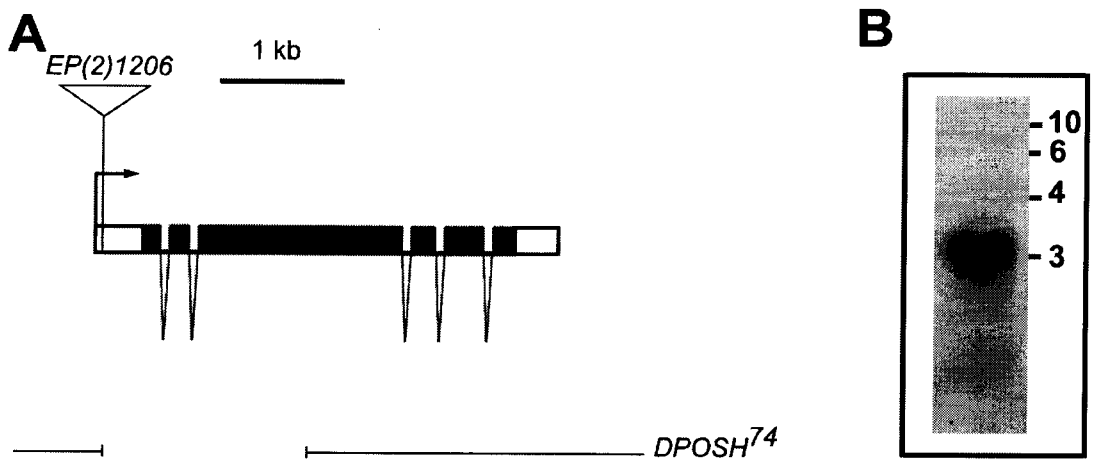

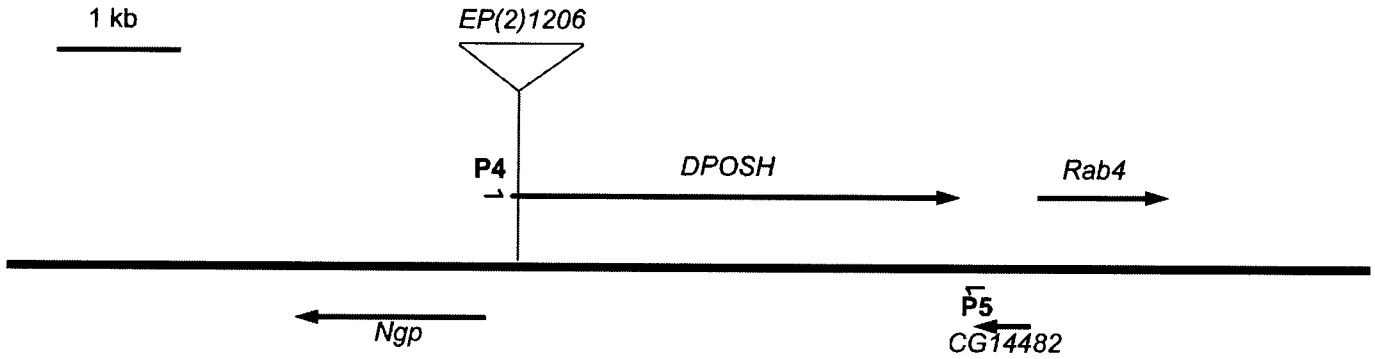

2R, 54C8-54C10

(Myers et al., 2000). A Northern blot analysis of poly A^+ mRNA from 0-12 hour old embryos revealed no evidence for alternative transcripts that may have been occluded by ribosomal RNA shadow bands in the total RNA, nor does the sequencing project predict more than one transcript. The cDNA encodes an open reading frame of 2514 nucleotides that translates to a protein containing 838 amino acids with a molecular mass of 92 kDa.

The theoretical *Drosophila* POSH protein was run against the InterPro database and was found to have a distinct series of domains that are specifically organized and highly similar to the mammalian homologs determined from tBLASTn searches against the PubMed translated nucleotide database. While RING finger and SH3 domains are found in a variety of proteins, only a single family of proteins in each species examined has a RING finger domain at the N terminal of the protein followed by four SH3 domains each of which is distinct and specifically similar to their counterpart (Fig. 4.2 and Table 4.1).

An EP-element insertion, *EP(2)1206,* that lies 229 base pairs upstream of the predicted start codon of *DPOSH* was found using BLAST and CytoSearch programs on Flybase and the stock was obtained from the Szeged Center (Fig. 4.1A). EP-elements contain engineered upstream activating sequences for the yeast GAL4 transcription factor, and can be used to direct GAL4-driven expression of any gene that they insert next to in the correct orientation (Rorth, 1996b). *EP(2)1206* is in the correct orientation to allow GAL-4 driven over-expression of *DPOSH.*

Figure 4.2 Schematic of DPOSH and homology comparison between DPOSH and *M. musculus* POSH.

(A) Schematic of *Drosophila* POSH protein showing specific organization of the RING finger and distinct SH3 domains. The mammalian and *Drosophila* POSH proteins are characterized by a RING finger domain at the N terminal followed by four SH3 domains. A serine rich region of unknown function and a putative 14-3-3 binding site are also shown. The largest possible protein product encoded by the deleted $DPOSH^{74}$ allele is shown. A line indicates the region of DPOSH generated as a GST-fusion protein and injected subcutaneously into rabbits as an antigen for the production of polyclonal anti-DPOSH antibodies.

(B) Alignment of the RING fingers (dashed box) and the first and second SH3 domains (solid boxes) of the *Drosophila* POSH (top) and *M. musculus* POSH (bottom). Yellow circles indicate the specific amino acids required for the co-ordination of the Zn^{+2} ions in the ring finger. (C) and (D) Alignment of the third and fourth (boxed) SH3 domains of the POSH proteins.

Alignment was performed using the Clustal method of the programme ALIGN of LASERGENE 99 package (DNAStar, Madison WI) that incorporates the method of Lipman and Pearson (Pearson and Lipman, 1988).

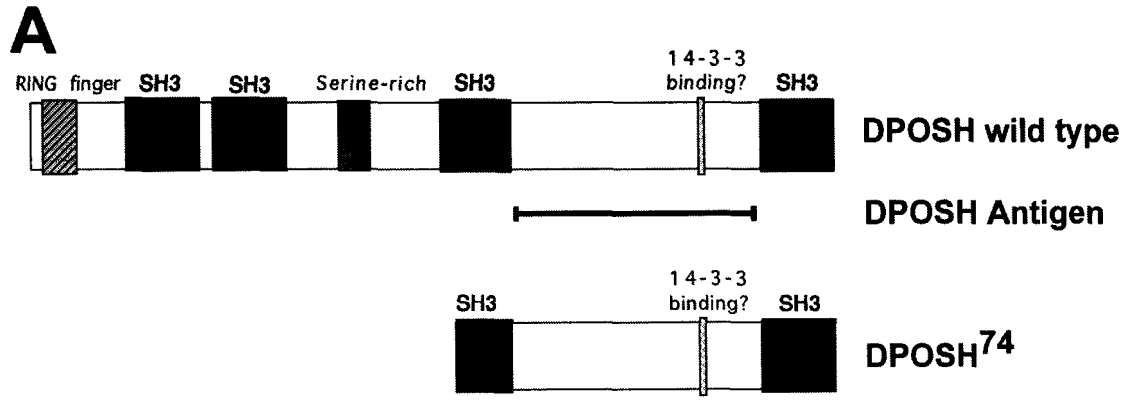

B

```
MDEHTLNDLLECSVCLERLDTTSKVLPCQHTFCRKCLQDIVASQHKLRCPECRILVSCKIDELPPNVLLM
MDE :L DLLEC:VCLERLD:::KVLPCQHTFC::CL :IV:S::.LRCPECR.LV:. :DELP:N:LL:
MDESALLDLLECPVCLERLDASAKVLPCQHTFCKRCLLGIVGSRNELRCPECRTLVGSGVDELPSNILLV

RILEGMKQNAAAGKGEEKGEETETQPERAKPQPPAESVAPPDNQLLQLQSHQQSHQPARHKQRR--FLLP
R:L:G:KQ.:     .. G..T T:. RA:  . .:.    .::L   Q. QQ:: .A:  . R    LP
RLLDGIKQRPWKPGPGGGGGTTCTNTLRAQGSTVVNC---GSKDLQSSQCGQQPRVQAWSPPVRGIPQLP

HAYALFDFASGEATDLKFKKGDLILIKHRNDNNWFVGQANGQEGTFPINYVKVSVPLPM--PQCIAMYDF
 A AL::::.: E:.DLKF.KGD I::::: D:NW: G:.:G :G FP.N:V::  PLP   PQC A:YDF
CAKALYNYEGKEPGDLKFSKGDTIILRRQVDENWYHGEVSGVHGFFPTNFVQIIKPLPQPPPQCKALYDF

KM-GPNDEEGCLEFKKSTVIQVMRRVDHNWAEGRIGQTIGIFPIAFVELNAAAKKLLD 263
.: : :.:.:CL F K..V: V:RRVD:NWAEG.:::.IGIFPI::VE:N:AAK:L::
EVKDKEADKDCLPFAKDDVLTVIRRVDENWAEGMLADKIGIFPISYVEFNSAAKQLIE 265
```

C

```
PWGYLALFPYKPRQTDELELKKGCVYIVTERCVDGWFKGKN-WLDITGVFPGNYLTPL 478
P  Y:A::PY.PR:.DELEL:KG :::V ERC DGW:KG.:   . .GVFPGNY::P:
PSVYVAIYPYTPRKEDELELRKGEMFLVFERCQDGWYKGTSMHTSKIGVFPGNYVAPV 511
```

D

```
HRKSHSLDASHVLSPSSNMITEAAIKASATTKSPYCTRESRFRCIVPYPPNSDIELELHL
HRK: SLD::  ::P::.   .:   . ..::: C.R   R :V:YPP:S: ELEL.
HRKTSSLDSAVPIAPPPRQACSSLGPVMNEARPVVCER---HRVVVSYPPQSEAELELKE

GDIIYVQRKQKNGWYKGTHARTHKTGLFPASFVEPDC 838
GDI::V::K:.:GW:KGT .R. KTGLFP:SFVE
GDIVFVHKKREDGWFKGTLQRNGKTGLFPGSFVENI 892
```

Table 4.1 Table depicting the identities and similarities of the specific domains of the POSH homologs as compared to *Drosophila* POSH.

Each distinct domain had a high degree of similarity across species. For example, the first SH3 domain had the highest degree of similarity to the first SH3 domain of the other homologs as opposed to the second, third or fourth SH3 domains.

First percent shown is identity, second is similarity. Data based upon tBLASTn searches on the PubMed database.

	RING finger	SH3 (1)	SH3 (2)	SH3 (3)	SH3 (4)
H. sapiens	71%/88%	45%/70%	50%/70%	58%/77%	56%/77%
M. musculus	71%/88%	43%/69%	50%/70%	60%/80%	59%/76%
R. norvegicus	71%/88%	45%/70%	50%/70%	53%/74%	56%/75%

First percent shown is identity, second is similarity as compared to DPOSH.

4.3 DPOSH expression pattern

Whole mount *in situ* localization experiments were performed on embryos with a DIG labelled anti-sense probe generated from the cDNA LD45365. *DPOSH* was found to be expressed ubiquitously throughout embryogenesis but was enriched in the leading edge cells of the epidermis during dorsal closure (Fig 16).

In order to examine the DPOSH protein expression pattern, the anti-DPOSH polyclonal antibodies were raised in rabbits. A GST fusion construct containing a truncated region from amino acids 479 to 781 of DPOSH was designed (Fig. 4.2A). This epitope was 37 kDa in size and excluded all regions of DPOSH that bore significant similarity to other proteins as determined by BLAST and InterPro analysis. 0.5 mg of GST-DPOSH was suspended in an equal volume of TITERMAX adjuvant and injected subcutaneously into two rabbits every two weeks.

During the generation of the antibodies, serum aliquots were taken from the rabbits every two weeks and tested for reactivity by Western blotting against DPOSH expressed *in vitro* using rabbit reticulocyte lysate (Promega, 1999). Antibodies were also tested for their ability to detect DPOSH over-expressed from a UAS transgene expressed in *ptc* stripes during embryonic development using the *ptc-GAL4* driver. *ptc-GAL4/UAS-DPOSH* embryos were fixed and stained with anti-DPOSH antibodies. An intense staining of *ptc* stripes indicated that anti-DPOSH could detect the protein in embryos (Fig. 4.4B). These tests were undertaken after each aliquot to assess the positive generation of an antibody.

Figure 4.3 Whole mount RNA *in situ* of *DPOSH*.

(A) and (B) Whole mount RNA *in situ* of embryo at onset of dorsal closure showing enrichment of DPOSH mRNA in leading edge cells of epidermis (arrowheads). *DPOSH* cDNA was used to generate an anti-sense DIG labelled probe.

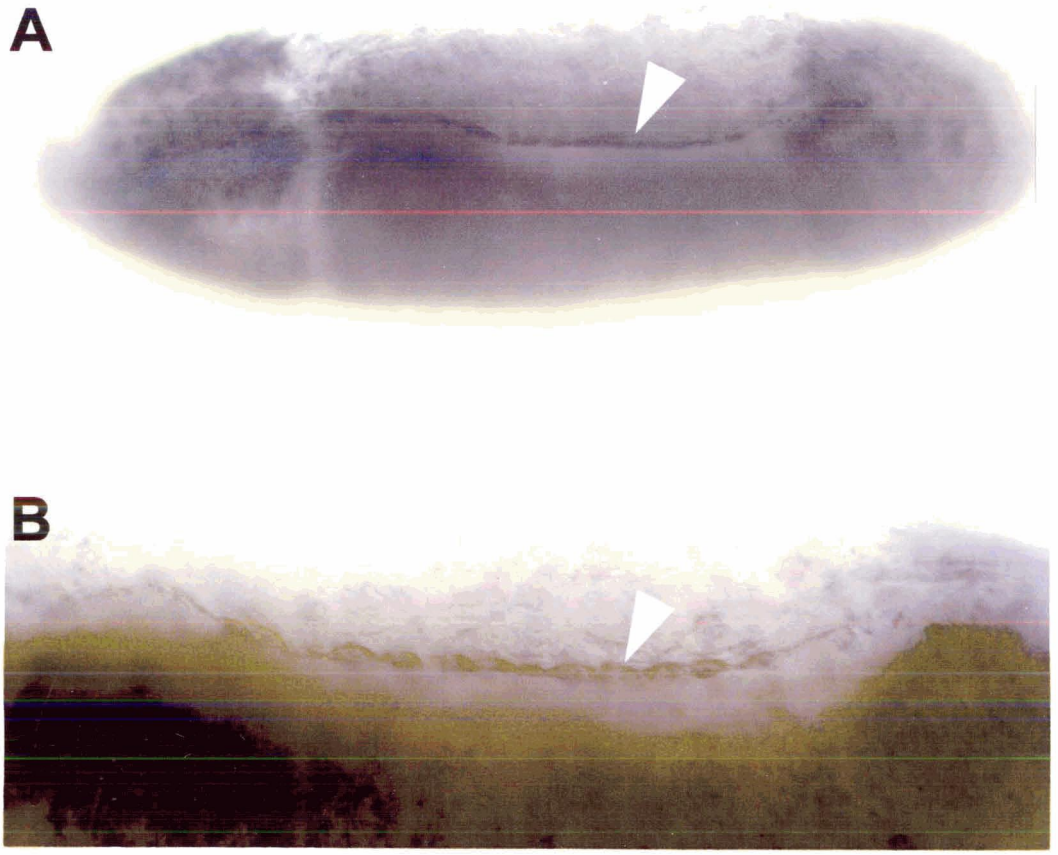
A
B

Unfortunately, Western blots of whole *Drosophila* lysate incubated with anti-DPOSH contained many unspecific bands, such that it was not possible to identify a specific DPOSH band. As described later (Results: DPOSH construction of transgenes), a transgenic *Drosophila* line was constructed in which a FLAG tagged (*UAS-FLAG-DPOSH*) could be expressed using GAL4 drivers. These were used as a control to mark the size of the specific DPOSH bands on Western blots of whole *Drosophila* lysates and used as positive controls for the antibody staining of the *ptc-GAL4/UAS-DPOSH* embryos as it is possible to express the FLAG-DPOSH fusion and use anti-FLAG antibodies to identify DPOSH specific bands (Fig. 4.4C).

The antiserum was capable of detecting the expressed DPOSH proteins both on Western blots and in *ptc-GAL4/UAS-DPOSH* embryos but not able to detect endogenous levels of DPOSH on Western blots. Concentration of the antibodies was attempted by affinity purification in order to try and resolve a definitive DPOSH band on Western blots. Anti-DPOSH antibodies were affinity purified by linking the constructed DPOSH antigen to nitrocellulose, exposing it to the anti-DPOSH serum, several washes, and separation of the antibody from the antigen via denaturation as described in Materials and Methods (Sambrook et al., 1989). However the affinity purified DPOSH antibodies still detected multiple bands on Western blots (Fig. 4.4A).

Staining of embryos with either unpurified or purified anti-DPOSH antibodies showed little signal, and no leading edge enrichment of DPOSH protein was seen as compared to the *DPOSH in situ* (results no shown). Taken together with the finding that even purified anti-DPOSH cross-reacted with extra bands on Western blots, it was

Figure 4.4 Anti-DPOSH antibodies.

(A) Western blot of whole cell lysate taken from the indicated flies and incubated using the affinity purified anti-DPOSH antibodies or anti-FLAG. The *hs-GAL4/UAS-FLAG-DPOSH* and control *hs-GAL4/+* flies were induced by heat shock at 37°C for the indicated times before sample preparation. A single band was seen in all the *UAS-FLAG-POSH* lanes indicating the expected approximate size of DPOSH as well as indicating the specificity of the anti-FLAG antibody to FLAG. The affinity purified anti-DPOSH antibodies detected a band at the same size as the anti-FLAG antibody, an approximate size of 90 kDa consistent with the predicted size of the fusion protein. In the control lysate no apparent DPOSH specific band was seen. The $POSH^{74}$ mutant lysate has a similar banding pattern to the wild type flies (results not shown).

(B) *ptc-GAL4/UAS-FLAG-POSH* embryos stained with anti-FLAG antibodies demonstrating staining in *ptc* stripes (arrows). (C) A similar pattern is also seen in *ptc-GAL4/UAS-POSH* embryos stained with anti-DPOSH serum indicating ability of anti-DPOSH antibodies to detect over-expressed DPOSH (arrows).

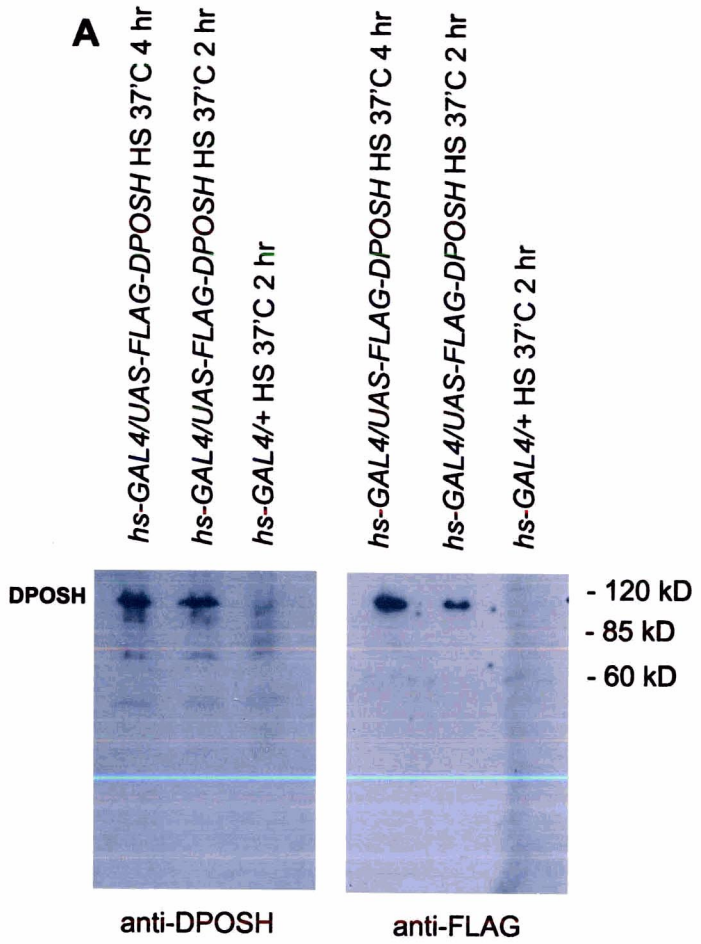
A
hs-GAL4/UAS-FLAG-DPOSH HS 37'C 4 hr
hs-GAL4/UAS-FLAG-DPOSH HS 37'C 2 hr
hs-GAL4/+ HS 37'C 2 hr
hs-GAL4/UAS-FLAG-DPOSH HS 37'C 4 hr
hs-GAL4/UAS-FLAG-DPOSH HS 37'C 2 hr
hs-GAL4/+ HS 37'C 2 hr
DPOSH
- 120 kD
- 85 kD
- 60 kD
anti-DPOSH
anti-FLAG


B


C

concluded that the DPOSH antibodies could not be used for immunohistochemistry in the developing embryo.

Futhermore as dicussed later (Discussion), DPOSH protein levels in the embryo may be low due to self-targeting of DPOSH for ubiquitination by its own Zinc RING finger and degradation through the proteosome degradation pathway (Xu et al., 2003).

4.4 Construction of transgenic DPOSH flies

Transgenic flies are used to rescue a particular phenotype in order to verify by reversion to wild type that the mutant is responsible for that phenotype. Transgenic lines can also be useful for large scale screening interactions as well as targeted interactions between genes or demonstration of epigenesis in genetic pathways.

Construction of transgenic lines is explained in detail in Materials and Methods. In brief, the *DPOSH* cDNA was cloned into pUAST in order to place it under the control of a *UAS* promoter such that available *GAL4* drivers could drive its expression in a tissue specific manner.

Transgenic *DPOSH* lines were created with insertions on the X, 2nd and 3rd chromosomes. The localization of the P-element insertions to each chromosome was determined by crossing the various lines to individual balancers for each chromosome and screening for the maintenance of heterozygosity of the balancer with the insertion in subsequent generations.

These lines were crossed with *hs-GAL4*^{M4}, heat shocked for 1 hour at 37°C, and Northern blot analysis performed to test the function of the transgenes (Fig. 4.5). The Northern blot revealed that the lines were successfully expressing *DPOSH*.

Figure 4.5 *UAS-DPOSH* transgenic flies can be used to induce *DPOSH* over-expression.

Northern blot demonstrating that *UAS-DPOSH* transgenes can be induced by *hs-GAL4*^{M4} through heat shock. Flies were heat shocked at 37°C for 1 hour and either immediately frozen on liquid nitrogen for RNA preparation or aged for 1 hour at 25°C to allow further expression of DPOSH before freezing. Control flies were *hs-GAL4*^{M4} crossed to Canton S.

Canton S/hs-GAL4M4
UAS-DPOSH10.1;hs-GAL4M4 HS 1 hr
hs-GAL4M4/UAS-DPOSH15.1 HS 1 hr
UAS-DPOSH10.1;hs-GAL4M4 HS 1 hr aged 1 hr
hs-GAL4M4/UAS-DPOSH15.1 HS 1 hr aged 1 hr
DPOSH
rp49

DPOSH has a putative Zinc RING finger motif at the N-terminal of the protein (Fig. 4.2B). Previous studies have revealed that the Zinc RING finger has a role in ubiquitylation of proteins for the proteosome mediated degradation pathway (Joazeiro and Weissman, 2000). One of these studies has defined the C_3HC_4 residues in the Zinc RING finger as being essential for this function (Ota et al., 2000). It was therefore decided to create RING finger mutant transgenes in order to test the requirement of the DPOSH RING finger in its function.

Site directed mutagenesis was performed using the primer, GGTGCTGCCAGCCCAGAACACCTTCGCCCGCAAAGCCTTGCAGGAC, in order to change the C_3HC_4 motif of the Zinc RING finger to an inactive $C_2ANA_2C_2$ motif (Fig. 4.6). The product of site directed mutagenesis was sequenced to ensure that the mutation had occurred correctly and then cloned into pUAST as previously described. The mutagenesis is designed to replace the amino acids cysteine and histidine with amino acids that are not able to properly co-ordinate the Zn^{2+} co-factor and disrupt the RING finger resulting in a non-functioning domain (Fig. 4.6C and 4.7D) (Ota et al., 2000).

FLAG-POSH fusion transgenic flies were generated in order to serve as positive controls for anti-DPOSH antibody testing. The FLAG antigen was fused to the DPOSH protein and could be detected by anti-FLAG antibodies on both Western blots and embryos. *UAS-FLAG-DPOSH* was constructed by cloning the DPOSH coding cDNA in frame into the FLAG vector pXJFLAG, and cut and cloned into the pUAST vector and transgenic animals generated as explained in Materials and Methods.

Figure 4.6 Generation of DPOSH Zinc RING finger transgenes.

(A) Sequence results demonstrating the site directed mutation of the *DPOSH* Zinc RING finger. Wild type bases are displayed in red type above the sequence data.

(B) A depiction of the wild type Zinc RING finger showing the co-ordination of the Zn^{2+} cations by the cysteine and histidine residues allowing the ring finger to adopt a helical structure. (C) Targeted mutation of the Zinc RING finger results in a disruption of the secondary structure of the enzymatic domain that is responsible for ubiquitylation and subsequent degradation of POSH and possibly other proteins.

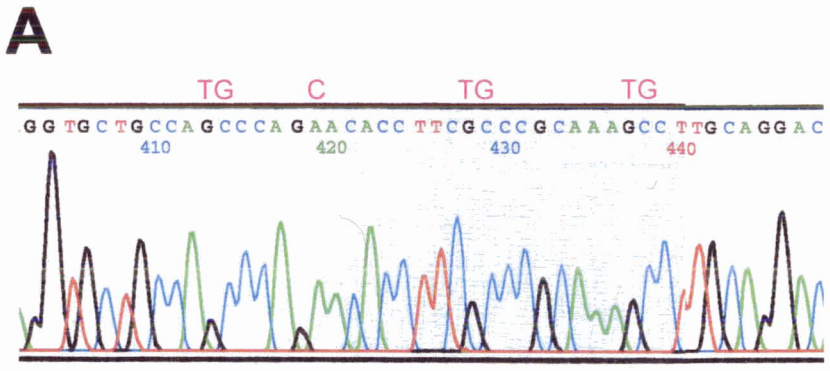
A
TG
C
TG
TG
GG TG C TG CCA G CCC A G AA CAC C TTC G C CC G CAAA G CC TTG CA GG A C
410
420
430
440

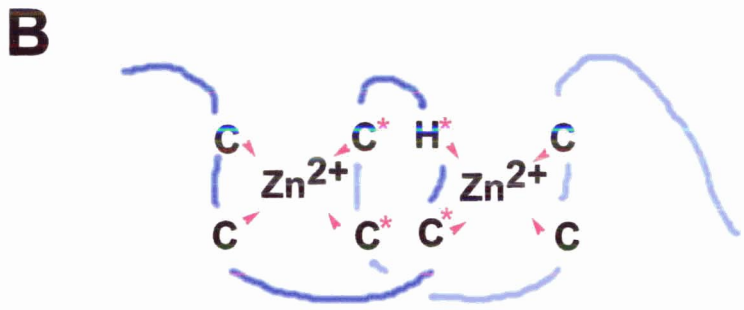
B
C
C*
H*
C
Zn2+
Zn2+
C
C*
C*
C


C
C
A
N
A
A
C
C

4.5 Over-expression of DPOSH

The over-expression of a gene in a model system such as *Drosophila* can offer insight into its function. For example, over-expression of *DRac1* in the *Drosophila* eye has provided evidence of the function of DRac1 in cell fate while over-expression of DRac1N17 in the wing indicated a role in cell polarity (Hariharan et al., 1995) (Eaton et al., 1996). Moreover genetic attempts at modification of over-expression phenotypes can also provide evidence of regulators of the over-expressed gene. For example, the *Drosophila* 'deficiency kits' can be used to screen for deletions containing genetic modifiers of the over-expression phenotype. Such an approach was used to find *myoblast city*, a suppressor of *Rac1* over-expression in the eye (Nolan et al., 1998).

When ectopically driven, *UAS-DPOSH* produced some interesting phenotypes. In combination with an eye specific driver, *GMR-GAL4*, *UAS-DPOSH*$^{10.1}$ flies developed a rough eye phenotype, which upon closer examination with Scanning Electron Microscopy (SEM), is seen to have a disorganized bristle and ommatidia structure (Fig.21A and 21B). The over-expression of *UAS-DPOSH*$^{RING19.1}$ also produced a visibly rough eye, but upon closer examination by SEM it appeared to not be nearly as disorganized as over-expression of wild type *DPOSH* (Fig. 4.7C). Over-expression of DPOSH along the wing anterior/posterior (A/P) boundary using *ptc-GAL4* in combination with *UAS-DPOSH*$^{15.1}$ caused a disorganized bristle polarity the length of the A/P boundary.

To examine if *DPOSH* over-expression would affect dorsal closure or germband retraction, two morphogenetic events that the *Drosophila Rac* proteins have been

Figure 4.7 Over-expression of *DPOSH* in the eye and the embryo.

(A) Scanning electron micrograph of wild type eye. Note the normal organized ommatidia and bristle pattern. (B) *GMR-GAL4/UAS-DPOSH*$^{I2.1}$ eye showing effects on organizational structure of the bristles and ommatidia but the eye itself maintains a normal shape. (C) *GMR-GAL4/UAS-DPOSH*$^{RING19.1}$ eye, expressing the Zinc ring finger mutant transgene. The eye pattern itself is more organized than the over-expression of wild type *DPOSH* but the eye shape is abnormal. All eyes are from female flies.

(D) and (F) Wild type embryo stained by anti-phosphotyrosine showing normal localization of phosphotyrosine at the boundaries of the cells. Dorsal and ventral views are shown respectively. (E) and (G) *hs-GAL4*^{M4}*/UAS-DPOSH* embryos heat shocked for 1 hour at 37˚C 6-12 hours AEL and stained with anti-phosphotyrosine showing a mislocalization of phosphotyrosine away from the cell boundary and into the cytosol.

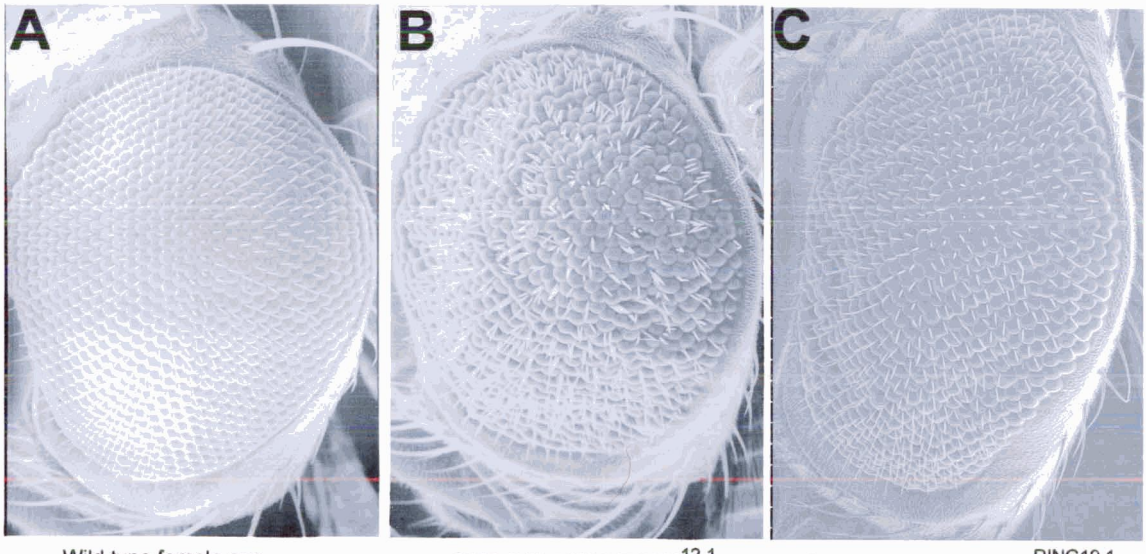

Wild type female eye

GMR-GAL4/UAS-POSH$^{12.1}$

GMR-GAL4/UAS-POSH$^{RING19.1}$

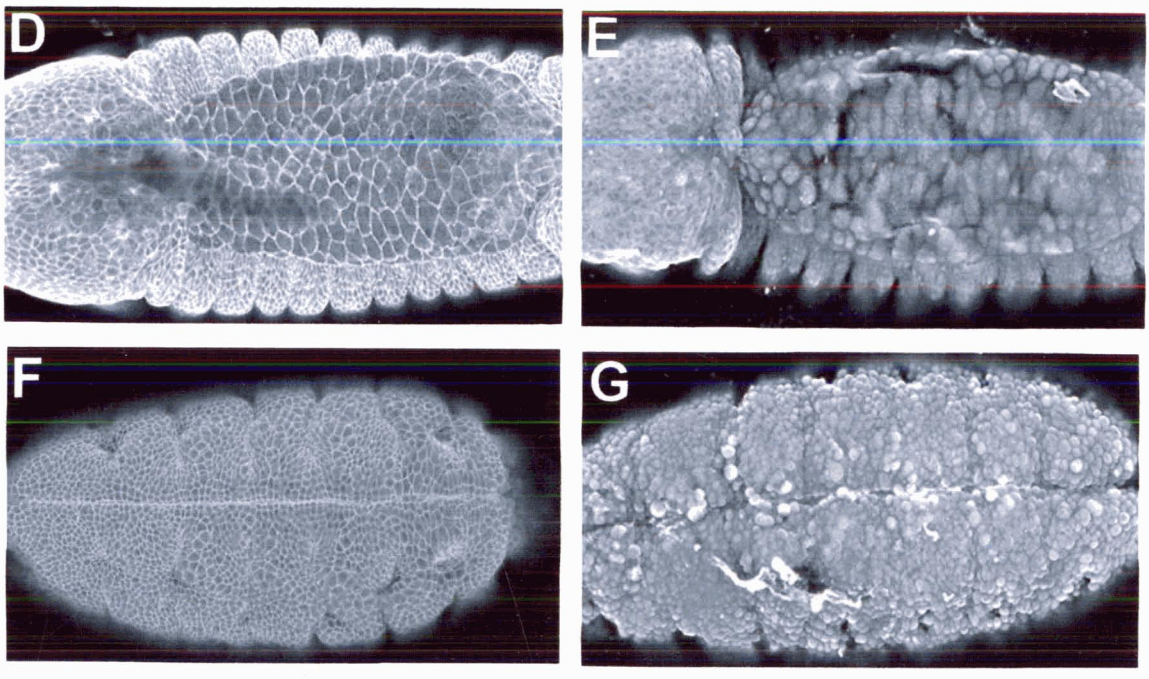

implicated in, *DPOSH* was over-expressed during embryogenesis (Harden et al., 1995). *DPOSH* was expressed for one hour at 37°C using *hs-GAL4*^{M4} to drive *UAS-DPOSH*$^{15.1}$ in 6-12 hour old embryos AEL and anti-phosphotyrosine was used to stain the periphery of the cells. Strikingly the embryos showed a shift of the phosphotyrosine staining from the membrane to the cytosol of the cells (Fig. 4.7D, 21E, 21F and 21G). This also caused lethality and cuticle preparations revealed a large number of embryos that had failed to develop cuticles. These embryos were also stained with Acridine Orange (AO) to mark apoptosis, however an increase in AO staining was not observed. Targeted over-expression of *DPOSH* in epidermal stripes in *ptc-GAL4;UAS-DPOSH*$^{15.1}$ embryos also did not cause dorsal closure defects when examined by cuticle preparations though the flies survived with wing defects as mentioned.

Over-expression of *DPOSH* during embryogenesis did not cause dorsal closure defects. One might have expected an effect on this process as the endogenous *DPOSH* transcript is amplified at the leading edge (Fig. 4.3). By its nature, the targeted expression of a gene in an organism is an artificial event and not necessarily a reliable indicator of a gene's functional role in development. For example, the over-expression of wild-type *DRac1* in the ectoderm of the developing *Drosophila* embryo seems to have no obvious effects, however the expression of *DRacV12*, an activated form of *DRac1*, causes a failure in dorsal closure (Harden et al., 1995). In the *Drosophila* eye, however, the over-expression of both these forms of *DRac1* cause eye defects (Hariharan et al., 1995).

4.6 Creation of a DPOSH mutant

In order to determine what processes *DPOSH* is required for, loss-of-function mutations were created. Since *DPOSH* RNA *in situ* revealed an increased level of

transcript at the leading edge, analysis of *DPOSH* mutant embryos for effects on development was a necessary part of the investigation.

The presence of an EP-element upstream allowed for targeted deletions of *DPOSH* by re-mobilization of the EP-element (Fig. 4.1A) (Hawley and Waring, 1988). Since imprecise excision events result in deletions of random length and direction about the insertion point, many lines generally needed to be screened to obtain deletions affecting only *DPOSH* and not neighbouring genes. Two hundred excision events from the *EP(2)1206* line were produced as described in Materials and Methods.

Excision lines were examined by PCR using upstream and downstream primers flanking *DPOSH* in order to determine the precise size of the deletions and ensure the preservation of the flanking genes. The upstream primer, P4, contained the sequence, ATCGACTACGAGGACTGGCCACAC, while the downstream primer, P5, contained the sequence, CTTTGTAGAGGGCACAAGGATCGG (Fig. 4.1A). Screening of the lines via PCR revealed a single line of interest, $DPOSH^{74}$, which had a smaller ~2 kb amplified band on an agarose gel compared to the wild type ~4 kb band (Fig. 4.8A and B).

Line $DPOSH^{74}$ is homozygous viable and is a loss-of-function mutation as no transcripts are seen on *DPOSH* Northern blots (Fig. 4.8C). After isolation and sequencing of the 2 kb PCR product, it was revealed that $DPOSH^{74}$ had an 1543 bp deletion in the *DPOSH* gene (Fig. 4.9A and 4.9B). This deletion is located downstream of the TATA box, removing the start codon and extending 1282 nucleotide bases into the coding region of *DPOSH* (427 amino acids) (Fig. 4.9B). The next available start codon that could

Figure 4.8 Molecular characterization of *DPOSH*^{74}.

(A) PCR amplification on wild type Canton S flies using *DPOSH* flanking primers. The screening method selects for deletions that are constrained to the *DPOSH* locus. The wild type band is about 4 kb. (B) PCR result of line *DPOSH*^{74}*/CyO* showing a smaller band at approximately 2 kb, in addition to the wild type *DPOSH* band coming from the balancer chromosome.

(C) Northern blot of *DPOSH*^{74}*/DPOSH*^{74} poly A+ mRNA from adult flies probed with *DPOSH*, demonstrating a lack of *DPOSH* transcript. The wild type DPOSH transcript is seen in the control sample from Canton S flies.

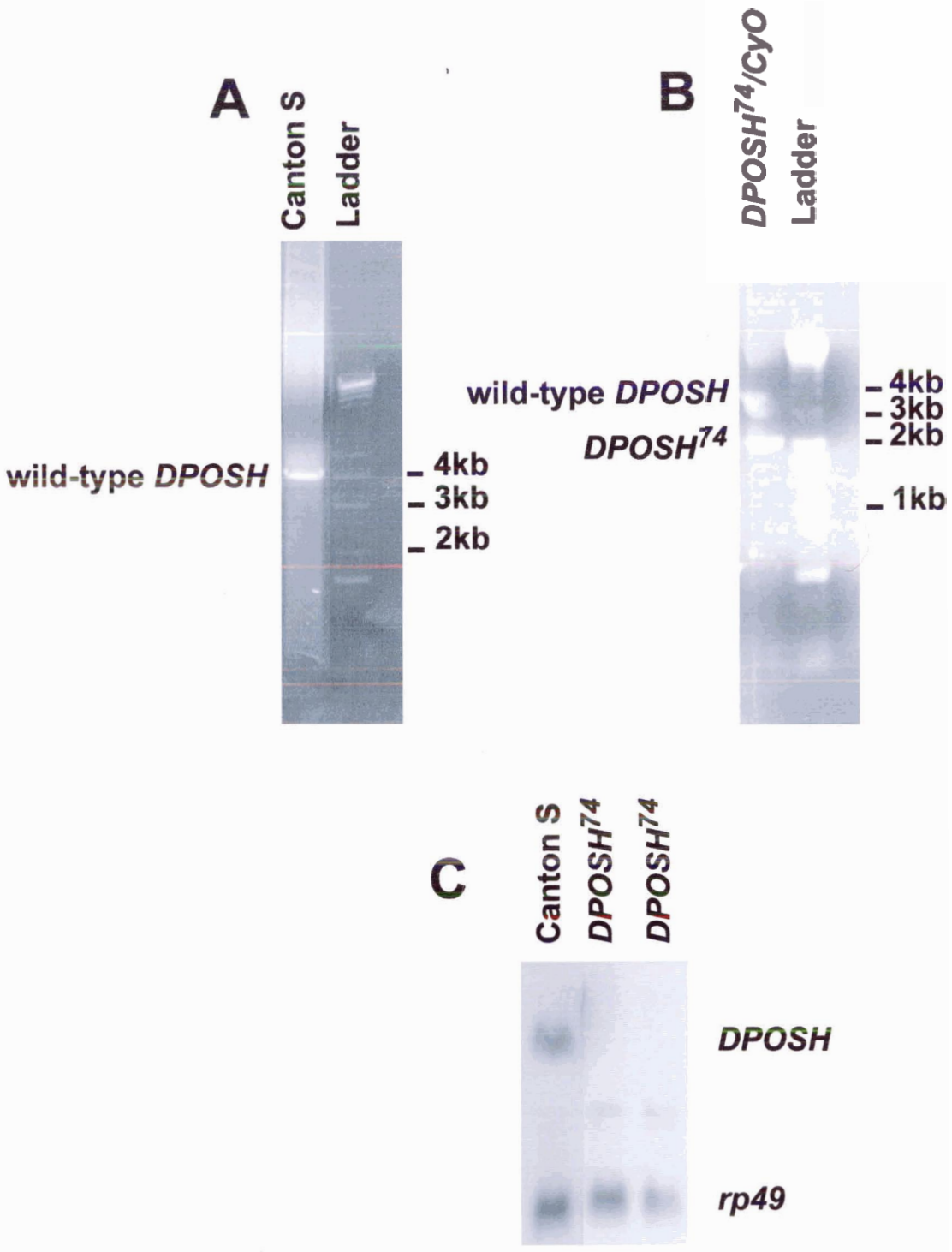
A
Canton S
Ladder
wild-type DPOSH
4kb
3kb
2kb
B
DPOSH74/CyO
Ladder
wild-type DPOSH
DPOSH74
4kb
3kb
2kb
1kb
C
Canton S
DPOSH74
DPOSH74
DPOSH
rp49

produce a truncated DPOSH protein is at amino acid 487 and would result in a protein lacking the RING finger, and the first three SH3 domains (Fig. 4.2A).

Line *DPOSH*^{74} was concluded to be a strong loss-of-function or null allele of *DPOSH* from these results and used in further mutant analysis.

4.7 A subset of DPOSH^{74} *mutant embryos have a head defect*

DPOSH^{74}/*DPOSH*^{74} flies were allowed to lay eggs for 24 hours, and the eggs were aged for another 24 hours in order to ensure that all embryos had an opportunity to make it through all the stages of embryogenesis and form cuticles. These were collected and cuticle preparations were performed in order to examine the morphology of the embryo. 12% (n = 412) of the progeny had a head defect, an open hole in the cuticle associated with a failure of head involution, as compared to the wild type level of 3% (n = 400) (Fig. 4.10).

To demonstrate that the head defect in line *DPOSH*^{74} is due to the loss of *DPOSH* function, a rescue of the phenotype by replacement of wild type DPOSH into the embryo was performed. *DPOSH* was expressed in *DPOSH*^{74}/*DPOSH*^{74};*UAS-DPOSH/hs-GAL4*^{M4} embryos by heat shock at 37°C for 30 minutes 5 hours AEL and embryos allowed to develop for 24 hours at room temperature followed by cuticle preparations. *DPOSH*^{74}/*DPOSH*^{74};+/*hs-GAL4*^{M4} embryos were used as a control. A reduction from 12% (n = 677) head defects to 7% (n = 666) was found.

The results suggest that loss of *DPOSH* function is responsible for a low number of head defects and that *DPOSH* may have a role in head involution in the developing embryo.

Figure 4.9 Sequence analysis of *DPOSH*^{74} deletion.

(A) Sequence results from PCR of *DPOSH*^{74} chromosomal DNA in the *DPOSH* locus. Arrow indicates 5′ end of 1.5 kb deletion in *DPOSH* caused by P-element remobilisation of *EP(2)1206*.

(B) Alignment comparison of sequences from wild-type *DPOSH* and *DPOSH*^{74} depicting 5′ and 3′ ends of the excision event (arrows). A few nucleotides that do not align remain as a result of the excision event. Numbers indicate the distance from the beginning of the wild type *DPOSH* cDNA. Bent arrow indicates the start site of translation. The Clustal method of the programme MEGALIGN of LASERGENE 99 package (DNAStar, Madison WI) was used. Shaded residues match the wild-type *DPOSH* sequence.

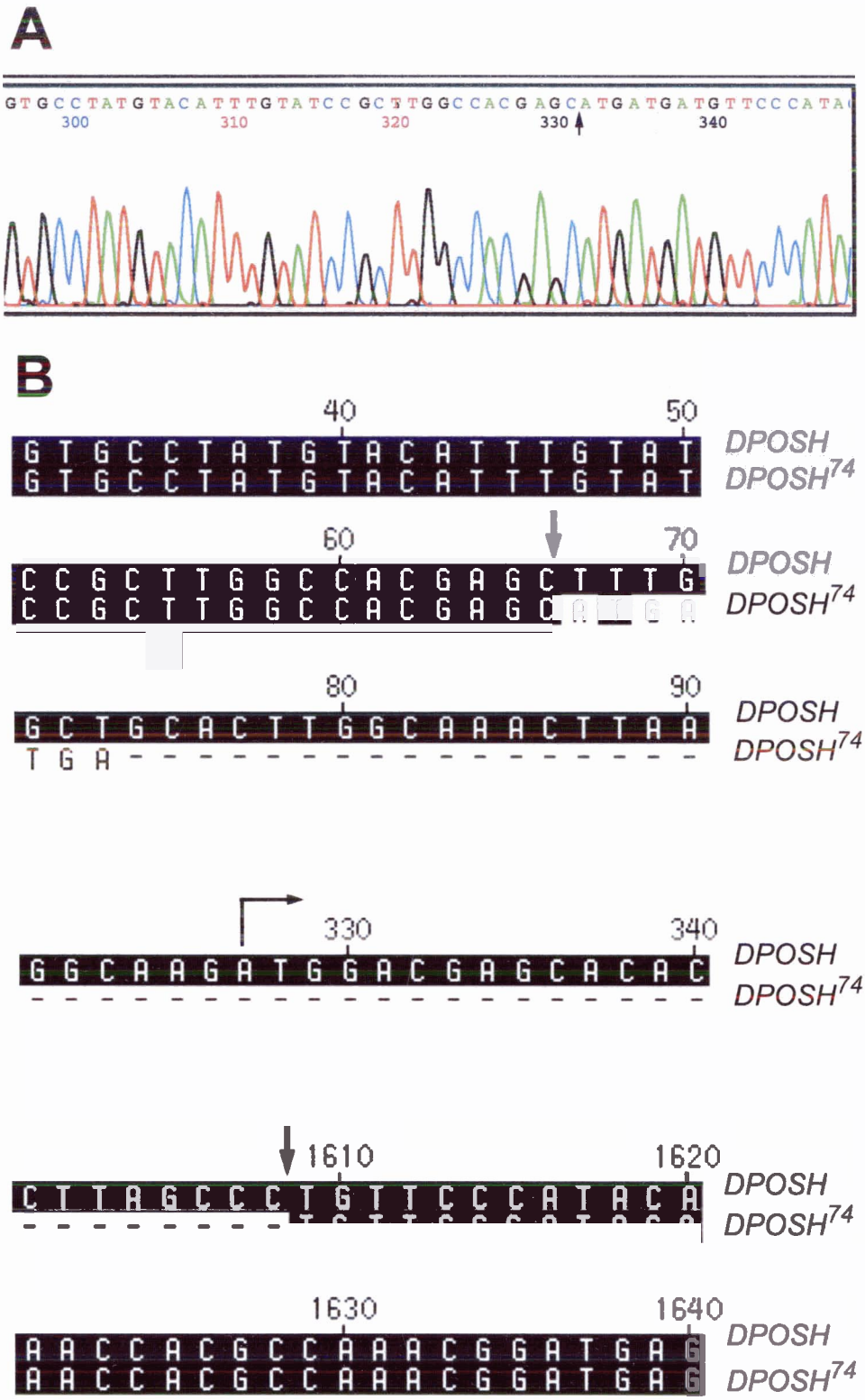
A
300
310
320
330
340
B
40
50
DPOSH
DPOSH74
60
70
DPOSH
DPOSH74
80
90
DPOSH
DPOSH74
330
340
DPOSH
DPOSH74
1610
1620
DPOSH
DPOSH74
1630
1640
DPOSH
DPOSH74

Figure 4.10 Head involution defects are seen in *DPOSH* mutant embryos.

(A) and (B) wild type embryos aged 24 hours. (C) and (D) $DPOSH^{74}/DPOSH^{74}$ embryos aged 24 hours. White arrow indicates head defect appearing as a hole in the cuticle associated with a failure of head involution.

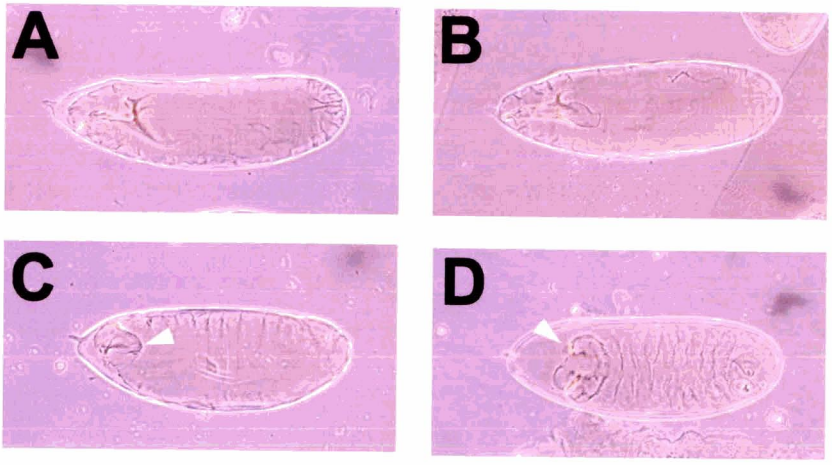
A
B
C
D

4.8 No defects in nervous system development have been detected to date in DPOSH^{74} mutants

DRac1 has been shown to have important roles in embryonic axon guidance, glial cell migration, and the adult photoreceptor (Kaufmann et al., 1998), (Hakeda-Suzuki et al., 2002), (Ng et al., 2002), (Sepp and Auld, 2003). *DPOSH^{74}* embryos were examined for a role in nervous system development using the nervous system specific antibody Mab22C10 (Zipursky et al., 1984). The central nervous system and peripheral nervous system of *DPOSH^{74}* mutant embryos appeared normal. This was expected as most embryos survive.

The imaginal discs of the developing *Drosophila* adult eye were stained with the monoclonal antibody 24C10 to examine the photoreceptor axons (Van Vactor et al., 1988). In *DPOSH^{74}* and *GMR-GAL4/UAS-DPOSH* imaginal discs no evidence was seen of axon guidance defects as compared to wild type imaginal discs.

4.9 Attempts to sensitize the DPOSH^{74} allele

In order to try and genetically sensitize the *DPOSH^{74}* mutants, fly stocks were created bearing mutations for genes involved in the JNK pathway or involved in the proteosome degradation pathway. The stocks were constructed such that they would be maternally and zygotically deficient for *DPOSH* while containing a balanced copy of a mutation in another gene, ie: *DPOSH^{74}/DPOSH^{74}; X^{x}/Balancer*. None of the constructed lines bearing mutant alleles in the following genes were found to modify *DPOSH^{74}* at the level of dorsal closure or adult morphology, *Sacl^{2107}*, *kayak*, *bsk^{1}*, *hep^{1}*, *slpr^{1}*, *Rac^{J11}-Rac2$^{\Delta}$-MTL$^{\Delta}$*, *puc^{E69}*, *H99*, *cbl*, and *Tbp-1* (proteosome endopeptidase).

4.10 Exploring the roles of DPOSH in Rac function

4.10.1 DPOSH fails to bind activated Rac1 in vitro GST-pull down assays

DPOSH was shown to bind preferentially to activated Rac1 in a yeast two-hybrid system (Tapon et al., 1998). In order to examine if the *Drosophila* protein behaves in a similar manner, GST-pull down assays in done as previously described for DSra-1 were performed. The *DPOSH* cDNA was cloned into pXJFLAG from which transcription by phage T7 polymerase and translation by rabbit reticulolysate in the presence of ^{35}S-methionine produced ^{35}S-labelled DPOSH. GST-DRac1 was expressed in BL21 cells, bound to glutathione sepharose beads, and exchanged with either an unhydrolyzable form of GTP (GTP-γS) or GDP to give the active and inactive forms of the p21s, respectively. Under the conditions of a fairly strict wash buffer of Tris pH 7.5 + 0.5% Triton-X, DPOSH was found to not bind GTP-γS –Drac1 or GDP-DRac1 (Fig. 4.11).

4.10.2 DPOSH does not bind activated Rac1 in yeast two hybrid system

The interaction trap yeast two hybrid method (see Materials and Methods) was used to further test the interaction between DPOSH and DRac1. *Drosophila Rac1V12* was cloned into pJG4-5 via *Eco*RI and *Xho*I. Using site directed mutagenesis a thymine was mutated to an adenosine in order to produce an amino acid mutation of a cysteine to a serine at amino acid position 189. This deactivates the CAAX box encoded in the C-terminal of the Rho family of GTPases that causes a localization of the protein to the cell membrane (Hancock et al., 1991). When transformed into the EGY48 yeast strain, the pJG4-5-Rac1V12 plasmid causes expression of, under the control of a GAL1 promoter, a fusion protein containing Rac1V12, a nuclear localization signal and an acid

Figure 4.11 GST-pull down assay showing lack of binding of DPOSH to GTP or GDP bound forms of DRac1.

In order to test DPOSH for its ability to bind GTP-bound Rac1, a GST-pull down assay was performed. DPOSH coding sequences were cloned into *pXJFLAG* from which transcription by phage T7 polymerase and translation by rabbit reticulolysate in the presence of ^{35}S-methionine produced ^{35}S-labelled DPOSH. GST-DRac1 and GST were expressed in the bacteria strain BL21, bound to glutathione sepharose beads, and exchanged with either an unhydrolysable form of GTP (GTP-γS) or GDP to give the active and inactive forms of the p21s, respectively. Under the conditions of a fairly strict wash buffer of Tris pH 7.5 + 0.5% Triton-X, DPOSH was found to be unable to bind GTP-γS -DRac1.

The lane labelled 10% input contains the protein products of the transcription and translation of *pXJFLAG-DPOSH* and is a control to demonstrate the expression of radiolabelled DPOSH as well as provide an indicator of its size.

This result is representative of several separate experiments. Coomassie blue staining of the gels indicated equal loading of the small GTPases (data not shown).

10% input
GST-GTPγS
GST-GDP
GST-Rac1-GTPγS
GST-Rac1-GDP
DPOSH

transcriptional activation domain (Golemis et al., 1999). The removal of the membrane localization signal, CAAX, is required to keep the Rac1V12 fusion protein inside the nucleus. A pJG4-5-Rac1N17 plasmid with an inactive CAAX box was constructed in a similar manner.

Full length *DPOSH* was cloned into pEG202, to express this as a fusion protein with a LexA DNA binding domain under the control of the ADH promoter (Golemis et al., 1999).

The lacZ reporter plasmid, pSH18, was used to determine if there was any interaction between Rac1 and DPOSH, and if binding of DRac1V12 is favoured over DRac1N17.

DPOSH did not cause self activation of the lacZ reporter, and it was demonstrated that the fusion protein localizes to the nucleus by a repression assay, where the LexA-DPOSH fusion protein is able to bind LexA operator sites on a pJK101 lacZ reporter plasmid and interfere with a GAL1 UAS upstream of two LexA domains (Golemis et al., 1999).

Using this assay, we were unable to demonstrate binding of DPOSH to DRac1V12 or N17.

The failure to demonstrate any binding of DPOSH with DRac1 contradicts mammalian data (Tapon et al., 1998). Perhaps in *Drosophila*, another protein or proteins, is required to couple DPOSH with DRac1. The requirement for such adaptor molecule(s) would preclude DPOSH binding DRac1 in the GST-pull down assay. Furthermore as

yeast does not have Rac, the adaptor may be lacking in this organism and as such the yeast two hybrid assay would not be expected to work either.

4.10.3 Over-expression of DPOSH enhances DRac1N17 over-expression phenotypes in embryos but has no effect on DRac1V12 over-expression phenotypes

Previous work had shown that over-expressed mammalian POSH could bind Rac1 and induce the JNK signalling pathway (Tapon et al., 1998). DRac1N17 is able to interfere with endogenous DRac1 signalling in a dominant negative fashion and has been partially rescued by over-expression of constitutively active *Djun* indicating that disrupted JNK signaling is a component of DRac1N17-induced dorsal closure defects (Harden et al., 1995), (Hou et al., 1997).

From the previous data it could be possible that *DPOSH* over-expression would activate the JNK pathway and suppress *DRac1N17*-induced dorsal closure defects. *hs-GAL4,hs-DRac1N17/EP(2)1206* 6-12 hour AEL embryos were heat shocked at 37°C for 1 hour and cuticle preparations were performed. *hs-GAL4,hs-DRac1N17/+* embryos were used as a control. 77.8% (n = 400) dorsal closure defects were counted in the over-expression of *DPOSH* and *DRac1N17* as compared to 50.2% (n = 217) of over-expression of *DRac1N17* alone. This was an increase of dorsal closure defects by 55%.

From this data it seemed to appear that DPOSH was actually acting as a antagonist of endogenous Rac1 and not a positive effector.

If DPOSH were acting as an antagonist than it would be possible that DPOSH could antagonize over-expression of *DRacV12*. Over-expression of *DRac1V12* in 6-12 hour AEL embryos causes puckering and contraction of the epidermis presumably due to

enhancement of the forces driving dorsal closure, as well as failure of the germ band to retract (Harden et al., 2002).

6-12 AEL old *hs-GAL4,UAS-DPOSH*$^{10.1}$*;UAS-DRac1V12* embryos were heat shocked at 37°C for 10 minutes and allowed to complete development before cuticle preparations were performed. *hs-GAL4;UASRac1V12* embryos were used as a control. 23.1% (n = 325) of the *DPOSH* modified embryos had dorsal defects as compared to 23.8% (n = 303) defects in the control.

It does not appear that over-expression of *DPOSH* can modify the effects of constitutively active *DRac1*.

4.10.4 DPOSH^{74} *suppresses the effects of over-expression of DRac1V12*

If DPOSH was acting as a negative regulator, removing DPOSH from the system should enhance the dorsal closure defects seen in over-expression of *DRac1V12*. *DPOSH*^{74}*/DPOSH*^{74}*;hs-GAL4*^{M4}*/UAS-DRac1V12* 6-12 hour AEL embryos were heat shocked at 37°C for 10 minutes and cuticle preparations were performed after the embryos were allowed to develop for 24 hours at room temperature or the embryos were fixed and stained with anti-phosphotyrosine to examine their morphology. *hsGAL4*^{M4}*/UAS-DRac1V12* embryos were used as a control.

Surprisingly, a dramatic *decrease* in the severity of the puckering and a rescue of the DRacV12 induced germband retraction failures were seen in almost all embryos that contained the *DPOSH*^{74} mutation (Fig. 4.12).

Figure 4.12 *DPOSH*^{74} suppresses over-expressed *DRac1V12* in the embryo.

(A) Cuticle preparation of *hsGAL4*^{M4}*/UAS-DRac1V12* 6-12 hour AEL embryo heat shocked at 37˚C for 10 minutes. Severe puckering is seen in the embryo in the area of the dorsal surface as well as the failure of the germ band to retract. (C) Severe puckering and failure of the germ band to retract is seen in the epidermis in this confocal micrograph of a *hsGAL4*^{M4}*/UAS-DRac1V12* embryo treated in a similar fashion as (A) and stained with anti-phosphotyrosine. (B) Cuticle preparation of *DPOSH*^{74}*/DPOSH*^{74}*;hs-GAL4*^{M4}*/UAS-DRac1V12* heat shocked as in (A). A dramatic reduction of the puckering phenotype and rescue of the germ band retraction failure is seen but the embryo fails to survive to past this stage. (D) Confocal micrograph of *DPOSH*^{74}*/DPOSH*^{74}*;hs-GAL4*^{M4}*/UAS-DRac1V12* embryo treated as in (A) and stained with anti-phosphotyrosine showing a reduction in the puckering of the epidermis and a rescue of the germ band retraction failure.

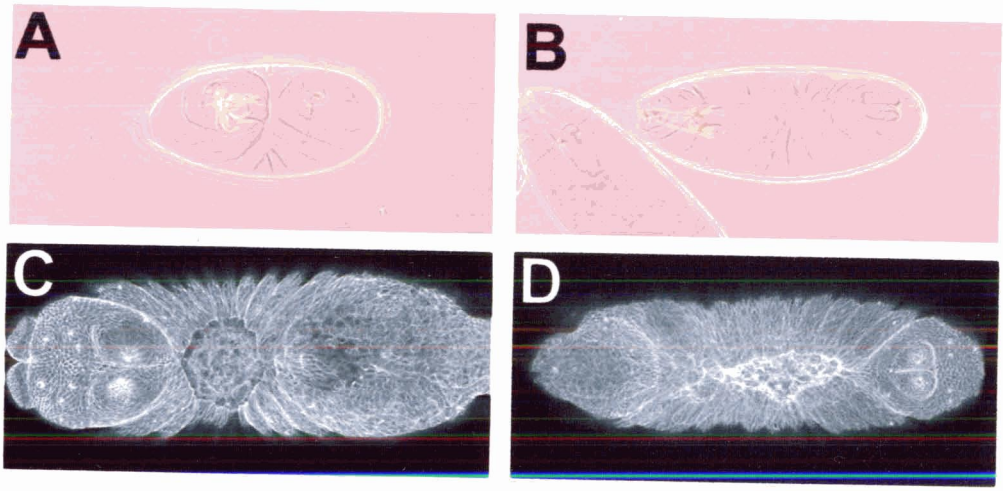
A
B
C
D

This data suggests that DPOSH was actually acting as a positive effector of DRac1 and not as an antagonist as previously demonstrated. These paradoxical results will be considered in the Discussion section.

4.10.5 DPOSH^{74} and Rac1^{J11},Rac2$^{\Delta}$,Mtl$^{\Delta}$ genetically interact during embryogenesis

Embryos homozygous for zygotic loss-of-function mutations for the three Rac proteins in *Drosophila* have a modest frequency of dorsal closure defects (Hakeda-Suzuki et al., 2002). From the previous data DPOSH appeared to have both positive and negative regulatory roles, and examining embryos deficient for both *DPOSH* and the *Drosophila* Rac proteins provide evidence on the function of DPOSH. If DPOSH was acting as a positive effector, the removal of both the maternal and zygotic *DPOSH* from the embryo could cause a worsening of the loss of *DRac* phenotype as signaling by remaining Rac protein would be impaired. If DPOSH was a negative regulator there could be a suppression of the *Rac* loss-of-function phenotype.

DPOSH^{74}/DPOSH^{74};Rac1^{J11},Rac2$^{\Delta}$,Mtl$^{\Delta}$/TM6 flies were constructed as a stock and 0-24 hour AEL embryos were collected and allowed to develop for another 24 hours in order to ensure each embryo proceeded through embryonic development before being dechorionated and cuticle preparations performed. *Rac1^{J11},Rac2$^{\Delta}$,Mtl$^{\Delta}$/TM6* embryos were used as a control.

It is important to note that only one quarter of the embryos on the slide will be homozygous for both *DPOSH^{74}* and *Rac1^{J11},Rac2$^{\Delta}$,Mtl$^{\Delta}$*. Embryo cuticles were examined for changes in a range of dorsal closure defects. The percentage of wild type survivors and embryos exhibiting a completely disrupted cuticle remained roughly the same,

however an increase in germband retraction failures from 8.2% (estimated 32.8% of homozygotes) in the *Rac1*^{J11},*Rac2*$^{\Delta}$,*Mtl*$^{\Delta}$/*TM6* embryos to 13.8% (estimated 55.2%) in the *DPOSH*^{74}/*DPOSH*^{74};*Rac1*^{J11},*Rac2*$^{\Delta}$,*Mtl*$^{\Delta}$/*TM6* embryos was observed, a change of 41%. At the same time the number of embryos exhibiting a wild-type retracted germ-band and a failure of dorsal closure dropped from 9.2% to 1.6% respectively. Over 100 embryos were counted for each experiment. It appears that the *DPOSH*^{74};*Rac1*^{J11},*Rac2*$^{\Delta}$,*Mtl*$^{\Delta}$ embryos are halting earlier, during germband retraction, and are not able to proceed past this point.

These results suggested that DPOSH and DRac co-operate in germband retraction during embryogenesis as demonstrated in the previous section.

4.10.6 Exploring interactions between DPOSH and DRac in the Drosophila eye

In an attempt to resolve the relationship of the interaction between DPOSH and Rac, the *Drosophila* eye was used as a reporter. As shown the over-expression of *DPOSH* in *Drosophila* eyes causes a disorganized structure but the eye shape is retained as compared to a wild type eye (Fig. 4.13A and Fig. 4.13B). Over-expression of *DRac1* and *DRac2* in the *Drosophila* eye increases apoptosis of the ommatidia and consequently a smaller, diamond-shaped organ (Fig. 4.13D and Fig.29F) (Hariharan et al., 1995).

To test if over-expression of *DPOSH* could be modified by the *DRac* mutations, flies bearing the genotype *GMR-GAL4,UAS-DPOSH*$^{10.1}$; *Rac1*^{J11},*Rac2*$^{\Delta}$,*Mtl*$^{\Delta}$/+ were examined (Fig. 4.13C). The eyes remained identical to the eyes of *GMR-GAL4,UAS-DPOSH*$^{10.1}$ flies (Fig. 4.13B). This result indicated that DPOSH does not act through Rac in generating a rough eye phenotype.

Figure 4.13 *DPOSH* and *Rac* Interact in the *Drosophila* eye.

(A) Wild type *Drosophila* eye. (B) *GMR-GAL4,UAS-DPOSH*$^{10.1}$ eyes are rough and disorganized but retain wild type size. (C) *GMR-GAL4,UAS-DPOSH*$^{10.1}$; *Rac1*^{J11},*Rac2*$^{\Delta}$,*Mtl*$^{\Delta}$/+ eye is identical to (B).

(D) *GMR-GAL4,UAS-DRac1* eye is small and almost completely ablated. (E) *GMR-GAL4,UAS-Rac1/UAS-DPOSH*$^{10.1}$ eye is identical to (D).

(F) Over-expression of *DRac2* in the eye, *GMR-GAL4;EP(3)3118*, at 18°C causes a consistently smaller eye than wild type (A). (G) *GMR-GAL4/UAS-DPOSH*$^{10.1}$*;EP(3)3118* flies at 18°C have an eye shape consistenly more severe than that of the eyes of over-expressed *DRac2* alone suggesting that DPOSH can either enhance DRac2 signalling or the effect on the eye is additive. While a large number of flies were mated and a large number of larvae were seen in several vials, only a few *GMR-GAL4/UAS-DPOSH*$^{10.1}$*;EP(3)3118* survivors were obtained from this cross. The eye phenotype shown is a consistent representation of the collection of only four survivors. (H) *GMR-GAL4;EP(3)3118/DPOSH*$^{RING9.1}$,*DPOSH*$^{RING19.1}$, at 18°C has a consistently more severe eye phenotype than (F), but has a much less severe phenotype than (G). (I) *GMR-GAL4/DPOSH*^{74}*;EP(3)3118* eyes at 18°C are also consistently reduced in size compared to (F).

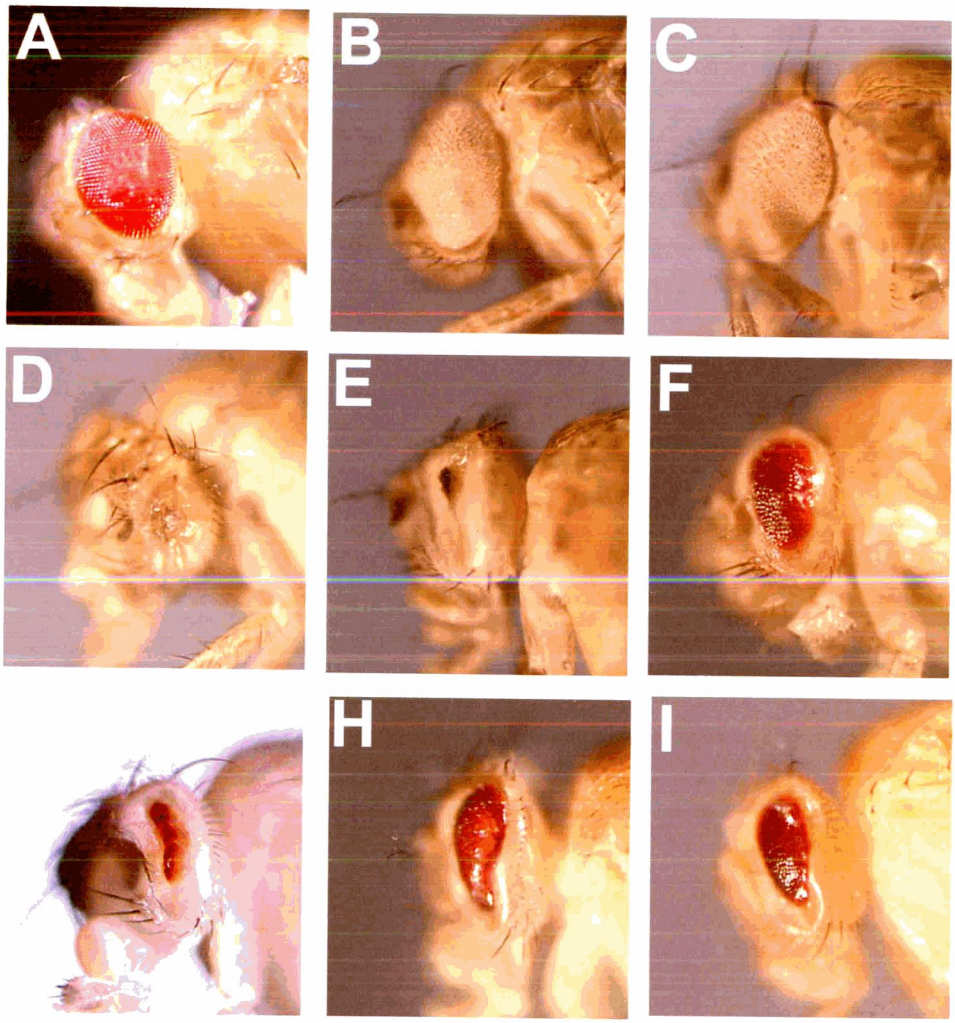
A
B
C
D
E
F
H
I

Flies bearing the genotype *GMR-GAL4, UAS-DRac1/UAS-DPOSH*$^{10.1}$ had eyes that were identical to *GMR-GAL4,UAS-DRac1* flies indicating that *DPOSH* over-expression could not modify the phenotypic effects of *DRac1* over-expression (Fig. 4.13D and Fig. 4.13E).

An EP insertion, *EP(3)3118* proximal to *DRac2* enables the over-expression of *DRac2* by *GAL4* drivers. *GMR-GAL4/UAS-DPOSH*$^{10.1}$*;EP(3)3118* flies at 25°C do not produce any survivors, thus the *DRac2* over-expression experiments were performed at 18◦C. Flies bearing the genotype *GMR-GAL4;EP(3)3118* exhibited diamond shaped eyes at 18°C (Fig. 4.13F). *GMR-GAL4/UAS-DPOSH*$^{10.1}$*;EP(3)3118* flies at 18°C have an eye shape more severe than that of the eyes of over-expressed *DRac2* alone suggesting that DPOSH either contributes to DRac2 signalling or the effect on the eye is additive (Fig. 4.13G).

Interestingly the over-expression of two copies of the *DPOSH* loss of function RING finger transgenes in the *DRac2* over-expressed background, *GMR-GAL4;EP(3)3118/DPOSH*$^{RING9.1}$*,DPOSH*$^{RING19.1}$ flies at 18°C causes a more severe eye phenotype than over-expression of *DRac2* alone. However, it has a much less severe phenotype than the co-expression of wild-type *DPOSH* and *DRac2* in the eye (Fig. 4.13H).

GMR-GAL4/ DPOSH^{74}*;EP(3)3118* eyes at 18°C are also reduced in size compared to over-expression of *DRac2* alone (Fig. 4.13I). This demonstrates that DPOSH is dowstream of DRac2 and suggests that DPOSH interacts with DRac2 in an antagonistic manner.

4.11 Exploring the roles of DPOSH in JNK signaling

4.11.1 DPOSH is not required for the JNK cascade during dorsal closure

Previously it has been shown that an over-expression of *DRac1V12* can cause the ectopic activation of the JNK cascade (Glise and Noselli, 1997). To determine if DPOSH is a member of the JNK cascade, a similar method was used. Embryos bearing the genotypes *ptc-GAL4;UAS-DPOSH*$^{15.1}$ and *ptc-GAL4;UAS-Rac1V12* were collected over 24 hours, fixed and *dpp* RNA *in situs* were performed. Over-expression of *DPOSH* using *ptc-GAL4*, a driver expressing GAL4 in distinct segmented stripes, failed to cause over-expression of *dpp* in *ptc-GAL4;UAS-DPOSH*$^{15.1}$ developing embryos as compared to *ptc-GAL4;UAS-Rac1V12* embryos (Fig. 4.14A and Fig. 4.14B). Even in a *puc*^{E69} 'sensitized' background no evidence of ectopic *dpp* expression was seen (data not shown). As a negative regulator of JNK, a loss of one copy of *puckered (puc)* could, in theory, sensitize the JNK pathway to a weak effector (Glise and Noselli, 1997).

Embryos bearing the genotype *ptc-GAL4;puc*^{E69}*/UAS-DPOSH*$^{15.1}$ were collected over 24 hours and stained with anti-βgalactosidase antibodies. This was done in the presence of a *puc-lacZ* enhancer-trap insertion *puc*^{E69} that allows transcriptional control of *puc* gene expression to be visualized by staining for β-galactosidase (Ring and Martinez Arias, 1993). As *puc* transcription is regulated by the JNK cascade, the pattern of β-galactosidase staining in such an experiment reveals areas of JNK cascade activation (Glise and Noselli, 1997). We looked for overstaining of β-galactosidase as evidence of upregulation of *puckered* caused by an over-expression of *DPOSH*. No evidence was found in over 100 embryos (Fig. 4.14 C).

Figure 4.14 DPOSH does not participate in the JNK pathway in the *Drosophila* embryo.

(A) *dpp in situ* of *ptc-GAL4;UAS-Rac1V12* embryo showing enhanced *dpp* expression along the *ptc* expression pattern (arrowheads). Constitutively activated DRac1 can upregulate the expression of *dpp* through activation of the Jun/Fos complex. (B) *dpp in situ* of *ptc-GAL4;UAS-DPOSH*$^{15.1}$ embryo showing a regular *dpp* expression pattern suggesting that over-expression of *DPOSH* cannot activate the JNK cascade (arrowhead). (C) *ptc-GAL4;puc*^{E69}*/UAS-DPOSH*$^{15.1}$ embryo stained with anti-lacZ to resolve the localization of puckered. Normal puckered staining pattern similar to the *dpp* expression pattern along the dorsal leading edge can be seen suggesting that over-expression of *DPOSH* does not activate the JNK cascade (arrowhead).

(D) and (E) *dpp in situ* of *DPOSH*^{74} embryo showing a regular *dpp* pattern suggesting that *DPOSH* loss of function cannot inhibit the JNK cascade (arrowhead). Wild type pattern can be seen in Fig. 3.11B.

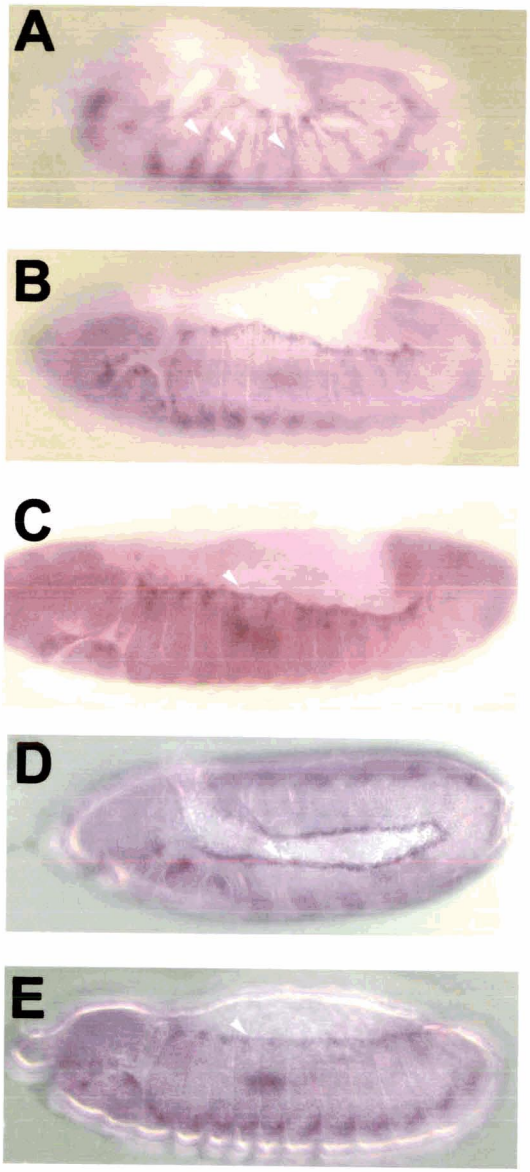
A
B
C
D
E

The effects of loss of maternal and zygotic DPOSH on the JNK cascade-dependent transcription of *dpp* in the leading edge cells were investigated to further search for a possible requirement for DPOSH in the JNK cascade. Embryos from the $DPOSH^{74}$ allele were fixed and examined using *dpp in situ*. The leading edge expression of *dpp* is maintained in $POSH^{74}$ homozygous embryos, indicating that DPOSH is not required for JNK cascade function (Fig. 4.14D and Fig. 4.14E).

As previously mentioned (Results Part 2: Attempts to sensitize the $DPOSH^{74}$ allele), components of the JNK signalling pathway failed to genetically interact with the mutant allele. Moreover, attempts to modify the rough eye generated by *DPOSH* over-expression by introduction of JNK components puc^{E69}, *kayak*, hep^{1}, and *basket*, failed (Results Part 2: Screening for genetic modifiers of *GMR-GAL4,UAS-DPOSH*). These results also suggest that DPOSH does not act through the JNK cascade.

4.12 DPOSH and Apoptosis

4.12.1 $DPOSH^{74}$ embryos fail to stain with Acridine Orange

POSH over-expression in mammalian cells induces JNK signalling and apoptosis (Tapon et al., 1998). $DPOSH^{74}$ embryos, 0-12 hours AEL (after egg laying), were examined for the levels of apoptosis by staining with Acridine Orange (AO). When a cell dies by apoptosis, AO binds duplex DNA and becomes highly flourescent (Abrams et al., 1993), (Delic et al., 1991). During *Drosophila* embryogenesis, apoptosis begins in stage 11, approximately 6 hours AEL and is concentrated in areas of the head and nervous system. $DPOSH^{74}$ embryos did not exhibit any patches of AO staining, while wild type embryos exhibited the regular pattern of apoptotic patches (Fig. 4.15A and Fig. 4.15B). The experiment was repeated several times with controls done in parallel. A rescue

experiment indicated that loss of AO is due to loss of *DPOSH*. *DPOSH^{74}/DPOSH74;hs-Gal4^{M4}/UAS-DPOSH$^{15.1}$* embryos were heat shocked at 37°C for 1 hour 6 hours AEL or were grown at 30°C for the full 12 hours in order to activate the heat shock driven GAL4 expression. Patches of AO were seen in a significant number of these embryos suggesting that the lack of AO staining is due to loss of *DPOSH* (Fig. 4.15C and 4.15D). *DPOSH^{74}/DPOSH74;hs-Gal4^{M4}/+* embryos treated similarly were used as control and did not exhibit AO staining (Fig. 4.15B).

DPOSH^{74} embryos were also stained with TUNEL, another method used to examine apoptosis in cells. *DPOSH^{74}* embryos showed a lower level of TUNEL staining compared to wild-type embryos suggesting that an aspect of apoptosis is inhibited by loss of *DPOSH* (Fig. 4.15E and Fig. 4.15F).

4.12.2 DPOSH^{74} and drICE

The lack of AO staining in *DPOSH^{74}* mutant embryos was surprising as embryos devoid of apoptosis normally dies with severe head defects (Grether et al., 1995). As stated earlier, *DPOSH^{74}* alleles survive to adulthood, and only 12% of *DPOSH^{74}* embryos die with mild head defects. To see if caspases were being activated in *DPOSH^{74}* mutant embryos the activity of drICE was examined. drICE is an effector caspase activated during apoptosis of *Drosophila* cells (Fraser et al., 1997). Antibodies specific for the activated form of drICE were obtained from Bruce Hay and were used to stain *DPOSH^{74}* embryos to examine the caspase activity (Yoo et al., 2002). *DPOSH^{74}* embryos had a similar staining pattern as wild type embryos indicating DPOSH has no role in the activation of drICE (Fig. 4.15G and 4.15H).

Figure 4.15 *DPOSH*^{74} embryos fail to stain with Acridine Orange.

(A) Wild type embryo stained with Acridine Orange (AO). Staining can be seen in the head and along the developing nervous system. (B) *DPOSH*^{74}*/DPOSH74;hs-Gal4*^{M4}/+ embryo heat shocked at 37°C for 1 hour 6 hours AEL showing a lack of AO staining. (C) Rescue of AO staining is seen in *DPOSH*^{74}*/DPOSH74;hs-Gal4*^{M4}*/UAS-DPOSH*$^{15.1}$ embryos heat shocked at 37°C for 1 hour 6 hours AEL (arrowhead). (D) Wider rescue of AO staining as in (C).

(E) TUNEL staining of wild-type and (F) *DPOSH*^{74} embryo. *DPOSH*^{74} embryos showed a lower level of TUNEL staining as compared to the wild-type in embryos fixed in parallel and stained under the same conditions.

(G) Confocal micrograph of wild-type embryo stained with anti-drICE antibodies showing staining pattern of activated caspase in the head and nervous system. (H) *DPOSH*^{74} embryos with a wild type drICE staining pattern.

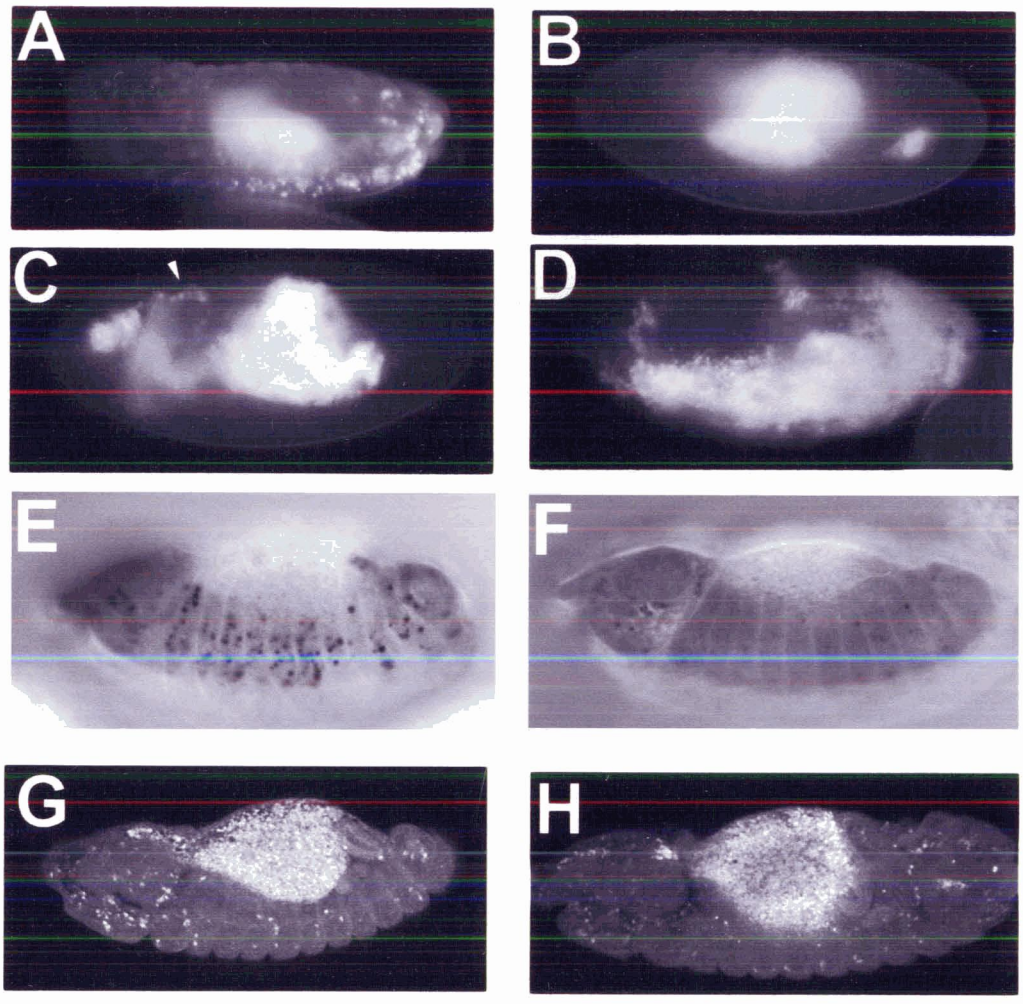
A
B
C
D
E
F
G
H

4.13 New Directions for DPOSH

4.13.1 Screening of Drosophila cDNA library using yeast two-hybrid system identifies 14-3-3ζ as a DPOSH binding partner

The yeast two hybrid screen has been successfully used to identify many interactions in *Drosophila*, for example activated Rac was shown in a yeast two hybrid screen to bind the semaphorin receptor, B plexin (Driessens et al., 2001). *DPOSH* was cloned into the yeast vector as previously described, and as it did not self-activate, it was satisfactory for use in a cDNA library screen for potential binding partners. The library consisted of cDNA isolated from 0-12 hour old embryos and cloned into *pJG4-5* (Finley and Brent). The library was transformed into the EGY48 strain pre-transformed with *pEG202-DPOSH* and the lacZ reporter, *pSH18*. The transformation produced 900,000 primary transformants, and was expanded and $2.7x10^8$ colonies were screened. Thus a 300X coverage of the original transformation was screened. 100 colonies were selected on leucine minus media and replated for selection on Xgal plates. Of these, plasmids were rescued from 10 strong interactors (Fig. 4.16). Sequencing of the library plasmids returned cDNAs encoding ribosomal proteins and 14-3-3ζ or Leonardo. Since ribosomal proteins often result in false positives they were discarded (Golemis et al., 1999). The plasmid containing *14-3-3ζ* was retransformed along with *pEG202-DPOSH* into fresh EGY48 yeast cells and retested for interaction to rule out background effects. *14-3-3ζ* was also transformed alone into yeast without the presence of *pEG202-DPOSH* to rule out self-activation.

Discovery of the common 14-3-3 binding domain, RSXSXP, in the amino acid sequence of DPOSH, was consistant with the yeast two hybrid result being genuine

Figure 4.16 Screening of *Drosophila* cDNA library using yeast two-hybrid system identifies 14-3-3ζ as a DPOSH binding partner.

(A) Yeast transformed with *pEG202-DPOSH* bait and *pJG4-5-14-3-3ζ* fail to grow on glucose^{+}/leucine^{-} plates. Glucose is able to repress the GAL1 promoter effectively repressing the expression of *14-3-3ζ* demonstrating that DPOSH is unable to self-activate *LEU2* expression by binding the LexA operator and activating transcription of *LEU2*. (B) Galactose-induced expression of *14-3-3ζ* in yeast transformed with *pEG202-DPOSH* bait and *pJG4-5-14-3-3ζ* on galactose^{+}/leucine^{-} plates. DPOSH and 14-3-3ζ bind to complete the transcription factor and induce *LEU2* expression and allow the yeast to grow on leucine deficient media. (C) Yeast transformed with *pEG202-DPOSH* bait, *pJG4-5-14-3-3ζ*, and *pSH18-34* Xgal reporter on glucose^{+}/Xgal plates cannot induce expression of lacZ and subsequent Xgal catalysis. This is a similar control to test that DPOSH cannot self_activate lacZ transcription as 14-3-3ζ is not expressed. (D) Yeast transformed with *pEG202-DPOSH* bait, *pJG4-5-14-3-3ζ*, and *pSH18-34* Xgal reporter on galactose^{+}/Xgal plates can induce expression of lacZ and subsequent Xgal catalysis resulting in a positive blue colour. This is the result of DPOSH and 14-3-3ζ binding to complete a transcription factor and inducing expression of lacZ under the control of a LexA promoter.

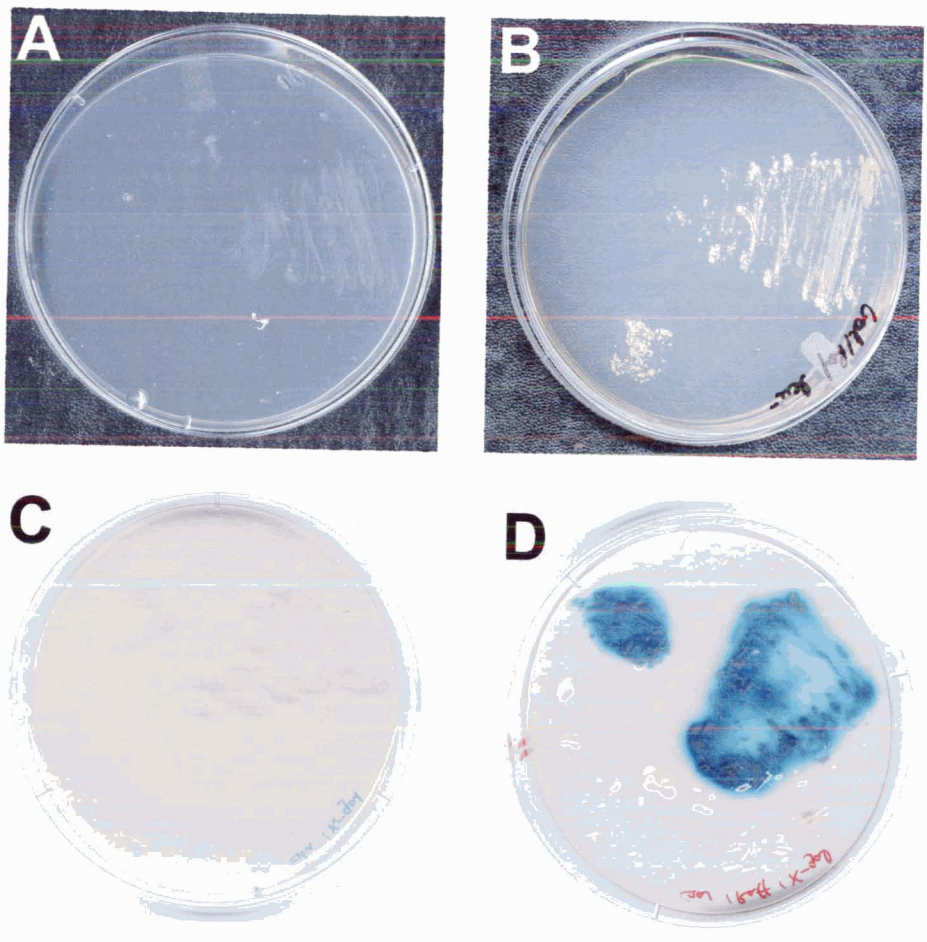
A
B
C
D

(Muslin et al., 1996). The proposed 14-3-3ζ domain in DPOSH consists of the sequence RSGSCP.

14-3-3ζ or Leonardo, has been implicated in the Torso (Tor) receptor tyrosine kinase Ras/Raf-1/MEK pathway that controls the transcription of *tailless* (*tll*) in 1-2 hour old *Drosophila* embryos (Li et al., 1997a). It may be possible that DPOSH is part of this signalling pathway or provides a link between that pathway and Rac1 signalling.

4.13.2 DPOSH may participate in 14-3-3ζ function

Since DPOSH was found to bind 14-3-3ζ in the yeast two hybrid screen and it was shown that over-expression of *14-3-3ζ* in embryos 1-2 hours AEL caused paired denticle belt defects, a similar experiment was performed with *DPOSH* (Li et al., 1997a). Over-expression of *DPOSH* using *hs-GAL4^{M4},EP(2)1206/CyO* in 1-2 hour old embryos at 37°C for 10 minutes revealed an increase in the number of embryos bearing paired denticle belts after cuticle preparation (Fig. 4.17A, 4.17B, and 4.17C). The percentage of embryos with the denticle belt defect was 5.6% vs a wild type background of 2.1%. Over 500 embryos were scored and a p value of .011 was returned from a paired T-test. Over-expression of *14-3-3zeta* during this time frame of embryogenesis also caused an increase in paired denticle belts, thus a role of *DPOSH* in this signalling pathway could be possible.

It has been shown that 14-3-3ζ acts through Raf to induce *tailless* transcription (Li et al., 1997a). As was shown, 14-3-3ζ binds DPOSH by yeast two hybrid, therefore a similar experiment was performed to determine if DPOSH could act similar to 14-3-3ζ and alter *tailless* transcription.

Figure 4.17 Over-expression of *DPOSH* causes denticle belt defects.

(A) Wild type embryo showing normal denticle belt pattern as indicated by the arrow. (B) and (C) *hs-GAL4M4/UAS-POSH* embryos where the expression of *DPOSH* has been driven by heat shocking the embryos at 37°C for 10 minutes 1-2 hours after egg laying (AEL). Denticle belt defects are seen where there is a pairing of denticle belts, as indicated by arrows.

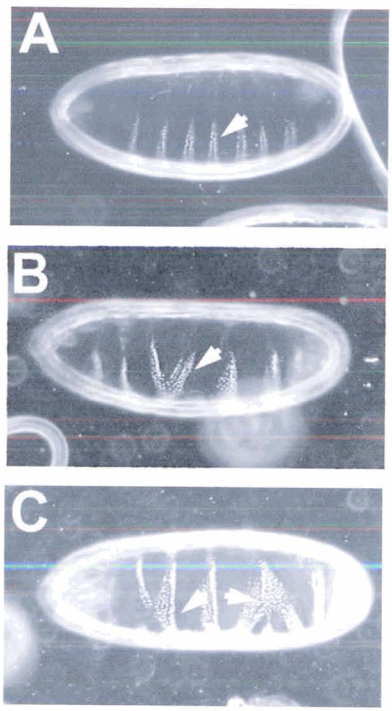
A
B
C

DPOSH was over-expressed using *nanos-GAL4*, a driver expressing GAL4 ubiquitously during the first hours of embyro development. 1-2 hour old progeny were collected, fixed and *in situs* were performed using a DIG labelled *tailless* antisense probe.

Wild type flies were crossed with nanos-GAL4 and their progeny were simultaneously collected and hybridized as a control. The quantification of *tailless* levels was calculated by measuring the length of the posterior *in situ tailless* band of expression as compared to the length of the embryo (Li et al., 1997a). In the late syncytial blastoderm stage, control embryos (*nanosGAL4/+;+/+*) had a *tailless* expression pattern extending an average of 9% of the length of the embryo (n=36) while in *nanosGAL4/+;UAS-DPOSH/+* embryos *tailless* expression extended an average of 13.65% of the embryo length, an increase of 52% (n=60) (Fig. 4.18A and 4.18B).

This data suggested that DPOSH may act with 14-3-3ζ to activate Raf and induce *tailless* transcription. However *tailless in situ* experiments on $DPOSH^{74}$ mutant embryos did not show any effect on normal expression suggesting that DPOSH is not required for *tailless* expression. The majority, 60%, of maternal and zygotic deficient *14-3-3ζ* embryos also show a normal *tailless* expression pattern, while 40% show reduced *tailless* expression (Li et al., 1997b).

4.13.3 Screening for genetic modifiers of GMR-GAL4,UAS-DPOSH

As shown previously the over-expression of *DPOSH* in the *Drosophila* eye produces a "rough eye" phenotype. This phenotype is easy to score and has been demonstrated to be useful for the purpose of determining genetic interactions especially since the eye is not required for survival (Barrett et al., 1997). The availability from the

Figure 4.18 Over-expression of DPOSH in 1-2 hour AEL embryos upregulates *tailless* expression.

A) *In situ tailless* pattern in *nanosGAL4/+;+/+* embryo showing a wild-type pattern of expression at both the anterior and posterior ends of the embryo. An arrow marks the *tailless* pattern boundary in the posterior end of the embryo. (B) *In situ tailless* pattern in *nanosGAL4/+;UAS-DPOSH/+* embryo showing a wider posterior domain of *tailless* expression compared to wild-type (arrow). RNA *in situs* on control and expressed embryos were done in parallel using the same set of reagents.

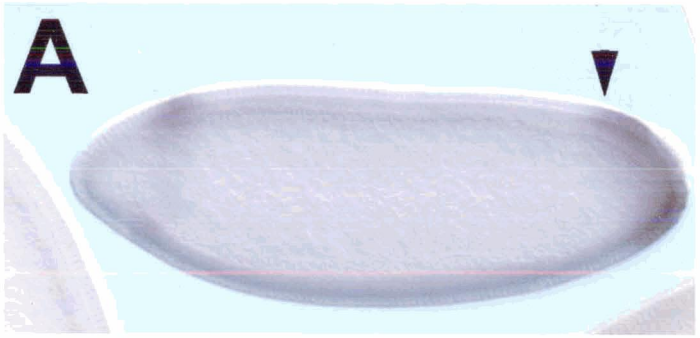
A


B

Bloomington Stock Center of large deficiency (Df) stocks covering most of the *Drosophila* genome allows one to rapidly search the genome for genetic interactions that either suppress or enhance rough eye phenotypes. *GMR-GAL4* was recombined onto a second chromosome *UAS-POSH* transgene and used for screening experiments. This was crossed to males from the deficiency kit and forty *GMR-GAL4,UAS-POSH/Df* progeny were examined for each cross (Table 3). No enhancers or suppressors were found in the screen. Logical lines were also tested such as the JNK pathway components: puc^{E69}, *kayak*, hep^{1}, and *basket;* the potential binding partner from the yeast two hybrid screen: *14-3-3epsilon* and *1 4-3-3zeta* (*leonardo*) and genes associated with the torso pathway, Btk^{1}; apoptosis inhibitors: *UAS-p35* and *H99;* apoptosis inducer: *GMR-reaper*; and proteosome pathway associated gene: *Tbp-1*, have all been tested and none were found to affect the rough eye.

An example of the screening methodology is shown with *GMR-reaper* (Fig. 4.19). Upregulation of *reaper* has been shown to induce apoptosis in the *Drosophila* eye (Fig. 4.19B) (White et al., 1996). Mammalian POSH could induce apoptosis and it was decided to test for interaction between DPOSH and reaper (Tapon et al., 1998). *GMR-reaper/GMR-GAL4,UAS-POSH* eyes were compared to *GMR-reaper/GMR-GAL4* eyes as a control. Eye sizes in both genotypes appeared similar suggesting that DPOSH and reaper were not interacting (Fig. 4.19E and Fig. 4.19F). The presence of two copies of *GMR* was enough to reduce the severity of the *GMR-reaper* eyes implying that perhaps two copies of *GMR* was enough to interfere with the stochiometry of the levels of the glass transcription factor present in the eye (Fig. 4.19B and Fig. 4.19E) (Hay et al., 1997).

Table 4.2 Results of screening for modifiers of the rough eye resulting from over-expression of *DPOSH* in the *Drosophila* eye.

GMR-GAL4,UAS-POSH flies were crossed with flies from the Bloomington deficiency kit designed to cover the *Drosophila* genome. Deficiencies on chromosomes 2 and 3 were used in the cross and the eyes of the resulting progeny, *GMR-GAL4,UAS-POSH/Df*, were examined for enhancement or suppression of the rough eye. C refers to the autosome number. The Number Screened is the number of flies of the relevant genotype that were examined for modification while the Modified Number is the number of flies bearing modified eyes. No modifiers were found.

Bloomington Stock Number	C	Genetic Name	Locus	Number Screened	Modified
3638	2	Df(2L)net-PMF	21A1;21B7-8	40	0
6283	2	Df(2L)BSC4	21B7-C1;21C2-3	40	0
6608	2	Df(2L)BSC16	21C3-4;21C6-8	40	0
3084	2	Df(2L)ast2	21D1-2;22B2-3	40	0
3133	2	Df(2L)dp-79b	22A2-3;22D5-E1	40	0
7144	2	Df(2L)BSC37	22D2-3;22F1-2	40	0
6648	2	Df(2L)dpp[d14]	22E4-F2;22F3-23A1	Eye glazed	-
90	2	Df(2L)C144	22F3-4;23C3-5	40	0
1567	2	Df(2L)JS17	23C1-2;23E1-2	40	0
6875	2	Df(2L)BSC28	23C5-D1;23E2	40	0
6965	2	Df(2L)BSC31	23E5;23F4-5	40	0
6507	2	Df(2L)drm-P2	23F3-4;24A1-2	40	0
5330	2	Df(2L)ed1	24A2;24D4	40	0
693	2	Df(2L)sc19-8	24C2-8;25C8-9	40	0
3813	2	Df(2L)sc19-4	25A5;25E5	40	0
781	2	Df(2L)cl-h3	25D2-4;26B2-5	40	0
490	2	Df(2L)E110	25F3-26A1;26D3-11	40	0
6299	2	Df(2L)BSC5	26B1-2;26D1-2	40	0
6338	2	Df(2L)BSC6	26D3-E1;26F4-7	40	0
6374	2	Df(2L)BSC7	26D10-E1;27C1		
2414	2	Df(2L)spd[j2]	27C1-2;28A	40	0
5420	2	Df(2L)Dwee1-W05	27C2-3;27C4-5		
4956	2	Df(2L)XE-3801	27E2;28D1	40	0
7147	2	Df(2L)BSC41	28A4-B1;28D3-9	40	0
140	2	Df(2L)Trf-C6R31	28DE;28DE	40	0
179	2	Df(2L)TE29Aa-11	28E4-7;29B2-C1	40	0
2892	2	Df(2L)N22-14	29C1-2;30C8-9	40	0
6478	2	Df(2L)BSC17	30C3-5;30F1	40	0
1045	2	Df(2L)Mdh	30D-30F;31F	40	0
3366	2	Df(2L)J2	31B;32A	40	0
7142	2	Df(2L)BSC32	32A1-2;32C5-D1	40	0
7143	2	Df(2L)BSC36	32D1;32D4-E1	40	0
5869	2	Df(2L)FCK-20	32D1;32F1-3	40	0
3079	2	Df(2L)Prl	32F1-3;33F1-2	40	0
6999	2	Df(2L)BSC30	34A3;34B7-9	40	0
3138	2	Df(2L)b87e25	34B12-C1;35B10-C1	40	0
3588	2	Df(2L)TE35BC-24	35B4-6;35F1-7	40	0
1491	2	Df(2L)r10	35D1;36A6-7	40	0
2583	2	Df(2L)cact-255rv64	35F-36A;36D	40	0
420	2	Df(2L)TW137	36C2-4;37B9-C1	40	0
567	2	Df(2L)pr-A16	37B2-12;38D2-5	40	0
167	2	Df(2L)TW161	38A6-B1;40A4-B1	40	0

4959	2	Df(2L)C'	h35;h38L	40	0
739	2	Df(2R)M41A4	41A;41A		
749	2	In(2R)bw[VDe2L]Cy[R]	41A-B;42A2-3	40	0
1007	2	Df(2R)nap9	42A1-2;42E6-F1	40	0
1888	2	Df(2R)ST1	42B3-5;43E15-18		
3368	2	Df(2R)cn9	42E;44C	40	0
198	2	Df(2R)H3C1	43F;44D3-8	40	0
201	2	Df(2R)H3E1	44D1-4;44F12	40	0
3591	2	Df(2R)Np5	44F10;45D9-E1	40	0
4966	2	Df(2R)w45-30n	45A6-7;45E2-3	40	0
6917	2	Df(2R)BSC29	45D3-4;45F2-6	40	0
1743	2	Df(2R)B5	46A;46C	40	0
1702	2	Df(2R)X1	46C;47A1	40	0
447	2	Df(2R)stan1	46D7-9;47F15-16	40	0
190	2	Df(2R)en-A	47D3;48B2	40	0
1145	2	Df(2R)en30	48A3-4;48C6-8	40	0
7145	2	Df(2R)BSC39	48C5-D1;48D5-E1	40	0
4960	2	Df(2R)CB21	48E;49A	40	0
7146	2	Df(2R)BSC40	48E1-2;48E2-10		
5879	2	Df(2R)BSC3	48E12-F4;49A11-B6	40	0
754	2	Df(2R)vg-C	49A4-13;49E7-F1	40	0
442	2	Df(2R)CX1	49C1-4;50C23-D2	40	0
6516	2	Df(2R)BSC18	50D1;50D2-7	40	0
6455	2	Df(2R)BSC11	50E6-F1;51E2-4	40	0
3518	2	Df(2R)Jp1	51D3-8;52F5-9	40	0
3520	2	Df(2R)Jp8	52F5-9;52F10-53A1	40	0
7445	2	Df(2R)BSC49	53D9-E1;54B5-10	40	0
6404	2	Df(2R)P803-Delta15	53E;53F11	40	0
6916	2	Df(2R)ED1	53E10;53F9		
7414	2	Df(2R)BSC44	54B1-2;54B7-10	40	0
5680	2	Df(2R)robl-c	54B17-C4;54C1-4	40	0
5574	2	Df(2R)k10408	54C1-4;54C1-4	40	0
7441	2	Df(2R)BSC45	54C8-D1;54E2-7	40	0
6779	2	Df(2R)14H10Y-53	54D1-2;54E5-7	40	0
6780	2	Df(2R)14H10W-35	54E5-7;55B5-7	40	0
1547	2	Df(2R)PC4	55A;55F	40	0
757	2	Df(2R)P34	55E2-4;56C1-11	40	0
6866	2	Df(2R)BSC26	56C4;56D6-10	40	0
6647	2	Df(2R)BSC22	56D7-E3;56F9-12	40	0
543	2	Df(2R)017	56F5;56F15	40	0
3467	2	Df(2R)AA21	56F9-17;57D11-12		
6609	2	Df(2R)BSC19	56F12-14;57A4	40	0
5246	2	Df(2R)Egfr5	57D2-8;58D1	40	0

282	2	Df(2R)X58-12	58D1-2;59A	40	0
3909	2	Df(2R)59AD	59A1-3;59D1-4	40	0
7273	2	Df(2R)vir130	59B;59D8-E1	40	0
1682	2	Df(2R)or-BR6	59D5-10;60B3-8	40	0
2604	2	Df(2R)Px2	60C5-6;60D9-10	40	0
2471	2	Df(2R)M60E	60E2-3;60E11-12	40	0
3157	2	Df(2R)ES1	60E6-8;60F1-2	40	0
4961	2	Df(2R)Kr10	60F1;60F5	40	0
2577	3	Df(3L)emc-E12	61A;61D3	40	0
439	3	Df(3L)Ar14-8	61C5-8;62A8	40	0
5411	3	Df(3L)Aprt-32	62B1;62E3	40	0
2400	3	Df(3L)R-G7	62B8-9;62F2-5	40	0
6755	3	Df(3L)BSC23	62E8;63B5-6	40	0
3650	3	Df(3L)M21	62F;63D	40	0
3649	3	Df(3L)HR119	63C2;63F7	40	0
463	3	Df(3L)GN34	63E6-9;64A8-9		
3686	3	Df(3L)GN24	63F6-7;64C13-15	40	0
3096	3	Df(3L)ZN47	64C;65C	40	0
4393	3	Df(3L)XDI98	65A2;65E1	40	0
6867	3	Df(3L)BSC27	65D4-5;65E4-6	40	0
6964	3	Df(3L)BSC33	65E10-F1;65F2-6	40	0
1420	3	Df(3L)pbl-X1	65F3;66B10	40	0
5877	3	Df(3L)ZP1	66A17-20;66C1-5	40	0
1541	3	Df(3L)66C-G28	66B8-9;66C9-10	40	0
6460	3	Df(3L)BSC13	66B12-C1;66D2-4	40	0
3024	3	Df(3L)h-i22	66D10-11;66E1-2	40	0
4500	3	Df(3L)Scf-R6	66E1-6;66F1-6	40	0
7079	3	Df(3L)BSC35	66F1-2;67B2-3		
997	3	Df(3L)AC1	67A2;67D11-13	40	0
6471	3	Df(3L)BSC14	67E3-7;68A2-6	40	0
2611	3	Df(3L)vin5	68A2-3;69A1-3	40	0
2612	3	Df(3L)vin7	68C8-11;69B4-5	40	0
5492	3	Df(3L)eyg[C1]	69A4-5;69D4-6	40	0
6456	3	Df(3L)BSC10	69D4-5;69F5-7	40	0
6457	3	Df(3L)BSC12	69F6-70A1;70A1-2	40	0
4366	3	In(3LR)C190[L]Ubx[42TR]	70A1-2;70C3-4	40	0
3124	3	Df(3L)fz-GF3b	70C1-2;70D4-5	40	0
3126	3	Df(3L)fz-M21	70D2-3;71E4-5	40	0
6551	3	Df(3L)XG5	71C2-3;72B1-C1	40	0
3640	3	Df(3L)brm11	71F1-4;72D1-10	40	0
2993	3	Df(3L)st-f13	72C1-D1;73A3-4	40	0
2998	3	Df(3L)81k19	73A3;74F	40	0
6411	3	Df(3L)BSC8	74D3-75A1;75B2-5	40	0
2608	3	Df(3L)W10	75A6-7;75C1-2	40	0

2990	3	Df(3L)Cat	75B8;75F1	40	0
6754	3	Df(3L)fz2	75F10-11;76A1-5	40	0
6646	3	Df(3L)BSC20	76A7-B1;76B4-5	40	0
3617	3	Df(3L)kto2	76B1-2;76D5		
5126	3	Df(3L)XS533	76B4;77B	40	0
2052	3	Df(3L)rdgC-co2	77A1;77D1		
3127	3	Df(3L)ri-79c	77B-C;77F-78A	40	0
5878	3	Df(3L)ri-XT1	77E2-4;78A2-4	40	0
4429	3	Df(3L)ME107	77F3;78C8-9		
4430	3	Df(3L)Pc-2q	78C5-6;78E3-79A1	40	0
4506	3	Df(3L)Ten-m-AL29	79C1-3;79E3-8	40	0
5951	3	Df(3L)HD1	79D3-E1;79F3-6		
6649	3	Df(3L)BSC21	79E5-F1;80A2-3	40	0
1518	3	Df(3R)ME15	81F3-6;82F5-7	40	0
4787	3	Df(3R)3-4	82F3-4;82F10-11	40	0
5694	3	Df(3R)e1025-14	82F8-10;83A1-3	40	0
7443	3	Df(3R)BSC47	83B7-C1;83C6-D1	40	0
1990	3	Df(3R)Tpl10	83C1-2;84B1-2	40	0
2393	3	Df(3R)WIN11	83E1-2;84A4-5	40	0
1884	3	Df(3R)Scr	84A1-2;84B1-2	40	0
1842	3	Df(3R)Antp17	84B1-2;84D11-12 or 84A6;84D14	40	0
1968	3	Df(3R)p712	84D4-6;85B6	40	0
1962	3	Df(3R)p-XT103	85A2;85C1-2	40	0
6756	3	Df(3R)BSC24	85C4-9;85D12-14	40	0
1931	3	Df(3R)by10	85D8-12;85E7-F1	40	0
7080	3	Df(3R)BSC38	85F1-2;86C7-8	40	0
3128	3	Df(3R)M-Kx1	86C1;87B1-5	40	0
3003	3	Df(3R)T-32	86E2-4;87C6-7	40	0
3007	3	Df(3R)ry615	87B11-13;87E8-11	40	0
1534	3	Tp(3;Y)ry506-85C	87D1-2;88E5-6	40	0
383	3	Df(3R)ea	88E7-13;89A1	40	0
756	3	Df(3R)sbd105	88F9-89A1;89B9-10	40	0
1920	3	Df(3R)sbd104	89B5;89C	40	0
1467	3	Df(3R)P115	89B7-8;89E7	40	0
4431	3	Df(3R)DG2	89E1-F4;91B1-B2	40	0
3011	3	Df(3R)Cha7	90F1-F4;91F5	40	0
3012	3	Df(3R)Dl-BX12	91F1-2;92D3-6	40	0
4962	3	Df(3R)H-B79	92B3;92F13	40	0
7413	3	Df(3R)BSC43	92F7-93A1;93B3-6		
2425	3	Df(3R)e-N19	93B;94	40	0
3340	3	Df(3R)e-R1	93B6-7;93D2	40	0
2586	3	Df(3R)23D1	94A3-4;94D1-4	40	0
4940	3	Df(3R)mbc-30	95A5-7;95C10-11		0
2585	3	Df(3R)mbc-R1	95A5-7;95D6-11	40	0

4432	3	Df(3R)crb-F89-4	95D7-D11;95F15	40	0
2363	3	Df(3R)crb87-5	95F7;96A17-18	40	0
3468	3	Df(3R)slo8	96A2-7;96D2-4	40	0
5601	3	Df(3R)Espl3	96F1;97B1	40	0
1910	3	Df(3R)Tl-P	97A;98A1-2	40	0
823	3	Df(3R)D605	97E3;98A5	40	0
7412	3	Df(3R)BSC42	98B1-2;98B3-5		0
430	3	Df(3R)3450	98E3;99A6-8	40	0
669	3	Df(3R)Dr-rv1	99A1-2;99B6-11	40	0
3547	3	Df(3R)L127	99B5-6;99E4-F1	40	0
3546	3	Df(3R)B81	99C8;100F5	40	0
		puc^{E69}		40	0
		kayak		40	0
		hep^{1}		40	0
		basket		40	0
		slpr^{1}		40	0
		14-3-3epsilon		40	0
		14-3-3zeta		40	0
		Btk^{1}		40	0
		UAS-DIAP1		40	0
		UAS-p35		40	0
		H99		40	0
		GMR-reaper		40	0
		Tbp-1		40	0

Figure 4.19 Example of screening methodology used to search for modifiers of *DPOSH*.

(A) Wild type eye. (B) *GMR-reaper/ GMR-reaper* eye with a classic wedge shape due to increased levels of apoptosis in the developing eye. (C) *GMR-reaper/+* eye with a reduction in apoptosis levels caused by removal of one copy of the *GMR-reaper* chromosome. (D) The over-expression phenotype of *reaper* in the eye is not modified by the *DPOSH* mutant allele $POSH^{74}$. *GMR-reaper/POSH74* eye has a similar shape to the *GMR-reaper/+* eye suggesting no evidence of genetic interaction in the eye. (E) *GMR-reaper/GMR-GAL4* with yet a further reduction in apoptosis levels as suggested by a larger eye, possibly due to saturation of the glass multimer reporter (GMR). (F) *GMR-reaper/GMR-GAL4,UAS-DPOSH* eye similar in size to the *GMR-reaper/GMR-GAL4* eye suggesting no evidence of interaction between reaper and DPOSH.

All eyes are from adult female flies.

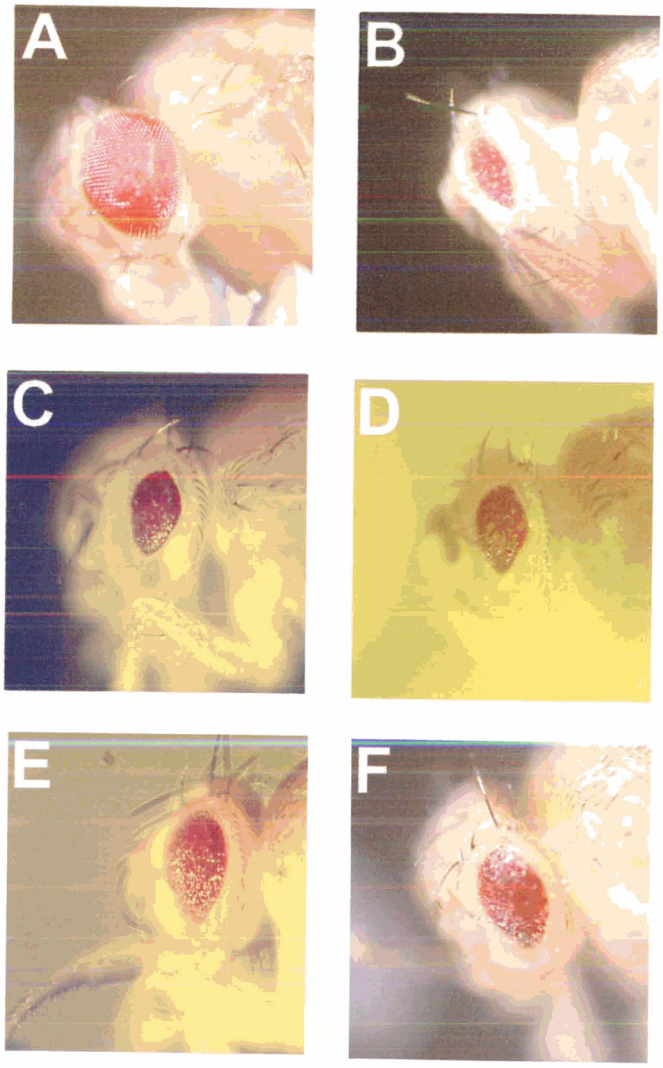
A
B
C
D
E
F

RESULTS PART 3

Drosophila Rho GTPase Activating Protein 68F

5.1 Drosophila RhoGAP68F has preferential affinity for activated Rho

As part of the search for regulators of Rac signalling in *Drosophila*, a RhoGAP was selected for investigation. GTPase activating proteins (GAPs) act as negative regulators of GTPases by activating the intrinsic GTPase activity of the GAPs, facilitating the cleavage of bound GTP to GDP, inactivating the signaling pathway. At the same time, there is evidence that GAPs can act as effectors of signalling downstream of GTPases. For example, n-chimaerin, a Rac1 GAP, was shown to be able to induce the formation of actin based structures lamellipodia and filopodia (Kozma et al., 1996). *RhoGAP68F*, reported in a survey of *Drosophila* GAPs by Billuart et al., was selected for study in *Drosophila* as it had an EP element, *EP(3)3152*, conveniently inserted upstream of the gene (Billuart et al., 2001). RhoGAP68F is homologous to the human p50RhoGAP that had been shown to be a GAP for Cdc42, which as stated earlier is very similar to Rac (Lancaster et al., 1994). Therefore DRhoGAP68F might regulate Cdc42/Rac signalling in *Drosophila*.

The cDNA clone of a *Drosophila RhoGAP68F* was inserted in frame into pXJFLAG and used in GST-pull down experiments to assess the binding preferences of DRhoGAP.

Binding assay experiments in a manner similar to those between DRac1 and DSra-1 were performed. The *pXJFLAG-RhoGAP68F* construct was used for transcription

of *RhoGAP68F* by phage T7 polymerase and translation by rabbit reticulolysate in the presence of ^{35}S-methionine produced ^{35}S labelled RhoGAP68F. GST-DRac1, GST-Dcdc42 and GST-DRho1 were expressed in BL21 cells, bound to glutathione sepharose beads, and exchanged with either an unhydrolyzable form of GTP (GTP-γS) or GDP to give the active and inactive forms of the p21s, respectively. Under the conditions of a fairly strict wash buffer of Tris pH 7.5 + 0.5% Triton-X, RhoGAP68F is found to preferentially bind GTP-γS –DRho (Fig. 5.1).

5.2 DRhoGAP preferentially activates Rho GTPase

To investigate whether RhoGAP68F could function as a GTPase activating protein (GAP) and increase the rate of hydrolysis of GTP to GDP by Rho GTPase, a GAP assay was performed.

The purified forms of human Rac1, RhoA and Cdc42 GTPases were prepared from pGEX constructs obtained from Edward Manser, IMCB, Singapore. The concentration of GTPases was quantified by Bradford assay and 2 μg of purified GTPase was loaded with [$^{\gamma 32}$P]GTP as explained in Materials and Methods. GST-RhoGAP68F was expressed in bacteria, purified, and added to the [$^{\gamma 32}$P]GTP bound GTPase at a final concentration of 0.001 mg/mL. Aliquots were taken from the reaction mix, halted and the [$^{\gamma 32}$P]GTP bound GTPase was linked to a 0.45 μm nitrocellulose filter. The filters were washed of unbound [$^{\gamma 32}$P]GTP and were placed in scintillation vials and the remaining bound radioactive phosphate was counted.

Final counts revealed that RhoGAP68F showed the strongest GAP activity against RhoA (Fig. 5.2).

Figure 5.1 GST-pull down assay demonstrating preferential binding of RhoGAP68F to GTP-bound DRhoA.

RhoGAP68F was expressed in the presence of ^{35}S methionine that incorporated the radioactively labelled amino acid into the protein. GST fusion constructs of the p21s were pulled out using GST beads, washed, and loaded on an acrylamide gel. Exposure of the gel to film revealed the presence of RhoGAP68F bound to activated DRho.

This result is representative of several separate experiments. Coomassie blue staining of the gels indicated equal loading of the small GTPases (data not shown).

RhoGAP68F
60% input
GST-GTPγS
GST-GDP
GST-DRac1-GTPγS
GST-DRac1-GDP
GST-DRhoA-GTPγS
GST-DRhoA-GDP
GST-Dcdc42-GTPγS
GST-Dcdc42-GDP

The use of the human GTPases in the GAP assays was favoured over the *Drosophila* GTPases as the *Drosophila* proteins have an extremely rapid rate of intrinsic GTPase function even at 4°C, such that the assay is extremely difficult to perform.

The combined results from the GST-pull down assay and the GAP assay suggest that RhoGAP68F functions as a GAP for RhoA in Drosophila. Given that the intent of this thesis was the study of Rac-specific signalling, work on RhoGAP68F was not pursued further.

Figure 5.2 Chart depicting the preferred GAP activity of RhoGAP68F for RhoA vs. Cdc42 or Rac1.

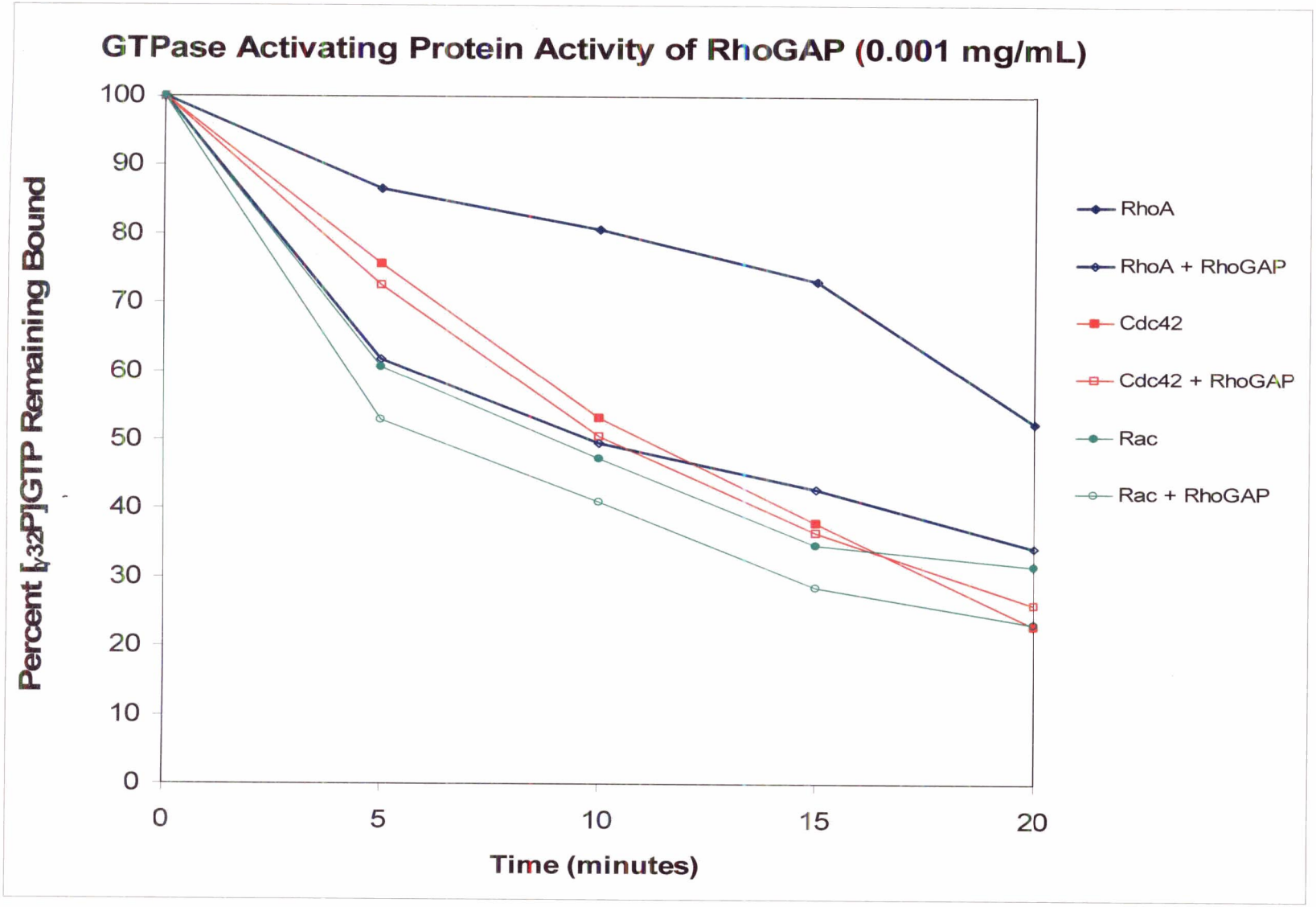
GTPase Activating Protein Activity of RhoGAP (0.001 mg/mL)
Percent [γ32P]GTP Remaining Bound
100
90
80
70
60
50
40
30
20
10
0
0
5
10
15
20
Time (minutes)
RhoA
RhoA + RhoGAP
Cdc42
Cdc42 + RhoGAP
Rac
Rac + RhoGAP

DISCUSSION PART 1

Drosophila Sra-1

A *Drosophila* homolog of *Sra-1* has been identified and cloned. It was sequenced and submitted to NCBI, designated accession number AY029211. *Sra-1* has only one *Drosophila* homolog, expressing a transcription product of 4.6kb, and the translated protein has a remarkable similarity to the human counterpart of 80%. No evident domains could be found within DSra-1.

As Sra-1 had been shown to bind to GTP-bound Rac1 as well as the cytoskeletal component, F-actin, and had a closely homologous *Drosophila* counterpart, it was decided to be a good candidate for investigation in a model organism (Kobayashi et al., 1998). DSra-1 was also found to be able to bind GTP-bound DRac1, suggesting a conserved route of function.

6.1 A role for DSra-1 cannot be demonstrated during dorsal closure

Dorsal closure is a well characterized model system for the study of epithelial cell motility and shape change, cellular functions that activated Rac1 has been shown to participate in (Harden, 2002). Indeed, Rac is a key regulator of the actin cytoskeleton in dorsal closure. Sra-1, with its association with F-actin and GTP-bound Rac1, seemed a promising candidate effector for Rac in this process.

The expression pattern of *DSra-1* during embryogenesis was not a promising indicator of a role for DSra-1 in dorsal closure. Enrichment of *DSra-1* transcript was seen

only in the central and peripheral nervous system, however, this did not preclude a role, as many participants in dorsal closure do not show an enrichment in leading edge cells as many participants in dorsal closure do not show an enrichment in the leading edge cells.

More promising was the cross-reactivity of the anti-human Sra-1 antibody to DSra-1 (Kobayashi et al., 1998). Staining of the embryos during embryogenesis revealed an enriched staining pattern of DSra-1 in the leading edge cells. Moreover, over-expression of *DSra-1* during embryogenesis caused dorsal closure defects. Taken together, these results suggested a role for DSra-1 in dorsal closure.

Genetic studies, however, failed to demonstrate a role for DSra-1 in Rac signaling during dorsal closure. The rescue of the phenotypic effects of *DRacN17* expression by over-expression of *DSra-1* was successful in increasing the survivability of the embryos, but had no effect on the frequency of dorsal defects. The increase in survivability is possibly due to the rescue of alternative defects caused by the global over-expression of *DRacN17*, in particular it may be possible that *DSra-1* over-expression was able to rescue various nervous system defects.

As our collaborators, Schenck et al., have shown, DSra-1 is a component of *Drosophila* Rac signaling in neural development (Schenck et al., 2003). However, their data suggests that DSra-1, at least in part, has a negative regulatory role in this Rac signaling. Therefore, DSra-1 might be a negative regulator of Rac function in dorsal closure rather than a positive effector. Expression of DRac1V12 causes disruption of dorsal closure, indicating that excessive Rac signaling impairs this process. Over-expression of wild-type DRac1 does not disrupt dorsal closure, and it was investigated whether a DSra-1 mutant background might make dorsal closure sensitive to elevated

levels of wild-type Rac. However, DRac1 over-expression in a *DSra-1* mutant background did not cause dorsal closure defects.

The most important evidence of a lack of a DSra-1 functional role during dorsal closure came from the generation of embryos deficient in maternal and zygotic *DSra-1*. No evidence of dorsal closure defects was seen, and it was concluded that another process would have to be identified for the mutational analysis of DSra-1's role in actin cytoskeletal regulation.

6.2 DSra-1 does not activate the JNK cascade during dorsal closure

From initial interpretation of mammalian data, it seemed that Sra-1 might function in a direct manner with the actin cytoskeleton, however, given that Sra-1 is a Rac-binding protein there was the possibility that it could contribute to JNK signaling (Bagrodia et al., 1995; Sells et al., 1997; Vadlamudi et al., 2002). A popular route of investigation of effectors of the JNK cascade in *Drosophila* is the study of gene expression events that occur during dorsal closure. Transcription levels of *puc* and *dpp* are enhanced at the leading edge and these are used as reporters for JNK activation (Glise and Noselli, 1997). The activation of the JNK cascade has been shown to have a role in the regulation of F-actin, for example the JNK cascade can induce transcription of *profilin* (*chickadee* in *Drosophila*) during dorsal closure (Jasper et al., 2001; Verheyen and Cooley, 1994b; Wills et al., 1999). Furthermore in JNK pathway mutants the leading edge cytoskeleton is disrupted (Harden, 2002).

No effect on *puc* or *dpp* levels was seen at the leading edge in maternal and zygotic deficient *DSra-1* embryos, and as the JNK cascade is required for successful

closure and loss of *DSra-1* does not cause dorsal closure defects, this is not surprising (Harden, 2002). The results indicate that the route of DSra-1's regulation of F-actin in *Drosophila* does not involve JNK.

6.3 DSra-1 can regulate F-actin

Despite the fact that embryos lacking DSra-1 have no dorsal closure defects, DSra-1 over-expression does cause defects in dorsal closure. DSra-1 may not normally have a role in F-actin regulation in the leading edge cell, but its ectopic over-expression may be affecting the cytoskeleton in these cells. This may reflect a genuine role in F-actin regulation for DSra-1 that normally occurs elsewhere in the organism.

Close examination of the effects of over-expression of *DSra-1* in the leading edge revealed a loss of the phosphotyrosine nodes, similar to what is seen with the expression of DRac1N17, and which probably reflects a loss of the leading edge F-actin (Harden et al., 1995).

The loss of phosphotyrosine nodes indicates the distruption of adherens junctions that, as previously mentioned, appear to be stabilized by activated Rac (Evers et al., 2000; Harden, 2002). The adherens junctions appear to be implicated in the localization of various proteins vital for dorsal closure such as Canoe and Polychaetoid (Harden, 2002). Mutations of *canoe* (*cno*) and *polychaetoid* (*pyd*), produce dorsal closure defects and seem to be responsible, in part, for activation of the JNK pathway.

Recently it has been shown that Sra-1 participates in the stability and localization of SCAR/WAVE to regulate the formation of F-actin based cellular structures such as lamellipodia (Blagg et al., 2003; Eden et al., 2002; Kunda et al., 2003). Analysis using

various *SCAR* alleles, and clones of *SCAR* alleles, indicates that *SCAR* mutations cause defects in the blastodem, axon growth in the CNS, eye development and egg chamber structure during oogenesis (Zallen et al., 2002). *DSra-1* also causes axon guidance defects similar to *SCAR* suggesting a possible route of regulation, however, unlike *DSra-1* maternal and zygotic mutants, which can progress to pupal development, maternal and zygotic SCAR loss-of-function mutants die in the very early syncytial blastoderm stage suggesting that DSra-1 is not required in all SCAR processes (Schenck et al., 2003; Zallen et al., 2002).

Rac has been shown to signal through SCAR to activate the Arp2/3 complex and induce actin polymerization (Bear et al., 1998; Miki et al., 1998). In *Drosophila*, SCAR appears to be the primary regulator of Arp2/3-dependent morphogenetic events, however, the Arp2/3 complex and SCAR, while having F-actin associated roles in development have no reported roles in dorsal closure (Miller, 2002; Zallen et al., 2002). There are routes other than SCAR by which Rac could affect cytoskeletal regulation in dorsal closure, such as through the effector kinase Pak (Conder et al., submitted for publication). Recent evidence indicates that the Arp2/3 complex is not the only route by which *de novo* actin polymerization can occur (Evangelista et al., 2003). Indeed, the *Drosophila* Arp2/3 complex is only required for a subset of F-actin rearrangments in development (Hudson and Cooley, 2002). This, DSra-1 may only participate in a subset of Rac-regulated cytoskeletal events during development.

The disruption of the leading edge F-actin in embryos over-expressing *DSra-1* may have been an ectopic event revealing a true role for DSra-1 in regulation of F-actin. Sra-1 along with Nap1 (Nck associated protein, Kette) has been shown *in vitro* to form a

complex with SCAR, in which SCAR is inactive. SCAR is then released upon the binding of GTP-bound Rac to Sra-1 (Eden et al., 2002). This regulation has been demonstrated *in vivo* in *Dictystelium* where *Sra-1* mutants display uncontrolled protrusions that could be associated with unregulated polymerization of F-actin by Arp2/3 (Blagg et al., 2003). DRac1V12-induced growth defects in the intersegmental neurons are rescued by over-expression of *DSra-1*, further implicating Sra-1 as a possible negative regulator of SCAR (Schenck et al., 2003).

However, from studies on *Drosophila* cell lines, it has been shown that binding of SCAR to DSra-1 prevents the proteosome mediated degradation of SCAR and that DSra-1 contributes positively to actin-based protrusions (Kunda et al., 2003; Rogers et al., 2003). Furthermore, in one study on fibroblasts, Sra-1 and Nap1 were shown to positively contribute to Rac-mediated lamellipodia formation (Steffen et al., 2004). Thus the exisiting literature supports the idea that Sra-1 has both positive and negative regulatory roles in the formation of actin based structures.

All the work to date on regulation of actin-based structures by DSra-1 has been done in *Drosophila* cell lines. There is a need to identify an actin regulation in the whole organism involving DSra-1 that would enable a genetic dissection of DSra-1 function. Such a process could be regulation of the basal F-actin cytoskeleton of follicle cells covering the oocyte.

During oogenesis, the *Drosophila* oocyte is surrounded by a layer of somatic follicle cells attached to a basal lamina. This attachment to the lamina may be aided by integrin receptors, which assemble and localize to the basal cell surface (Goode and Perrimon, 1997). In each of the follicle cells, F-actin is arranged in parallel bundles at the

basal surface exhibiting a polarity perpendicular to the A-P plane of the oocyte (Gutzeit, 1990a). This arrangement of F-actin is thought to act like a molecular corset, restricting growth perpendicular to the A-P axis, and indeed the loss of the F-actin polarity produces round oocytes as seen in *Drosophila β-integrin* (*myospheroid* (*mys*)) mutants (Bateman et al., 2001a).

A possible link between DRac and the regulation of the basal F-actin could be the *Drosophila* receptor tyrosine phophatase, Leucocyte Common Antigen-Related (Dlar). *Dlar* mutants exhibited a disorganized follicular basal F-actin structure and produced oocyte phenotypes closely resembling those produced in *mys* mutants (Bateman et al., 2001a). Genetic interactions were also demonstrated between *Dlar* and *mys* suggesting a role between integrins and the organization of F-actin.

Dlar mutants have been shown to aggravate DRac1N17 induced intersegmental nerve path-finding defects and mutations of the Rac GEF, *Trio*, has also been demonstrated to genetically potentiate the *Dlar* guidance phenotype (Bateman et al., 2000; Debant et al., 1996). These results suggest a possible pathway for F-actin co-ordination in follicular cells, but to date a role for Rac has not been described.

The data from this thesis indicates that DSra-1 is required for the assembly of the F-actin in these cells. As several other proteins with known links to Rac signaling are also required: integrins, Dlar, and Pak, the F-actin of the follicle cells may present an excellent system for assembling a pathway of Rac-mediated regulation of the cytoskeleton through DSra-1 (Bateman et al., 2001a; Conder et al., submitted for publication).

DISCUSSION PART 2

Drosophila Plenty of SH3s

A *Drosophila* homolog of *POSH* has been identified and cloned. *DPOSH* has only one *Drosophila* homolog, expressing a transcription product of 3.0kb. The POSH proteins are characterized by a Zinc RING finger at the N-terminal followed by four SH3 domains. The Zinc RING finger in DPOSH has been shown to act as an E3 ubiquitin ligase, targeting itself for proteosomal degradation, a common characteristic of these proteins (Matheny et al., 2004; Xu et al., 2003).

Initial studies of *DPOSH* embryonic *in situs* revealed an increase in transcript levels along what appeared to be the leading edge of the epidermis during dorsal closure. As stated earlier, Rac is a key participant in dorsal closure acting in part through a JNK cascade (Harden, 2002). Given that mammalian POSH can bind Rac and activate JNK, POSH was considered a good candidate participant in JNK signaling during dorsal closure in *Drosophila* (Tapon et al., 1998). Other proteins homologous to mammalian activators of the JNK cascade, such as Slpr or Msn, have been well studied in *Drosophila* (Brown et al., 1996; Stronach and Perrimon, 2002; Su et al., 2000; Su et al., 1998; Tibbles et al., 1996).

Anti-DPOSH antibodies were generated, but Western blots were unable to produce any identifiable wild-type DPOSH signals. It may be that this is due to rapid degradation of DPOSH by self ubiquitylation via its internal E3 ubiquitin ligase (Tapon et al., 1998; Xu et al., 2003). Xu et al. also report that endogenous POSH is undetectable

in mammalian cell lines (Xu et al., 2003). Attempts to stain embryos to determine the localization of DPOSH and provide indication of its developmental role did not produce reliable data.

In order to study the role of DPOSH during development, a loss-of-function mutation was successfully created in *Drosophila.*

7.1 DPOSH does not activate the JNK cascade during dorsal closure

Over-expression of POSH in Cos-1 cells can activate the JNK cascade (Tapon et al., 1998). As previously mentioned, a popular route of investigation of effectors of the JNK cascade in *Drosophila* is through the study of dorsal closure. Transcription levels of *puc* and *dpp* are enhanced at the leading edge and these are used as reporters for JNK activation (Glise and Noselli, 1997). No effects on *dpp* or *puc* levels were seen at the leading edge in embryos deficient in maternal and zygotic *DPOSH.* The result is not surprising, as *DPOSH* mutant embryos do not show dorsal closure defects.

However, contrasting results were seen from work done by our collaborators in the Aigaki lab, who showed that over-expression of *DPOSH* in the wing imaginal disc caused activation of the JNK cascade, as well as an increase in *puc* transcription (Seong et al., 2001). Interestingly, when the level of Dpp is reduced in the wing disc, the JNK cascade is activated at the wing tip causing apoptosis (Adachi-Yamada and O'Connor, 2002). This suggests a possible role for DPOSH activating apoptosis through JNK in the wing disc, though no evidence of wing defects were seen in *DPOSH* loss-of-function mutants.

7.2 DPOSH and apoptosis

Over-expression of mammalian POSH was shown to induce apoptosis in PC12 and NIH-3T3 cells (Tapon et al., 1998; Xu et al., 2003). Over-expression of DPOSH during embryogenesis caused cells in the embryo to round up, a phenotype similar to that seen in *Drosophila inhibitor of apoptosis 1* (*DIAP1*) mutants that have increased caspase activity (Wang et al., 1999). *DPOSH* loss-of-function embryos fail to stain with AO, have a reduced level of TUNEL staining, and embryos exhibit a low frequency of head involution defects. Head involution defects are commonly seen in mutants with reduced levels of apoptosis, for example *hid* mutant embryos (Grether et al., 1995). Furthermore, *DPOSH* mutants enhance *Rac* mutant-induced germ band retraction failures. A significant amount of cell death occurs in the germ band during development and germ band retraction defects are also seen in *DIAP1* mutant embryos (Pazdera et al., 1998; Wang et al., 1999). These results suggest that DPOSH contributes to apoptosis during embryonic development.

Unlike mutations in other activators of apoptosis, homozygous loss-of-function *DPOSH* is not lethal and this is puzzling (Chen et al., 1996; Wang et al., 1999; White et al., 1994; Zhou et al., 1995). One possibility is that other mutants deficient in apoptosis are not dying due to a lack of apoptosis. As mentioned earlier, the inducers of programmed cell death in *Drosophila*, *grim*, *reaper* (*rpr*), and *hid,* all lie within a deletion on the third chromosome designated *H99* (White et al., 1994). It has been shown that while apoptosis does not occur in embryos deficient in these three genes, engulfment of the appropriate cells by macrophages still occurs. It has been speculated that caspase-inhibited embryos may be dying due to secondary effects on morphogenesis rather than a

lack of apoptosis (Mergliano and Minden, 2003), (Nassif et al., 1998; Pazdera et al., 1998). Thus, in *DPOSH* mutant embryos a defect in apoptosis may not be lethal.

Another consideration is that not all features of apoptosis are lacking in *DPOSH* mutant embryos. Despite the fact that these embryos are devoid of AO staining and reduced TUNEL staining, they show normal activation of the caspase, drICE. The exact nature of the mechanism behind the staining of apoptotic cells by AO is unknown (Abrams et al., 1993). AO has been shown in the studies of other genes to reveal a subset of the mechanisms behind apoptosis, for example, *DIAP1* mutants show an increase in TUNEL staining and caspase activity but no corresponding increase in AO staining (Wang et al., 1999). DPOSH may be involved in regulation of particular aspects of apoptosis, as the maintenance of activated drICE levels during embryogenesis in *DPOSH* mutants is conserved and *DPOSH* did not show any genetic interaction with reaper, p35, or DIAP1.

Work by our collaborators in the Ruden lab, using our *DPOSH* mutants, further implicated DPOSH in the regulation of apoptosis. Although apoptosis appears to be normal in DPOSH mutant eye discs, they exhibit greatly increased levels of X-ray induced apoptosis as compared to wild-type (Xiao and Ruden, unpublished results). In this context, DPOSH might be acting as a negative regulator of apoptosis occurring in response to DNA damage.

7.3 DPOSH interacts with Rac

Unlike mammalian POSH, DPOSH doesn't seem to bind Rac in a GST-pull down assay or in the yeast two-hybrid system. This, however, does not preclude the binding of the two through an intermediary adaptor protein.

Interestingly, *DPOSH* was shown to genetically interact with *Rac* in both the embryo and the eye. Over-expression of *DPOSH* in embryos expressing *DRac1N17* caused an increase in the number of *DRac1N17*-induced dorsal closure defects by 55% suggesting that DPOSH could function as a negative regulator of Rac.

Conversely, expressing *DRac1V12* in *DPOSH* loss-of-function embryos alleviated the *DRac1V12*-induced failure of germ band retraction, suggesting DPOSH could function as a positive effector. Germ band retraction failures are also seen in the *Rac* triple mutant embryos bearing the genotype, $Rac1^{J11}$,$Rac2^{\Delta}$,Mtl^{Δ} (Hakeda-Suzuki et al., 2002). When *Rac* mutant embryos are placed in a *DPOSH* homozygous mutant background, embryos exhibit an increase of 41% in the number of germ band retraction failures. Those two sets of results suggest that DPOSH is a positive effector for Rac in germ band retraction.

Genetic interaction experiments in the *Drosophila* eye also indicated that DPOSH could act as both an agonist and antagonist of Rac, specifically DRac2. Over-expression of either *DRac1* or *DRac2* in the *Drosophila* eye causes a rough, wedge shaped eye (Hariharan et al., 1995). Over-expression of *DRac1* was not modified by over-expression of *DPOSH*, while over-expression of *DRac2* together with *DPOSH* caused complete lethality at 25°C, and modifier experiments were performed at 18°C in order to weaken the penetrence of the phenotype. Both over-expression and loss-of-

function *DPOSH* caused an enhancement of the DRac2-induced rough eye, indicating that DPOSH may have both positive and negative regulatory roles in DRac2 signaling. DPOSH may be downstream of Rac in this regulation as the loss of all three *Drosophila Racs* has no effect on rough eyes induced by *DPOSH* over-expression. Interestingly, over-expression of two copies of *DPOSH* with inactivating mutations in the Zinc RING finger also caused an enhancement of the over-expression of *DRac2*, but the enhancement was not nearly as severe as that caused by over-expressing wild-type *DPOSH*. Hence the DPOSH Zinc RING finger may have a role in in its effector function in Rac signaling.

7.4 Building a working model of DPOSH function in Drosophila

Clearly DPOSH is not functioning to activate the JNK cascade during dorsal closure. However, DPOSH does seem to have a role in apoptosis, possibly through the JNK cascade (Fig. 7.1). It has recently been shown that POSH can respond to activated Rac1, acting as a MLK binding scaffold protein, and subsequently activating the JNK cascade to induce apoptosis in neuronal PC-12 cells (Xu et al., 2003). MLKs have been shown to act at the level of a JNKKK in the JNK cascade (Davis, 2000). The *Drosophila* MLK, Slipper, was not shown to genetically interact with DPOSH, however, as Slipper has been shown to be the JNKKK to likely activate the JNK cascade during dorsal closure, and DPOSH has no role in dorsal closure, this is not surprising (Stronach and Perrimon, 2002).

The JNKKK that DPOSH may interact with to activate the JNK cascade could be *Drosophila* TAK1 (dTAK1). Interestingly, *Drosophila* Tumour Necrosis Factor (TNF) ligand, Eiger, has been shown to stimulate the *Drosophila* TNF receptor, Wengen, to

Figure 7.1 Putative DPOSH pathway.

DPOSH may be involved in a scaffolding complex with Rac and a JNKKK, possibly dTAK1 that could be activated by the upstream TNF receptor (Wengen). Activation of the JNK cascade leads to apoptosis and activation of NF-κB-induced immune response. DPOSH may act to mediate the response by both positive signaling and degradation of effectors.

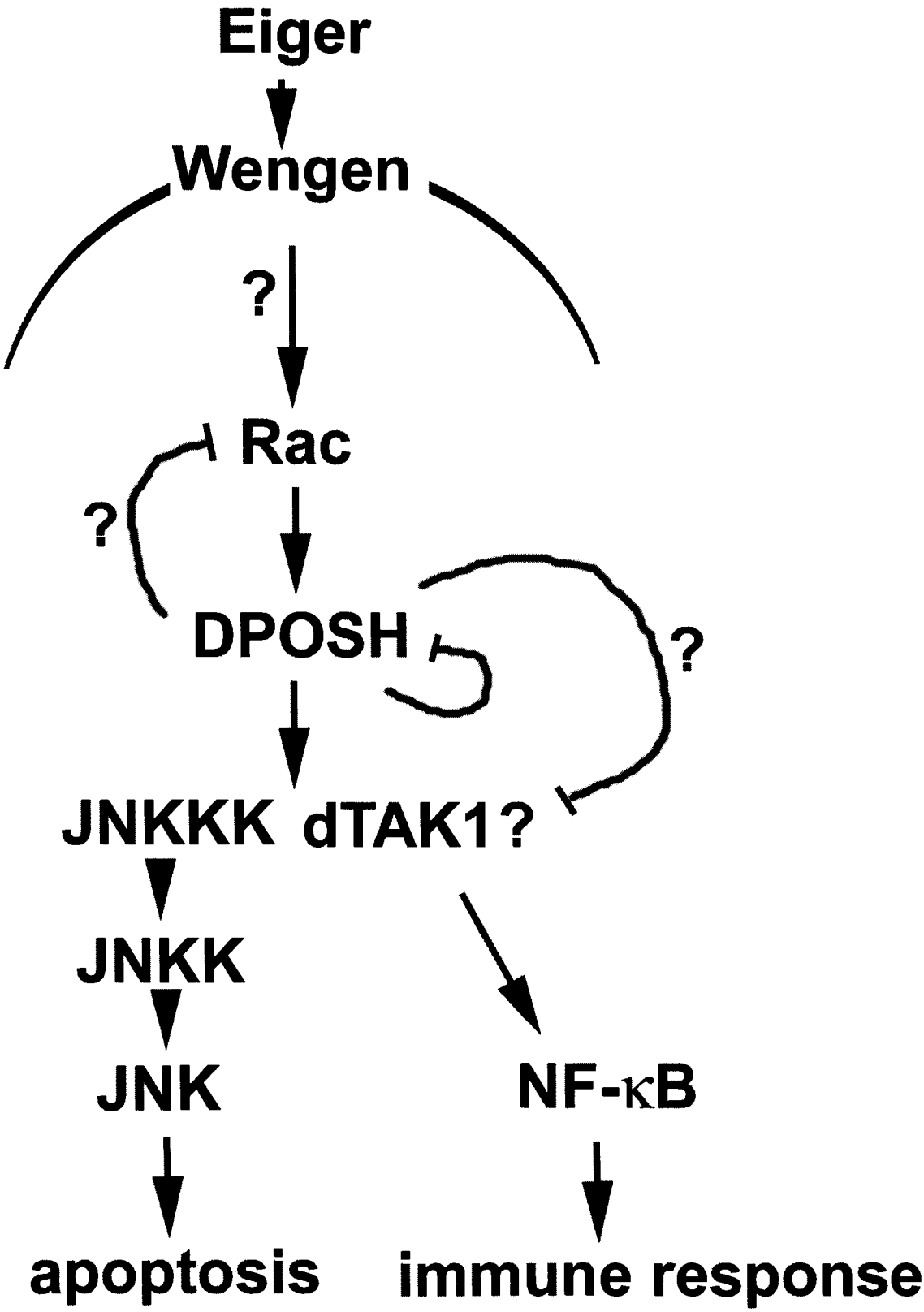
Eiger
Wengen
?
Rac
?
DPOSH
?
JNKKK
dTAK1?
JNKK
JNK
NF-κB
apoptosis
immune response

induce apoptosis through dTAK1 (Igaki et al., 2002; Kauppila et al., 2003). This pathway of activation of apoptosis can be inhibited by *bsk* (JNKK) and *hep* (JNK) mutant backgrounds, suggesting that the JNK cascade is responsible for apoptosis (Igaki et al., 2002). It is also interesting to note that this method of apoptosis does not seem to require the initiator or activator caspases. As seen in *DPOSH* mutants, activated drICE levels are unaffected while lacking in AO staining, lending some support to a possible link between DPOSH and dTAK1. It is possible that this cascade is required for apoptosis during development, such as during head involution and germ band retraction, and is therefore responsible for the phenotypes seen with the *DPOSH* mutants and genetic interactions with the *Rac* mutants.

POSH was originally shown to activate the immune response transcription factor, NF-κB, in Cos-1 cells (Tapon et al., 1998). dTAK1 has also been shown to activate the *Drosophila* NF-κB protein, Relish, after infection by Gram-negative bacteria (Silverman et al., 2003). Our collaborators in the Aigaki lab, have shown a genetic interaction between DPOSH and TAK1 in the *Drosophila* eye, and furthermore, have shown that our mutant *DPOSH* flies have decreased transcription levels of *relish* after exposure to Gram-negative bacteria.

The activation of Relish may actually lead to a negative feedback loop that causes the proteosomal degradation of dTAK1 and the downregulation of the JNK cascade (Park et al., 2004). The molecule responsible for the direct degradation of dTAK1 is unknown and a possible ubiquitin ligase that could act here might be DPOSH. It may be that DPOSH is controlling the levels of signaling, as our collaborators in the Ruden lab show that *DPOSH* mutants have higher levels of AO staining in the eye while we have shown

that *DPOSH* mutants show no AO staining. The Aigaki lab has shown that DPOSH over-expression induces apoptosis, but that both over-expression and *DPOSH* mutants can suppress Eiger induced apoptosis. A complicated mechanism likely exists behind DPOSH signaling.

7.5 Future Directions for DPOSH

The obvious route of investigation appears to be through dTAK1. Genetic interaction studies with *dTAK1* and members of its cascade, such as *relish* are worth pursuing in the eye. Moreover, biochemical binding assays could be performed with DPOSH and dTAK1 as compared to other JNKKKs such as Slipper. Investigation of DPOSH as an E3 ubiquitin ligase for dTAK1 could be examined.

What is interesting to note is that while a large amount of developmentally regulated apoptosis occurs during embryogenesis, mutants in the JNK cascade, *TAK1*, and *Rac* have not been examined for possible roles. Could it be possible that mutants of JNK components have defects in apoptosis similar to *DPOSH* mutants, but that their morpogenetic defects cause lethality? Indeed it has been shown that mutants in *grim*, *reaper*, and *hid* cause morphogenetic problems (Nassif et al., 1998; Pazdera et al., 1998).

As DPOSH protein levels were undetectable in *Drosophila* lysate, it could be possible that DPOSH levels are strictly regulated in the organism. It could be possible that it responds or is stabilized by Rac or dTAK. Expression of dominant negative or constitutively active forms of these proteins in the embryo followed by Western and embryo staining could be examined for DPOSH stability.

BIBLIOGRAPHY

Abrams, J. M., White, K., Fessler, L. I. and Steller, H. (1993). Programmed cell death during Drosophila embryogenesis. *Development* **117**, 29-43.

Adachi-Yamada, T. and O'Connor, M. B. (2002). Morphogenetic apoptosis: a mechanism for correcting discontinuities in morphogen gradients. *Dev Biol* **251**, 74-90.

Affolter, M., Nellen, D., Nussbaumer, U. and Basler, K. (1994). Multiple requirements for the receptor serine/threonine kinase *thick veins* reveal novel functions of TGF β homologs during Drosophila embryogenesis. *Development* **120**, 3105-3117.

Ashburner, M. (1989). Drosophila: A Laboratory Manual. Cold Spring Harbor, NY: Cold Spring Harbor Laboratory Press.

Bagrodia, S., Derijard, B., Davis, R. J. and Cerione, R. A. (1995). Cdc42 and PAK-mediated signaling leads to Jun kinase and p38 mitogen-activated protein kinase activation. *J Biol Chem* **270**, 27995-8.

Barrett, K., Leptin, M. and Settleman, J. (1997). The Rho GTPase and a putative RhoGEF mediate a signaling pathway for the cell shape changes in Drosophila gastrulation. *Cell* **91**, 905-15.

Bateman, J., Reddy, R. S., Saito, H. and Van Vactor, D. (2001a). The receptor tyrosine phosphatase Dlar and integrins organize actin filaments in the *Drosophila* follicular epithelium. *Curr Biol* **11**, 1317-27.

Bateman, J., Reddy, R. S., Saito, H. and Van Vactor, D. (2001b). The receptor tyrosine phosphatase Dlar and integrins organize actin filaments in the Drosophila follicular epithelium. *Curr Biol* **11**, 1317-27.

Bateman, J., Shu, H. and Van Vactor, D. (2000). The guanine nucleotide exchange factor Trio mediates axonal development in the *Drosophila* embryo. *Neuron* **26**, 93-106.

Bear, J. E., Rawls, J. F. and Saxe, C. L., 3rd. (1998). SCAR, a WASP-related protein, isolated as a suppressor of receptor defects in late Dictyostelium development. *J Cell Biol* **142**, 1325-35.

Betson, M., Lozano, E., Zhang, J. and Braga, V. M. (2002). Rac activation upon cell-cell contact formation is dependent on signaling from the epidermal growth factor receptor. *J Biol Chem* **277**, 36962-9.

Billuart, P., Winter, C. G., Maresh, A., Zhao, X. and Luo, L. (2001). Regulating axon branch stability: the role of p190 RhoGAP in repressing a retraction signaling pathway. *Cell* **107**, 195-207.

Bishop, A. L. and Hall, A. (2000). Rho GTPases and their effector proteins. *Biochem J* **348 Pt 2**, 241-255.

Blagg, S. L., Stewart, M., Sambles, C. and Insall, R. H. (2003). PIR121 regulates pseudopod dynamics and SCAR activity in Dictyostelium. *Curr Biol* **13**, 1480-7.

Bokoch, G. M. (2003). Biology of the p21-Activated Kinases. *Annu Rev Biochem* **72**, 743-781.

Braga, V. M., Machesky, L. M., Hall, A. and Hotchin, N. A. (1997). The small GTPases Rho and Rac are required for the establishment of cadherin-dependent cell-cell contacts. *J Cell Biol* **137**, 1421-31.

Brand, A. H. and Perrimon, N. (1993). Targeted gene expression as a means of altering cell fates and generating dominant phenotypes. *Development* **118**, 401-415.

Brown, J. L., Stowers, L., Baer, M., Trejo, J., Coughlin, S. and Chant, J. (1996). Human Ste20 homologue hPAK1 links GTPases to the JNK MAP kinase pathway. *Curr Biol* **6**, 598-605.

Brown, N. H., Gregory, S. L. and Martin-Bermudo, M. D. (2000). Integrins as mediators of morphogenesis in *Drosophila*. *Dev Biol* **223**, 1-16.

Brummel, T. J., Twombly, V., Marques, G., Wrana, J. L., Newfeld, S. J., Attisano, L., Massague, J., O'Connor, M. B. and Gelbart, W. M. (1994). Characterization and relationship of Dpp receptors encoded by the *saxophone* and *thick veins* genes in Drosophila. *Cell* **78**, 251-261.

Burbelo, P. D., Drechsel, D. and Hall, A. (1995). A conserved binding motif defines numerous candidate target proteins for both Cdc42 and Rac GTPases. *J Biol Chem* **270**, 29071-29074.

Burridge, K. and Wennerberg, K. (2004). Rho and Rac take center stage. *Cell* **116**, 167-79.

Bustelo, X. R. (1996). The VAV family of signal transduction molecules. *Crit Rev Oncog* **7**, 65-88.

Campos-Ortega, J. A. and Hartenstein, V. (1985). The embryonic development of Drosophila melanogaster. Berlin ; New York: Springer-Verlag.

Chasan, R. and Anderson, K. V. (1989). The role of *easter*, an apparent serine protease, in organizing the dorsal-ventral pattern of the *Drosophila* embryo. *Cell* **56**, 391-400.

Chen, P., Nordstrom, W., Gish, B. and Abrams, J. M. (1996). grim, a novel cell death gene in Drosophila. *Genes Dev* **10**, 1773-82.

Childs, S. R., Wrana, J. L., Arora, K., Attisano, L., O'Connor, M. B. and Massague, J. (1993). Identification of a *Drosophila* activin receptor. *Proc. Natl. Acad. Sci. U S A* **90**, 9475-9479.

Choi, K. W. and Benzer, S. (1994). Rotation of photoreceptor clusters in the developing Drosophila eye requires the nemo gene. *Cell* **78**, 125-36.

Chou, T. B. and Perrimon, N. (1996). The autosomal FLP-DFS technique for generating germline mosaics in Drosophila melanogaster. *Genetics* **144**, 1673-9.

Conder, R., Yu, H., Ricos, M., Hing, H., Chia, W., Lim, L. and Harden, N. (submitted for publication). dPak is transcriptionally regulated by small GTPase signaling during Drosophila dorsal closure and is required for integrity of the leading edge cytoskeleton, (ed.

Coso, O. A., Chiariello, M., Yu, J. C., Teramoto, H., Crespo, P., Xu, N., Miki, T. and Gutkind, J. S. (1995). The small GTP-binding proteins Rac1 and Cdc42 regulate the activity of the JNK/SAPK signaling pathway. *Cell* **81**, 1137-1146.

Cote, J. F. and Vuori, K. (2002). Identification of an evolutionarily conserved superfamily of DOCK180-related proteins with guanine nucleotide exchange activity. *J Cell Sci* **115**, 4901-13.

Dan, I., Watanabe, N. M. and Kusumi, A. (2001). The Ste20 group kinases as regulators of MAP kinase cascades. *Trends Cell Biol* **11**, 220-230.

Danial, N. N. and Korsmeyer, S. J. (2004). Cell death: critical control points. *Cell* **116**, 205-19.

Davis, R. J. (2000). Signal transduction by the JNK group of MAP kinases. *Cell* **103**, 239-52.

Debant, A., Serra-Pages, C., Seipel, K., O'Brien, S., Tang, M., Park, S. H. and Streuli, M. (1996). The multidomain protein Trio binds the LAR transmembrane tyrosine phosphatase, contains a protein kinase domain, and has separate rac-specific and rho-specific guanine nucleotide exchange factor domains. *Proc Natl Acad Sci U S A* **93**, 5466-71.

Delic, J., Coppey, J., Magdelenat, H. and Coppey-Moisan, M. (1991). Impossibility of acridine orange intercalation in nuclear DNA of the living cell. *Exp Cell Res* **194**, 147-53.

Diekmann, D., Brill, S., Garrett, M. D., Totty, N., Hsuan, J., Monfries, C., Hall, C., Lim, L. and Hall, A. (1991). Bcr encodes a GTPase-activating protein for p21rac. *Nature* **351**, 400-2.

Driessens, M. H., Hu, H., Nobes, C. D., Self, A., Jordens, I., Goodman, C. S. and Hall, A. (2001). Plexin-B semaphorin receptors interact directly with active Rac and regulate the actin cytoskeleton by activating Rho. *Curr Biol* **11**, 339-44.

Eaton, S., Auvinen, P., Luo, L., Jan, Y. N. and Simons, K. (1995). CDC42 and Rac1 control different actin-dependent processes in the *Drosophila* wing disc epithelium. *J Cell Biol* **131**, 151-64.

Eaton, S., Wepf, R. and Simons, K. (1996). Roles for Rac1 and Cdc42 in planar polarization and hair outgrowth in the wing of *Drosophila*. *J Cell Biol* **135**, 1277-89.

Eden, S., Rohatgi, R., Podtelejnikov, A. V., Mann, M. and Kirschner, M. W. (2002). Mechanism of regulation of WAVE1-induced actin nucleation by Rac1 and Nck. *Nature* **418**, 790-3.

Evangelista, M., Zigmond, S. and Boone, C. (2003). Formins: signaling effectors for assembly and polarization of actin filaments. *J Cell Sci* **116**, 2603-11.

Evers, E. E., Zondag, G. C., Malliri, A., Price, L. S., ten Klooster, J. P., van der Kammen, R. A. and Collard, J. G. (2000). Rho family proteins in cell adhesion and cell migration. *Eur J Cancer* **36**, 1269-74.

Finley, R. L. and Brent, R. rfly Drosophila cDNA yeast two hybrid library, (ed. E. Verheyen).

Fraser, A. G., McCarthy, N. J. and Evan, G. I. (1997). drICE is an essential caspase required for apoptotic activity in Drosophila cells. *Embo J* **16**, 6192-9.

Glise, B., Bourbon, H. and Noselli, S. (1995). *hemipterous* encodes a novel Drosophila MAP kinase kinase, required for epithelial cell sheet movement. *Cell* **83**, 451-461.

Glise, B. and Noselli, S. (1997). Coupling of Jun amino-terminal kinase and Decapentaplegic signaling pathways in *Drosophila* morphogenesis. *Genes Dev* **11**, 1738-1747.

Golemis, E. A., Serebriiskii, I. and Law, S. F. (1999). The yeast two-hybrid system: criteria for detecting physiologically significant protein-protein interactions. *Curr Issues Mol Biol* **1**, 31-45.

Golemis, E. A., Serebriiskii, R. I., Finley, R. L., Kolonin, M. G., Gyuris, J. and Brent, R. (1989). Interaction Trap/Two-Hybrid System to Identify Interacting Proteins.

In *Current protocols in molecular biology*, (ed. F. M. Ausubel), pp. 20.1.16. New York: Published by Greene Pub. Associates and Wiley-Interscience : J. Wiley.

Goode, S. and Perrimon, N. (1997). Inhibition of patterned cell shape change and cell invasion by Discs large during Drosophila oogenesis. *Genes Dev* **11**, 2532-44.

Grether, M. E., Abrams, J. M., Agapite, J., White, K. and Steller, H. (1995). The head involution defective gene of Drosophila melanogaster functions in programmed cell death. *Genes Dev* **9**, 1694-708.

Gutzeit, H. O. (1990a). The microfilament pattern in the somatic follicle cells of mid-vitellogenic ovarian follicles of Drosophila. *Eur J Cell Biol* **53**, 349-56.

Gutzeit, H. O. (1990b). The microfilament pattern in the somatic follicle cells of mid-vitellogenic ovarian follicles of Drosophila. *Eur J Cell Biol* **53**, 349-56.

Hakeda-Suzuki, S., Ng, J., Tzu, J., Dietzl, G., Sun, Y., Harms, M., Nardine, T., Luo, L. and Dickson, B. J. (2002). Rac function and regulation during *Drosophila* development. *Nature* **416**, 438-42.

Hall, A. (1998). Rho GTPases and the actin cytoskeleton. *Science* **279**, 509-14.

Hancock, J. F., Cadwallader, K., Paterson, H. and Marshall, C. J. (1991). A CAAX or a CAAL motif and a second signal are sufficient for plasma membrane targeting of ras proteins. *Embo J* **10**, 4033-9.

Hancock, J. F., Cadwaller, K., Paterson, H. and Marshall, C. J. (1992). A CAAX or a CAAL motif and a second signal are sufficient for plasma membrane targeting of ras proteins. EMBO J. 10, 4033-4039. *Trends Cell Biol* **2**, 73.

Harden, N. (2002). Signaling pathways directing the movement and fusion of epithelial sheets: lessons from dorsal closure in *Drosophila*. *Differentiation* **70**, 181-203.

Harden, N., Lee, J., Loh, H. Y., Ong, Y. M., Tan, I., Leung, T., Manser, E. and Lim, L. (1996). A *Drosophila* homolog of the Rac- and Cdc42-activated serine/threonine kinase PAK is a potential focal adhesion and focal complex protein that colocalizes with dynamic actin structures. *Mol Cell Biol* **16**, 1896-1908.

Harden, N., Loh, H. Y., Chia, W. and Lim, L. (1995). A dominant inhibitory version of the small GTP-binding protein Rac disrupts cytoskeletal structures and inhibits developmental cell shape changes in *Drosophila*. *Development* **121**, 903-914.

Harden, N., Ricos, M., Ong, Y. M., Chia, W. and Lim, L. (1999). Participation of small GTPases in dorsal closure of the *Drosophila* embryo: distinct roles for Rho subfamily proteins in epithelial morphogenesis. *J Cell Sci* **112**, 273-284.

Harden, N., Ricos, M., Yee, K., Sanny, J., Langmann, C., Yu, H., Chia, W. and Lim, L. (2002). Drac1 and Crumbs participate in amnioserosa morphogenesis during dorsal closure in *Drosophila*. *J Cell Sci* **115**, 2119-2129.

Hariharan, I. K., Hu, K. Q., Asha, H., Quintanilla, A., Ezzell, R. M. and Settleman, J. (1995). Characterization of rho GTPase family homologues in Drosophila melanogaster: overexpressing Rho1 in retinal cells causes a late developmental defect. *Embo J* **14**, 292-302.

Hartenstein, V. (1993). Atlas of Drosophila development. Plainview, N.Y.: Cold Spring Harbor Laboratory Press.

Hattori, S., Maekawa, M. and Nakamura, S. (1992). Identification of neurofibromatosis type I gene product as an insoluble GTPase-activating protein toward ras p21. *Oncogene* **7**, 481-5.

Hawkins, P. T., Eguinoa, A., Qiu, R. G., Stokoe, D., Cooke, F. T., Walters, R., Wennstrom, S., Claesson-Welsh, L., Evans, T., Symons, M. et al. (1995). PDGF stimulates an increase in GTP-Rac via activation of phosphoinositide 3-kinase. *Curr Biol* **5**, 393-403.

Hawley, R. J. and Waring, G. L. (1988). Cloning and analysis of the dec-1 female-sterile locus, a gene required for proper assembly of the Drosophila eggshell. *Genes Dev* **2**, 341-9.

Hay, B. A., Maile, R. and Rubin, G. M. (1997). P element insertion-dependent gene activation in the Drosophila eye. *Proceedings of the National Academy of Sciences U.S.A.* **94**, 5195-5200.

Hibi, M., Lin, A., Smeal, T., Minden, A. and Karin, M. (1993). Identification of an oncoprotein- and UV-responsive protein kinase that binds and potentiates the c-Jun activation domain. *Genes Dev* **7**, 2135-48.

Hing, H., Xiao, J., Harden, N., Lim, L. and Zipursky, S. L. (1999). Pak functions downstream of Dock to regulate photoreceptor axon guidance in *Drosophila*. *Cell* **97**, 853-863.

Hinz, U., Giebel, B. and Campos-Ortega, J. A. (1994). The basic-helix-loop-helix domain of Drosophila lethal of scute protein is sufficient for proneural function and activates neurogenic genes. *Cell* **76**, 77-87.

Hoffmann, F. M. and Goodman, W. (1987). Identification in transgenic animals of the Drosophila decapentaplegic sequences required for embryonic dorsal pattern formation. *Genes Dev* **1**, 615-25.

Hou, X. S., Goldstein, E. S. and Perrimon, N. (1997). *Drosophila* Jun relays the Jun amino-terminal kinase signal transduction pathway to the Decapentaplegic signal transduction pathway in regulating epithelial cell sheet movement. *Genes Dev* **11**, 1728-1737.

Hudson, A. M. and Cooley, L. (2002). A subset of dynamic actin rearrangements in Drosophila requires the Arp2/3 complex. *J Cell Biol* **156**, 677-87.

Igaki, T., Kanda, H., Yamamoto-Goto, Y., Kanuka, H., Kuranaga, E., Aigaki, T. and Miura, M. (2002). Eiger, a TNF superfamily ligand that triggers the Drosophila JNK pathway. *Embo J* **21**, 3009-18.

Inohara, N. and Nunez, G. (1999). Genes with homology to DFF/CIDEs found in Drosophila melanogaster. *Cell Death Differ* **6**, 823-4.

Ip, Y. T. and Davis, R. J. (1998). Signal transduction by the c-Jun N-terminal kinase (JNK)--from inflammation to development. *Curr Opin Cell Biol* **10**, 205-19.

Jacinto, A., Wood, W., Balayo, T., Turmaine, M., Martinez-Arias, A. and Martin, P. (2000). Dynamic actin-based epithelial adhesion and cell matching during *Drosophila* dorsal closure. *Curr Biol* **10**, 1420-1426.

Jackson, P. D. and Hoffmann, F. M. (1994). Embryonic expression patterns of the *Drosophila decapentaplegic* gene: separate regulatory elements control blastoderm expression and lateral ectodermal expression. *Dev. Dyn.* **199**, 28-44.

Jasper, H., Benes, V., Schwager, C., Sauer, S., Clauder-Munster, S., Ansorge, W. and Bohmann, D. (2001). The genomic response of the *Drosophila* embryo to JNK signaling. *Dev. Cell* **1**, 579-586.

Jin, S., Martinek, S., Joo, W. S., Wortman, J. R., Mirkovic, N., Sali, A., Yandell, M. D., Pavletich, N. P., Young, M. W. and Levine, A. J. (2000). Identification and characterization of a p53 homologue in Drosophila melanogaster. *Proc Natl Acad Sci U S A* **97**, 7301-6.

Joazeiro, C. A. and Weissman, A. M. (2000). RING finger proteins: mediators of ubiquitin ligase activity. *Cell* **102**, 549-52.

Jurgens, G., Wieschaus, E., Nusslein-Volhard, C. and Kluding, H. (1984). Mutations affecting the pattern of the larval cuticle in *Drosophila melanogaster* II. Zygotic loci on the third chromosome. *Roux's Arch. Dev. Biol.* **193**, 283-295.

Kaiser, W. J., Vucic, D. and Miller, L. K. (1998). The Drosophila inhibitor of apoptosis D-IAP1 suppresses cell death induced by the caspase drICE. *FEBS Lett* **440**, 243-8.

Kanda, H., Igaki, T., Kanuka, H., Yagi, T. and Miura, M. (2002). Wengen, a member of the Drosophila tumor necrosis factor receptor superfamily, is required for Eiger signaling. *J Biol Chem* **277**, 28372-5.

Kaufmann, N., Wills, Z. P. and Van Vactor, D. (1998). Drosophila Rac1 controls motor axon guidance. *Development* **125**, 453-61.

Kauppila, S., Maaty, W. S., Chen, P., Tomar, R. S., Eby, M. T., Chapo, J., Chew, S., Rathore, N., Zachariah, S., Sinha, S. K. et al. (2003). Eiger and its receptor, Wengen, comprise a TNF-like system in Drosophila. *Oncogene* **22**, 4860-7.

Kiehart, D. P. and Franke, J. D. (2002). Actin dynamics: the arp2/3 complex branches out. *Curr Biol* **12**, R557-9.

Kiehart, D. P., Galbraith, C. G., Edwards, K. A., Rickoll, W. L. and Montague, R. A. (2000). Multiple forces contribute to cell sheet morphogenesis for dorsal closure in *Drosophila*. *J Cell Biol* **149**, 471-490.

Kiosses, W. B., Shattil, S. J., Pampori, N. and Schwartz, M. A. (2001). Rac recruits high-affinity integrin alphavbeta3 to lamellipodia in endothelial cell migration. *Nat Cell Biol* **3**, 316-20.

Kiyokawa, E., Hashimoto, Y., Kobayashi, S., Sugimura, H., Kurata, T. and Matsuda, M. (1998). Activation of Rac1 by a Crk SH3-binding protein, DOCK180. *Genes Dev* **12**, 3331-3336.

Kobayashi, K., Kuroda, S., Fukata, M., Nakamura, T., Nagase, T., Nomura, N., Matsuura, Y., Yoshida-Kubomura, N., Iwamatsu, A. and Kaibuchi, K. (1998). p140Sra-1 (specifically Rac1-associated protein) is a novel specific target for Rac1 small GTPase. *J Biol Chem* **273**, 291-5.

Kockel, L., Zeitlinger, J., Staszewski, L. M., Mlodzik, M. and Bohmann, D. (1997). Jun in *Drosophila* development: redundant and nonredundant functions and regulation by two MAPK signal transduction pathways. *Genes Dev* **11**, 1748-1758.

Kotani, K., Yonezawa, K., Hara, K., Ueda, H., Kitamura, Y., Sakaue, H., Ando, A., Chavanieu, A., Calas, B., Grigorescu, F. et al. (1994). Involvement of phosphoinositide 3-kinase in insulin- or IGF-1-induced membrane ruffling. *Embo J* **13**, 2313-21.

Kovacs, E. M., Ali, R. G., McCormack, A. J. and Yap, A. S. (2002). E-cadherin homophilic ligation directly signals through Rac and phosphatidylinositol 3-kinase to regulate adhesive contacts. *J Biol Chem* **277**, 6708-18.

Kozma, R., Ahmed, S., Best, A. and Lim, L. (1996). The GTPase-activating protein n-chimaerin cooperates with Rac1 and Cdc42Hs to induce the formation of lamellipodia and filopodia. *Mol Cell Biol* **16**, 5069-80.

Kraynov, V. S., Chamberlain, C., Bokoch, G. M., Schwartz, M. A., Slabaugh, S. and Hahn, K. M. (2000). Localized Rac activation dynamics visualized in living cells. *Science* **290**, 333-7.

Kunda, P., Craig, G., Dominguez, V. and Baum, B. (2003). Abi, Sra1, and Kette Control the Stability and Localization of SCAR/WAVE to Regulate the Formation of Actin-Based Protrusions. *Curr Biol* **13**, 1867-75.

Lancaster, C. A., Taylor-Harris, P. M., Self, A. J., Brill, S., van Erp, H. E. and Hall, A. (1994). Characterization of rhoGAP. A GTPase-activating protein for rho-related small GTPases. *J Biol Chem* **269**, 1137-42.

Letsou, A., Arora, K., Wrana, J. L., Simin, K., Twombly, V., Jamal, J., Staehling-Hampton, K., Hoffmann, F. M., Gelbart, W. M., Massague, J. et al. (1995). Drosophila Dpp signaling is mediated by the *punt* gene product: a dual ligand-binding type II receptor of the TGF β receptor family. *Cell* **80**, 899-908.

Leung, I. W. and Lassam, N. (2001). The kinase activation loop is the key to mixed lineage kinase-3 activation via both autophosphorylation and hematopoietic progenitor kinase 1 phosphorylation. *J Biol Chem* **276**, 1961-7.

Li, W., Skoulakis, E. M., Davis, R. L. and Perrimon, N. (1997a). The Drosophila 14-3-3 protein Leonardo enhances Torso signaling through D-Raf in a Ras 1-dependent manner. *Development* **124**, 4163-71.

Li, W., Skoulakis, E. M., Davis, R. L. and Perrimon, N. (1997b). The Drosophila 14-3-3 protein Leonardo enhances Torso signaling through D-Raf in a Ras 1-dependent manner. *Development* **124**, 4163-71.

Lin, A. (2003). Activation of the JNK signaling pathway: breaking the brake on apoptosis. *Bioessays* **25**, 17-24.

Lu, Z. G., Zhang, C. M. and Zhai, Z. H. (2004). LDFF, the large molecular weight DNA fragmentation factor, is responsible for the large molecular weight DNA degradation during apoptosis in Xenopus egg extracts. *Cell Res* **14**, 134-40.

Luo, L. (2000). Rho GTPases in neuronal morphogenesis. *Nat Rev Neurosci* **1**, 173-80.

Luo, L., Liao, Y. J., Jan, L. Y. and Jan, Y. N. (1994). Distinct morphogenetic functions of similar small GTPases: Drosophila Drac1 is involved in axonal outgrowth and myoblast fusion. *Genes Dev* **8**, 1787-802.

Magie, C. R., Meyer, M. R., Gorsuch, M. S. and Parkhurst, S. M. (1999). Mutations in the Rho1 small GTPase disrupt morphogenesis and segmentation during early *Drosophila* development. *Development* **126**, 5353-5364.

Malecz, N., McCabe, P. C., Spaargaren, C., Qiu, R., Chuang, Y. and Symons, M. (2000). Synaptojanin 2, a novel Rac1 effector that regulates clathrin-mediated endocytosis. *Curr Biol* **10**, 1383-6.

Manser, E., Chong, C., Zhao, Z. S., Leung, T., Michael, G., Hall, C. and Lim, L. (1995). Molecular cloning of a new member of the p21-Cdc42/Rac-activated kinase (PAK) family. *J Biol Chem* **270**, 25070-8.

Manser, E., Huang, H. Y., Loo, T. H., Chen, X. Q., Dong, J. M., Leung, T. and Lim, L. (1997). Expression of constitutively active α-PAK reveals effects of the kinase on actin and focal complexes. *Mol Cell Biol* **17**, 1129-43.

Margolis, J. and Spradling, A. (1995). Identification and behavior of epithelial stem cells in the Drosophila ovary. *Development* **121**, 3797-807.

Martin-Blanco, E., Gampel, A., Ring, J., Virdee, K., Kirov, N., Tolkovsky, A. M. and Martinez-Arias, A. (1998). *puckered* encodes a phosphatase that mediates a feedback loop regulating JNK activity during dorsal closure in *Drosophila*. *Genes Dev* **12**, 557-570.

Matheny, S. A., Chen, C., Kortum, R. L., Razidlo, G. L., Lewis, R. E. and White, M. A. (2004). Ras regulates assembly of mitogenic signalling complexes through the effector protein IMP. *Nature* **427**, 256-60.

McCall, K., Baum, J. S., Cullen, K. and Peterson, J. S. (2004). Visualizing apoptosis. *Methods Mol Biol* **247**, 431-42.

Mergliano, J. and Minden, J. S. (2003). Caspase-independent cell engulfment mirrors cell death pattern in Drosophila embryos. *Development* **130**, 5779-89.

Mihaly, J., Kockel, L., Gaengel, K., Weber, U., Bohmann, D. and Mlodzik, M. (2001). The role of the Drosophila TAK homologue dTAK during development. *Mech Dev* **102**, 67-79.

Miki, H., Suetsugu, S. and Takenawa, T. (1998). WAVE, a novel WASP-family protein involved in actin reorganization induced by Rac. *Embo J* **17**, 6932-41.

Miller, K. G. (2002). Extending the Arp2/3 complex and its regulation beyond the leading edge. *J Cell Biol* **156**, 591-3.

Mirkovic, I., Charish, K., Gorski, S. M., McKnight, K. and Verheyen, E. M. (2002). Drosophila nemo is an essential gene involved in the regulation of programmed cell death. *Mech Dev* **119**, 9-20.

Moreno, E., Yan, M. and Basler, K. (2002). Evolution of TNF signaling mechanisms: JNK-dependent apoptosis triggered by Eiger, the Drosophila homolog of the TNF superfamily. *Curr Biol* **12**, 1263-8.

Morisato, D. and Anderson, K. V. (1995). Signaling pathways that establish the dorsal-ventral pattern of the *Drosophila* embryo. *Annu. Rev. Genet.* **29**, 371-399.

Muro, I., Hay, B. A. and Clem, R. J. (2002). The Drosophila DIAP1 protein is required to prevent accumulation of a continuously generated, processed form of the apical caspase DRONC. *J Biol Chem* **277**, 49644-50.

Muslin, A. J., Tanner, J. W., Allen, P. M. and Shaw, A. S. (1996). Interaction of 14-3-3 with signaling proteins is mediated by the recognition of phosphoserine. *Cell* **84**, 889-97.

Myers, E. W., Sutton, G. G., Delcher, A. L., Dew, I. M., Fasulo, D. P., Flanigan, M. J., Kravitz, S. A., Mobarry, C. M., Reinert, K. H., Remington, K. A. et al. (2000). A whole-genome assembly of *Drosophila*. *Science* **287**, 2196-204.

Nakagawa, M., Fukata, M., Yamaga, M., Itoh, N. and Kaibuchi, K. (2001). Recruitment and activation of Rac1 by the formation of E-cadherin-mediated cell-cell adhesion sites. *J Cell Sci* **114**, 1829-38.

Nassif, C., Daniel, A., Lengyel, J. A. and Hartenstein, V. (1998). The role of morphogenetic cell death during Drosophila embryonic head development. *Dev Biol* **197**, 170-86.

Nath, R., Raser, K. J., McGinnis, K., Nadimpalli, R., Stafford, D. and Wang, K. K. (1996a). Effects of ICE-like protease and calpain inhibitors on neuronal apoptosis. *Neuroreport* **8**, 249-55.

Nath, R., Raser, K. J., Stafford, D., Hajimohammadreza, I., Posner, A., Allen, H., Talanian, R. V., Yuen, P., Gilbertsen, R. B. and Wang, K. K. (1996b). Non-erythroid alpha-spectrin breakdown by calpain and interleukin 1 beta-converting-enzyme-like protease(s) in apoptotic cells: contributory roles of both protease families in neuronal apoptosis. *Biochem J* **319 (Pt 3)**, 683-90.

Nellen, D., Affolter, M. and Basler, K. (1994). Receptor serine/threonine kinases implicated in the control of Drosophila body pattern by *decapentaplegic*. *Cell* **78**, 225-237.

Newsome, T. P., Schmidt, S., Dietzl, G., Keleman, K., Asling, B., Debant, A. and Dickson, B. J. (2000). Trio combines with Dock to regulate Pak activity during photoreceptor axon pathfinding in *Drosophila*. *Cell* **101**, 283-94.

Ng, J., Nardine, T., Harms, M., Tzu, J., Goldstein, A., Sun, Y., Dietzl, G., Dickson, B. J. and Luo, L. (2002). Rac GTPases control axon growth, guidance and branching. *Nature* **416**, 442-7.

Nobes, C. D. and Hall, A. (1995). Rho, rac, and cdc42 GTPases regulate the assembly of multimolecular focal complexes associated with actin stress fibers, lamellipodia, and filopodia. *Cell* **81**, 53-62.

Nobes, C. D., Hawkins, P., Stephens, L. and Hall, A. (1995). Activation of the small GTP-binding proteins rho and rac by growth factor receptors. *J Cell Sci* **108**, 225-33.

Nolan, K. M., Barrett, K., Lu, Y., Hu, K. Q., Vincent, S. and Settleman, J. (1998). Myoblast city, the *Drosophila* homolog of DOCK180/CED-5, is required in a Rac signaling pathway utilized for multiple developmental processes. *Genes Dev* **12**, 3337-3342.

Noren, N. K., Niessen, C. M., Gumbiner, B. M. and Burridge, K. (2001). Cadherin engagement regulates Rho family GTPases. *J Biol Chem* **16**, 16.

Noselli, S. and Agnes, F. (1999). Roles of the JNK signaling pathway in *Drosophila* morphogenesis. *Curr Opin Genet Dev* **9**, 466-72.

Nusslein-Volhard, C., Wieschaus, E. and Kluding, H. (1984). Mutations affecting the pattern of the larval cuticle in *Drosophila melanogaster* I. Zygotic loci on the second chromosome. *Roux's Arch. Dev. Biol.* **193**, 267-282.

O'Connell, P. O. and Rosbash, M. (1984). Sequence, structure, and codon preference of the Drosophila ribosomal protein 49 gene. *Nucleic Acids Res* **12**, 5495-513.

O'Connor, M. and Chia, W. (1993). P Element-Mediated Germ-Line Transformation of *Drosophila.* In *Transgenesis Techniques: Priniciples and Protocols*, vol. 18 (ed. D. Murphy and D. A. Carter), pp. 75-85. Totowa, NJ: Humana Press.

Ota, S., Hazeki, K., Rao, N., Lupher, M. L., Jr., Andoniou, C. E., Druker, B. and Band, H. (2000). The RING finger domain of Cbl is essential for negative regulation of the Syk tyrosine kinase. *J Biol Chem* **275**, 414-22.

Ozanne, B. W., McGarry, L., Spence, H. J., Johnston, I., Winnie, J., Meagher, L. and Stapleton, G. (2000). Transcriptional regulation of cell invasion: AP-1 regulation of a multigenic invasion programme. *Eur J Cancer* **36**, 1640-8.

Park, J. M., Brady, H., Ruocco, M. G., Sun, H., Williams, D., Lee, S. J., Kato, T., Jr., Richards, N., Chan, K., Mercurio, F. et al. (2004). Targeting of TAK1 by the NF-kappa B protein Relish regulates the JNK-mediated immune response in Drosophila. *Genes Dev* **18**, 584-94.

Pazdera, T. M., Janardhan, P. and Minden, J. S. (1998). Patterned epidermal cell death in wild-type and segment polarity mutant Drosophila embryos. *Development* **125**, 3427-36.

Pearson, W. R. and Lipman, D. J. (1988). Improved tools for biological sequence comparison. *Proc Natl Acad Sci U S A* **85**, 2444-8.

Penton, A., Chen, Y., Staehling-Hampton, K., Wrana, J. L., Attisano, L., Szidonya, J., Cassill, J. A., Massague, J. and Hoffmann, F. M. (1994). Identification of two bone morphogenetic protein type I receptors in Drosophila and evidence that Brk25D is a Decapentaplegic receptor. *Cell* **78**, 239-250.

Peppelenbosch, M. P., Qiu, R. G., de Vries-Smits, A. M., Tertoolen, L. G., de Laat, S. W., McCormick, F., Hall, A., Symons, M. H. and Bos, J. L. (1995). Rac mediates growth factor-induced arachidonic acid release. *Cell* **81**, 849-56.

Pignoni, F., Baldarelli, R. M., Steingrimsson, E., Diaz, R. J., Patapoutian, A., Merriam, J. R. and Lengyel, J. A. (1990). The Drosophila gene tailless is expressed at the embryonic termini and is a member of the steroid receptor superfamily. *Cell* **62**, 151-63.

Promega. (1999). TnT Quick Coupled Transcription/Translation System.

Ridley, A. J., Paterson, H. F., Johnston, C. L., Diekmann, D. and Hall, A. (1992). The small GTP-binding protein rac regulates growth factor-induced membrane ruffling. *Cell* **70**, 401-10.

Riesgo-Escovar, J. R. and Hafen, E. (1997a). Common and distinct roles of DFos and DJun during *Drosophila* development. *Science* **278**, 669-672.

Riesgo-Escovar, J. R. and Hafen, E. (1997b). *Drosophila* Jun kinase regulates expression of *decapentaplegic* via the ETS-domain protein Aop and the AP-1 transcription factor DJun during dorsal closure. *Genes Dev* **11**, 1717-1727.

Riesgo-Escovar, J. R., Jenni, M., Fritz, A. and Hafen, E. (1996). The *Drosophila* Jun-N-terminal kinase is required for cell morphogenesis but not for DJun-dependent cell fate specification in the eye. *Genes Dev* **10**, 2759-2768.

Ring, J. M. and Martinez Arias, A. (1993). *puckered*, a gene involved in position-specific cell differentiation in the dorsal epidermis of the *Drosophila* larva. *Development Suppl.*, 251-259.

Rio, D. C., Laski, F. A. and Rubin, G. M. (1986). Identification and immunochemical analysis of biologically active Drosophila P element transposase. *Cell* **44**, 21-32.

Rogers, S. L., Wiedemann, U., Stuurman, N. and Vale, R. D. (2003). Molecular requirements for actin-based lamella formation in Drosophila S2 cells. *J Cell Biol* **162**, 1079-88.

Rorth, P. (1996a). A modular misexpression screen in Drosophila detecting tissue-specific phenotypes. *Proc Natl Acad Sci U S A* **93**, 12418-22.

Rorth, P. (1996b). A modular misexpression screen in Drosophila detecting tissue-specific phenotypes. *Proc Natl Acad Sci U S A* **93**, 12418-22.

Ruberte, E., Marty, T., Nellen, D., Affolter, M. and Basler, K. (1995). An absolute requirement for both the type II and type I receptors, Punt and Thick veins, for Dpp signaling in vivo. *Cell* **80**, 889-897.

Saller, E., Tom, E., Brunori, M., Otter, M., Estreicher, A., Mack, D. H. and Iggo, R. (1999). Increased apoptosis induction by 121F mutant p53. *Embo J* **18**, 4424-37.

Sambrook, J., Fritsch, E. F. and Maniatis, T. (1989). Molecular Cloning: A Laboratory Manual. Cold Spring Harbor, NY: Cold Spring Harbor Laboratory Press.

Schenck, A., Bardoni, B., Langmann, C., Harden, N., Mandel, J. L. and Giangrande, A. (2003). CYFIP/Sra-1 controls neuronal connectivity in Drosophila and links the Rac1 GTPase pathway to the fragile X protein. *Neuron* **38**, 887-98.

Schenck, A., Bardoni, B., Moro, A., Bagni, C. and Mandel, J. L. (2001). A highly conserved protein family interacting with the fragile X mental retardation protein (FMRP) and displaying selective interactions with FMRP-related proteins FXR1P and FXR2P. *Proc Natl Acad Sci U S A* **98**, 8844-9.

Schmidt, A. and Hall, A. (2002). Guanine nucleotide exchange factors for Rho GTPases: turning on the switch. *Genes Dev* **16**, 1587-609.

Sells, M. A., Knaus, U. G., Bagrodia, S., Ambrose, D. M., Bokoch, G. M. and Chernoff, J. (1997). Human p21-activated kinase (Pak1) regulates actin organization in mammalian cells. *Curr Biol* **7**, 202-10.

Seong, K. H. (2000). Molecular cloning and characterization of Drosophila POSH, (ed. Tokyo: Tokyo Metropolitan University.

Seong, K. H., Matsuo, T., Fuyama, Y. and Aigaki, T. (2001). Neural-specific overexpression of drosophila plenty of SH3s (DPOSH) extends the longevity of adult flies. *Biogerontology* **2**, 271-81.

Sepp, K. J. and Auld, V. J. (2003). RhoA and Rac1 GTPases mediate the dynamic rearrangement of actin in peripheral glia. *Development* **130**, 1825-35.

Sepp, K. J., Schulte, J. and Auld, V. J. (2000). Developmental dynamics of peripheral glia in Drosophila melanogaster. *Glia* **30**, 122-33.

Sepp, K. J., Schulte, J. and Auld, V. J. (2001). Peripheral glia direct axon guidance across the CNS/PNS transition zone. *Dev Biol* **238**, 47-63.

Settleman, J. (2001). Rac 'n Rho: the music that shapes a developing embryo. *Dev Cell* **1**, 321-31.

Shaulian, E. and Karin, M. (2002). AP-1 as a regulator of cell life and death. *Nat Cell Biol* **4**, E131-6.

Silverman, N., Zhou, R., Erlich, R. L., Hunter, M., Bernstein, E., Schneider, D. and Maniatis, T. (2003). Immune activation of NF-kappaB and JNK requires Drosophila TAK1. *J Biol Chem* **278**, 48928-34.

Sluss, H. K., Han, Z., Barrett, T., Davis, R. J. and Ip, Y. T. (1996). A JNK signal transduction pathway that mediates morphogenesis and an immune response in *Drosophila*. *Genes Dev* **10**, 2745-2758.

Spradling, A. C. (1986). P element mediated transformation. In *Drosophila: A Practical Approach*, pp. 175-197. Oxford, England: IRL Press.

St Johnston, R. D. and Gelbart, W. M. (1987). Decapentaplegic transcripts are localized along the dorsal-ventral axis of the *Drosophila* embryo. *Embo J* **6**, 2785-2791.

Staehling-Hampton, K., Hoffmann, F. M., Baylies, M. K., Rushton, E. and Bate, M. (1994). dpp induces mesodermal gene expression in Drosophila. *Nature* **372**, 783-6.

Steffen, A., Rottner, K., Ehinger, J., Innocenti, M., Scita, G., Wehland, J. and Stradal, T. E. (2004). Sra-1 and Nap1 link Rac to actin assembly driving lamellipodia formation. *Embo J* **23**, 749-59.

Stronach, B. and Perrimon, N. (2002). Activation of the JNK pathway during dorsal closure in *Drosophila* requires the mixed lineage kinase, *slipper*. *Genes Dev* **16**, 377-387.

Su, Y. C., Maurel-Zaffran, C., Treisman, J. E. and Skolnik, E. Y. (2000). The Ste20 kinase Misshapen regulates both photoreceptor axon targeting and dorsal closure, acting downstream of distinct signals. *Mol Cell Biol* **20**, 4736-4744.

Su, Y. C., Treisman, J. E. and Skolnik, E. Y. (1998). The *Drosophila* Ste20-related kinase *misshapen* is required for embryonic dorsal closure and acts through a JNK MAPK module on an evolutionarily conserved signaling pathway. *Genes Dev* **12**, 2371-2380.

Sved, J. A., Blackman, L. M., Gilchrist, A. S. and Engels, W. R. (1991). High levels of recombination induced by homologous P elements in Drosophila melanogaster. *Mol Gen Genet* **225**, 443-7.

Takahashi, K., Sasaki, T., Mammoto, A., Takaishi, K., Kameyama, T., Tsukita, S. and Takai, Y. (1997). Direct interaction of the Rho GDP dissociation inhibitor with ezrin/radixin/moesin initiates the activation of the Rho small G protein. *J Biol Chem* **272**, 23371-5.

Tapon, N. and Hall, A. (1997). Rho, Rac and Cdc42 GTPases regulate the organization of the actin cytoskeleton. *Curr Opin Cell Biol* **9**, 86-92.

Tapon, N., Nagata, K., Lamarche, N. and Hall, A. (1998). A new rac target POSH is an SH3-containing scaffold protein involved in the JNK and NF-kappaB signalling pathways. *Embo J* **17**, 1395-404.

Theodosiou, N. A. and Xu, T. (1998). Use of FLP/FRT system to study Drosophila development. *Methods* **14**, 355-65.

Tibbles, L. A., Ing, Y. L., Kiefer, F., Chan, J., Iscove, N., Woodgett, J. R. and Lassam, N. J. (1996). MLK-3 activates the SAPK/JNK and p38/RK pathways via SEK1 and MKK3/6. *Embo J* **15**, 7026-35.

Vadlamudi, R. K., Li, F., Adam, L., Nguyen, D., Ohta, Y., Stossel, T. P. and Kumar, R. (2002). Filamin is essential in actin cytoskeletal assembly mediated by p21- activated kinase 1. *Nat Cell Biol* **4**, 681-90.

Van Aelst, L. and D'Souza-Schorey, C. (1997). Rho GTPases and signaling networks. *Genes Dev* **11**, 2295-2322.

Van Vactor, D., Jr., Krantz, D. E., Reinke, R. and Zipursky, S. L. (1988). Analysis of mutants in chaoptin, a photoreceptor cell-specific glycoprotein in Drosophila, reveals its role in cellular morphogenesis. *Cell* **52**, 281-90.

Varfolomeev, E. E. and Ashkenazi, A. (2004). Tumor necrosis factor: an apoptosis JuNKie? *Cell* **116**, 491-7.

Verheyen, E. and Cooley, L. (1994a). Looking at oogenesis. *Methods Cell Biol* **44**, 545-61.

Verheyen, E. M. and Cooley, L. (1994b). Profilin mutations disrupt multiple actin-dependent processes during Drosophila development. *Development* **120**, 717-28.

Virca, G. D., Northemann, W., Shiels, B. R., Widera, G. and Broome, S. (1990). Simplified northern blot hybridization using 5% sodium dodecyl sulfate. *Biotechniques* **8**, 370-1.

Volkmann, N., Amann, K. J., Stoilova-McPhie, S., Egile, C., Winter, D. C., Hazelwood, L., Heuser, J. E., Li, R., Pollard, T. D. and Hanein, D. (2001). Structure of Arp2/3 complex in its activated state and in actin filament branch junctions. *Science* **293**, 2456-9.

Wang, S. L., Hawkins, C. J., Yoo, S. J., Muller, H. A. and Hay, B. A. (1999). The Drosophila caspase inhibitor DIAP1 is essential for cell survival and is negatively regulated by HID. *Cell* **98**, 453-63.

Webster, M., Moretti, P. and Brink, N. G. (1992). Supernova (spno), a new maternal mutant producing variable-sized cleavage nuclei in Drosophila. *Genet Res* **60**, 131-7.

White, K., Grether, M. E., Abrams, J. M., Young, L., Farrell, K. and Steller, H. (1994). Genetic control of programmed cell death in Drosophila. *Science* **264**, 677-83.

White, K., Tahaoglu, E. and Steller, H. (1996). Cell killing by the Drosophila gene reaper. *Science* **271**, 805-7.

Widlak, P. (2000). The DFF40/CAD endonuclease and its role in apoptosis. *Acta Biochim Pol* **47**, 1037-44.

Wills, Z., Marr, L., Zinn, K., Goodman, C. S. and Van Vactor, D. (1999). Profilin and the Abl tyrosine kinase are required for motor axon outgrowth in the Drosophila embryo. *Neuron* **22**, 291-9.

Wolf, W. A., Chew, T. L. and Chisholm, R. L. (1999). Regulation of cytokinesis. *Cell Mol Life Sci* **55**, 108-20.

Xiao, L. and Ruden, D. M. (unpublished results). DPOSH regulates Xray induced apoptosis, (ed.

Xu, Z., Kukekov, N. V. and Greene, L. A. (2003). POSH acts as a scaffold for a multiprotein complex that mediates JNK activation in apoptosis. *Embo J* **22**, 252-61.

Yoo, S. J., Huh, J. R., Muro, I., Yu, H., Wang, L., Wang, S. L., Feldman, R. M., Clem, R. J., Muller, H. A. and Hay, B. A. (2002). Hid, Rpr and Grim negatively regulate DIAP1 levels through distinct mechanisms. *Nat Cell Biol* **4**, 416-24.

Young, P. E., Richman, A. M., Ketchum, A. S. and Kiehart, D. P. (1993). Morphogenesis in *Drosophila* requires nonmuscle myosin heavy chain function. *Genes Dev* **7**, 29-41.

Zallen, J. A., Cohen, Y., Hudson, A. M., Cooley, L., Wieschaus, E. and Schejter, E. D. (2002). SCAR is a primary regulator of Arp2/3-dependent morphological events in Drosophila. *J Cell Biol* **156**, 689-701.

Zeitlinger, J., Kockel, L., Peverali, F. A., Jackson, D. B., Mlodzik, M. and Bohmann, D. (1997). Defective dorsal closure and loss of epidermal *decapentaplegic* expression in *Drosophila fos* mutants. *Embo J* **16**, 7393-7401.

Zhou, L., Hashimi, H., Schwartz, L. M. and Nambu, J. R. (1995). Programmed cell death in the Drosophila central nervous system midline. *Curr Biol* **5**, 784-90.

Zipursky, S. L., Venkatesh, T. R., Teplow, D. B. and Benzer, S. (1984). Neuronal development in the Drosophila retina: monoclonal antibodies as molecular probes. *Cell* **36**, 15-26.